Distinct Roles of Class 1 PI3K Isoforms in the Regulation of Beta Cell Exocytosis and Insulin Secretion

by

Jelena Kolic

A thesis submitted in partial fulfillment of the requirements for the degree of

Doctor of Philosophy

Department of Pharmacology
University of Alberta

ABSTRACT

Distinct Roles of Class 1 PI3K Isoforms in the Regulation of Beta Cell Exocytosis and Insulin Secretion

PhD Thesis 2014, Jelena Kolic

Department of Pharmacology, University of Alberta

Type 2 diabetes (T2D) is characterized by peripheral insulin resistance and an insufficiency of insulin secretion from the pancreatic beta cell. The incidence of T2D is rising worldwide at an alarming rate. An increase in population growth, increased prevalence of obesity, and an aging population are all thought to be contributing to this rise in T2D incidence. The economic burden of this disease is increasing globally; but more importantly, despite numerous treatment options, many type 2 diabetic patients still suffer from a decreased life expectancy.

The mechanisms that regulate insulin secretion from the pancreatic beta cell are still not fully understood. Thus in order to understand beta cell dysfunction in disease state, it is essential to fully understand the mechanisms that regulate insulin secretion from the healthy pancreatic beta cell. The present thesis will thus investigate the role of class 1 phosphoinositide 3-kinase (PI3K) isoforms in the regulation of beta cell exocytosis and insulin secretion.

The PI3K family of enzymes is linked to a large number of diverse cellular functions, and is essential to almost all aspects of cell and tissue biology. PI3Ks are known to have critical roles in the control of islet mass and function, and alterations in PI3K signaling are shown to be associated with T2D. The chronic genetic impairment of

upstream PI3K signaling in islets results in impaired insulin secretion; but this is contrasted by findings showing that pharmacologic PI3K inhibition increases glucose-stimulated insulin secretion. However, PI3Ks are a diverse family of enzymes, and recently there has been a broadening recognition of the importance of distinct PI3K isoforms.

The work presented here confirms the expression of three class 1 PI3K isoforms: p110α, -β and -γ in mouse and human islets, and identifies a distinct role for each in insulin secretion and beta cell exocytosis. Using selective pharmacologic inhibition and shRNA-mediated knockdown, p110α is shown to negatively regulate glucose-stimulated insulin secretion (GSIS) by limiting Ca^{2+}-dependent exocytosis in beta cells. p110β however, exerts a positive insulinotropic effect upstream of exocytosis, by promoting insulin granule localization to the plasma membrane, independent of its catalytic activity. Finally, the G-protein coupled p110γ is shown to be a positive regulator of insulin secretion and exocytosis. It plays an important role in maintaining a membrane-docked, readily releasable pool of secretory granules, (at least in part) through the regulation of cortical F-actin polymerization.

The requirement for p110γ signaling in GIP-R and GLP-1-R induced insulin secretion is also examined in this thesis. p110γ inhibition or shRNA-mediated knockdown impairs the insulinotropic effects of GIP-R (but not GLP-1-R) activation in mouse and human islets. We propose that this is due to GIPs inability to induce actin depolymerization following p110γ inhibition. We suggest that this p110γ-dependent pathway facilitates insulin granule access to the plasma membrane (in concert with classical cAMP/PKA-dependent signaling) to potentiate exocytosis and insulin secretion.

PREFACE

The research project, of which this thesis is a part, received research ethics approval from the University of Alberta Research Ethics Board, "Cell Biology of Human Pancreatic Islets", No. Pro00001754, updated September 22, 2014; and "Pancreatic β-cell Function and Breeding Colony", No. AUP00000291, updated September 11, 2014.

A version of Chapter 2 of this thesis has been published as Jelena Kolic, Aliya F. Spigelman, Greg Plummer, Eric Leung, Catherine Hajmrle, Tatsuya Kin, James AM. Shapiro, Jocelyn E. Manning Fox, Patrick E. MacDonald. (2013) Distinct and opposing roles for p110α and p110β in the regulation of insulin secretion from rodent and human beta cells. *Diabetologia* **56**(6): 1339-1349. I was responsible for the majority of the data collection, data analysis, and manuscript composition. A.F.S., G.P., E.L., C.L., and J.E.M.F. contributed to data collection as outlined in the figure legends in chapter 2. T.K. and J.A.M.S. contributed to concept formation. P.E.M. was the supervisory author and was involved with concept formation and editing of the manuscript.

A version of Chapter 3 of this thesis has been published as Gary M. Pigeau*, Jelena Kolic*, Brandon J. Ball, Michael B. Hoppa, Ying W. Wang, Thomas Rückle, Minna Woo, Jocelyn E. Manning Fox, and Patrick E. MacDonald (2009) Distinct and opposing roles for p110α and p110β in the regulation of insulin secretion from rodent and human beta cells. *Diabetes* **58**(9): 2084-1349. I was responsible for data collection, data analysis, and contributed to the manuscript composition. G.M.P contributed equally to data collection, data analysis, and the manuscript composition. B.J.B., J.E.M.F., M.B.H, and Y.W.W. contributed to data collection as outlined in the figure legends in chapter 3. T.R. and M.W. contributed to concept formation. P.E.M. was the supervisory author and was involved with concept formation and editing of the manuscript.

A version of Chapter 4 of this thesis has been submitted to the Journal of Biochemistry as Jelena Kolic, Aliya F. Spigelman, Alannah M. Smith, Jocelyn E. Manning Fox, and Patrick E. MacDonald (2014) Insulin secretion induced by glucose-dependent insulinotropic polypeptide requires PI3Kγ in rodent and human beta cells. I was responsible for the majority of the data collection, data analysis, and manuscript composition. A.F.S., and A.M.S contributed to data collection as outlined in the figure legends in chapter 4. J.E.M.F. contributed to concept formation. P.E.M. was the supervisory author and was involved with concept formation and editing of the manuscript.

Some of the research conducted for this thesis (referred to in chapter 5) forms part of a research collaboration, led by Dr. Daniel J. Drucker (Figure 37) at the Lunenfeld-Tanenbaum Research Institute (Mount Sinai Hospital), and Dr. Vincent Poitout at the Montreal Diabetes Research Center (Figure 38), with Dr. Patrick E. MacDonald being the lead collaborator at the University of Alberta. Figures 37 and 38 are my original work.

Figure 38 has been published as a part of: Ferdaoussi M, Bergeron V, Zarrouki B, Kolic J, Cantley J, Fielitz J, Olson EN, Prentki M, Biden T, MacDonald PE, Poitout V. (2012)

G protein-coupled receptor (GPR)40-dependent potentiation of insulin secretion in mouse islets is mediated by protein kinase D1. *Diabetologia* **55**(10):2682-92. I was responsible for the sample preparation, data collection, and analysis for Figure 38 in this thesis.

ACKNOWLEDGEMENTS

First and foremost I would like to express my deep gratitude to my research supervisor Dr. Patrick Macdonald for his patient guidance, enthusiastic encouragement and useful critiques of this research work. I have been extremely lucky to have a supervisor who cared so much about my work, and who was always available to discuss any hurdles encountered. Thank you for the all the opportunities you have provided for me over the past 6 years!

I would also like to thank the members of my supervisory committee, Dr. Fred Tse and Dr. Catherine Chan for their advice, encouragement and support during my studies.

I also thank the Department of Pharmacology, and the funding agencies that have supported my PhD studies: The Canadian Institutes of Health Research, Alberta Innovates Health Solutions, The Canadian Diabetes Association, and the Alberta Diabetes Institute.

A big thanks to my lab-mates for all the laughs, fun and support! Joss Manning Fox, Xiao Qing Dai, Mourad Ferdaoussi, Greg Plummer, James Lyon, Aliya Spigelman, Cathy Pretzlaw, Nancy Smith, Robbie Wright, Alannah Smith: the last 6 years would have been much more difficult and dull without your presence! You truly made me enjoy my time in grad school!

Finally, I would like to express my gratitude to my family, my friends, and my James, who have endured my PhD experience with me. Thank you for putting up with my numerous moments of insanity! Without your love and support this thesis would not have been possible.

ABBREVIATIONS

$[Ca^{2+}]_I$	Intracellular concentration of Ca^{2+}
μg	microgram
μl	microliter
μM	micromolar
ABCC	Administrative and Bioinformatics Coordinating Center
ABD	Adaptor Binding Domain
ABP	Actin Binding Protein
ADP	Adenosine diphosphate
ANOVA	Analysis of Variance
AS605240	5-(6-Quinoxalinylmethylene)-2,4-thiazolidinedione
ATP	Adenosine triphosphate
ATPase	Adenosine Triphosphatase
AU	Arbitrary Unit
AUC	Area Under the Curve
AZD6482	(R)-2-(1-(7-methyl-2-morpholino-4-oxo-4H-pyrido[1,2-a]pyrimidin-9-yl)ethylamino)benzoic acid
BCH	Breakpoint Cluster region-Homology domain
cAMP	Cyclic Adenosine Monophosphate
Cdc42	Cell division control protein 42 homolog
DAG	Diacylglycerol
PKD	Protein Kinase D
DMEM	Dulbecco's Modified Eagle's Medium
DMSO	Dimethyl sulfoxide
DNase 1	Deoxyribonuclease I
DPP-4	Dipeptidyl peptidase-4
EGFR	Epidermal Growth Factor Receptor
EGTA	Ethylene Glycol Tetraacetic Acid
Epac	Rap guanine nucleotide exchange factor 3
Ex-4	Exendin-4
F-actin	Filamentous actin
fF	femtofarad
FBS	Fetal Bovine Serum
FoxO1	Forkhead Transcription Factor 1
G-actin	Globular actin
GAP	GTPase-Activating Protein
GDI	Guanosine nucleotide Dissociation Inhibitors
GEF	Guanine nucleotide Exchange Factor
GFP	Green Fluorescent Protein
GFP-PH_{AKT}	Green Fluorescent Protein tagged Pleckstrin homology domain
GIP	Glucose-Dependent Insulinotropic Peptide
GIP-R	Glucose-Dependent Insulinotropic Peptide-Receptor
GLP-1	Glucagon Like Peptide-1
GLP-1-R	Glucagon Like Peptide-1-Receptor
GLUT	Glucose Transporter

GPCR	G-protein Coupled Receptor
GPR40	G-protein Coupled Receptor regulating free fatty acid
GSIS	Glucose Stimulated Insulin Secretion
GST	Glutathione S-Transferase
GTP	Guanosine Triphosphate
GTPase	Guanosine Triphosphatase
HD	Helical Domain
HEPES	N-2-Hydroxyethylpiperazine-N'-2-Ethanesulfonic Acid
HG	High Glucose
HIT cells	Hamster Insulin Secreting Cell line
IAPP–mCherry	Islet Amyloid Polypeptide tagged with mCherry Fluorophore
IC_{50}	Half Maximal Inhibitory Concentration
IGF-1	Insulin-Like Growth Factor 1
IGF1R	Insulin-Like Growth Factor 1 Receptor
INS-1	Rat Insulinoma Cell Line
INS-1E	Rat Insulinoma Cell Line
IR	Insulin Receptor
IRS	Insulin Receptor Substrate
iSH2	inter-Src Homology 2 domain
K_{ATP}	ATP- sensitive potassium
Kd	Dissociation constant
KO	Knock-out
KRB	Krebs-Ringer Buffer
Kv	Voltage-dependent potassium
LDCV	Large Dense Core Vesicles
LG	Low Glucose
LPA	Lysophosphatidic Acid
LY294002	2-(4-Morpholinyl)-8-phenyl-4H-1-benzopyran-4-one
MAPK	Mitogen-Activated Protein Kinase
min	minute
MIN6	Mouse Insulinoma Cell Line
mM	millimolar
mTOR	Mammalian Target of Rapamycin
mRNA	Messenger RNA
ms	Milliseconds
mV	Millivolts
NPY-mCherry	Neuropeptide Y tagged with mCherry Fluorophore
OGTT	Oral Glucose Tolerance Test
p-AKT	Phospho-Akt
PACAP	Pituitary adenylate cyclase-activating polypeptide
PAK1	P21-Activated Kinase 1
PAK2	P21-Activated Kinase 2
PC1	Prohormone Convertase 1
PDE3B	Phosphodiesterase 3B
PDK1	Phosphoinositide-Dependent Kinase-1
Pdx-1	Pancreatic/ Duodenal Homeobox transcription factor -1

pF	picofarads
PH domain	Plekstrin Homology domain
PI3K	Phosphatidylinositol 3-OH kinases
PI3KC1	Class 1 Phosphatidylinositol 3-OH kinase
PI3KC2	Class 2 Phosphatidylinositol 3-OH kinase
PI3KC3	Class 3 Phosphatidylinositol 3-OH kinase
PIK-75	2- methyl- 5- nitro- 2- [(6- bromoimidazo[1, 2- a]pyridin- 3- yl)methylene]- 1- methylhydrazide- benzenesulfonic acid, monohydrochloride
PIK3CA	Phosphatidylinositol 3-OH kinase alpha
PIK3CB	Phosphatidylinositol 3-OH kinase beta
PIK3CD	Phosphatidylinositol 3-OH kinase delta
PIK3CG	Phosphatidylinositol 3-OH kinase gamma
pik3r1	Phosphatidylinositol 3-OH kinase regulatory subunit alpha
pik3r2	Phosphatidylinositol 3-OH kinase regulatory subunit beta
PIP_2	Phosphatidylinositol 4,5 bisphosphate
PIP_3	Phosphatidylinositol 3,4,5-trisphosphate
PKA	Protein Kinase A
PKB	Protein Kinase B
PKC	Protein Kinase C zeta type
PtdInsP5K	Phosphatidylinositol-4-phosphate 5-Kinase
qPCR	Quantitative Polymerase Chain Reaction
Rac1	Ras-related C3 Botulinum Toxin Substrate 1
Ras	Rat Sarcoma family of small GTPase proteins
RANTES	Regulated on Activation, Normal T cell Expressed and Secreted
RBD	Ras Binding Domain
RFP	Red Fluorescent Protein
Rho	Rho small GTPase proteins
RIP	Rat Insulin Promoter
RP	Reserve Pool
RPMI	Roswell Park Memorial Institute Media
RRP	Readily Releasable Pool
RTK	Receptor Tyrosine Kinase
s	Seconds
SDS-PAGE	Sodium Dodecyl Sulfate Polyacrylamide Gel Electrophoresis
SH2	Src Homology 2 Domain
SH3	Src Homology 3 Domain
shRNA	Short Hairpin Ribonucleic Acid
pA	picoamp
PTEN	Phosphatase and Tensin Homolog
SNAP	Soluble NSF Attachment Protein
SNARE	SNAP Receptor Protein
STZ	Streptozotocin
T2D	Type 2 Diabetes
TCF7L2	T-cell specific, High Mobility Group box transcription factor
TEM	Transmission electron microscopy

TGX-221	7-methyl-2-morpholino-9-(1-(phenylamino)ethyl)-4H-pyrido[1,2-a]pyrimidin-4-one
TIRF	Total Internal Reflection Fluorescence
TUNEL	Terminal Deoxynucleotidyl Transferase dUTP Nick End Labeling
VAMP	Vesicle Associated Membrane Proteins
VAMP-pHlourin	VAMP tagged with pH-sensitive GFP
VGCC	Voltage Gated Calcium Channels
VIP	Vasoactive intestinal peptide
V	Voltage
Vm	Membrane Potential
WASP	Wiskott–Aldrich Syndrome Protein
WAVE	WASP-Family Verprolin-Homologous Protein
Wnt	Drosophila Melanogaster Wingless protein
Z-FIX	Zinc Formalin Fixative

LIST OF FIGURES

LIST OF TABLES

TABLE OF CONTENTS

Chapter 1

Introduction

1.1 OVERVIEW OF INSULIN SECRETION AND BETA CELL EXOCYTOSIS

1.1.1 The Pancreatic Beta Cell and T2D

In mammals, pancreatic beta cells constitute anywhere from 55-80% of the cells within the Islets of Langerhans (Cabrera et al., 2006). Murine islets tend to have a higher proportion of beta cells than human islets, 77% vs. 55% (Cabrera et al., 2006). Under physiological conditions, the beta cell, being pivotal to glucose homeostasis, senses rising blood glucose levels, and secretes insulin accordingly. Any sort of malfunction, or destruction of the beta cell, is associated with the pathological state of diabetes.

Type 2 diabetes (T2D), a metabolic disorder, characterized by high blood glucose levels and insulin resistance, is associated with varying degrees of beta cell dysfunction. Driven by an aging population and an increased prevalence of obesity, the incidence of T2D is rising at an alarming rate (Danaei et al., 2011; Herman and Zimmet, 2012; Shaw et al., 2010). It is estimated that by 2030 there will be a 69% increase in numbers of diabetics in developing countries and a 20% increase in developed countries (Shaw et al., 2010). The economic burden of this disease is increasing globally; in Canada the cost of diabetes is expected to rise from $6.3 billion annually in 2000 to $16.9 billion annually by 2020 (Canadian Diabetes Association, 2009).

Whilst it is essential to mention that beta cell dysfunction is only one factor contributing to the hyperglycemic state, the bulk focus of this thesis will be on signaling within the beta cell. A greater understanding of the signaling mechanisms by which beta cells secrete insulin will allow us to better understand the malfunctions that occur in disease state. This will allow us to manipulate signaling pathways to regulate secretion of insulin from the beta cells; which in turn may lead to better treatment options.

1.1.2 Beta Cell Stimulus Secretion Coupling

Similar to a neuronal cell, the pancreatic beta cell is electrically excitable and can produce action potentials following a depolarizing stimulus (Dean and Matthews, 1968; Dean and Matthews, 1970a; Dean and Matthews, 1970b). The resting membrane potential (Vm) of a beta cell lies close to -70 mV and is determined largely by a small outward K^+ conductance through the ATP-sensitive potassium (K_{ATP}) channel (Ashcroft and Rorsman, 1990; Doyle et al., 1998; Hille, 1992; Meissner and Schmelz, 1974). Various ion channels and transporters contribute to the regulation of beta cell membrane potential **(Figure 1)** (LeRoith et al., 2004).

During a fed state, when the extracellular glucose concentration rises above 5.5 mM, the threshold for initiation of electrical activity of the beta cell is reached, leading to depolarization, and subsequent bursts of action potential firing (Bokvist et al., 1991). The trigger for this series of events is facilitated glucose uptake into the beta cell through the glucose transporter 2 (GLUT2), which has a high capacity, but low affinity for glucose (Ashcroft and Rorsman, 1990; Bokvist et al., 1991). In human beta cells, GLUT1 and 3 are also involved, but the relative contribution of each is still under debate (McCulloch et al., 2011; Sechi and Wehland, 2000). Subsequent glucose metabolism by the beta cell leads to changes in the concentration of cytosolic adenine nucleotides. In particular, the elevation of intracellular concentration ratio of ATP to ADP leads to the closure of the K_{ATP} channel (Ashcroft and Rorsman, 1990; Bokvist et al., 1991; LeRoith et al., 2004). This decrease in the efflux of K^+ ions causes membrane depolarization to – 50 mV (Ashcroft and Rorsman, 1990; Bokvist et al., 1991; LeRoith et al., 2004), which subsequently activates voltage-gated calcium channels (VGCC) (Braun et al., 2008; Yang

and Berggren, 2006). The resulting increase in Ca^{2+} influx further depolarizes the beta cell, activates additional VGCC channels (and Na^{+} channels in human beta cells), initiates action potentials, and triggers insulin granule exocytosis (Ashcroft and Rorsman, 1989; Braun et al., 2008; Pressel and Misler, 1990; Rorsman et al., 2011). Action potentials are terminated by the opening of voltage-gated potassium (K_v) channels, and inactivation of VGCC channels (Ashcroft and Rorsman, 1989; Smith et al., 1990).

Figure 1: Ion channels and transporters involved in beta cell insulin excitability.

Figure 1 illustrates a number of key ion channels and transporters involved in beta cell insulin exocytosis. Glucose is transported from the extracellular space into the beta cell via a GLUT transporter (GLUT2 in rodent cells, GLUT1 and 3, in human cells.) Glucose is subsequently metabolized via the glycolytic pathway, and enters the mitochondria as pyruvate, where it is further metabolized by the mitochondria to generate ATP. This rise in cellular ATP levels leads to the closure of ATP-sensitive potassium (K_{ATP}) channels (which set the resting membrane potential, by passing a small outward positive current), and causes membrane depolarization. Membrane depolarization leads to the opening of voltage-gated calcium channels (VGCCs), which further leads to membrane depolarization, and subsequent rise in $[Ca^{2+}]_i$, which is the trigger for insulin granule exocytosis. Delayed activation of voltage-gated K^+ channels (along with inactivation of VGCCs) hyperpolarizes the beta cell membrane and returns the cell to resting potential.

Figure 1

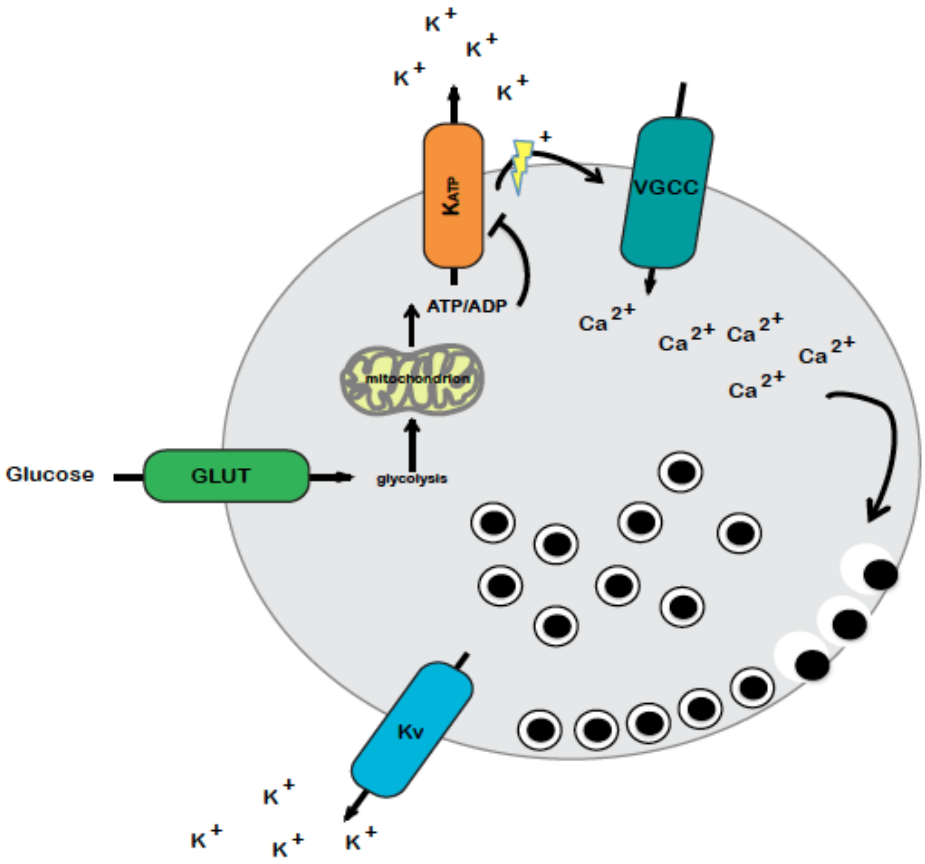
K+
K+
K+
K+
K+
KATP
VGCC
ATP/ADP
Ca2+
Ca2+
Ca2+
Ca2+
Ca2+
mitochondrion
Glucose
GLUT
glycolysis
Kv
K+
K+
K+
K+

1.1.3 Overview of Beta Cell Exocytotic Machinery

In the beta cell insulin is crystalized with zinc and calcium and packaged in large dense core vesicles (LDCV), generally termed secretory granules (Rorsman and Renström, 2003). Secretory granule exocytosis is a tightly regulated multistage process that requires transport, docking and priming of granules to the plasma membrane followed by membrane fusion and the subsequent release of the granule contents into the extracellular space (Ma et al., 2004; Rorsman and Renström, 2003). A large number of proteins that aid in this exocytotic process have been identified, and the key molecular machinery essential to exocytosis are members of the SNARE (soluble N-ethylmaleimide-sensitive factor attachment protein receptor) family of proteins (Kiraly-Borri et al., 1996; Regazzi et al., 1995; Wheeler et al., 1996). SNARE proteins are found both on the lipid membranes of secretory granules and the plasma membrane of the beta cell (Kiraly-Borri et al., 1996; Regazzi et al., 1995; Wheeler et al., 1996). Originally SNARE proteins that were found on the vesicle were termed v-SNAREs, and those found on target compartments were termed t-SNAREs. The SNARE proteins have recently been reclassified into R- and Q – SNARES, which is based on their structural features. R-SNAREs contribute an arginine residue to the formation of the SNARE complex, whilst Q-SNAREs contribute a glutamine residue (Gerst, 2003; Seino and Bell, 2008). In the beta cell, the fusion of insulin granules with the plasma membrane involves the assembly of the R-SNARE VAMP-2 (vesicle-associated membrane protein-2), and the plasma membrane associated SNAREs syntaxin-1 and SNAP-25 (Synaptosomal-associated protein-25) **(Figure 2)** (Rorsman and Renström, 2003; Seino and Bell, 2008; Wheeler et al., 1996). However, pancreatic beta cells contain numerous Syntaxin, VAMP and SNAP

isoforms, suggesting that additional SNARE complexes participate in the regulation of insulin secretion (Jacobsson et al., 1994; Sadoul et al., 1997; Spurlin and Thurmond, 2006; Wheeler et al., 1996). There are also a large number of accessory proteins (including Munc13, Munc18, and Tomosyn for example) that contribute to the formation of this core complex, and thereby regulate exocytosis (Gerst, 2003; Oh et al., 2012; Rossner et al., 2004; Saltiel and Pessin, 2007).

SNARE proteins regulate exocytosis by bringing the vesicular lipid membrane in very close contact to the plasma membrane of the cell. Whilst this was first identified in neuronal cells (Söllner et al., 1993a; Söllner et al., 1993b), beta cell SNARE proteins regulate exocytosis in the same manner (Jacobsson et al., 1994; Kiraly-Borri et al., 1996; Sadoul et al., 1995). Syntaxin-1 and SNAP-25 constitute an acceptor complex for VAMP-2, and form an extremely stable heterotrimeric complex (Poirier et al., 1998; Söllner et al., 1993a; Sutton et al., 1998). One α-helix from VAMP-2 and Syntaxin-1, and 2 α-helices from SNAP-25 intertwine in a Zipper-like manner to form a four-helix stable complex (Sutton et al., 1998). Under stimulatory conditions, the SNARE proteins change conformation, and interact in such a way that vesicles are forced down towards the plasma membrane and held tightly against the plasma membrane lipid bilayer; this allows for an intermediate fusion pore to form before vesicle exocytosis occurs (reviewed by Chen and Scheller, 2001).

Figure 2: Beta cell SNARE complex.

Figure 2 depicts the basic SNARE (soluble N-ethylmaleimide-sensitive factor attachment protein receptor) core complex proteins that are necessary for glucose-stimulated insulin secretion from the pancreatic beta cell. Syntaxin-1 and SNAP-25 are found on the plasma membrane, whilst VAMP-2 is found on the membrane of the beta cell. Vesicle fusion (such as the insulin containing Large Dense Core Vesicles (LDCV)) occurs when SNARE proteins change conformation, and vesicles are forced down towards the plasma membrane and held tightly against the plasma membrane lipid bilayer, which allows for an intermediate fusion pore to form before vesicle exocytosis occurs.

Figure 2

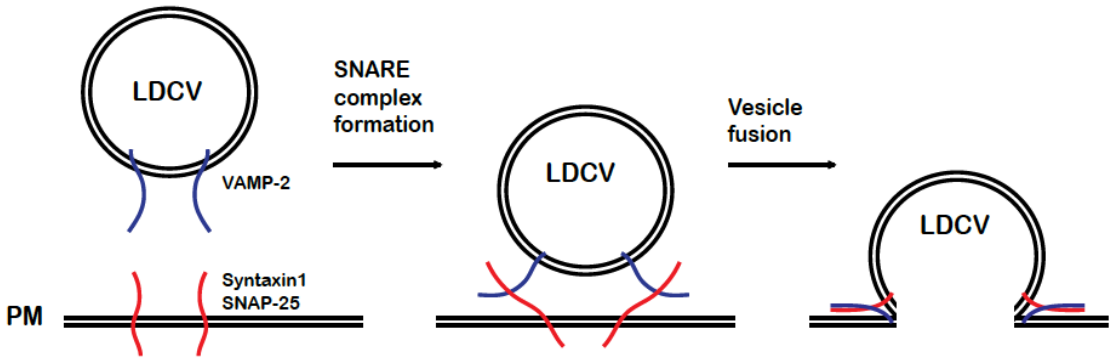
LDCV
VAMP-2
SNARE
complex
formation
LDCV
Vesicle
fusion
LDCV
Syntaxin1
SNAP-25
PM

1.1.4 Beta Cell Biphasic Insulin Secretion

Insulin secretion is bi-phasic (Barg et al., 2002; Curry et al., 1968; Heinemann et al., 1993; Henquin et al., 2002). The prompt generation of action potentials following a glucose stimulus (described above in section 1.1.2) is termed as the "first phase" of insulin secretion, and is generally well established. The first phase of insulin secretion is however limited by the small percentage (~ 1-5%) of insulin granules that form the "readily releasable pool" (RRP) (Neher, 1998; Rorsman and Renström, 2003; Wang and Thurmond, 2009). These granules, physically docked at the plasma membrane, are readily available for release. However, once the RRP has been depleted, the replenishment of this pool of granules becomes the rate-limiting step in insulin secretion. Thus in order to maintain sustained insulin secretion in response to a prolonged stimulus, a "second phase" follows. This second phase of insulin secretion involves both K_{ATP} channel-dependent pathway (because of the need for elevated intracellular Ca^{2+}) and additional signals from K_{ATP} channel-independent pathways) (Neher, 1998; Rorsman and Renström, 2003; Wang and Thurmond, 2009).

Ca^{2+} acts as a second messenger, activating numerous enzymes, and proteins, which maintain prolonged insulin release (Barclay et al., 2005; Dean and Matthews, 1970b; Neher, 1998; Rorsman and Renström, 2003). It is proposed that new insulin granules are mobilized from the "reserve pool" (RP) of granules in the cytosol, and trafficked to the plasma membrane to replenish the RRP (Rorsman et al., 2000). However, granules that belong to the RP are not immediately available for release once they reach the plasma membrane. They must undergo a series of events referred to as vesicle "priming". Vesicle priming involves chemical modifications of the granules,

which renders them readily releasable in response to a Ca^2 trigger (Henquin et al., 2002; Jackson and Chapman, 2006). Though still not fully understood, this priming involves the pairing of SNARE proteins on the plasma membrane and the SNARE proteins of the vesicle membrane (Barg et al., 2001; Hanson et al., 1997; Sutton et al., 1998). The priming process involves a number of key proteins including N-ethylmaleimide Sensitive Factor (NSF), Munc-13 and phosphatidylinositol-4-phosphate-5- kinase (PtdInsP5K) (Hay et al., 1995; Kang et al., 2006; Rossner et al., 2004; Wang and Thurmond, 2009). Despite years of research, the exact molecular mechanisms that underlie this second phase of secretion still remain unresolved.

1.1.5 Overview of Incretin Hormone Signaling

In 1906, gut secretions were hypothesized to contain a hormone that could regulate the "internal" secretion of the pancreas (Moore, 1906). The term "internal" was used to describe the endocrine function of the pancreas, as opposed to the exocrine or "external" function (Moore, 1906). By administering an extract obtained from the small intestine of the pig to patients with diabetes Moore *et al.* (2006) were able to decrease the amount of glycosuria (a prominent symptom of diabetes where excess glucose is excreted into the urine). This gut extract was purified in 1930, and named incretin (INtestine seCRETtion Insulin) (Moore, 1906; Vanhaesebroeck et al., 2010; Zunz and La Barre, 1930). However, the ability to reproduce these results over the next 10 years was not consistent, and thus the existence of the incretin hormone remained questionable (Loew et al., 1940). The existence of an incretin effect was forgotten until radioimmunoassays to measure insulin levels became available in the 1960s (Yalow and Berson, 1960). An oral glucose load was shown to result in much more insulin release than an intravenous

injection of glucose (Elrick et al., 1964; McIntyre et al., 1964). The hormones GIP (Glucose-Dependent Insulinotropic Polypeptide) and GLP-1 (Glucagon – Like Peptide-1) have since been identified as the incretin hormones that lower blood glucose levels by stimulating insulin secretion from the beta cell (Bell et al., 1983; Dupre et al., 1973; Kreymann et al., 1987; Schmidt et al., 1985; Taminato et al., 1977). Both GIP and GLP-1 mediate their incretin effect by binding to their respective 7-transmembrane domain G-protein coupled receptors (GIP-R and GLP1-R) (Dillon et al., 1993; Gremlich et al., 1995; Kapeller et al., 1994; Thorens, 1992; Wheeler et al., 1995). GPCR activation leads to the activation of adenylate cyclase, and subsequent rise in intracellular cAMP, which potentiates insulin secretion through the activation of protein kinase A (PKA) and Epac2 (exchange protein directly activated by cAMP) (Seino et al., 2009; Yabe and Seino, 2011). In addition to an increase in cAMP, GIP-R and GLP1-R activation has been linked to PI3K and MAP kinase activation (Buteau et al., 2001; Buteau et al., 1999; Kim et al., 2005; Kubota et al., 1997).

1.1.5a Glucose-Dependent Insulinotropic Polypeptide

Bioactive GIP is a 42 amino acid peptide secreted from the K-cells of mucosa of the duodenum and proximal jejunum. The half-life of GIP is relatively short due to its rapid degradation by the peptidase DPP-4 (Kieffer et al., 1995). GIP receptor mRNA is present in the pancreas, as well as numerous other tissues including: gut, adipose, heart, and various brain regions (Usdin et al., 1993). In addition to its incretin effect, GIP also promotes beta cell proliferation and survival, and stimulates proinsulin gene expression (Trümper et al., 2001). Furthermore, GIP stimulates glucagon secretion from the pancreatic alpha cells (Meier et al., 2003b).

To further validate the role of GIP signaling, GIP-R knockout mice (GIP-R-/-) were generated in 1999 (Miyawaki et al., 1999). These mice were shown to have higher blood glucose levels, with an impaired first phase of insulin secretion following an oral glucose load. Body weight and fasting blood glucose levels were not affected in these mice. These results showed the important role of GIP as incretin hormone, and confirmed that insulin secretion from the pancreatic beta cell is regulated not only by glucose and GLP-1 but also by GIP.

Despite the fact that T2D patients have normal, (or sometimes elevated serum levels of GIP) (Alssema et al., 2013; Meier and Nauck, 2010; Ross et al., 1977), GIP-induced insulin secretion is generally impaired in these individuals (Nauck et al., 1993b). Some T2D patients also have missense mutation in the GIP-R gene that causes a decreased cAMP response to GIP stimulation (Saxena et al., 2010; Thorens, 1992). This suggests a significant disturbance in the GIP entero-insular axis, and is thus one of the main reasons for which GIP administration is not used as a clinical treatment for T2D (Creutzfeldt et al., 1983; Miyawaki et al., 1999).

1.1.5b Glucagon – Like Peptide-1

GLP-1 (7-37) and GLP-1 (7-36)NH_2, are the biologically active forms of GLP-1, and are secreted from the enteroendocrine L-cells of the distal ileum and colon following a meal. In humans, the majority of bioactive GLP-1 is circulating in the GLP-1 (7-36)NH_2 form (Dhanvantari and Brubaker, 1998; Elliott et al., 1993; Sjölund et al., 1983). GLP-1 is a post-translational product of the proglucagon gene. Proglucagon can be processed differently in the L-cells (or alpha cells) to yield either GLP-1 or glucagon (Patzelt and Schiltz, 1984; Rouillé et al., 1994; Whalley et al., 2011). In particular,

prohormone convertase 1 (PC1) cleaves the proglucagon gene to GLP-1 in the L-cells (Whalley et al., 2011). Like GIP, the half-life of GLP-1 is relatively short due to its rapid metabolism and inactivation by the peptidase DPP-4 (Kieffer et al., 1995).

GLP-1 acts to stimulate glucose-induced insulin secretion following a meal, and inhibit glucagon secretion (Hare, 2010; Leech et al., 2011; MacDonald et al., 2002; Nauck et al., 1993b). By binding to its specific receptor, GLP-1 both stimulates insulin secretion, and induces insulin gene biosynthesis and transcription (Drucker et al., 1987; Fehmann and Habener, 1992). This stimulation of insulin gene biosynthesis and transcription is thought to prevent beta ell exhaustion. Some reports have also linked GLP-1 signaling to beta cell neogenesis, showing that Streptozotocin (STZ) -treated newborn rats had improved glucose homeostasis as adults if GLP-1 was administered shortly following STZ treatment (Tourrel et al., 2001). GLP-1 signaling is also linked to increased beta cell mass and decreased beta cell apoptosis (Drucker, 2003; Farilla et al., 2003; Li et al., 2003; Xu et al., 1999).

The role of GLP-1 as an essential incretin hormone was further validated with the generation of a GLP-1 receptor KO mouse model (GLP1R-/-) (Scrocchi et al., 1996). GLP1R-/- mice are normal in body weight, but exhibit fasting hyperglycemia, an impairment in glucose tolerance and decreased insulin secretion in response to either an oral, or intravenous glucose load (Scrocchi et al., 1996).

T2D patients generally show a significant reduction in the incretin effect, however the significance of this incretin effect and the underlying reason for this loss, remain controversial (Meier and Nauck, 2010; Nauck et al., 1993b; Nauck et al., 1986). The secretion of GLP-1 in T2D patients is quite complex, with some studies showing

significant reductions in circulating GLP-1 after mixed meal ingestion (Toft-Nielsen et al., 2001; Vilsbøll et al., 2001), and other studies showing no changes in in circulating GLP-1 (compared to non-diabetic patients) (Alssema et al., 2013; Meier and Nauck, 2008). In fact, circulating GLP-1 concentrations seem to be very variable between individuals, independent of their glycemic state (Meier and Nauck, 2008). However, unlike with GIP, exogenous administration of supra-physiological concentrations of GLP-1 normalizes hyperglycemia in T2D patients (Meier et al., 2003a; Nauck et al., 1993b). Thus, GLP-1 mimetics are used clinically as treatment of T2D.

1.2 ACTIN REMODELING AND ROLE IN INSULIN SECRETION

1.2.1 Structure of Actin

Actin is one of the most abundant proteins found in all eukaryotic cells, typically constituting about 5-10% of total cell protein (Holmes et al., 1990). W. D. Halliburton first observed actin experimentally in 1887 when he extracted a protein from muscle that seemed to be bound with myosin (Halliburton, 1887). He called this protein "myosin-ferment", but was unable to further identify its characteristics. Thus, it is Brúnó F. Straub who is officially credited for the discovery of actin in 1942, after he found a way to extract large amounts of relatively pure actin from muscle protein (Straub, 1943).

Actin is a 43 kDa protein, which exists in two forms: G-actin (globular) and F-actin (filamentous) (reviewed by Holmes, 2009). The first X-ray crystallography model of G-actin was shown by W. Kabsch and K. Holmes in 1990 (Holmes et al., 1990). Crystal structures of G-actin have since been shown independently over 30 times (reviewed by Reisler and Egelman, 2007). These crystal structures show that G-actin has a globular structure and that each of these globules consists of two individual lobes separated by a cleft. The cleft provides the binding sites for ATP or its hydrolyzed version ADP.

Filamentous actin is made up of polymerized G-actin monomers (reviewed by Dominguez and Holmes, 2011). Electron-microscopy has shown F-actin to be made of two parallel strands that are rotated 166 degrees to lie on top of each other (Graceffa and Dominguez, 2003; Reisler, 1993; Reisler and Egelman, 2007). This is the double helix structure that forms the microfilaments found in the cytoskeletons of cells (Graceffa and Dominguez, 2003; Reisler, 1993). However, because of its ever-changing dynamic state, researchers have had trouble with obtaining a detailed crystal structure of F-actin, and

have failed to capture the G-F actin transition state.

Actin filaments are polarized; they are characterized by a plus/barbed end (fast growing) and a minus end (slow growing) (reviewed by Disanza et al., 2005). The polymerization of G-actin into helical filaments involves the continuous hydrolysis of ATP at the barbed end. As Mg-ATP bound G-actin is incorporated into the growing filaments, the ATP is slowly hydrolyzed to ADP by actin's own ATPase activity. During the depolymerization stage, which occurs at the rear pointed end of the filament, ADP actin is released, and ATP-actin is subsequently regenerated. This term actin filament "treadmilling" is used to describe this steady-state mechanism of actin polymerization/depolymerization **(Figure 3)**.

Figure 3: Actin Treadmilling.

Figure 3 depicts the actin remodeling process. Actin exists in two forms; G-actin (globular) and F-actin (filamentous). G-actin globules consists of two individual lobes separated by a cleft which provides the binding sites for ATP, or its hydrolyzed version ADP. The polymerization of G-actin involves the continuous hydrolysis of ATP at the barbed (+) end. Actin has intrinsic ATPase activity, and thus incorporated ATP is slowly hydrolyzed to ADP at the (-) pointed end. The binding sites of various small molecules that disrupt or stabilize actin filaments are shown in red. Cytochalasins bind to and cap the barbed end of the actin filament, thus preventing incorporation of new G-actin monomers. Latrunculins bind and sequester G-actin monomers, thus preventing their binding to the F-actin filament. They can also directly cause disassembly of the filament. Both Jasplakinolide and phalloidins bind to F-actin and prevent disassembly at the pointed end. They also lower the dissociation rate constant for barbed-end actin, resulting in faster incorporation of G-actin monomers.

Figure 3

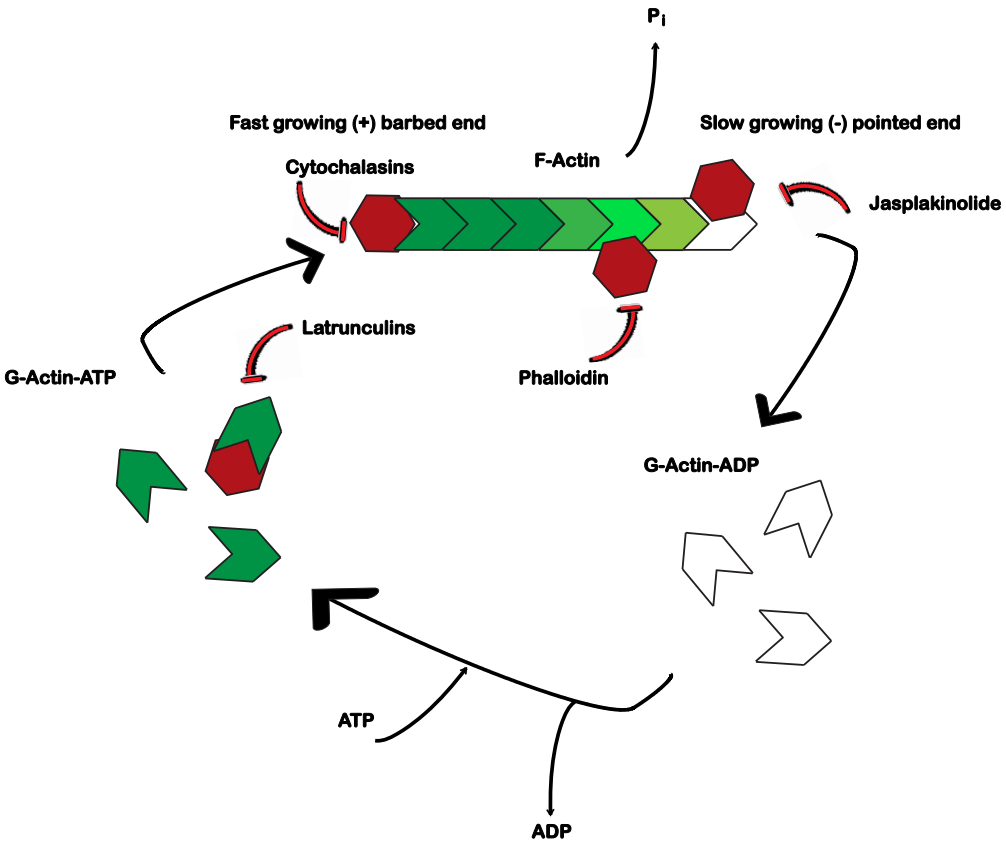
P_i
Fast growing (+) barbed end
Slow growing (-) pointed end
Cytochalasins
F-Actin
Jasplakinolide
Latrunculins
G-Actin-ATP
Phalloidin
G-Actin-ADP
ATP
ADP

1.2.2 Actin Binding Proteins Involved in Actin Remodeling

Numerous essential actin binding proteins (ABPs) that aid in the regulation of the actin remodeling process have been identified (Barroso et al., 2003; Hansen et al., 1997; Remedios and Chhabra, 2010). These proteins have many diverse functions including: stabilizing of G-actin, actin filament severing, capping of filament plus and minus ends, and actin monomer sequestration. A number of key ABPs are described in detail below.

1.2.2a Gelsolin

Gelsolin is a primarily cytosolic actin severing protein, which belongs to the family of actin severing and actin capping proteins (Janmey et al., 1985; Kinosian et al., 1998; Wegner et al., 1994). It is said to be the most potent actin filament severing protein identified to date. Once activated by Ca^{2+}, gelsolin binds to the side of an actin filament to initiate severing (Kinosian et al., 1998). In the pancreatic beta cell, gelsolin is thought to act as a positive regulator of glucose stimulated insulin secretion, as knock-down of gelsolin reduces glucose-stimulated insulin secretion, whereas gelsolin over-expression potentiates secretion from an insulin secreting cell line (Tomas et al., 2006; Vanhaesebroeck et al., 2010).

A mechanism by which gelsolin may have a role in insulin secretion has recently been proposed (reviewed by Kalwat and Thurmond, 2013). Gelsolin can bind to the N-terminus of the SNARE protein syntaxin-4 (Kalwat et al., 2012). Gelsolin remains bound to syntaxin-4 under basal (un-stimulated) conditions, and is dissociated upon acute glucose or KCl stimulation. Once dissociated from gelsolin, syntaxin-4 is free to complex with other exocytotic proteins (such as Munc13), and aid in insulin vesicle release.

1.2.2b ADF/cofilin and profilin

ADF/cofilin are a family of ubiquitously conserved proteins that aid in the depolymerization of actin and are generally involved in the recycling of actin monomers during processes involving rapid cytoskeleton turnover (Andrianantoandro and Pollard, 2006; Galkin et al., 2011; Pollard, 2007). These binding proteins, preferentially bind to the ADP-form of actin. They increase the rate of actin depolymerization by promoting the release of ADP-G actin from the barbed ends. In contrast, another protein, profilin, binds preferentially to the ATP-actin form and promotes actin growth (Goldschmidt-Clermont et al., 1990; Kang et al., 1999; Pollard et al., 2000). It catalyzes the exchange of ADP for ATP, and thus increases the association of the ATP-bound-profilin-actin complex at the barbed ends.

1.2.2c Arp2/3 complex

Another important set of ABPs, the Arp2/3 complex, is involved in both the growth and branching of actin filaments (Machesky et al., 1994; Robinson et al., 2001). The Arp2/3 complex stimulates actin polymerization by creating a new nucleation core (Galletta et al., 2008; Machesky et al., 1994; Robinson et al., 2001). It is also capable of inducing the formation of daughter filaments. How exactly this occurs is still unknown, but two theories have been proposed. One suggests that branching occurs at the sides of the pre-existing filaments, whilst the other suggests that this branching is only possible at the barbed ends (Disanza et al., 2005; Fischer and Fowler, 2003). The major activators of Arp2/3 complex are, however, known. They are proteins of the WASP (Wiskott-Aldrich syndrome protein) and WAVE (WASP family verprolin-homologous) families (Machesky and Insall, 1998; Machesky et al., 1999; Rohatgi et al., 1999). They contain a

conserved C-terminal (VCA) domain that helps bring together the Arp2/3 complex with the actin monomers, thereby aiding in polymerization.

1.2.3 Small Molecules That Disrupt or Stabilize Actin Filaments

Compounds that inhibit actin polymerization, cause actin depolymerization or compounds that stabilize actin filaments and thus prevent actin depolymerization are very useful in the laboratory setting (reviewed by Fenteany and Zhu, 2003). A few of the key actin-disrupting and actin-stabilizing molecules are described in more detail below and in **Figure 3** above.

1.2.3a Cytochalasins

The cytochalasins are the most well studied actin-disrupting small molecules. Cytochalasin D, for example, is a fungal toxin that has been used for decades to study motility-related phenomena in a number of different cell types (reviewed by Fenteany and Zhu, 2003). This toxin has a number of profound effects on cell morphology and motility (Cooper, 1987; Goddette and Frieden, 1986a; Goddette and Frieden, 1986b). Electron microscopy studies have indicated that Cytochalasin D binds to the barbed end of actin filaments (as opposed to the pointed end) and inhibits both the association and dissociation of actin monomers (reviewed by Fenteany and Zhu, 2003; Schliwa, 1982). Cytochalasin D is a useful tool in the laboratory setting as it has a high affinity for the barbed end of actin filaments (Kd = 2 nM), and thus possible off target effects like inhibition of protein synthesis can be controlled by using low concentrations (Cooper, 1987; reviewed by Fenteany and Zhu, 2003; Goddette and Frieden, 1986a; Goddette and Frieden, 1986b). Cytochalasin B, which acts in a very similar manner to Cytochalasin D, has also been used frequently in the laboratory setting, but because it may have more off

target effects (may inhibit monosaccharide transport), it is less desirable (Dancker and Löw, 1979).

1.2.3b Latrunculins

The Latrunculins are macrolide toxins produced by marine sponges. They have an advantage over the cytochalasins because they tend to be more potent, and have a simpler mechanism of action (reviewed by Fenteany and Zhu, 2003). Latrunculin A was first isolated from *Negombata magnifica* (The Red Sea Sponge), and was identified as an inhibitor of actin polymerization based on its structure, and the effects it had on actin filament distribution in cultured cells (Spector et al., 1989; Spector et al., 1983). The binding site of Latrunculin A has still not been conclusively identified, but it likely resides on the nucleotide-binding cleft of actin. Certain mutations in the actin gene near the nucleotide-binding cleft of actin, provide resistance to the actions of Latrunculin A (Ayscough et al., 1997). The main actin depolymerizing mechanism of Latrunculin A is its ability to sequester actin monomers. The Latrunculin A/actin complex shows a conformational change in G-actin, which disfavors polymerization (Morton et al., 2000). The mechanism of action of Latrunculin B is identical to those of Latrunculin A, apart from it being slightly less potent (Spector et al., 1989). It is thought that Latrunculin B can be inactivated in the prolonged presence of serum; but for this reason Latrunculin B may have fewer side effects, and is quite useful in shorter term studies (Spector et al., 1989).

1.2.3c Phalloidin

Phalloidin was first crystalized in 1937 by the German biochemist Feodor Lynen (Lynen, 1937). Phalloidin belongs to the group of poisonous mushroom (*Amanita*

phalloides) isolated phallotoxins (Wieland and Faulstich, 1978). It stabilizes actin filaments by preferentially binding to actin filaments, rather than actin monomers. The monomer to filament equilibrium is also shifted by phalloidin in favor of the filament form because the critical concentration for polymerization is lowered by 10-30 fold (reviewed by Cooper, 1987). The binding site of phalloidin is shown to be adjacent to the ATP binding site, and is thought that the two sites share certain residues; and thus overlap (Barden et al., 1987). However, once the monomers have combined to form filamentous actin, they are generally unable to dissociate, and thus phalloidin will essentially poison the cell. In the laboratory setting phalloidin use is generally restricted to non-living cells. Its use in non-living cells is also limited by its inability to permeate cell membranes (reviewed by Cooper, 1987). However, the properties of phalloidin make it a very useful tool for imaging experiments for visualization of F-actin in non-living cells. Fluorescent derivatives of phalloidin have been generated and the fluorescence generated can be used as a quantitative measurement of the amount of F-actin actin present (Wehland and Weber, 1981; Wulf et al., 1979).

1.2.3d Jasplakinolide

Jasplakinolide was first isolated from the marine sponge *Jaspis johnstoni* in 1987 (Braekman et al., 1987), but did not become commercially available until the late 1990s due to numerous synthesis problems (Chu et al., 1991; Holmes, 2009; Kahn et al., 1991). Jasplakinolide specifically targets F-actin and enhances the rate of actin filament nucleation, thus stabilizing actin filaments (Bubb et al., 1994). Jasplakinolide is known to compete with phalloidin for binding to actin, and is said to have a slightly higher affinity for actin over phalloidin (Bubb et al., 1994). However, its mechanism of action on actin

filaments is far less understood than that of phalloidin (Bubb et al., 1994). In addition, unlike phalloidin, it is cell permeable and can thus be used on live cells, making it very useful in the laboratory setting (reviewed by Fenteany and Zhu, 2003).

1.2.4 Actin in the Beta Cell

In the 1970s, Orci *et al.* discovered the presence of microfilamentous structures in individual beta cells, and found that isolated insulin-containing granules generally co-sedimented with F-actin (Orci et al., 1972). Electron microscopy-based ultrastructural analysis showed F-actin to be organized as "a dense web beneath the plasma membrane" (Orci et al., 1972). On the basis of this, it was hypothesized that F-actin acts as a barrier to the movement of insulin containing granules to the plasma membrane. Early experiments showed that certain clostridial toxins and cytochalasins, which disrupt the F-actin structure, also increase secretagogue-induced insulin secretion (Lacy et al., 1973; Orci et al., 1972; Wang et al., 1990). These were the first reports that linked the cytoskeleton to having a negative role in insulin secretion.

However, these results were later confounded by research ascribing a positive role for F-actin in insulin secretion, thereby raising controversy in regards to the role of F-actin in insulin granule mobilization (Li et al., 1994; Stutchfield and Howell, 1984; Swanston-Flatt et al., 1980). Using a DNase 1 inhibition assay (Blikstad et al., 1978). Swanston-Flatt *et al.* showed that exposure of mouse islets to high glucose was associated with a significant increase in polymerized actin (Swanston-Flatt et al., 1980). In 1984 Stutchfield *et al.* showed that permeabilized rat islets treated with phalloidin showed enhanced calcium-stimulated insulin secretion (Stutchfield and Howell, 1984). Li *et al.* showed that disruption of F-actin using *Clostridium botulinum* C2 toxin reduced both

glucose and forskolin-stimulated insulin secretion in a hamster insulin secreting cell line (Li et al., 1994). Thus, these authors suggested that an increase in actin polymerization might be a trigger for increased insulin secretion from the beta cell.

Improved techniques in microscopy, and better actin probes have allowed for the imaging of live cells, thus showing time-dependent changes in secretagogue induced F-actin remodeling (Ivarsson et al., 2005; Kalwat and Thurmond, 2013; Riedl et al., 2008). Glucose is shown to induce remodeling of F-actin in both primary beta cells and clonal beta cell lines, and this promotes insulin granule mobilization to the plasma membrane (Nevins and Thurmond, 2003; Thurmond et al., 2003; Tomas et al., 2006). This glucose induced remodeling of F-actin involves a precise, concerted and localized cycle of F-actin depolymerization and polymerization across the cell membrane (reviewed by Kalwat and Thurmond, 2013). Thus, the confounding results seen in previous studies were merely an artifact of the cyclic nature of actin remodeling, limited imaging techniques, and off-target effects of pharmacological agents used.

1.2.5 Involvement of Rho-family GTPases

A number of studies suggest that the key to the glucose induced remodeling of F-actin in the pancreatic beta cell lies in two Rho family GTPase proteins: cell division control protein 42 homolog (Cdc42) and Ras-related C3 botulinum toxin substrate 1 (Rac1) **(Figure 4)** (reviewed by Bishop and Hall, 2000; Isgandarova et al., 2007; reviewed by Kalwat and Thurmond, 2013; Li et al., 2004). The Rho family of GTPase proteins belongs to the Ras superfamily, which is composed of more than 50 members (reviewed by Wennerberg et al., 2005). These proteins exist in two conformations: an active GTP-bound form, and an inactive GDP-bound form (reviewed by Bustelo et al.,

2007). The inactive form is sequestered in the cell cytosol, whilst the active form is normally localized at the plasma membrane. Guanine nucleotide Exchange Factors (GEFs) catalyze the replacement of GDP by GTP, and thereby activate signaling. GTPase Activating Proteins (GAPs), on the other hand, accelerate the intrinsic GTPase activity, thereby favoring the GDP bound form and leading to an inactivation of signaling. In addition, a second level of regulation is provided by GDI proteins (Guanine Dissociation Inhibitors), which act by binding to the GDP form of the protein, and prevent the action of GEFs. These proteins also prevent the translocation of the GTPase to the plasma membrane (the biologically active site of the proteins).

1.2.5a Cdc42

Cdc42 is a protein involved in the regulation of the cell division cycle, and is also involved in a number of diverse cellular functions including cell morphology, migration, endocytosis and cell cycle progression (reviewed by Heasman and Ridley, 2008). In the beta cell, under basal conditions, Cdc42 is sequestered in the cytosol (primarily found on insulin-containing granules) in its inactive form, through interaction with Caveolin-1 (a GDI protein) (Nevins and Thurmond, 2006). About three minutes upon glucose stimulation the complex dissociates and Cdc42 translocates to the plasma membrane (Jayaram et al., 2011; Nevins and Thurmond, 2003; Wang et al., 2007). Various mutant forms of Cdc42 that prevent cycling of Cdc42 from the GDP to the GTP bound state also prevent the cortical F-actin reorganization seen upon beta cell glucose stimulation (Nevins and Thurmond, 2003). siRNA-mediated knockdown of Cdc42 also impairs glucose-stimulated insulin secretion from the beta cell; in particular the second phase of insulin secretion is affected (Wang et al., 2010; Wang et al., 2007). Cdc42 is known to be

involved in actin remodeling through interaction with nucleation promoting factors and the Arp2/3 complex (Carlier et al., 1999; Uenishi et al., 2013), however the complete signaling cascade that mediates Cdc42 induced remodeling of F-actin remains to be discovered.

1.2.5b Rac1

Rac1 is a 21-kDa Rho family GTPase that has been implicated in insulin secretion (Asahara et al., 2013; Li et al., 2004). Rac1 has numerous actions in other cell types including the control of cell growth, cytoskeletal reorganization, and the activation of protein kinases (reviewed by Heasman and Ridley, 2008). Rac1 is activated downstream of Cdc42 in response to glucose stimulation in insulin secreting cells (Li et al., 2004; Wang et al., 2007). shRNA-mediated knockdown of Cdc42 blocks glucose-induced Rac1 activation. This is not due to a decrease in Rac1 expression, but is rather due to a failure of Rac1 to become activated at the plasma membrane.

In the beta cell, Rac1 is activated and translocated to the plasma membrane within 15 minutes of glucose stimulation (Li et al., 2004). INS-1 cells (a rat insulin secreting cell line) expressing dominant-negative mutations of Rac1 are smaller, and tend to have less lamellipodia, compared to control INS1 cells (Li et al., 2004). F-actin staining in these cells is almost non-existent, and glucose-stimulated insulin secretion (GSIS) is significantly reduced, (with no effect on membrane potential or intracellular Ca^{2+}). However, INS-1 cells expressing a dominant-active form of Rac1, or wild type Rac1 do not have impairments in GSIS, nor do they show major morphological changes or F-actin staining. Thus this study implicates a role for the dominant-negative form of Rac1 in F-actin organization and GSIS.

Asahara *et al.* further implicate Rac1 in GSIS and actin remodeling *in vivo* and *in vitro* (Asahara et al., 2013). Heterozygous pancreatic beta cell-specific Rac1-knockout (betaRac1-/-) mice have an impaired oral glucose tolerance test (OGTT). This is due to an impairment of insulin secretion in response to glucose from isolated islets. shRNA mediated knockdown of Rac1 in INS-1 cells also impairs GSIS. Furthermore, Rac1 knockdown in INS-1 cells blocks glucose stimulated F-actin depolymerization, and limits insulin granule recruitment to the plasma membrane; whilst forced depolymerization of F-actin by Latrunculin B restores GSIS in these cells. This study demonstrated the importance of Rac1 activation in promoting insulin secretion via depolymerisation of F-actin.

Figure 4: Involvement of Rho-family GTPases in Actin Remodeling.

Rac1 and Cdc42 exist in two conformations: an active GTP-bound form, and an inactive GDP-bound form. The inactive forms are sequestered in the cell cytosol by GDI (Guanosine nucleotide dissociation inhibitor) proteins. About three minutes upon glucose stimulation Cdc42 is activated. Cdc42 activation can activate PAK 1 (a serine/threonine-protein kinase). PAK 1 can also be activated by PKA (Protein Kinase A). PAK 1 activation promotes the activation of Rac1 (amongst numerous other effectors), and facilitates actin remodeling. Furthermore, PKA can directly activate Rac1 by activation of Rac GEFs (Guanine nucleotide exchange factors)

Figure 4

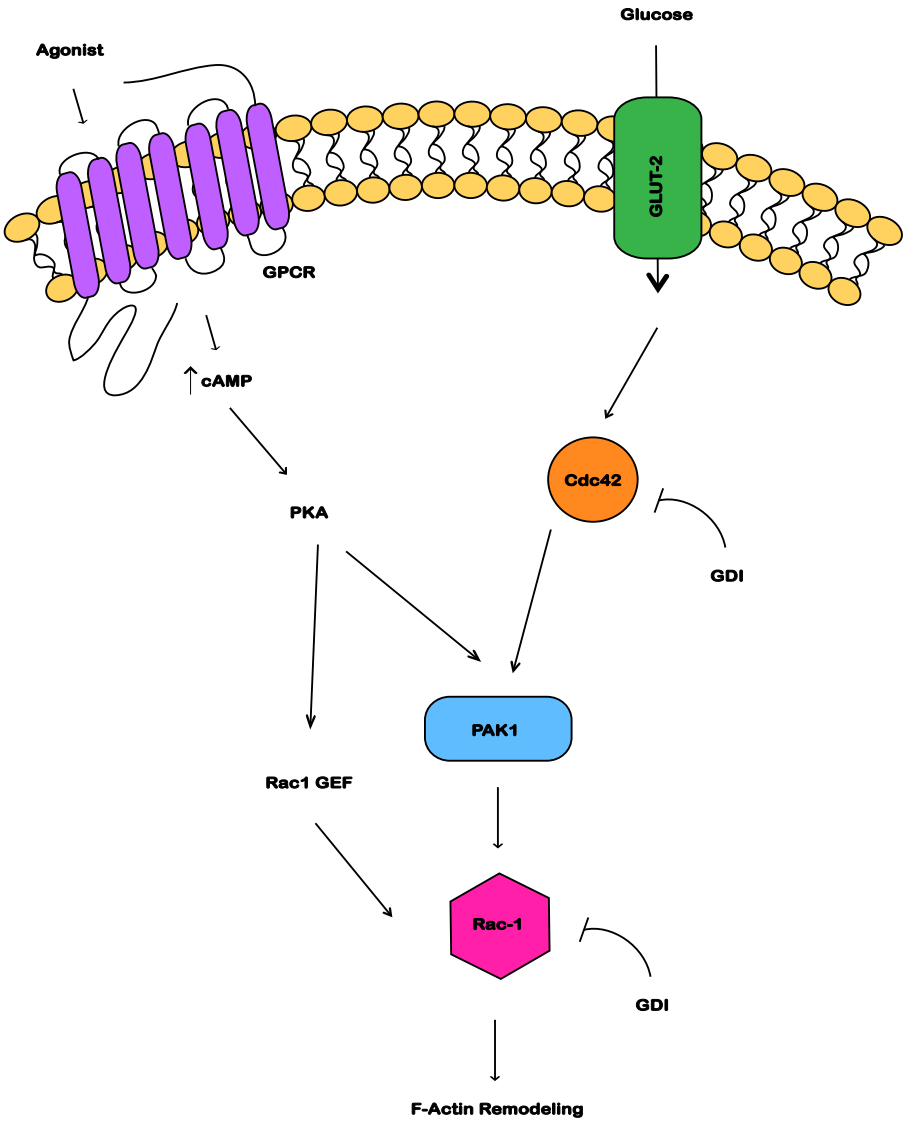
Glucose
Agonist
GLUT-2
GPCR
cAMP
Cdc42
PKA
GDI
PAK1
Rac1 GEF
Rac-1
GDI
F-Actin Remodeling

1.3 PHOSPHATIDYLINOSITOL 3-OH KINASE SIGNALING

1.3.1 Overview of Phosphatidylinositol 3-OH Kinase Signaling

Phosphatidylinositol 3-OH kinases (PI3Ks) are a family of enzymes that are involved in a number of essential cellular processes including: cell proliferation and growth, cell motility, cytoskeletal remodeling, and intracellular trafficking (reviewed by Vanhaesebroeck et al., 2012). PI3Ks are also been strongly implicated in influencing insulin secretion from the pancreatic beta cell (Dominguez and Holmes, 2011; Eto et al., 2002; Kaneko et al., 2010; Zawalich et al., 2002). Several PI3K polymorphisms have been associated with an increased risk in T2D (Barroso et al., 2003; Hansen et al., 1997). Furthermore, the non-specific PI3K inhibitors wortmannin and LY294002 have been known to increase insulin secretion for many years further implicating PI3K signaling in insulin secretion (Hagiwara et al., 1995; Nunoi et al., 2000; Zawalich et al., 2002).

PI3K signaling is opposed by the actions of phosphatase and tensin homolog (PTEN) (Song et al., 2012). PTEN is a phosphatase enzyme found in almost all tissues of the body; its main function is to act as a tumor suppressor gene (Song et al., 2012). Its specific function is to catalyze the dephosporylation of the 3` phosphate of the inositol ring in phosphatidylinositol 3,4,5-trisphosphate (PIP_3), resulting in phosphatidylinositol 4,5-bisphosphate (PIP_2) production (Song et al., 2012).

The focus of this thesis is on the class 1 PI3Ks (also known as PIK3C), which are responsible for the production of PIP_3 from PIP_2 (reviewed by Vanhaesebroeck et al., 2010; Whitman et al., 1988). Class I PI3Ks phosphorylate PIP_2 at the 3 position of the inositol ring **(Figure 5)** (Gunn and Hailes, 2008; Whitman et al., 1988). The product PIP_3, functions as a second cellular messenger that controls a number of cellular

processes described above. Class I PI3Ks are obligate heterodimeric proteins consisting of a p110 α, β, δ, or γ catalytic subunit, and a wide variety of regulatory subunits (reviewed by Fruman, 2010; Fruman et al., 1998). The regulatory (or adapter subunits) can influence the subcellular location and activity of the catalytic subunit (reviewed by Fruman, 2010; Fruman et al., 1998). The regulatory subunits also have functions that are independent of their role in regulating PI3K activity (reviewed by Jean and Kiger, 2014).

It is important to mention that 2 other classes of PI3Ks exist (class II or PI3KC2 and class III or PI3KC3); they are differentiated from the class I PI3Ks by their structure and function, as well as product and substrate specificities (reviewed by Jean and Kiger, 2014). Only class I PI3Ks are known to use PIP_2 to generate PIP_3. Class II PI3Ks can produce the 3,4-bisphosphate and the 3-monophosphate of inositol lipids, whilst and class III can only make the 3-monophosphate (Zhao and Vogt, 2008a). Both class I and II PI3Ks are expressed in pancreatic beta cells, and have been implicated in the regulation of insulin secretion (Dominguez and Holmes, 2011; Kaneko et al., 2010). Whether class III PI3K signaling has a role in pancreatic beta cell insulin secretion has not been explored, however Vps34, (the only known class III PI3K) has been shown to play a role positive role in autophagy in adult rat islets (Liu et al., 2013).

Figure 5: Phosphatidylinositol (3,4,5)-triphosphate production.

Phosphatidylinositols are a family of phospholipids with a glycerol backbone, two non-polar fatty acid tails, and a phosphate group on the 1' position of the inositol ring. The inositol ring can be further phosphorylated by a number of different kinases on the 3', 4' and/or 5' hydroxyl group positions. (The two and six hydroxyl groups are typically not phosphorylated due to steric hindrance). Class 1 PI3Ks primarily prefer (PIP_2) Phosphatidylinositol 4,5-bisphosphate $PI(4,5)P_2$ substrates. Class 1 PI3K phosphorylates the 3' position of the inositol ring to generate Phosphatidylinositol 3,4,5-trisphosphate (PIP_3). PI3K signaling is opposed by the actions of PTEN, which dephosphorylates the 3` phosphate of the inositol ring in PIP_3.

Figure 5

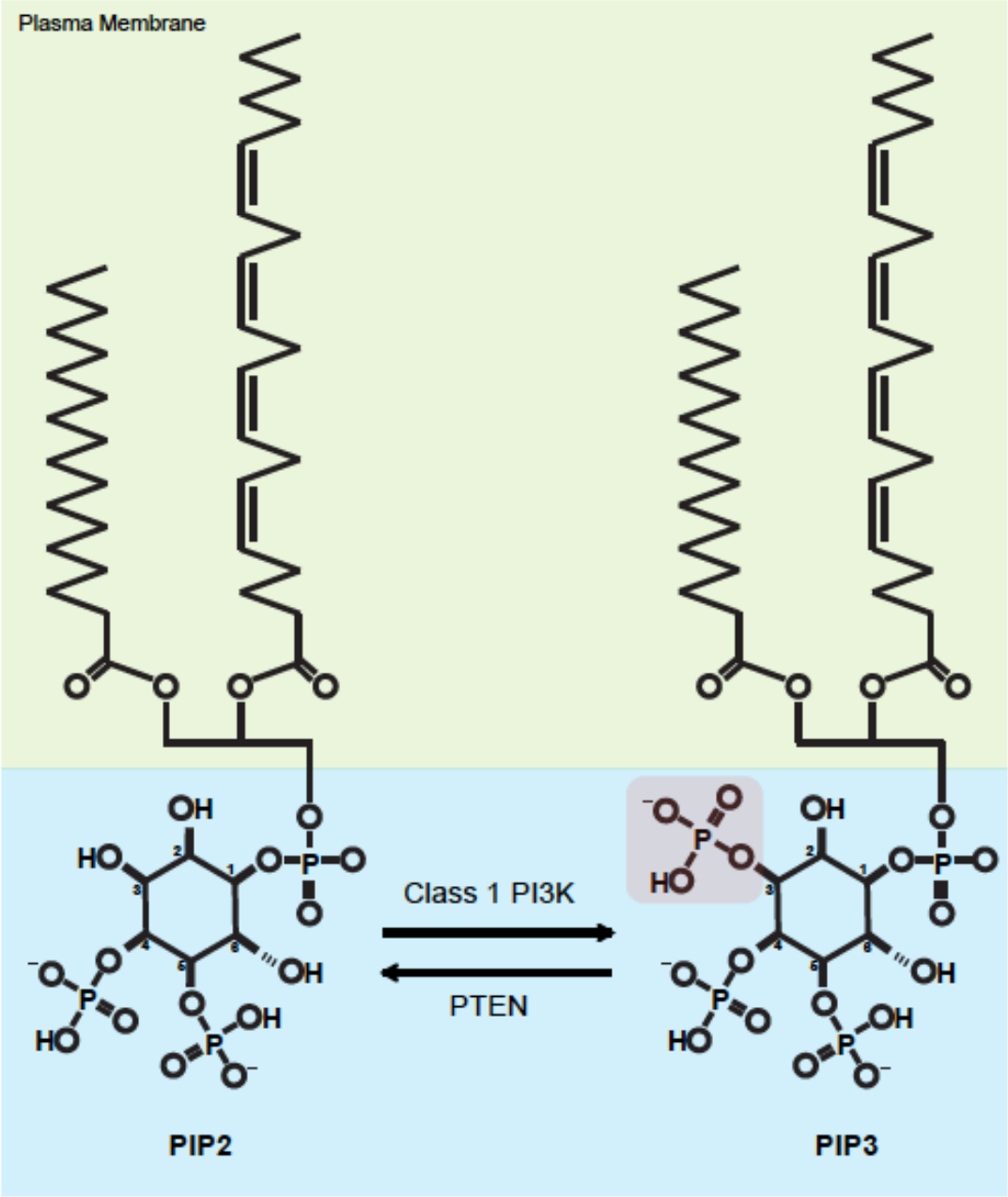

1.3.2 Class 1 PI3Ks

Class I PI3Ks are further subdivided between IA and IB subsets. In mammalian cells three genes (PIK3CA, PIK3CB and PIK3CD) encode for the catalytic subunits of class IA PI3K enzymes PI3Kα, PI3Kβ and PI3Kδ, respectively. PIK3CG encodes for the lone Class 1B PI3K isoform PI3Kγ (reviewed by Vanhaesebroeck et al., 2012).

Class 1A PI3Ks bind to a p85 (or the truncated p50/55) regulatory subunit, whilst Class1B bind to a p101 or p87 regulatory subunits (reviewed by Vanhaesebroeck et al., 2012; Vanhaesebroeck et al., 2001). Because p85 can bind to a phosphorylated tyrosine in a specific amino sequence (whilst p101 and p87 cannot), the main distinction between IA and IB subsets was originally thought to be correlated with the capacity to be activated by tyrosine kinase receptors (Vanhaesebroeck et al., 2001). Class IA PI3Ks are primarily activated by cell surface receptor tyrosine kinases (RTKs), (such as the insulin receptor), whilst class IB are activated by G-protein coupled receptors (GPCRs). Whilst this classification is still widely accepted, recent evidence suggests that p110β may be activated by a GPCR, either directly through Gβγ protein subunits, or by the small GTPase protein Ras (Vanhaesebroeck et al., 2010).

Activation of PI3Kβ by G-protein coupled receptors has previously been reported (Hazeki et al., 1998; Maier et al., 1999; Murga et al., 2000; Roche et al., 1998). Whilst knocking out PI3Kβ in mice does not affect AKT phosphorylation in response to insulin and epidermal-like growth factor, AKT phosphorylation is decreased in response to the G-protein activation ligand lysophosphatidic acid (LPA) in cells lacking p110β (Ciraolo et al., 2008).

Ras is activated both by RTKs and GPCRs (Crespo et al., 1994; Lopez-Ilasaca et

al., 1997; Margolis and Skolnik, 1994). Some evidence has been put forth suggesting that p110α may also be activated by Ras, thus suggesting that class1A PI3Ks may be more influenced by GPCRs than previously thought (Vanhaesebroeck et al., 2010; Vanhaesebroeck et al., 2012) **(Figure 6)**. In addition, Ras may have some role in the activation of p110γ, thus suggesting that RTKs activation may have some indirect role in the activation of class 1B PI3Ks (Kurig et al., 2009; Pacold et al., 2000).

1.3.3 Class 1A PI3K Structure

PI3Kα and – β are ubiquitously expressed, whilst PI3Kδ is restricted to cells of the immune system (leukocytes) (Vanhaesebroeck et al., 2010; Vanhaesebroeck et al., 2012). The catalytic subunits of class IA PI3Ks consist of several domains including: an N-terminal adaptor binding domain (ABD), a Ras binding domain (RBD), a C2 domain, a helical domain (HD) (also known as a phosphatidylinositol kinase homology (PIK) domain), and a C-terminal catalytic kinase domain (Vanhaesebroeck et al., 2010; Vanhaesebroeck et al., 2012). The ABD is the binding site of the regulatory subunit. The RBD is the binding site of the small GTPase protein Ras. Ras binding to the RBD directly activates PI3K, and is shown to affect cell growth and proliferation (reviewed by Castellano and Downward, 2011). The C2 domain acts as a calcium-dependent (or sometimes calcium-independent) phospholipid-binding motif, and is important for PI3K binding to the phospholipid membrane. The helical domain of PI3Ks seems to be preserved between all three classes, however no clear function has been ascribed to this region. A few studies have however shown that certain point mutations in this region of the PI3Kα catalytic subunit can induce a gain of function mutation, indicating that the HD may have some role in catalysis (Zhao and Vogt, 2008b; Zhao and Vogt, 2010). The

catalytic kinase domain is the site of ATP binding, and phosphorylation of PIP_2 (Zhao and Vogt, 2008b; Zhao and Vogt, 2010).

The catalytic subunits of the class IA PI3Ks form heterodimers with specific regulatory subunits (Vanhaesebroeck et al., 2010; Vanhaesebroeck et al., 2012). For class 1A PI3Ks in particular, these regulatory subunits are restricted to one of five Src-homology 2 (SH2) domain- subunits; p85α, p85β, p55α, p55γ and p50α. The regulatory subunits are responsible for the activation and subcellular localization of the catalytic subunits, but do not possess an intrinsic enzymatic activity. Whilst they provide thermal stability to the catalytic subunit, they also suppress the catalytic subunit's activity under non-stimulated conditions (Vanhaesebroeck et al., 2010; Yu et al., 1998).

Like the catalytic subunits, the regulatory subunits are composed of several domains including: an N-teminal src-homology 3(SH3) domain, a breakpoint cluster region-homology domain (BCH) between two proline rich regions, and two C-terminal SH2 domains separated by a an inter-SH2 (iSH2) region, which is the binding site for the ABD of the catalytic subunit (Ashcroft and Rorsman, 1990; Bokvist et al., 1991; LeRoith et al., 2004; Vanhaesebroeck et al., 2010; Yu et al., 1998). The shorter (p50/55) regulatory subunits lack the SH3 and BCH domains (Pons et al., 1995; Yu et al., 1998).

The SH3 domain mediates protein-protein interactions by binding to proline rich segments of target proteins (including the proline rich segments of its own regulatory subunit) (Kapeller et al., 1994; Yu et al., 1998). The BCH has GTPase-Activating Protein (GAP) activity and interact with Cdc42 and Rac but not with Rho *in vitro* (Vanhaesebroeck et al., 2010; Vanhaesebroeck et al., 2012). The SH2 domains are essential to the activation of class IA PI3K by RTKs (Engelman et al., 2006). They bind

to phospho-tyrosine residues on activated RTKs (or adapter molecules such as the insulin receptor substrate IRS1). This binding of the SH2 domain to RTKs relieves the basal inhibition of the catalytic subunit, and recruits the PI3K heterodimer to its PIP_2 substrate at the plasma membrane (Engelman et al., 2006).

1.3.4 Class 1B PI3K Structure

The catalytic subunit structure of lone class 1B PI3K isoform PI3Kγ is very similar to that of the class 1A PI3K (reviewed by Vanhaesebroeck et al., 2010). Like the class 1A PI3K catalytic subunits, p110γ has an N-terminal RBD, a C2 domain, a PIK domain, and a C-terminal catalytic domain (reviewed by Vanhaesebroeck et al., 2010). These domains are homologues between classes and thus have identical functions to the ones described above. The catalytic subunit of PI3Kγ however, lacks the p85 N-terminal adaptor-binding domain. Instead, Class 1B PI3K is a heterodimer consisting of a p101 regulatory subunit and a p110γ catalytic subunit.

The p101 adapter subunit of PI3Kγ binds to the Gβγ subunit of GPCR and, thereby, recruits the catalytic p110γ subunit to the plasma membrane. Both p110γ and p101 have been shown to be able to bind to Gβγ *in vitro*, however p101 binds to Gβγ with 5-fold higher affinity (Stephens et al., 1997; Voigt et al., 2005), and *in vivo*, when both subunits are present, the p101 subunit has shown to be essential for to Gβγ - mediated activation of PI3Kγ (Voigt et al., 2005).

The p101 regulatory subunit is distinct from p85 (or any other known proteins), but despite its crucial role in the activation of p110γ, its structure is still not well understood (Voigt et al., 2005). It is thought that the binding site for p110γ is found near

the N-terminus of p101, whilst binding of Gβγ is mediated by a C-terminal domain (Voigt et al., 2005). This was determined by constructing different deletion mutants of p101, and assaying their ability to bind to either p110γ or Gβγ (Voigt et al., 2005). Both domains are required for GPCR activation of PI3Kγ, as the deletion of either one leads to compete loss of PI3Kγ activity (Voigt et al., 2005).

It is important to mention that the catalytic subunit of PI3Kγ may also interact with p87 (instead of p101). The p87 regulatory subunit was first identified in 2006, and has been shown to be highly expressed in the heart (by contrast p101 expression in the heart is very weak) (Voigt et al., 2006). Similarly to p101, p87 interacts with p110γ and Gβγ, but even less is known about its structure (Voigt et al., 2006). In addition, p87 is also involved in the regulation of PDE3B (a phosphodiesterase with important roles in regulating heart and vascular smooth muscle) (Voigt et al., 2006). **Figure 6** depicts the structure of class1 PI3K catalytic and regulatory subunits.

Figure 6: Structure of class 1 PI3K Isoforms and PTEN.

Figure 6 depicts the structure of the catalytic and regulatory subunits of both class 1A and class 1B PI3K isoforms. The function of each domain depicted is described in detail in the text above.

Figure 6

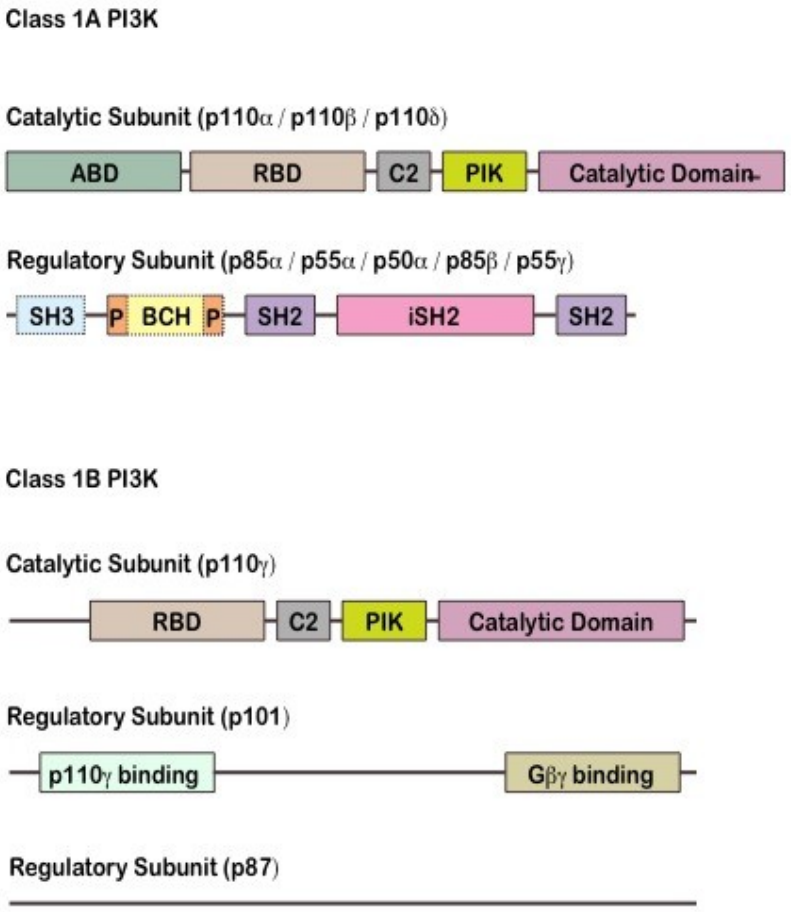
Class 1A PI3K
Catalytic Subunit (p110α / p110β / p110δ)
ABD
RBD
C2
PIK
Catalytic Domain
Regulatory Subunit (p85α / p55α / p50α / p85β / p55γ)
SH3
P
BCH
P
SH2
iSH2
SH2
Class 1B PI3K
Catalytic Subunit (p110γ)
RBD
C2
PIK
Catalytic Domain
Regulatory Subunit (p101)
p110γ binding
Gβγ binding
Regulatory Subunit (p87)

1.3.5 Pharmacological Inhibitors of Class 1 PI3K Activity

Inhibitors of PI3K activity are generally divided into three classes: pan-inhibitors, isoform-selective inhibitors, and dual PI3K/mTOR inhibitors. These distinctions between classes are primarily based on isoform selectivity for the ATP binding site of PI3Ks (reviewed by Vadas et al., 2011). For the purpose of this thesis, only the relevant PI3K inhibitors used in our studies will be discussed.

1.3.5a Pan-PI3K Inhibitor

Wortmannin, a fungal steroid metabolite, is a covalent PI3K inhibitor at nanonmolar concentrations (Arcaro and Wymann, 1993; Ui et al., 1995; Yano et al., 1993). Wortmannin is a pan-PI3K inhibitor as it displays similar potency *in vitro* for the class I, II, and III PI3Ks. Site directed mutagenesis was used to show that wortmannin covalently binds to a conserved lysine residue in the ATP binding pocket of PI3K (Walker et al., 2000; Wymann et al., 1996). Because of this covalent bond, the IC_{50} of wortmannin is in the 1-10nM range (Arcaro and Wymann, 1993; Ui et al., 1995; Yano et al., 1993). However, wortmannin is quite unstable in aqueous solutions and thus this drug needs to be used in an acute setting (Vanhaesebroeck and Waterfield, 1999).

1.3.5b Isoform Selective PI3K Inhibitors

PIK-75 is one of the first selective inhibitors of p110α generated (Hayakawa et al., 2007); it inhibits p110α with an IC_{50} of 8 nM (*versus* 907 nmol/l for p110β) (Chaussade et al., 2007; Hayakawa et al., 2007). PIK-75 is a noncompetitive inhibitor at the ATP binding pocket of p110α (Zheng et al., 2011). Two amino acids, Ser773 and His855 are shown to be critical for the binding of PIK-75, and are thought to be responsible for the p110α selectivity.

TGX-221 is one of the most potent inhibitors of p110β generated, with an IC_{50} of 5 nM for p110β (*versus* 1 μM for p110α) (Jackson et al., 2005). TGX-221 shows >1000-fold selectivity for p110β over a broad range of protein kinases. Unlike PIK-75, TGX-221 is a competitive inhibitor at the ATP binding pocket of p110β. AZD6482 is a novel inhibitor of p110β generated with an IC_{50} of 21 nmol/l (*versus* 1.4 μM for p110α) (Nylander et al., 2012). Like TGX-221, AZD6482 is a competitive inhibitor at the ATP binding pocket.

AS605240 and AS604850 are potent non covalent inhibitors of p110γ with an with an IC_{50} for p110γ of 8 nM and 250 nM, respectively (Camps et al., 2005). Both are 30 fold more selective for p110β, and 18 and 7.5 fold more selective over p110α, respectively. Both molecules bind to the ATP-binding pocket of PI3Kγ in a competitive manner. Two residues in the ATP binding pocket (Lysine 833 and Valine 822) are important for formation of hydrogen bonds with the inhibitors.

1.4 PI3K SGNALING IN THE ENDOCRINE PANCREAS

1.4.1 Positive Role of Class 1A PI3K Signaling

PI3Ks have important roles in the control of beta cell function. **Figure 7** summarizes class 1A and class 1B PI3K signaling in the beta cell.

Mice lacking the beta cell insulin receptor (IR) (and thus exhibiting decreased downstream PI3K activity) lack first phase insulin secretion in response to glucose and their ability to handle a glucose challenge severely declines with age (Kulkarni et al., 1999a). Isolated islets from mice lacking the beta cell insulin-like growth factor 1 (IGF-1) receptor (IGF1R) show impaired glucose-stimulated insulin secretion (Kulkarni et al., 2002).

IR and IGF1R receptor signaling pathways share homologous receptors and common downstream signaling pathways, including PI3K signaling. Thus, the full effects of loss of impairment of upstream PI3K signaling are not seen following chronic loss of either the IR or IGF1R. Whereas chronic beta cell specific ablation of either the IR or IGF1R presents with mild glucose intolerance, mice lacking both the IR and IGF1R (βDKO) develop full blown diabetes (Ueki et al., 2006). These βDKO mice die by six weeks of age due to severe hyperglycemia resulting from significantly decreased circulating insulin levels.

Since Class 1A PI3Ks are activated through tyrosine kinase receptors, PI3K signaling disruption is associated with the overt diabetes seen following chronic loss of IR and IGF1R signaling. Beta cell-specific *pik3r1* (βPik3r1KO) and *pik3r2* knockout (βPik3r2KO) in mice results in glucose intolerance (Kaneko et al., 2010). (*pik3r1* and *pik3r2* encode for the p85α and p85β regulatory subunits of PI3K, respectively).

Thus, these above experiments ascribe a positive role of PI3K signaling in the endocrine pancreas, as loss of the IR or IGF1R, or genetic ablation of the classic tyrosine-kinase-linked PI3Ks causes reduced islet insulin secretion.

Knock-out of the class 1B PI3K isoform, p110γ, is also associated with an impairment of glucose stimulated insulin secretion (MacDonald et al., 2004). Mice lacking p110γ (p110γ-/-) are not diabetic, but they show a reduced plasma insulin response to an i.p glucose injection. The p110γ-/- mice also show impairment in both first and second phase glucose-stimulated insulin secretion from *ex vivo* perfused pancreata, indicating a positive role for p110γ in pancreatic beta cell signaling (MacDonald et al., 2004).

1.4.2 Negative Role of PI3K Signaling

The role of PI3K signaling in the endocrine pancreas has been confounded by findings that pharmacologic PI3K inhibition increases glucose-stimulated insulin secretion (El-Kholy et al., 2003; Zawalich and Zawalich, 2000; Zawalich et al., 2002). The pan-PI3K inhibitor wortmannin amplifies GSIS from perifused mouse and rat islets (Zawalich et al., 2002). However, the effects of wortmannin are negligible when measuring GSIS in an obese mouse model (ob/ob mice), indicating impairment in PI3K signaling.

GSIS in mouse islets is also amplified by the use of another PI3K inhibitor LY294002 (Vlahos et al., 1994; Zawalich et al., 2002). However, the effects of LY294002 on insulin secretion are confounded its ability to strongly inhibit voltage-gated potassium channels (Kv), irrespective of its action on PI3Ks (El-Kholy et al., 2003; Hong et al., 2013). Inhibition of Kv channels prolongs the action potential duration, delays

repolarization of the beta cell and thus contributes to the increase in insulin secretion seen. Wortmannin on the other hand has no effects on Kv current (El-Kholy et al., 2003), and is generally preferred over LY294002 as a PI3K inhibitor.

A negative role for PI3K signaling has also been shown in class I PI3K p85α regulatory subunit–deficient (p85α-/-) mice (Eto et al., 2002). Despite a significant decrease in insulin content in p85α-/- mouse islets, GSIS from these islets is significantly higher than from the wild-type controls. This increase in insulin secretion is due to a potentiating effect distal to the increase in cytosolic [Ca^{2+}] following a glucose stimulus.

1.4.3 PI3K and Incretin Hormone Signaling

1.4.3a Beta cell survival

Both GIP and GLP-1 are suggested to signal through PI3K in the endocrine pancreas. For example, GIP's effects on pancreatic beta cell survival is shown to be dependent on PI3K/PKB signaling (Kim et al., 2005). The activation of the PI3K signaling pathway by GIP increases PKB activation, which in turn inhibits pro-apoptotic components (such as *bax* gene activation) of the intrinsic cell death machinery by preventing translocation of the transcription factor FoxO1 to the nucleus. The use of the non-specific PI3K inhibitor wortmannin prevents GIP-induced activation of PKB, and subsequently prevents *bax* expression.

GIP also directly stimulates cell proliferation and activates the class 1B PI3K isoform p110γ in an insulinoma cell line (Trümper et al., 2001). PIP_3 levels were increased in insulinoma cells lysates that were subjected to immunoprecipitation with the p110γ antibody and treated with GIP under high glucose conditions (Trümper et al.,

2001). This increase in PIP_3 was not seem in cells lysates that were subjected to immunoprecipitation with the p110α or p110β antibody, suggesting that GIP's ability to increase PIP_3 production was the result of p110γ activation.

The effects of GLP-1 on pancreatic beta cell survival are also dependent on PI3K/PKB signaling and subsequent FoxO1 inactivation (Buteau et al., 2006). GLP-1 mediated inhibition of FoxO1 increases beta cell mass, by increasing Pdx-1 expression (Kim et al., 2005). Pdx-1 (pancreatic and duodenal homeobox 1) is a nuclear transcription factor that is necessary for pancreatic development and beta cell maturation, and plays a major role in glucose-dependent regulation of insulin gene expression (Fujimoto and Polonsky, 2009; Kitamura et al., 2002; Kulkarni et al., 2004). LY294002-mediated inhibition of PI3K suppressed the GLP-1 mediated inhibition of FoxO1 in insulinoma cells; and thus further supporting a role of PI3Ks in GLP-1 mediated signaling (Buteau et al., 2006).

GLP-1 activates PI3K through receptor-mediated activation of c-Src (a non-receptor tyrosine kinase), which in turn transactivates the EGF receptor (EGFR) (Buteau et al., 2003). EGFR activation is known to activate PI3K signaling, and thus induce beta cell proliferation (Buteau et al., 2003; Humtsoe and Kramer, 2010). However, there is also evidence that GLP-1 can activate Epac (an exchange protein directly activated by cAMP) and subsequently activate PKB **(Figure 7)** (Buteau et al., 2003; Widenmaier et al., 2009).

1.4.3b Beta cell insulin secretion

PI3K signaling has also been implicated in the incretin effect of GIP. Wortmannin strongly inhibits the incretin effects of GIP in HIT cells (a hamster insulin-secreting cell

line) in both perifusion and static incubation studies (Straub and Sharp, 1996b). However, insulin secretion is not affected by wortmannin when the cAMP-inducing agent forskolin is used, indicating the presence of a wortmannin-sensitive pathway that exists in the stimulation of insulin secretion by GIP.

The link between GLP-1 signaling and the G-protein coupled PI3Kγ has been examined using PI3Kγ knockout (KO) mice (Li et al., 2006). Because PI3Kγ mice exhibit an increase in beta cell mass, and growth-mediated effects of GLP-1 are dependent on PI3K/PKB signaling, it was hypothesized that PI3Kγ may serve as an essential link between the GLP-1 receptor and PKB activation (Li et al., 2006). However, chronic treatments with the GLP-1 analogue Ex-4 treatment abolished the increase in beta cell mass seen following chronic PI3Kγ deletion (likely due to a reduced metabolic demand on the beta cell) (Li et al., 2006). Chronic Ex-4 treatment in KO animals also restored the secretory defect seen in isolated islets (Li et al., 2006). Thus it was determined that PI3Kγ likely does link GLP-1 receptor signaling and PI3K/PKB activation, and suggested that other isoforms of PI3K may be involved (consistent with the transactivation of class 1A PI3K isoforms) (Li et al., 2006).

Figure 7: Class 1A and class 1B PI3K signaling in the beta cell.

Class IA PI3Ks are primarily activated by cell surface receptor tyrosine kinases (RTKs), (such as the insulin receptor), whilst class IB are activated by G-protein coupled receptors (GPCRs). In the simplest scenario, agonist binding to the RTK leads to receptor autophosporylation. The phosphorylated residue on the RTK becomes a docking site for the p85 subunit PI3K. In the case of insulin receptor activation, however, receptor phosphorylation leads to the recruitment of the adaptor protein insulin receptor substrate (IRS), which is required for p85 subunit binding. The recruitment of class 1A PI3K to activated receptors initiates the phosphorylation of PIP_2 to PIP_3.

Class 1B PI3Ks are primarily activated by cell surface protein coupled receptors. GPCRs activate PI3Kγ through direct interaction of the regulatory subunit (or in some cases catalytic subunit) with free Gβγ. Like with class 1A PI3Ks, following activation, the catalytic subunit translocates to the inner leaflet of the plasma membrane, giving p110γ access to its lipid substrate PIP_2.

The generation of PIP_3 in turn leads to the activation and/or recruitment of numerous Pleckstrin Homology (PH) domain-containing proteins such as phosphoinositide-dependent kinase 1 (PDK1), and subsequent activation of effector proteins such as PKB/AKT.

Figure 7

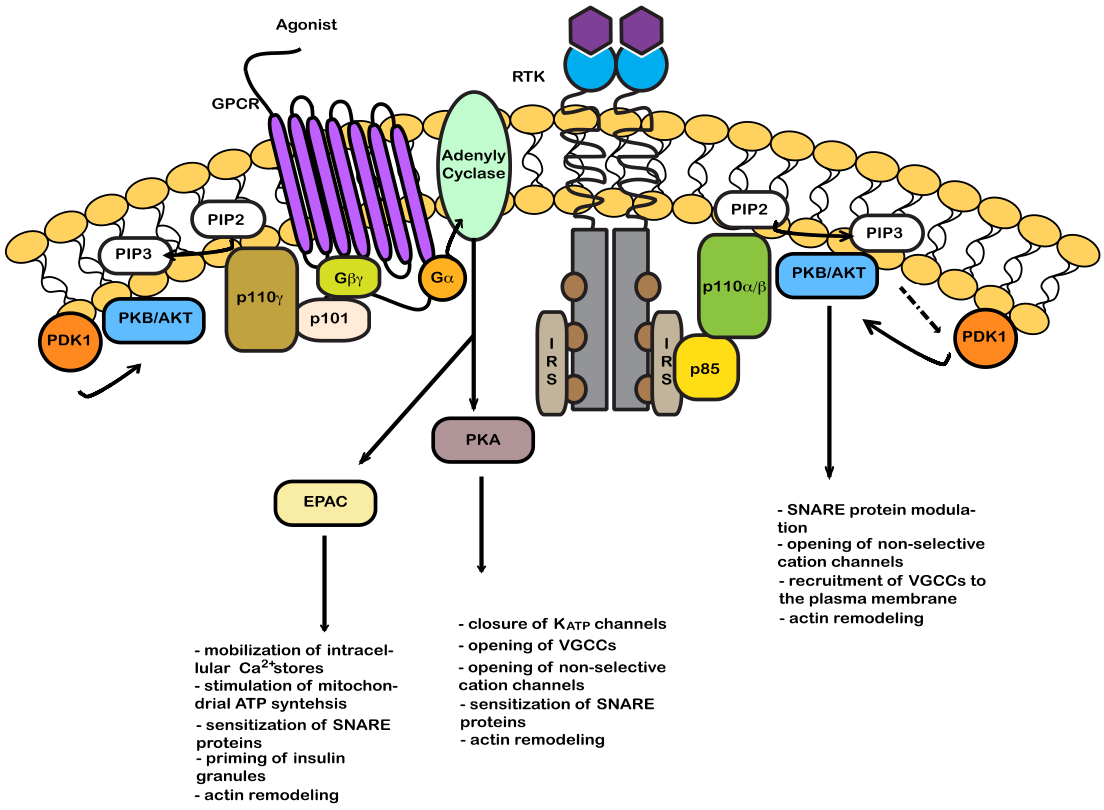
Agonist
GPCR
RTK
Adenyly Cyclase
PIP2
PIP3
PKB/AKT
PDK1
p110γ
p101
Gβγ
Gα
IRS
IRS
p110α/β
p85
PIP2
PIP3
PKB/AKT
PDK1
PKA
EPAC
- mobilization of intracellular Ca2+stores
- stimulation of mitochondrial ATP syntehsis
- sensitization of SNARE proteins
- priming of insulin granules
- actin remodeling
- closure of KATP channels
- opening of VGCCs
- opening of non-selective cation channels
- sensitization of SNARE proteins
- actin remodeling
- SNARE protein modulation
- opening of non-selective cation channels
- recruitment of VGCCs to the plasma membrane
- actin remodeling

1.5 GENERAL HYPOTHESIS

The disturbances in glycemia seen following alterations in insulin receptor and PI3K signaling demonstrate the important role of this pathway in maintaining proper metabolic homeostasis. However, the precise role of PI3K signaling in the insulin secretory pathway is not well understood due to conflicting results ascribing both positive and negative secretory roles to PI3K. Thus, a broader recognition of the importance of distinct roles of PI3K isoforms (both between, and within distinct classes) is necessary. I hypothesize that different Class 1 PI3K isoforms (p110α, -β, and -γ) have distinct roles in the regulation of beta cell exocytosis and insulin secretion. Furthermore, given the evidence that incretin hormones activate PI3K (in particular p110γ in response to GIP) I hypothesize a role for p110γ in the incretin effect of GIP and GLP-1 receptor activation.

1.6. AIMS

1.6.1 AIM 1: Characterization of the distinct roles of class1A PI3K isoforms (p110α and p110β) in mouse and human beta cell exocytosis and insulin secretion

The expression of p110α and -β in mouse and human islets was examined using western blot analysis. GSIS and single-cell exocytosis were measured from mouse and human islets and beta cells following p110α or -β selective pharmacologic inhibition or shRNA-mediated knockdown.

1.6.2 AIM 2: Characterization of the distinct role of the lone class1B PI3K isoform (p110γ) in mouse and human beta cell exocytosis and insulin secretion

The expression of p110γ was examined in an-insulin secreting cell line (INS-1 832/13) and human islets using western blot analysis. Glucose-stimulated insulin secretion and single-cell exocytosis were measured from INS-1 cells, mouse and human

islets and beta cells following p110γ selective pharmacologic inhibition or shRNA-mediated knockdown. Insulin granule recruitment to the plasma membrane was measured using TEM (Transmission Electron Microscopy) and TIRF (total internal reflection fluorescence) microscopy. F-actin density following p110γ inhibition was measured using TIRF microscopy.

1.6.3 AIM 3: Examining the role of PI3Kγ in the insulinotropic effects of GIP and GLP-1 receptor activation

The role of the PI3Kγ catalytic subunit (p110γ) in insulin secretion and beta cell exocytosis stimulated by GIP-R or GLP-1-R activation was examined in mouse and human islets, and beta cells. p110γ was inhibited pharmacologically, or knocked-down using an shRNA adenovirus. Actin remodeling in response to GIP-R or GLP-1-R activation was measured in mouse beta cells following p110γ pharmacological inhibition. Glucose and GIP mediated activation of the small GTPase protein Rac1 was measured in INS-1 cells using western blot analysis.

Chapter 2

Distinct and opposing roles for the phosphatidylinositol 3-OH kinase catalytic subunits p110α and p110β in the regulation of insulin secretion from rodent and human beta cells

The following chapter is published in Diabetologia, and is reprinted with the permission of the European Association for the Study of Diabetes:

Jelena Kolic, Aliya F. Spigelman, Greg Plummer, Eric Leung, Catherine Hajmrle, Tatsuya Kin, James AM. Shapiro, Jocelyn E. Manning Fox, Patrick E. MacDonald. (2013) Distinct and opposing roles for p110α and p110β in the regulation of insulin secretion from rodent and human beta cells. *Diabetologia* **56**(6): 1339-1349.

Contributions by co-authors to the figures presented are stated in the figure legends, accompanied by the appropriate co-authors' initials.

2.1 ABSTRACT

Phosphatidylinositol 3-OH kinases (PI3Ks) regulate beta cell mass, gene transcription, and function, although the contribution of the various PI3K isoforms is unknown. Since reduced class 1A PI3K signaling is thought to contribute to impaired insulin secretion, we investigated the role of the class 1A catalytic subunits p110α and -β in insulin granule recruitment and exocytosis in mouse and human islets. p110α or -β were inhibited by selective pharmacologic agents or shRNA-mediated knockdown. GSIS and single-cell exocytosis were measured from mouse and human islets and beta cells. Granule localization to the plasma membrane and actin density were monitored in INS-1 832/13 cells by total internal reflection fluorescence (TIRF) microscopy.

Inhibition or knockdown of p110α increased glucose-stimulated insulin secretion. This was not due to altered Ca^{2+} responses, depolymerization of cortical F-actin at the time points studied, or increased cortical granule density; but due to enhanced Ca^{2+}-dependent exocytosis. Intracellular infusion of recombinant PI3Kα blocked exocytosis. Conversely, knockdown (but not pharmacologic inhibition) of p110β blunted GSIS, reduced cortical granule density and impaired exocytosis. Exocytosis was rescued by direct intracellular infusion of recombinant PI3Kβ even when p110β catalytic activity was inhibited. Conversely, expression of both the wild type p110β and a catalytically inactive mutant directly facilitated exocytosis.

Type 1A PI3K isoforms have distinct and opposing roles in the acute regulation of insulin secretion. While p110α acts as a negative regulator of beta cell exocytosis and insulin secretion, p110β is a positive regulator of insulin secretion through a mechanism separate from its catalytic activity.

2.2 INTRODUCTION

Phosphatidylinositol 3-OH kinases (PI3Ks) have important roles in the control of islet mass and function. The chronic genetic impairment of upstream PI3K signaling in islets (Kulkarni et al., 1999a; Kulkarni et al., 2002; Kulkarni et al., 1999b; Ueki et al., 2006) results in impaired insulin secretion, and demonstrates an important positive role for this pathway in maintaining islet function. Genetic ablation of the classic tyrosine-kinase-linked PI3Ks causes reduced islet mass and insulin secretion (Kaneko et al., 2010). This is contrasted by increases in glucose-stimulated insulin secretion (GSIS) observed upon pharmacologic PI3K inhibition (El-Kholy et al., 2003; Eto et al., 2002; Zawalich and Zawalich, 2000). While consistent with the idea of an acute negative feedback role for insulin (Nunemaker et al., 2004; Persaud et al., 2002), these reports rely on non-selective inhibitors.

Of the three different classes of PI3K isoforms expressed in the endocrine pancreas (Dominguez and Holmes, 2011; Leibiger et al., 2010; Muller et al., 2007; Muller et al., 2006), the class 1 isoforms are the most studied. These are composed of regulatory and catalytic subunits that catalyze the phosphorylation of PIP2 to generate PIP3 (Fruman et al., 1998; Kulkarni et al., 1999a; Kulkarni et al., 1999b; Kulkarni et al., 2002; Ueki et al., 2006). Class 1 PI3Ks are further divided between class 1A and 1B subsets, regulated by tyrosine kinase and G-protein coupled receptors, respectively (Kaneko et al., 2010; Koyasu, 2003; Okkenhaug and Vanhaesebroeck, 2003). The catalytic subunit of class 1A PI3Ks is one of three p110 isoforms (α, β and δ). These associate with one of five regulatory subunits; p85α (and its splice variants p50α, and p55α), p85β and p55γ (El-Kholy et al., 2003; Eto et al., 2002; Okkenhaug and

Vanhaesebroeck, 2003; Zawalich and Zawalich, 2000). Pharmacologic inhibition of these class 1A isoforms (in a manner that is non-specific between p110α, β and δ) enhances insulin secretion (Aoyagi et al., 2012). The class 1B PI3K consists of p110γ catalytic and p101 regulatory subunits, and although stimulated by glucose-dependent insulinotropic polypeptide (Trümper et al., 2001), it contributes a minor fraction of islet PI3K activity. We have shown that inhibition or ablation of p110γ inhibits insulin secretion by increasing the density of the cortical actin network and preventing insulin granule trafficking to the plasma membrane (MacDonald et al., 2004; Pigeau et al., 2009).

Class 1A PI3K isoforms account for the majority of islet PI3K activity (Eto et al., 2002). Human beta cells express both p110α and -β mRNA (Muller et al., 2006), and INS-1 cells demonstrate p110α and -β associated lipid kinase activity (Trümper et al., 2001). Up-regulation of the class 1A PI3K is associated with islet compensation in *db/db* mice (Kaneko et al., 2010). De-compensation in this model is associated with loss of class 1A PI3K signalling, and is mimicked by the beta cell specific ablation of class 1A PI3Ks (Kaneko et al., 2010). This was accomplished by knockout of the p85 regulatory subunits, which also causes a loss of p110α and -β expression (Brachmann et al., 2005). Given the importance of class 1A PI3Ks to secretory dysfunction in T2D, we investigated the role of p110α and -β catalytic subunits in human and rodent beta cell function.

Using selective pharmacologic inhibition and shRNA-mediated knockdown we demonstrate that p110α negatively regulates GSIS by limiting Ca^{2+}-dependent exocytosis. In contrast, p110β exerts a positive insulinotropic effect by increasing beta cell exocytosis independent of its catalytic activity, perhaps by increasing cortical granule

density. Thus, the catalytic subunit isoforms of the class 1A PI3K play opposite and distinct roles in the acute regulation of insulin secretion in rodents and humans.

2.3 MATERIALS AND METHODS

Cells and cell culture

Islets from male C57/BL6 mice were isolated by collagenase digestion and hand-picking. Human islets, from 17 healthy donors (48+/-3 years of age), were from the Clinical Islet Laboratory at the University of Alberta. Islets were dispersed to single cells in Ca^{2+}-free buffer. INS-1 832/13 cells were a gift of Prof. Christopher Newgard (Duke University).

INS-1 832/13 cells were cultured in RPMI-1640 containing (in mmol/l) 11.1 glucose, 10 HEPES, 1 sodium pyruvate, 50 μM β-mercaptoethanol, 10% FBS and 100 units/ml penicillin/streptomycin at 37°C and 5% CO_2. Mouse islets and cells were cultured in RPMI with L-glutamine, 10% FBS, and 100 units/ml penicillin/streptomycin. Human islets and cells were cultured in low-glucose (1 g/l) DMEM with L-glutamine, 110 mg/l sodium pyruvate, 10% FBS, and 100 units/ml penicillin/streptomycin.

All studies were approved by the Animal Care and Use Committee and the Human Research Ethics Board at the University of Alberta.

DNA, adenovirus constructs, and and recombinant peptides

Three p110α and two p110β shRNA sequences targeting identical regions in mouse, rat and human, and a scrambled control **(Table 1)** were generated using small-interfering RNA target finder software from Genscript (Piscataway, NJ) and synthesized as described previously (Pigeau et al., 2009). These were transfected into INS-1 832/13 or human beta cells by lipid transfection (Lipofectamine 2000) or expressed via recombinant adenovirus, and experiments were performed after 72 hrs (Pigeau et al., 2009). Plasmids containing wild type $p110\beta^{WT}$ and p85α were from GeneCopoeia

(Rockville, MD). A catalytically inactive p110β^{K805R} mutant (Ciraolo et al., 2008) was generated using the QuickChange (Agilent Technologies, Santa Clara, CA) mutagenesis protocol. The islet amyloid polypeptide (IAPP)-mCherry was described previously (Pigeau et al., 2009). The GFP-tagged PH domain (GFP-PH_{AKT}) was a gift from Prof. Anders Tengholm (Uppsala, Sweden) (Tengholm and Meyer, 2002). Recombinant human PI3Kβ (p110β/p85β) was from Genway Biotech, Inc. (San Diego, CA). Recombinant human PI3Kα (p110α/p85β) was from Abcam Inc. (Ontario, Canada). Glutathione S-transferase (GST) was from Sigma Aldrich Canada (Oakville, Canada).

Pharmacologic inhibitors

PIK-75 (Symansis, Shanghai, China) is a non competitive ATP inhibitor of p110α (IC_{50} = 8 nmol/L for p110α *versus* 907 nmol/l for p110β) (Chaussade et al., 2007). TGX-221 (Symansis) is an ATP competitive inhibitor of p110β (IC_{50} 5 nmol/l for p110β *versus* 1 μmol/l for p110α) (Chaussade et al., 2007). These exhibit no notable activity against a wide array of kinases at 1 and 10 μmol/l, respectively (Jackson et al., 2005). AZD6482 (Selleckchem) inhibits p110β with an IC_{50} of 21 nmol/l (*versus* 1.4 μmol/l for p110α) (Nylander et al., 2012). Wortmannin is a covalent inhibitor of PI3Ks, displaying similar potency for class I, II and III PI3Ks (Wymann et al., 1996). Media was supplemented with 100 nmol/l PIK-75, TGX-221 or wortmannin in DMSO or an equal volume of DMSO alone.

Immunoblotting

Cell lysates were subjected to SDS-PAGE and transferred to polyvinylidene difluoride membranes (Millipore, Billerica, MA), probed with primary antibodies (anti-

p110α, anti-p110β, anti-p110γ, anti-p85; Cell Signaling Technology, Beverly, MA, anti–β-actin, anti-AKT, and anti-phospho-AKT (Ser473); Santa Cruz Biotechnology, Santa Cruz, CA), and visualized by chemiluminescence (ECL-Plus; GE Healthcare, Mississauga, Canada) and exposure to X-ray film (Fujifilm, Tokyo, Japan). Sizes of p110α and p110β were confirmed using over-expression constructs, and loss of bands following shRNA knockdown.

Electrophysiology

We used the standard whole-cell technique with the sine+DC lockin function of an EPC10 amplifier and Patchmaster software (HEKA Electronics, Lambrecht/Pfalz, Germany). Experiments were performed at 32–35°C. For capacitance measurements, the extracellular bath solution contained (in mmol/l) 118 NaCl, 20 TEA, 5.6 KCl, 1.2 $MgCl_2 \bullet 6H_2O$, 2.6 $CaCl_2$, 5 glucose, and 5 HEPES (pH 7.4 with NaOH). The pipette solution contained (in mmol/l) 125 Cs-glutamate, 10 CsCl, 10 NaCl, 1 $MgCl_2 \bullet 6H_2O$, 0.05 EGTA, 5 HEPES, 3 MgATP and 0.1 cAMP (pH 7.15 with CsOH). For measurement of voltage-dependent Ca^{2+} currents, the pipette solution was (in mmol/l): 140 Cs glutamate, 1 $MgCl_2$, 20-tetraethyl ammonium chloride, 5 EGTA, 20 HEPES and 3 MgATP (pH 7.3 with CsOH). The extracellular bath contained (in mmol/l): 10 $BaCl_2$, 100 NaCl, 5 CsCl, 1 $MgCl_2$, 5 glucose, 10 HEPES, and 0.5 μmol/l tetrodotoxin (pH 7.35 with CsOH). Patch pipettes, pulled from thin-walled borosilicate glass and coated with Sylgard, had resistances of 4–6 megaohm (MΩ) when filled with pipette solution. Capacitance responses and Ca^{2+} currents were normalized to initial cell size and expressed as femtofarad per picofarad (fF/pF) and picoampere per pF (pA/pF). Mouse beta cells were identified by size, whereas human beta cells were positively identified by

insulin immunostaining.

Insulin Secretion Measurements

Insulin secretion measurements were performed at 37°C in KRB (in mmol/l: 115 NaCl, 5 KCl, 24 $NaHCO_3$, 2.5 $CaCl_2$, 1 $MgCl_2$, 10 HEPES; and 0.1% BSA, pH 7.4). Fifteen mouse or human islets per group were pre-incubated for 2 hours in 2.8 or 1 mmol/l glucose KRB, respectively, then for 1 hour in these basal buffers followed by 1 h with 16.7 mmol/l glucose. Acid/ethanol extractions were used for insulin content. Human islet perifusion was performed at 37°C using a Brandel SF-06 system (Gaithersburg, MD) after a 2 hour pre-incubation in KRB with 1 mmol/l glucose. Thirty-five islets per lane were perifused (0.5 ml/min) with KRB. Glucose was increased as indicated. Samples were stored at -20°C and assayed for insulin via enzyme-linked immunosorbent assay (Alpco, Salem, NH).

Fluorescence Imaging

Total internal reflection fluorescence (TIRF) imaging was performed as described previously (Pigeau et al., 2009).For visualization of actin, cells were fixed with Z-FIX (Anatech, Battle Creek, MI) and stained with Alexa Fluor Rhodamine–conjugated phalloidin (Invitrogen, Madison, WI). For visualization of secretory granules, cells were transfected with IAPP–mCherry that localizes to insulin granules. Images were analyzed with ImageJ 1.38X (National Institutes of Health).

For measurement of intracellular Ca^{2+}, islets were incubated for 45 minutes with 10 μmol/l Fura Red-AM (Invitrogen, Carlsbad, CA) and 0.08% pluronic acid (Invitrogen, Madison, WI) in an extracellular imaging solution containing (in mmol/l) 130 NaCl, 5 KCl, 2 $CaCl_2$, 1 $MgCl_2 \bullet 6H_2O$, 5 $NaHCO_3$, and 10 HEPES (pH 7.4 with NaOH). Islets

were then imaged in fresh imaging solution with 0.5 mmol/l glucose at 37°C with constant bath perfusion. Glucose was increased as indicated. Fluorescence was measured every 5 s at 440 nm and 490 nm (excitation). Emission was collected using a 660/50 nm bandpass filter. Images were analyzed with Ratio Cam software (Metamorph).

For measurement of PI3K activation, INS-1832/13 cells expressing GFP-PH_{AKT} were treated with TGX-221 (100 nmol/l) or DMSO overnight, and then treated with insulin (200 nmol/l, 20min). Cells were visualized on a Perkin Elmer ERS6 spinning disk confocal microscope equipped with a 100X/1.4 NA lens and Hamamatsu 9100-50 EMCCD camera. Images were acquired and analyzed in VOLOCITY 5.2 software (Perkin Elmer, Waltham MA).

Statistical Analysis

For single-cell studies the n-values represent the number of cells studied, from at least three separate experiments. For Ca^{2+} imaging, n-values represent the number of islets studied from four experiments. For GSIS studies, n-values represent numbers of distinct islet preparations (each in triplicate). Electrophysiology data was analyzed using FitMaster v2.32 (HEKA Electronik). All data was analyzed using the Student t-test. The Student t-test (with a Bonferroni correction) was used *post hoc* one-way ANOVA where more than 2 groups were present. The Grubb's test was used to remove outliers. Data is expressed as means±SE, and $p<0.05$ was considered significant.

Table 1: p110 shRNA sequences.

We examined three shRNA sequences targeting p110α and two shRNA sequences targeting p110β, shown in ESM Table 1. These sequences all target identical regions in the mouse, rat and human p110 isoforms. For generation of recombinant adenovirus, we used the sh-p110α-1, sh-p110β-2, and sh-scram sequences.

(JMF designed the shRNA sequences)

Table 1.

shRNA	Sequence
Scrambled Control	GCTAAATAATCGGATGATGT
p110α-1	TTTAACAGAGCAGATTGAAAG
p110α-2	TATTTCCTGGCCTCTCTGAAC
p110α-3	TCTTTGCAAACATTCAGAATG
p110β-1	TCTTTCCTGATATCTCTGAGC
p110β-2	TTCTAGTCACTAGTTTGAGAA

2.4 RESULTS

2.4.1 Effect of p110α and p110β pharmacological inhibition on insulin secretion

We detected mRNA expression of p110α and -β, but not δ, in INS-1 832/13 cells and mouse islets by RT-PCR. Expression of p110α and -β protein was confirmed by western blot of human and mouse islet, and INS1 832/13 cell lysates **(Figure 8A)** in agreement with reports indicating mRNA expression for these in human islets (Muller et al., 2006), and lipid kinase activity in INS-1 cells (Trümper et al., 2001) .

Pharmacological inhibition of p110α with PIK-75 (100 nmol/l, overnight) in mouse islets increased glucose-stimulated insulin secretion by 1.8 fold (n=5, $p<0.05$; **Figure 8B)**, without affecting p110α or p110β expression **(Figure 8C)**. Overnight inhibition with PIK-75 was needed to observe the full effect **(Figure 8D)**. Consistent with previous studies (Collier et al., 2004; Nunoi et al., 2000), non-specific pharmacological inhibition of PI3Ks with wortmannin (100 nmol/l), increased glucose-stimulated insulin secretion by 2.4 fold **(**n=5, $p<0.05$; **Figure 8B).** In line with previous reports suggesting that wortmannin also inhibits other classes of PI3Ks, and related enzymes such as mammalian target of rapamycin (mTOR) and myosin light chain kinase (MLCK) (Brunn et al., 1996; Nakanishi et al., 1992), we observed a further 1.4 fold (n=4, $p<0.05$) increase in insulin secretion by wortmannin treatment when p110α was inhibited **(Figure 8E)**.

Pharmacological inhibition of p110β with TGX-221 (100 nmol/l, overnight) had no effect on glucose-stimulated insulin secretion from mouse islets **(**n=5; **Figure 8B)**, indicating that p110β activity may not be a crucial regulator of insulin secretion. To ensure efficacy of the p110β inhibitor, we examined recruitment of GFP-PH_{AKT}

(Tengholm and Meyer, 2002) to the plasma membrane of INS-1 832/13 cells following insulin stimulation (200 nmol/l). Insulin treatment increased GFP-PH_{AKT} recruitment to the plasma membrane by 1.6 fold (n=21, $p<0.01$) in control cells, but had no effect in cells treated with TGX-221 (100 nmol/l, overnight) **(**n=24; **Figure 8F,G)**. To further confirm the lack of effect of p110β inhibition we tested another p110β inhibitor, AZD6482 (100 nmol/l, overnight), which had no effect on GSIS **(**n=4; **Figure 8H)**.

Figure 8: Evidence that PI3K catalytic subunits p110α and p110β are expressed in mouse and human islets, and the effect of pharmacological inhibition on insulin secretion from mouse islets.

(A) Representative western blots showing p110α and p110β (black arrows) in human islets (H), mouse islets (M) and INS1 832/13 cells (I). A non-specific higher-molecular weight band was occasionally observed (grey arrows).

(B) Insulin secretion was measured from isolated mouse islets treated overnight with DMSO alone (white bars), 100 nmol/l PIK-75 (light grey bars),100 nmol/l TGX-221 (dark grey bars) or 100 nmol/l wortmannin (black bars).

(C) Representative western blots indicating no change in expression levels of p110α (*left*) or p110β (*right*) following overnight treatment with either DMSO, PIK-75 (100 nmol/l), or TGX-221 (100 nmol/l).

In panel **(D)**, insulin secretion was measured from isolated mouse islets (n=5 individual experiments) treated overnight with DMSO alone (*open bar*), overnight with 100 nmol/l TGX-221 (*black bar*), acutely with 100 nmol/l PIK-75 (*light gray bar*), overnight with 100 nmol/l PIK-75 (*dark gray bar*), or acutely with 100 nmol/l wortmannin (*stripped bar*).

In panel (**E)**, insulin secretion was measured from isolated mouse islets (n=4 individual experiments) treated overnight with DMSO alone (*open bar*), 100 nmol/l PIK-75 (*black bar*), or a combination of 100 nmol/l wortmannin and 100 nmol/l PIK-75 (*gray bar*).

(F,G) PI3K activation was monitored in INS-1 832/13 cells producing GFP-PHAkt and treated with DMSO (white bars) or 100 nmol/l TGX-221 (black bars) overnight. Cells were stimulated with insulin (200 nmol/l, 20 min) and imaged by confocal microscopy. Representative pictures and average intensity line scans are shown.

(H) Insulin secretion was measured from isolated mouse islets treated overnight with DMSO alone (white bars), 100 nmol/l TGX-221 (light grey bars), 100 nmol/l AZD6482 (dark grey bars) or 100 nmol/l wortmannin (black bars). *p,0.05, **p<0.01 and ***p<0.001

(JK performed the western blot experiments, JK and AS performed the GSIS experiments, AS ran the ELISAs, GP helped with GFP-PHAkt imaging, JK prepared all samples and analyzed all data.)

Figure 8

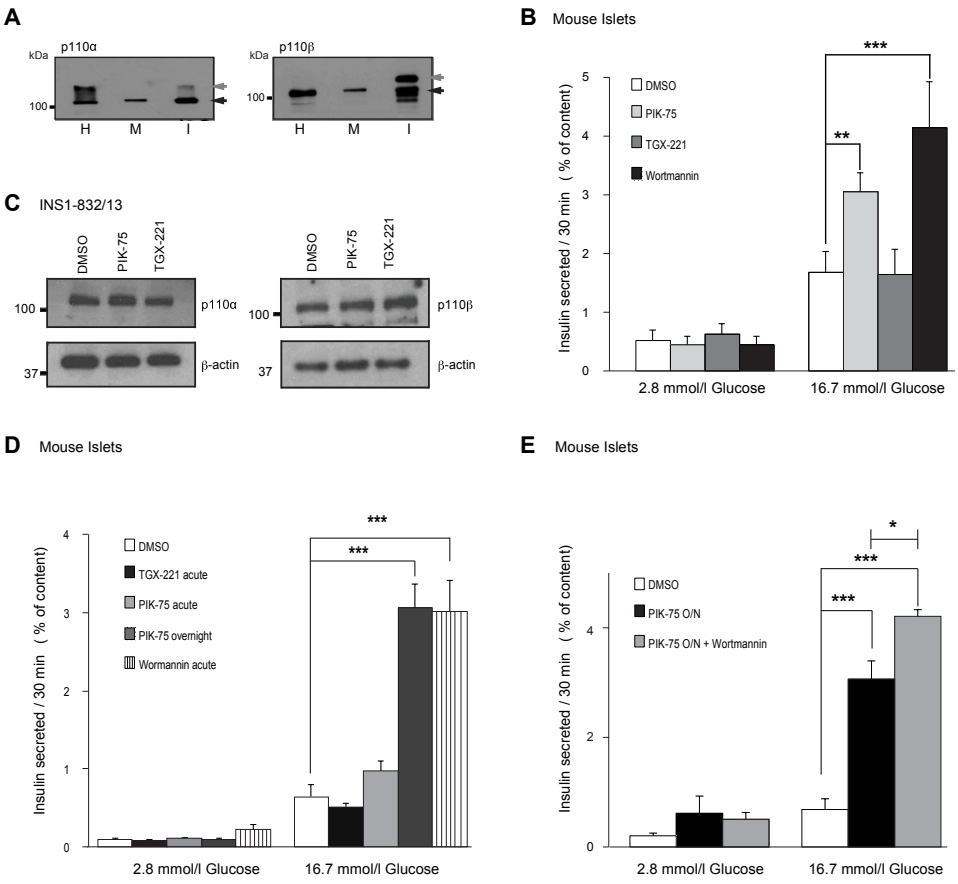
A
p110α
kDa
100
H
M
I
p110β
kDa
100
H
M
I
B
Mouse Islets
DMSO
PIK-75
TGX-221
Wortmannin
Insulin secreted / 30 min (% of content)
2.8 mmol/l Glucose
16.7 mmol/l Glucose
C
INS1-832/13
DMSO
PIK-75
TGX-221
100
p110α
37
β-actin
DMSO
PIK-75
TGX-221
100
p110β
37
β-actin
D
Mouse Islets
DMSO
TGX-221 acute
PIK-75 acute
PIK-75 overnight
Wormannin acute
Insulin secreted / 30 min (% of content)
2.8 mmol/l Glucose
16.7 mmol/l Glucose
E
Mouse Islets
DMSO
PIK-75 O/N
PIK-75 O/N + Wortmannin
Insulin secreted / 30 min (% of content)
2.8 mmol/l Glucose
16.7 mmol/l Glucose

Figure 8

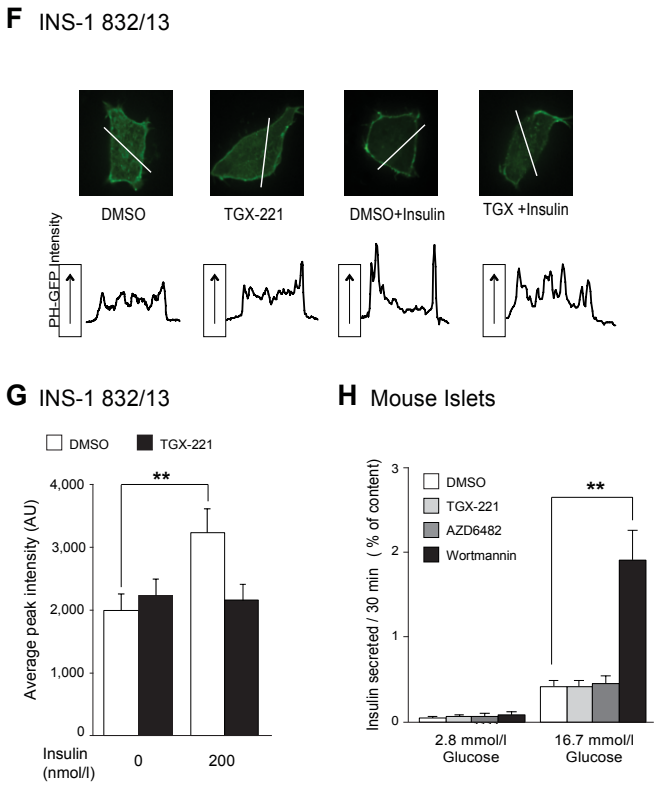
F INS-1 832/13
DMSO
TGX-221
DMSO+Insulin
TGX +Insulin
PH-GFP Intensity
G INS-1 832/13
DMSO
TGX-221
**
4,000
3,000
2,000
1,000
0
Average peak intensity (AU)
Insulin (nmol/l)
0
200
H Mouse Islets
DMSO
TGX-221
AZD6482
Wortmannin
**
3
2
1
0
Insulin secreted / 30 min (% of content)
2.8 mmol/l Glucose
16.7 mmol/l Glucose

2.4.2 Effect of p110α and p110β shRNA-mediated knockdown on insulin secretion in mouse islets.

An adenoviral-shRNA construct targeted against p110α (Adsh-p110α) reduced p110α expression in INS-1 832/13 cells by 41% (n=3, $p<0.05$) compared with a scrambled control (Adscram), while expression of p110β, p110γ and p85 were unaffected **(Figure 9A).** Similarly, an adenovirus targeting p110β knockdown (Adsh-p110β) reduced p110β expression in INS1 832/13 cells by 78% (n=3, $p<0.05$) compared with Adscram, without affecting p85 or p110γ (Fig. 8A), which can functionally compensate for p110β (Guillermet-Guibert et al., 2008; Trümper et al., 2001). Knockdown of p110α resulted in a 1.8 fold increase in GSIS **(**n=6, $p<0.05$; **Figure 9B)**, consistent with the pharmacologic inhibition of p110α. Surprisingly, in contrast to the negligible effects of the p110β inhibitors, p110β knockdown reduced insulin secretion by 53% **(**n=6, $p<0.05$; **Figure 9B)**, suggesting that p110β expression rather than activity may be critical. Insulin content was unchanged following either p110α or p110β knockdown. Additionally, there was no difference in glucose-stimulated $[Ca^{2+}]_i$ responses following p110α knockdown compared to the scrambled control **(**n=16-18; **Figure 9C)**, while there was a modest but significant 8.5% decrease **(**n=14-18, $p<0.05$; **Figure 9C)** in the glucose-stimulated $[Ca^{2+}]_i$ response following p110β knockdown.

Figure 9: Knockdown of p110α and p110β has opposite effects on GSIS.

In panel **(A)**, expression of p110α (but not p110β, p110γ, or p85) was reduced by an adenovirus delivered sh-p110α construct in INS-1 832/13 cells. Expression of p110β (but not p110γ or p85) was reduced by an adenovirus-delivered sh-p110β construct in INS-1 832/13 cells. These constructs targeted identical rat, mouse and human sequences within p110α and p110β.

In panel **(B)**, Insulin secretion was measured from isolated mouse islets expressing Adscram (*open bars*), Adsh-p110α (*grey bars*) or Adsh-p110β (*black bars*).

Panel **(C)** shows the glucose-stimulated increase in the Fura Red-AM ratio in mouse islets expressing Adscram (*open bar*), Adsh-p110α (*grey bar*) or Adsh-p110β (*black bar*). Representative responses are shown.

* $p<0.05$.

(JK performed the western blot experiments, JK and AS performed the GSIS experiments, AS ran the ELISAs, CH performed the calcium imaging experiments, JK prepared all samples, and analyzed all data.)

Figure 9

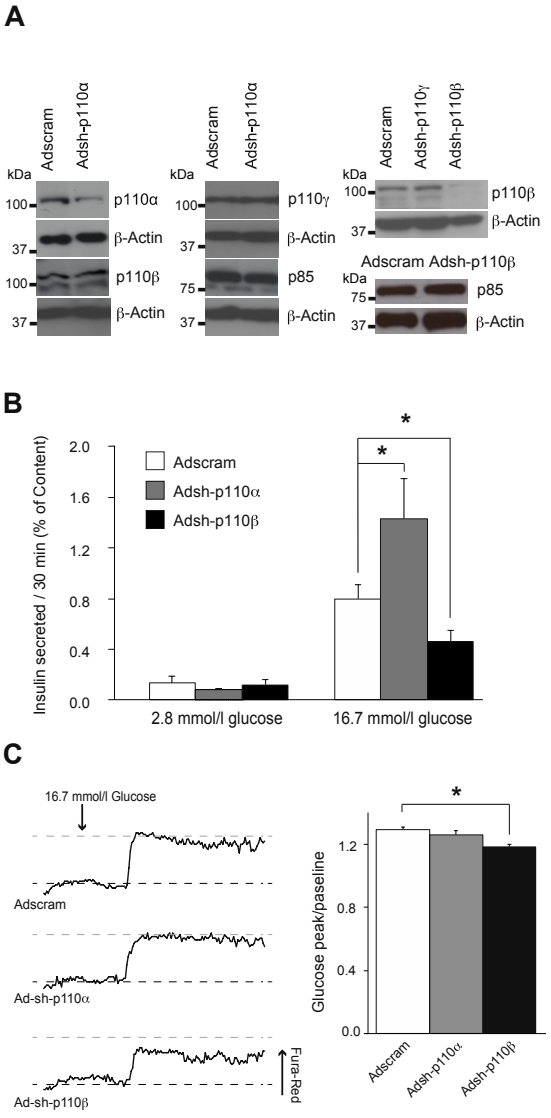
A
Adscram
Adsh-p110α
kDa
100
37
p110α
β-Actin
p110β
β-Actin
Adscram
Adsh-p110α
kDa
100
37
p110γ
β-Actin
75
p85
β-Actin
Adscram
Adsh-p110γ
Adsh-p110β
kDa
100
37
p110β
β-Actin
Adscram Adsh-p110β
kDa
75
37
p85
β-Actin
B
Insulin secreted / 30 min (% of Content)
2.0
1.6
1.2
0.8
0.4
0.0
Adscram
Adsh-p110α
Adsh-p110β
*
*
2.8 mmol/l glucose
16.7 mmol/l glucose
C
16.7 mmol/l Glucose
Adscram
Ad-sh-p110α
Ad-sh-p110β
Fura-Red
*
Glucose peak/paseline
1.2
0.8
0.4
0.0
Adscram
Adsh-p110α
Adsh-p110β

2.4.3 Effect of p110α and p110β shRNA mediated knockdown on exocytosis in mouse beta cells.

Whole-cell capacitance increases in response to a train of membrane depolarizations were monitored as a measure of exocytosis, which was increased in mouse beta cells by 1.8 fold upon p110α knockdown **(**n=20-21, p<0.01; **Figure 10A)**. This was not secondary to changes in Ca^{2+} channel activity **(Figure 11A,B)**, consistent with the lack of effect on $[Ca^{2+}]_i$ responses, and was similar between three distinct p110α-targeted shRNA sequences **(Figure 12A)**. Conversely, exocytosis was decreased by 60% in mouse beta cells following knockdown of p110β **(**n=18-21, p<0.001; **Figure 10B)**, whilst the pharmacological inhibition of p110β (100 nmol/l TGX-221) had no effect **(**n=13-16; **Figure 10C)**, suggesting that p110β may affect exocytosis independently of its catalytic activity. Despite the small but significant decrease in islet $[Ca^{2+}]_i$, we were unable to detect a significant reduction in Ca^{2+} channel activity following p110β knockdown in INS-1 832/13 **(Figure 11A,B)** and mouse beta cells **(**n=17-21; **Figure 10C)**, although the latter may trend towards decreased Ca^{2+} current. Nonetheless, these data indicate that the modest decrease in $[Ca^{2+}]_i$ does not account for the impaired exocytosis following p110β knockdown; an effect observed using two distinct p110β-targeted shRNAs **(Figure 12B)**.

We next directly infused PI3Kα and PI3Kβ (p110α/p85β and p110β/p85β heterodimers) into INS-1 832/13 cells **(Figure 13)**. In cells expressing scrambled shRNA, infusion of PI3Kα (1 μg/ml, 3 minutes) blunted exocytosis by 86% **(**n=9-20, p<0.001; **Figure 13)**. Furthermore, infusion of PI3Kα reduced exocytosis following p110α knockdown to levels similar to that following PI3Kα infusion in the control cells **(**n=23-

27, $p<0.001$; **Figure 13)**. Conversely, the direct infusion of PI3Kβ (1 μg/ml, 3 minutes) into INS-1 832/13 cells expressing the scrambled shRNA increased exocytosis by 1.7 fold (n=9-20, $p<0.01$), and was sufficient to rescue the impaired exocytotic response following p110β knockdown **(**n=20-22, $p<0.001$; **Figure 13**).

Figure 10: Knockdown of p110α and p110β has opposite effects on exocytosis in mouse beta cells.

In panel **(A)**, capacitance recordings and averaged data are shown from mouse beta cells expressing Adscram (*grey trace; open circles*) or Adsh-p110α (*black trace; black circles*).

In panel **(B)**, capacitance recordings and averaged data are shown from mouse beta cells expressing Adscram (*grey trace; open circles*) or Adsh-p110β (*black trace; black circles*).

In panel **(C)**, capacitance recordings and averaged data are shown from mouse beta cells treated overnight with DMSO alone (*grey trace; open circles*) or the p110β inhibitor TGX- 221 (100 nmol/l; *black trace; black circles*).

In panel **(D)**, voltage-dependent Ca^{2+} channel activity was measured in mouse beta cells expressing Adscram (*open circles*) or Adsh-p110β (*black circles*). * $p<0.05$, ** $p<0.01$, ***$p<0.001$.

(JK performed all electrophysiological experiments and analyzed data.)

Figure 10

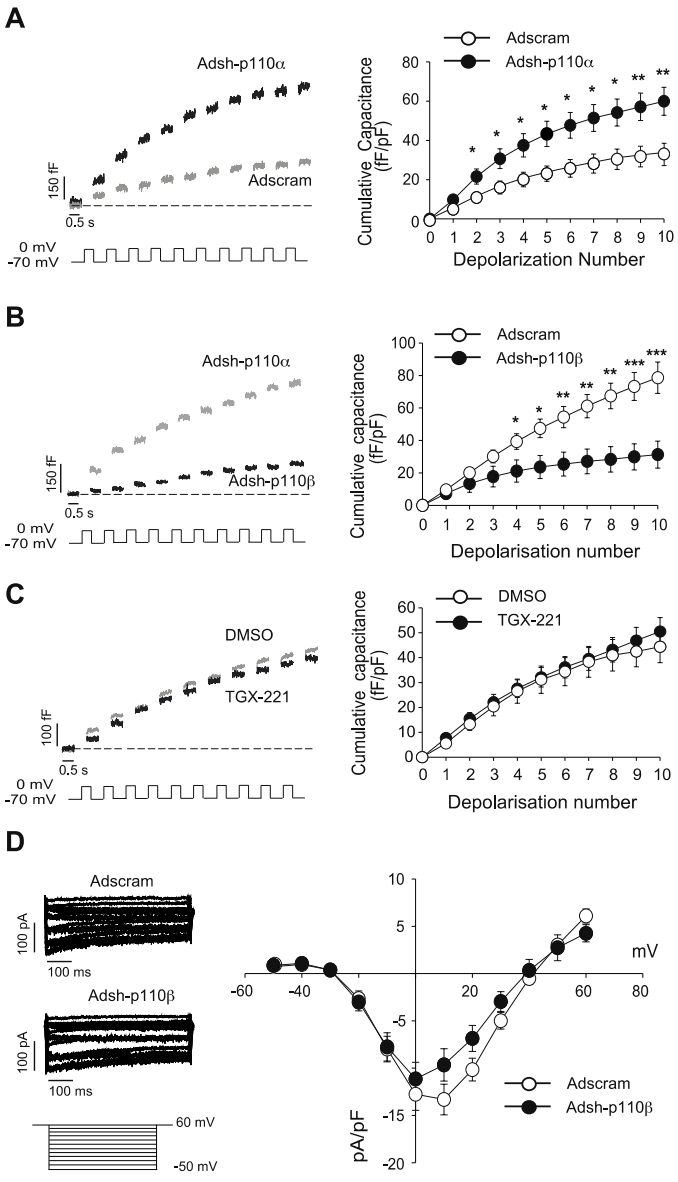
A
Adsh-p110α
150 fF
Adscram
0.5 s
0 mV
-70 mV
Adscram
Adsh-p110α
Cumulative Capacitance (fF/pF)
Depolarization Number
B
Adsh-p110α
150 fF
Adsh-p110β
0.5 s
0 mV
-70 mV
Adscram
Adsh-p110β
Cumulative capacitance (fF/pF)
Depolarisation number
C
DMSO
TGX-221
100 fF
0.5 s
0 mV
-70 mV
DMSO
TGX-221
Cumulative capacitance (fF/pF)
Depolarisation number
D
Adscram
100 pA
100 ms
Adsh-p110β
100 pA
100 ms
60 mV
-50 mV
mV
pA/pF
Adscram
Adsh-p110β

Figure 11: No change in Ca^{2+} channel activity is seen following shRNA-mediated knockdown of p110α or p110β in INS-1 cells.

We monitored Ca^{2+} channel activity during a single depolarization from -70 to 0 mV. Panel **(A)** shows representative inward Ca^{2+} currents from INS-1 832/13 cells expressing sh-scram, sh-p110α or sh-p110β cells.

Panel **(B)** shows the average Ca^{2+} charge entry during the depolarization (pC/pF) in these cells.

(JK performed all electrophysiological experiments and analyzed data.)

Figure 11

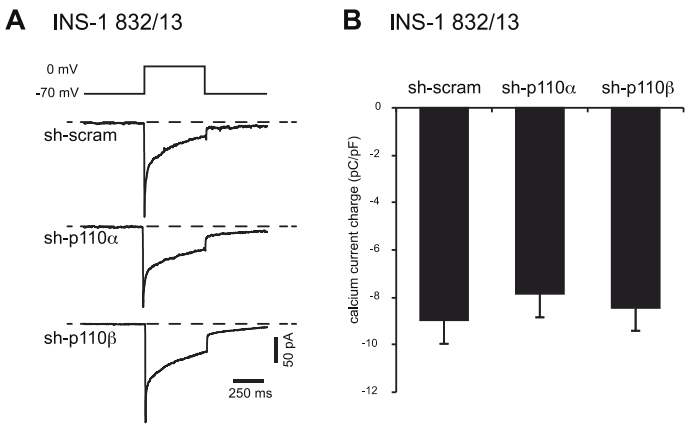
A
INS-1 832/13
0 mV
-70 mV
sh-scram
sh-p110α
sh-p110β
50 pA
250 ms
B
INS-1 832/13
sh-scram
sh-p110α
sh-p110β
calcium current charge (pC/pF)
0
-2
-4
-6
-8
-10
-12

Figure 12: p110α and p110β have opposing effects on INS-1 cell exocytosis – effects and direct rescue of multiple shRNA sequences.

In panel **(A)**, the effects of three distinct sh-p110α sequences on the cumulative capacitance response during a train of ten membrane depolarizations from -70 to 10 mV were measured in INS-1 832/13 cells. At the same time, we directly infused either the control peptide GST (*black bars*), or a recombinant PI3Kα peptide (1 μg/ml for 3 minutes) (*open bars*). N-values for each group are shown within the bars. There was no significant difference between the three different shRNA sequences.

In panel **(B)**, the effects of two distinct sh-p110β sequences on whole cell capacitance were measured in INS-1 832/13 cells. At the same time, we directly infused either the control peptide GST (*black bars*), or a recombinant PI3Kβ peptide (1 μg/ml for 3 minutes) (*open bars*). N-values for each group are shown within the bars. There was no significant difference (ns) between the two different shRNA sequences.

#-$p < 0.05$ compared with sh-scram. ** $p<0.01$ and ***$p<0.001$ as indicated.

(JK performed all infusion electrophysiological experiments and analyzed data.)

Figure 12

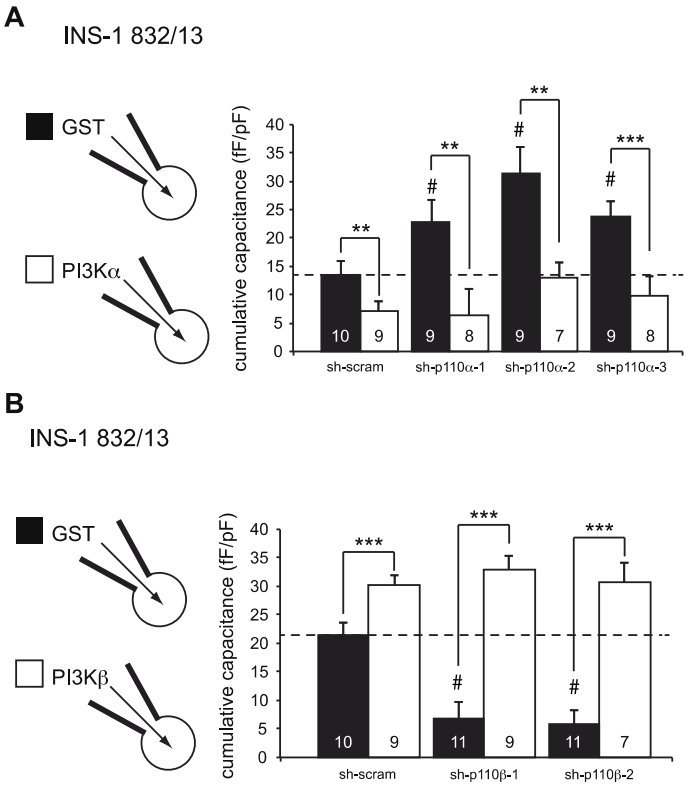
A
INS-1 832/13
GST
PI3Kα
cumulative capacitance (fF/pF)
40
35
30
25
20
15
10
5
0
**
**
**
***
#
#
#
10
9
9
8
9
7
9
8
sh-scram
sh-p110α-1
sh-p110α-2
sh-p110α-3
B
INS-1 832/13
GST
PI3Kβ
cumulative capacitance (fF/pF)
40
35
30
25
20
15
10
5
0
***
***
***
#
#
10
9
11
9
11
7
sh-scram
sh-p110β-1
sh-p110β-2

Figure 13: Intracellular dialysis of PI3Kα blunts, while PI3Kβ enhances, beta cell exocytosis.

In panel **(A)**, representative capacitance recordings are shown from INS-1 832/13 cells expressing scram, sh-p110α or sh-p110β and acutely infused with GST (*black*), PI3Kα (*dark grey*) or PI3Kβ (*light grey*) as indicated in panel **(B)**.

In panel **(C)**, the average cumulative capacitance responses under these conditions are shown. Data is pooled from experiments with three distinct sh-p110α and two distinct sh-p110β sequences.

There was no difference in the effect of the various shRNA sequences used, which are each shown separately **Figure 12**.

# $p < 0.05$ compared with the scrambled control.

** $p<0.01$, ***$p<0.001$ as indicated. ns – not significantly different compared with the scrambled control.

(JK performed all infusion electrophysiological experiments and analyzed data.)

Figure 13

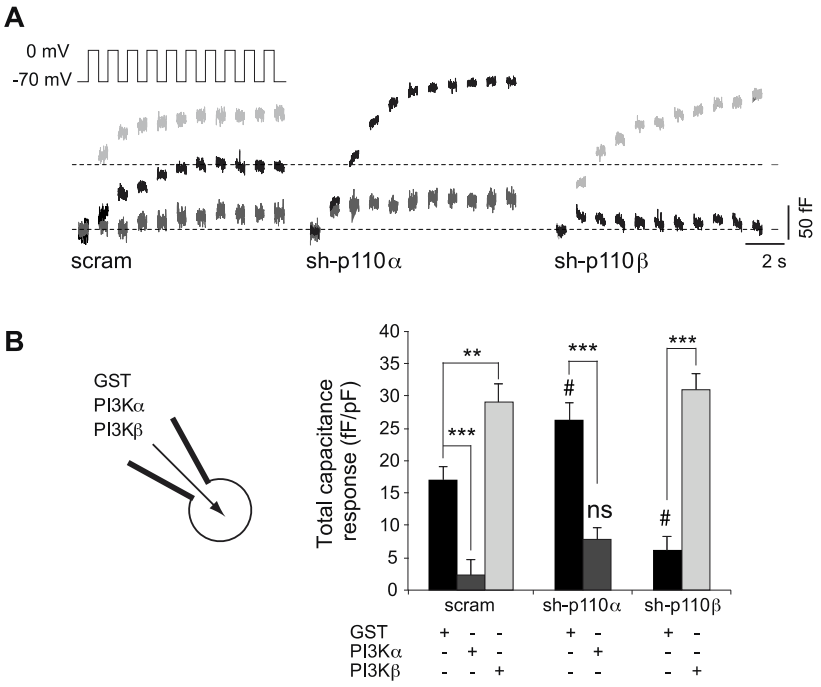
A
0 mV
-70 mV
50 fF
scram
sh-p110α
sh-p110β
2 s
B
GST
PI3Kα
PI3Kβ
Total capacitance response (fF/pF)
40
35
30
25
20
15
10
5
0
**
***
***
***
#
ns
#
scram
sh-p110α
sh-p110β
GST + - - + - + -
PI3Kα - + - - + - -
PI3Kβ - - + - - - +

2.4.4 p110β facilitates beta cell exocytosis independent of its catalytic activity

The observation that p110β knockdown, but not pharmacologic inhibition, blunts GSIS and exocytosis suggests a role for the PI3Kβ isoform that is independent of its kinase activity. Thus, we infused PI3Kβ directly into mouse beta cells while inhibiting p110β catalytic activity with 100 nmol/l TGX-221. In mouse beta cells p110β knockdown decreased exocytosis by 50% upon infusion of a control peptide (GST) **(**n=9-11, $p<0.01$; **Figure 14A)**, whilst infusion of PI3Kβ (1 μg/ml for 3 minutes together with 100 nmol/l TGX-221) rescued the exocytotic response **(**n=9-12, $p<0.001$; **Figure 14B)**. The fact that this occurs in the presence of the p110β inhibitor TGX-221, supports the idea that p110β increases exocytosis and insulin secretion independent of its catalytic activity.

To test this more directly, we generated a catalytically inactive mutant ($p110\beta^{K805R}$) as characterized previously (Ciraolo et al., 2008). We co-expressed the wild type p110β ($p110\beta^{WT}$) or $p110\beta^{K805R}$ together with p85 (required for p110 expression) in INS-1 832/13 cells. These expressed at similar levels and displayed the expected activities, as detected by changes in phosphorylated AKT (p-AKT) compared with a GFP-only control **(Figure 14C)**. INS-1 832/13 cells expressing either $p110\beta^{WT}$ or $p110\beta^{K805R}$ showed identical 2.3 fold increases (n=13-17, $p<0.01$) in exocytosis, compared with cells expressing GFP alone **(Figure 14D,E)**.

Figure 14: PI3Kβ rescues beta cell exocytosis following knockdown of p110β and facilitates exocytosis independent of its catalytic activity.

In panel **(A)** representative capacitance traces and averaged data are shown from mouse beta cells expressing Adscram (*grey trace; open circles*) or Adsh-p110β (*black trace; black circles*) following the acute infusion of GST.

In panel **(B)**, representative capacitance traces and averaged data are shown from mouse beta cells expressing Adscram (*grey line; open circles*) or Adsh-p110β (*black line; black circles*) following the acute infusion of a catalytically inhibited (with 100 nmol/l TGX-221) PI3Kβ peptide.

In panel **(C)**, the $p110\beta^{K805R}$ mutant was over-expressed at levels similar to $p110\beta^{WT}$, but was ineffective at elevating p-AKT levels above that of control cells.

In panel **(D)**, representative capacitance traces and averaged data are shown from INS-1 832/13 cells expressing GFP alone (*grey line; open circles*) or $p110\beta^{WT}$ (*black line; black circles*).

In panel **(E)**, representative capacitance traces and averaged data are shown from INS-1 832/13 cells expressing GFP alone (*grey line; open circles*) or $p110\beta^{K805R}$ (*black line; black circles*).

* $p<0.05$, ** $p<0.01$, ***$p<0.001$.

(JK performed all western blot and electrophysiological experiments and analyzed data.)

Figure 14

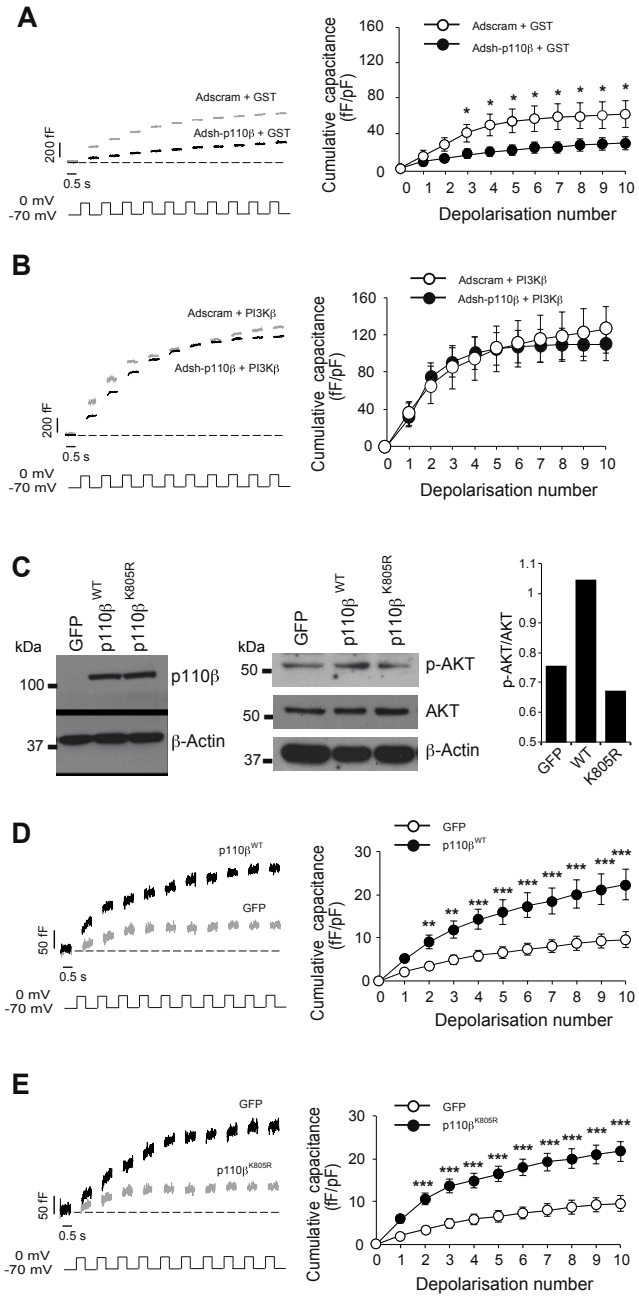
A
Adscram + GST
Adsh-p110β + GST
200 fF
0.5 s
0 mV
-70 mV
Cumulative capacitance (fF/pF)
Depolarisation number
B
Adscram + PI3Kβ
Adsh-p110β + PI3Kβ
C
GFP
p110β WT
p110β K805R
kDa
p110β
β-Actin
p-AKT
AKT
p-AKT/AKT
D
p110β WT
GFP
50 fF
E
p110β K805R

2.4.5 Knockdown of p110β reduces cortical granule density

Since cortical actin is an important determinant of the exocytotic response (Kaneko et al., 2010; Wang and Thurmond, 2009), our recent demonstration that p110γ controls cortical actin in beta cells (Pigeau et al., 2009), and the recent demonstration that p110δ inhibition leads to actin depolymerization and secretory granule recruitment in neurosecretory cells (Wen et al., 2011), we examined whether p110α or -β knockdown influences actin density and/or secretory cortical granule density by TIRF microscopy of INS-1 832/13 cells. Cortical actin density was unaffected by knockdown of either p110α or p110β **(**n=33-34 and n=31-33; **Figure 15A)**. While the density of cortical secretory granules labeled with IAPP-mCherry was slightly (22%) decreased following knockdown of p110α **(**n=39-48, $p<0.05$; **Figure 15B,C)**, this cannot account for the increased secretory and exocytotic responses observed. Knockdown of p110β, however, results in a 61% reduction of secretory granules **(**n=38-48, $p<0.001$; **Figure 15B,C)**. While this was similar to what we observed previously upon knockdown of the type 1B p110γ isoform (Pigeau et al., 2009), we could not rescue cortical granule density with forskolin (5 μmol/l, 10 min, n=39-48, $p<0.001$) **(Figure 15B,C)** as we could in the previous study. This reduction in cortical granule density may contribute to impaired exocytosis upon p110β knockdown, but appears to occur independently of any major changes in cortical actin density at the time-point studied here.

Figure 15: Knockdown of p110α or p110β reduces cortical granule density of INS-1 cells.

In panel **(A)**, INS-1 832/13 cells expressing sh-scram, sh-p110α or sh-p110β were stained for F-actin with rhodamine phalloidin 594 and imaged by TIRF microscopy. Intensity line scans, obtained from the regions indicated, are shown. Average actin line scan area under the curve (AUC - arbitrary units) are also shown.

Panel **(B)** shows cortical granules (labeled with IAPP-mCherry) imaged by TIRF microscopy of INS-1 832/13 cells expressing sh-scram, sh-p110α, or sh-p110β (+/- 5 μmol/l forskolin, 5 minutes).

Panel **(C)** shows average cortical granule density.

* $p<0.05$, ** $p<0.01$, ***$p<0.001$.

(JK and GP both contributed to the actin and vesicle imaging experiments and analyzed data. JK prepared all samples.)

Figure 15

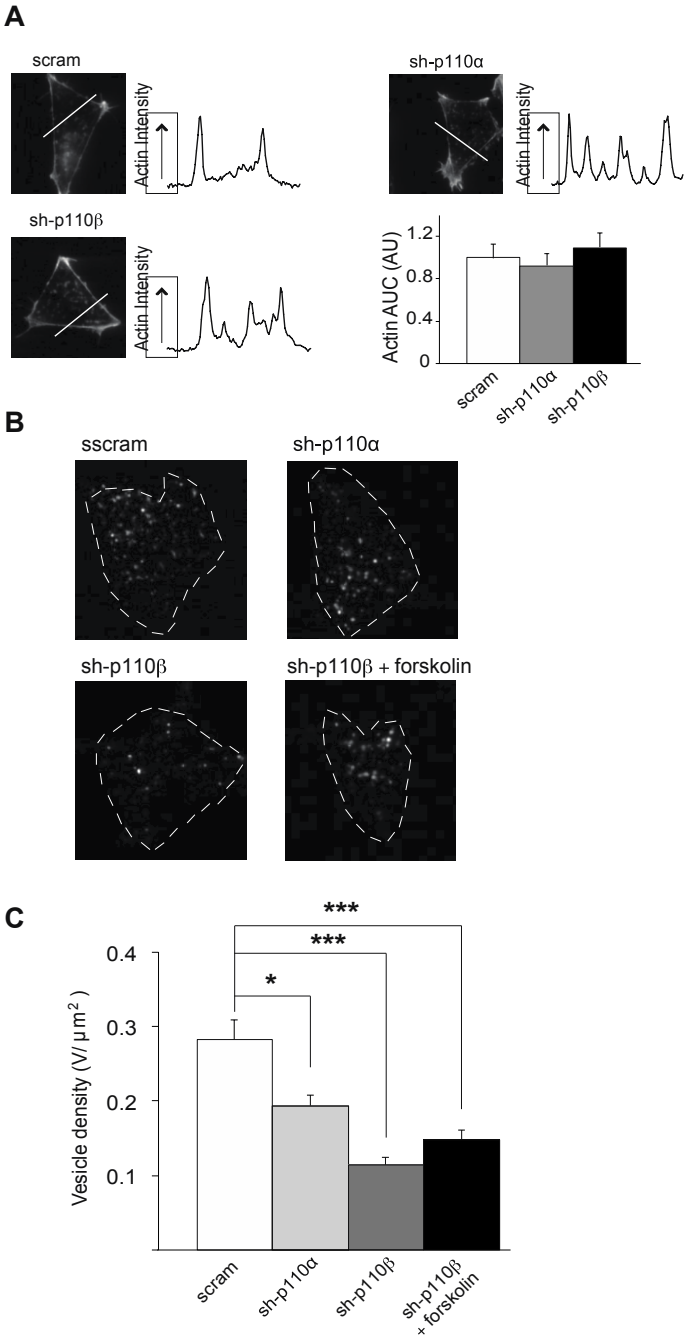
A
scram
Actin Intensity
sh-p110α
Actin Intensity
sh-p110β
Actin Intensity
Actin AUC (AU)
1.2
0.8
0.4
0
scram
sh-p110α
sh-p110β
B
sscram
sh-p110α
sh-p110β
sh-p110β + forskolin
C
***
***
*
Vesicle density (V/ µm2)
0.4
0.3
0.2
0.1
scram
sh-p110α
sh-p110β
sh-p110β + forskolin

2.4.6 p110α and p110β have opposing roles in insulin secretion and exocytosis in human beta cells

In line with our observations in mouse islets, inhibition of p110α (PIK-75, 100 nmol/l, overnight) increased GSIS by 2 fold (n=7 donors, $p<0.05$; Fig. 7A) in non-diabetic human islets, while wortmannin (100 nM, overnight) increased in GSIS by 3.2 fold **(**n=7 donors, $p<0.05$; **Figure 16A)**. The relatively larger effect of wortmannin may suggest a greater contribution of the type II and III PI3Ks than in mice. In human islets the p110β inhibitor (100 nmol/l TGX-221, overnight) had no effect on GSIS **(**n=7 donors; **Figure 16A)**, while p110β knockdown resulted in decreased GSIS (n=3 donors, $p<0.05$; **Figure 16B)**, with no change in total insulin content. Again, similar to observations in mouse, the GSIS results were paralleled by changes in beta cell exocytosis. Overnight inhibition of p110α (100 nmol/l PIK-75) increased human beta cell exocytosis by 1.4 fold **(**n=16-21, from 5 donors, $p<0.05$; **Figure 16C)**, while inhibition of p110β (100 nmol/l TGX-221, overnight) had no effect **(**n=14-17, from 4 donors; **Figure 16D)**. However, when p110β was knocked down using shRNA, the total capacitance response was decreased by 54% **(**n=21-22, from 4 donors, $p<0.05$; **Figure 16E)** in human beta cells.

Figure 16: The p110α and p110β catalytic subunits have opposing roles in GSIS from human islets and exocytosis from human beta cells.

In panel **(A)**, insulin secretion was measured from human islets treated overnight with DMSO (*open bar*), 100 nmol/l PIK-75 (*light grey bar*), 100 nmol/l TGX-221 (*dark grey bar*) or 100 nmol/l wortmannin (*black bar*).

In panel **(B)**, insulin secretion was measured by perifusion of isolated human islets expressing Adsh-p110β (*black circles*) or Adscram (*open circles*).

In panel **(C)**, representative capacitance traces and averaged data are shown from human beta cells (identified by positive insulin immunostaining) treated overnight with DMSO alone (*grey traces; open circles*) or 100 nmol/l PIK-75 (*black lines; black circles*).

In panel **(D)**, representative capacitance traces and averaged data are shown from human beta cells treated overnight with DMSO alone (*grey traces; open circles*) or 100 nmol/l TGX-221 (*black lines; black circles*).

In panel **(E)**, representative capacitance traces and averaged data are shown from human beta cells expressing Adscram (*grey lines, open circles*) or Adsh-p110β (*black lines; black circles*).

* $p<0.05$, ** $p<0.01$, ***$p<0.001$.

(JK performed all GSIS and electrophysiological experiments, AS ran the ELISAs, JK analyzed all data.)

Figure 16

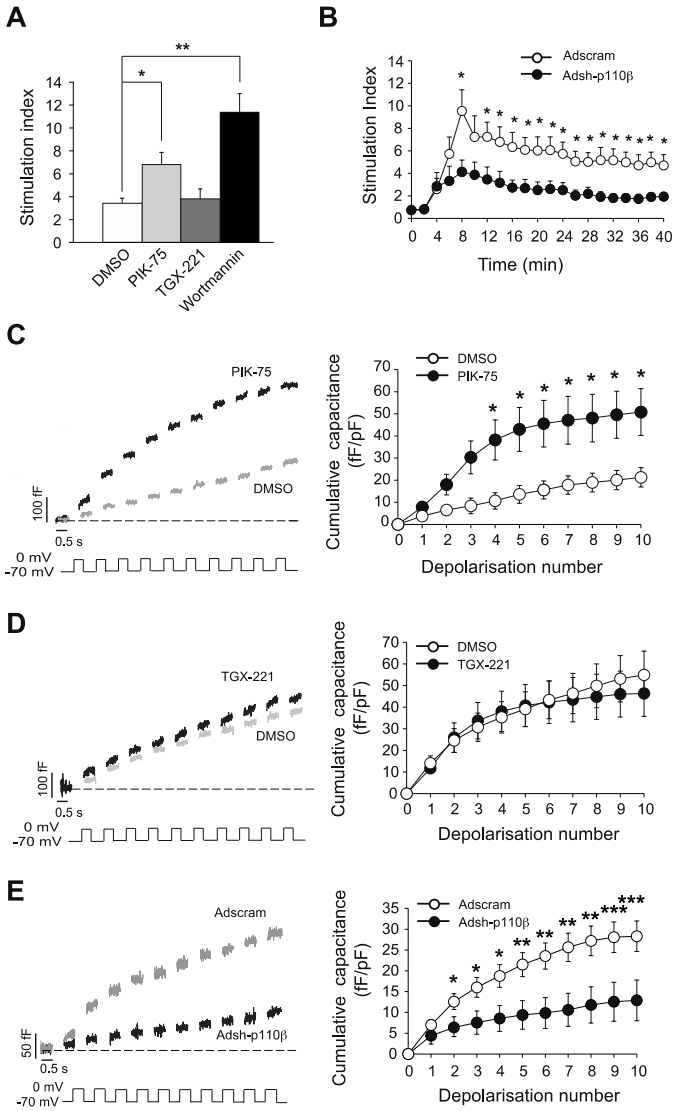
A
B
C
D
E
Stimulation index
DMSO
PIK-75
TGX-221
Wortmannin
Stimulation Index
Time (min)
Adscram
Adsh-p110β
PIK-75
DMSO
100 fF
0.5 s
0 mV
-70 mV
Cumulative capacitance (fF/pF)
Depolarisation number
TGX-221
50 fF

2.5 DISCUSSION

We showed previously that p110γ, the lone class 1B PI3K catalytic subunit, positively regulates insulin secretion by controlling cortical actin density and targeting of secretory granules to the plasma membrane (Pigeau et al., 2009). However, this G-protein coupled PI3K is responsible for only a fraction of islet PI3K activity, whilst the classical tyrosine kinase-linked class 1A isoforms account for the majority (Chaussade et al., 2007; Eto et al., 2002; Trümper et al., 2001). The importance of class 1A isoforms is recently demonstrated by work showing that expression of these declines together with islet secretory function in *db/db* mice (Kaneko et al., 2010), and knockout of type 1A PI3K activity in islets (through deletion of p85α in the beta cells and p85β globally) recapitulates an islet secretory defect (Terauchi et al., 1999; Ueki et al., 2002). Interestingly, loss of p85 also causes the loss of p110α and p110β expression (Fruman et al., 2000; Luo et al., 2005) although the specific function of these isoforms in insulin secretion is unknown. Therefore, we investigated the roles of these class 1A PI3K catalytic subunits in insulin secretion in rodent and human islets.

Mouse and human islets express p110α and p110β at the protein level, consistent with mRNA expression data in humans (Muller et al., 2006) and enzymatic activity in insulinoma cells (Trümper et al., 2001). The third class 1A isoform, p110δ, which is expressed mainly in white blood cells (Vanhaesebroeck et al., 1997), is not present. The commonly used PI3K inhibitors, including wortmannin, are non-selective between these (and other) PI3K isoforms and may account for findings ascribing both negative (El-Kholy et al., 2003; Eto et al., 2002; Zawalich and Zawalich, 2000) and positive (Kaneko et al., 2010; Kulkarni et al., 1999a; Kulkarni et al., 1999b; Kulkarni et al., 2002; Ueki et

al., 2006) roles to PI3K in insulin secretion. Using isoform selective inhibitors and shRNA-mediated knockdown we find that p110α and p110β play surprisingly opposite roles in the control of insulin secretion. While these have important roles in determining islet mass and gene transcription (Bernal-Mizrachi et al., 2001; Hügl et al., 1998), we observed no changes in insulin content upon relatively acute PI3K inhibition. Distinct roles for p110α and -β have previously been suggested: for example in Akt activation in myoblasts (Matheny and Adamo, 2010) and in platelet-derived growth factor induced actin reorganization in porcine aortic endothelial cells (Hooshmand-Rad et al., 2000).

We demonstrate that p110α activity negatively regulates insulin secretion. While this is in apparent contrast to the deleterious effects arising from knockout of insulin receptor signaling (Kulkarni et al., 1999a; Kulkarni et al., 1999b) or class 1A PI3Ks (Kaneko et al., 2010) it is notable that our inhibition of p110α was relatively acute (either overnight, or by 3 day exposure to shRNA) and not sufficient to affect insulin content. The p110α inhibitor PIK-75 had little effect when added at the time of glucose-stimulation, however, unlike the effect of the pan-PI3K inhibitor wortmannin **(Figure 8D)**. While we cannot entirely exclude the possibility of off-target effects of PIK-75 during the overnight treatment, this finding suggests that the acute insulinotropic effect of wortmannin is likely due to its inhibition of other PI3Ks (Brunn et al., 1996; Nakanishi et al., 1992). Though longer-term suppression of p110α activity is expected to result in reduced islet mass or insulin content, our results are consistent with short term *in vivo* inhibition of p110α which increases insulin secretion (Smith et al., 2012). Although the increased plasma insulin response in that study occurred in the face of glucose intolerance, there was no major blunting of insulin secretion upon p110α inhibition. An

acute negative role for p110α is also supported by a recent report showing that p110α inhibition increases secretion of an intestinal peptide secreted from N-cells in the small bowel by increasing granule trafficking (Li et al., 2012).

The increased GSIS, observed with either selective pharmacological inhibition or knockdown of p110α, was paralleled by an increase in beta cell exocytosis; while infusion of recombinant PI3Kα had the opposite effect. The increased exocytosis cannot be explained by alterations in membrane potential, which was clamped in these experiments. Likewise, we observed no significant differences in Ca^{2+} channel activity or $[Ca^{2+}]_i$ responses. We observed a 22% decrease in the density of cortical secretory granules following p110α knockdown. However, the robust increase in insulin secretion and exocytosis under this condition suggests that cortical granule density was not limiting. If anything, the lower granule density here results in an under-estimation of the effect of p110α knockdown on exocytosis *per se*. Thus we conclude that p110α exerts a negative effect on insulin secretion by limiting Ca^{2+}-dependent exocytosis. Although the exact mechanism is unclear, our results are consistent with a recent report (Aoyagi et al., 2012) demonstrating that PIK-75 (at a non-selective concentration of 0.3-3.0 μmol/l) promotes the fusion of newcomer insulin granules, without affecting intracellular Ca^{2+} responses or previously docked granules, in a PDK1-Akt-dependent manner.

In contrast, p110β is a positive regulator of insulin secretion. The decreased secretion following p110β knockdown is paralleled by impaired single-cell exocytosis. Although we cannot rule out entirely a role for impaired Ca^{2+} responses under this condition, as the $[Ca^{2+}]_i$ response to glucose was slightly decreased, this seems insufficient to explain the large reductions in GSIS and exocytosis. The impaired

exocytosis could be explained by the >60% reduction in cortical secretory granule density, although the exact mechanism remains to be determined. Unlike the effect of inhibiting the class 1B p110γ isoform (Pigeau et al., 2009), we observed no change in the cortical actin network following p110β knockdown as observed by TIRF microscopy. It should be noted however that we cannot presently rule out a role for altered actin reorganization at earlier time points, or at levels beyond the resolution of TIRF microscopy following p110β knockdown.

That pharmacological p110β inhibition did not affect GSIS or exocytosis is consistent with the lack of effect of a p110β inhibitor on glucose metabolism *in vivo* (Smith et al., 2012), and suggests that p110β can act in a lipid kinase-independent manner. The fact that the inhibitory effect of p110β knockdown is rescued by re-introduction of PI3Kβ, even when TGX-221 is present, and the identical ability of $p110\beta^{WT}$ and the inactive $p110\beta^{K805R}$ to facilitate exocytosis, support an important kinase-independent role for p110β in insulin secretion. This is in line with previous reports suggesting kinase-independent roles for p110β in clathrin-mediated endocytosis (Ciraolo et al., 2008), non-catalytic oncogenic activities (Vogt et al., 2009), and regulation of ERK phosphorylation (Matheny and Adamo, 2010).

In summary, p110α and p110β have opposing roles in beta cell function in humans and rodents. p110α is a negative regulator of insulin secretion by limiting Ca^{2+}-dependent exocytosis, whilst p110β is a positive regulator of insulin secretion by promoting Ca^{2+}-dependent exocytosis independent of it's catalytic activity. Loss of the class 1A PI3K pathway, as proposed to occur in diabetes, may impair the acute secretory response in a manner that will depend on the specific isoforms affected. A loss of p110β

expression *per se* may impair insulin secretion independent of a reduction in PI3K signaling.

2.6 CONCLUDING REMARKS

Previous studies have shown that class 1A PI3Ks control insulin secretion by multiple mechanisms, however the specific contribution of p110α and p110β had not been examined. PIK-75, when used at > 100 nmol/l will inhibit both p110α and p110β. The increase in insulin secretion from both mouse and human islets (and exocytosis from beta cells) we see following acute and selective inhibition of p110α, compliments the results obtained by studies examining PIK-75 mediated inhibition of both p110α and p110β. These experiments showed that acute (up to 24 hr) PIK-75 treatment (0.3 – 1 μmol/l) enhanced glucose stimulated insulin secretion in mouse islets (Aoyagi et al., 2012). However, unlike Aoyagi *et al.* (2012), I did not observe an increase in insulin secretion following a more acute (30 min) PIK-75 treatment (Kolic et al., 2013). However, Aoyagi *et al.* (2012) pre-incubated their islets with PIK-75 for 30 min before their GSIS experiment, whilst in my acute studies I added PIK-75 simultaneously with high glucose (Kolic et al., 2013).

Interestingly more chronic PIK-75 treatment (24-72 hrs) inhibited GSIS, and was associated with a reduction of the SNARE complex proteins SNAP-25 and Syntaxin (Aoyagi et al., 2012). This is in contrast to my results, which show that shRNA-mediated knockdown of p110α (a more chronic effect), stimulates insulin secretion and exocytosis, just as well as acute pharmacological inhibition. However, the high concentration of PIK-75 used by Aoyagi *et al*. (2012) is known to have off target effects (including inhibition of p110γ and a number of protein kinases), which could be contributing to the impairment

of insulin secretion following a more chronic treatment (Aoyagi et al., 2012). And whilst it is possible that the 100 nmol/l concentration of PIK-75 used in our studies also may have off target effects, my results were confirmed with the specific sh-RNA mediated knockdown of p110α, and match those of *in vivo* studies, where p110α inhibition is associated with increased plasma insulin levels in response to a glucose challenge (Smith et al., 2012)

I saw a slight decrease in the number of insulin granules that were within 100 nm of the plasma membrane (docked) following shRNA mediated p110α knockdown. It is possible that the reduction in docked granules observed was due to a slight reduction in SNARE complex proteins, as suggested by Aoyagi *et al.* (2012). However, despite this slight decrease in insulin granules at the plasma membrane, I still observed increased exocytosis and insulin secretion. TIRF microscopy studies examining granule localization in my studies were done with cells fixed at a specific time point, and not stimulated by glucose. I did not examine live granule fusion events in response to a glucose stimulus. Aoyagi *et al.* (2012) show that following acute inhibition of class 1 PI3K isoforms, there is an increase in "newcomer granule" fusion events from mouse beta cells, and a decrease in fusion events of the docked granules. These "newcomer granules" are intracellular insulin granules that move to the plasma membrane following a stimulus.

Furthermore, the TIRF method of imaging F-actin in INS-1 cells is not be best way to get an accurate representation of F- actin density. When cells adhere to coverslips, stress fibers and focal adhesions form at the cell-glass interface (reviewed by Kalwat and Thurmond, 2013). Remodeling of focal adhesions contributes to GSIS (Cai et al., 2012; Kalwat et al., 2012; Rondas et al., 2011; Rondas et al., 2012). Thus, because TIRF

imaging examines structures that are within about 100 nm of the plasma membrane, it is difficult to discern between cortical F-actin and focal adhesions or stress fibers. However, these methodological limitations are improved in later chapters with the use of biochemical measurements and wide-field epifluorescent microscopy.

My results also suggest a non-catalytic role for PI3Kβ in regulating exocytosis and insulin secretion. My results match those of *in vivo* studies showing that p110β pharmacological inhibition has no effect on plasma insulin levels in response to a glucose challenge in mice (Smith et al., 2012). PI3Kβ is implicated in non-catalytic functions. Conditional p110β knockout mice show severe altered glucose homeostasis, whilst having minimal effects on AKT-phosphorylation, thus suggesting a kinase independent role (Jia et al., 2008). Ciraolo *et al.* (2008) also suggested that PI3Kβ has a kinase-independent role in clathrin-mediated endocytosis (Ciraolo et al., 2008). The kinase independent method by which PI3Kβ promotes exocytosis and insulin secretion in my studies was however not determined. Based on the reduced number of (docked) granules at the plasma membrane however, and the lack of effect on actin polymerization (at the time points studied) one plausible suggestion is that PI3Kβ might be interacting directly (or indirectly) with SNARE protein complexes in a non-catalytic manner, and thus promoting the number of granules at the plasma membrane. Interactions between PI3Ks and SNARE proteins have previously been suggested. Expression of SNARE proteins (such as SNAP-25 and VAMP-2) are reduced in mice lacking both p110α and p110β (Kaneko et al., 2010). Thus, examining the plausible interaction between p110β and SNARE proteins would be an interesting area of future study.

Chapter 3

Insulin granule recruitment and exocytosis is dependent on p110γ in insulinoma and human beta cells

A version of the following chapter is published in Diabetes and is reprinted with the permission of the American Diabetes Association:

Gary M. Pigeau*, Jelena Kolic*, Brandon J. Ball, Michael B. Hoppa, Ying W. Wang, Thomas Rückle, Minna Woo, Jocelyn E. Manning Fox, and Patrick E. MacDonald (2009) Insulin granule recruitment and exocytosis is dependent on p110γ in insulinoma and human beta cells. *Diabetes* **58**(9): 2084-2092.

*These authors contributed equally

Contributions by co-authors to the figures presented are stated in the figure legends, accompanied by the appropriate co-authors initials.

3.1 ABSTRACT

Phosphatidylinositol 3-OH kinases (PI3Ks) have a long recognized role in beta cell mass regulation and gene transcription, and are implicated in the modulation of insulin secretion. However, the specific role of the lone G-protein activated PI3Kγ isoform is largely unexplored. We therefore investigated the role of PI3Kgamma (p110γ) in the regulation of insulin granule recruitment and exocytosis. The expression of p110γ was knocked-down by shRNA and p110γ activity was selectively inhibited with AS605240 (40 nM). Exocytosis and granule recruitment was monitored by islet perifusion, whole-cell capacitance, total internal reflection fluorescence (TIRF) microscopy and electron microscopy in INS-1 and human beta cells. Cortical F-actin was examined in INS-1 cells and human islets, and in mouse beta cells lacking the phosphatase and tensin homolog (PTEN).

Knockdown or inhibition of p110γ markedly blunted insulin secretion and exocytosis, and ablated the exocytotic response to direct Ca^{2+} infusion. This was correlated with a reduction in granule localization to the plasma membrane and was associated with increased cortical F-actin. Inhibition of p110γ had no effect on F-actin in beta cells lacking PTEN (phosphate and tensin homolog), a protein tyrosine phosphatase that preferentially dephosphorylates phosphoinositide substrates. Finally, agents that promote actin de-polymerization rapidly reversed the effect of p110γ inhibition on granule localization and exocytosis.

Thus, we show that the G-protein coupled PI3Kγ is an important determinant of secretory granule trafficking to the plasma membrane, at least in part through the negative regulation of cortical F-actin. We provide evidence suggesting that p110γ

activity plays an important role in maintaining a membrane-docked readily releasable pool of secretory granules in insulinoma and human beta cells, and is important in the insulin secretory response.

3.2 INTRODUCTION

Phosphatidylinositol 3-OH kinase (PI3K) signaling has well-defined roles in the regulation of islet gene transcription and mass, however its function in regulating glucose-stimulated insulin secretion remains a matter of debate. The use of non-selective pharmacological inhibitors has suggested both negative (Eto et al., 2002; Hagiwara et al., 1995; Zawalich et al., 2002) and positive (Straub and Sharp, 1996a; Straub and Sharp, 1996b) roles for PI3K in insulin secretion. While a negative role is supported by the enhanced secretion seen following genetic down-regulation of PI3K (Eto et al., 2002), a positive role is indicated by a reduced insulin secretion following knockout of the insulin or IGF-1 receptor (Kulkarni et al., 1999a; Kulkarni et al., 2002) or IRS-1 (Kulkarni et al., 1999b). In line with these observations, secretion is enhanced following beta cell-specific ablation of the phosphatase and tensin homolog (PTEN), which antagonizes PI3K signaling (Nguyen et al., 2006).

Class I PI3Ks catalyze the phosphorylation of PtdIns(4,5)P_2 to generate PtdIns(3,4,5)P_3 (Stephens et al., 1993). Receptor tyrosine kinase-linked PI3Ks, which include the class 1A catalytic subunits (p110α, β and δ), modulate ion channel activity, Ca^{2+} signaling and exocytosis (Aspinwall et al., 2000; Chasserot-Golaz et al., 1998; Gatof et al., 2004; Kolic et al., 2013). The lone class 1B PI3K, p110γ, is activated by G protein-coupled receptors (Koyasu, 2003), exhibits basal lipid kinase activity (Sasaki et al., 2007) and regulates cardiac contractility and inflammation (Rückle et al., 2006). Activity of p110γ has been detected in insulinoma cells, where it is activated by glucose-dependent insulinotropic polypeptide (GIP) (Trümper et al., 2001). Furthermore, we have demonstrated expression of this isoform in mouse and human islets (MacDonald et al.,

2004), and a lack of first phase insulin secretion in p110γ knockout mice (Li et al., 2006; MacDonald et al., 2004).

We have now examined the mechanism by which p110γ regulates insulin exocytosis in INS-1, mouse and human beta cells. We find that this PI3K isoform regulates beta cell Ca^{2+}-dependent exocytosis by controlling the size of the membrane-associated pool of secretory granules. Furthermore, we identify a role for p110γ in the modulation of cortical F-actin density as a mechanism by which it can regulate access of secretory granules to the plasma membrane. Thus, we now show that p110γ plays an important role in maintaining the ability of beta cells to undergo a robust secretory response following stimulation.

3.3 MATERIALS AND METHODS

Cells and Cell Culture

INS-1 832/13 and 833/15 cells (Chen et al., 2000; Hohmeier et al., 2000) from Prof. C. Newgard (Duke University), were transfected with Lipofectamine 2000 (Invitrogen, Carlsbad, CA) according to supplier instructions and re-plated on glass coverslips for total internal reflection fluorescence (TIRF) or 35-mm culture dishes for patch-clamp.

Islets from RIP-cre^{+}/PTEN$^{+/+}$ and RIP-cre^{+}/PTEN$^{fl/fl}$ mice (Nguyen et al., 2006) and from wild-type C57/bl6 mice were isolated by collagenase digestion followed by hand-picking. Human islets from 13 healthy donors were from Dr. J. Shapiro and the ABCC Human Islet Distribution Program at the University of Alberta. The Animal Care and Use Committee and the Human Research Ethics Board, at the University of Alberta, approved all studies. Islets were dispersed to single cells by incubation for 11 min at 37°C in Ca^{2+}-free dispersion buffer followed by gentle trituration with a flame-polished glass pipette. Mouse islets and cells were cultured in RPMI media with L-glutamine and supplemented with 10% FBS and 100U/ml penicillin/streptomycin. Human islets and cells were cultured in low glucose (1g/l) DMEM with L-glutamine, 110 mg/l sodium pyruvate and supplemented with 10% FBS and 100U/mL penicillin/streptomycin.

Islet perifusion was performed using a Brandel SF-06 system (Gaithersburg, MD) following 2hr static pre-incubation in 5mM KCl KRB (in mM: NaCl 115; KCl 5; NaHCO3 24; CaCl2 2.5; MgCl2 1; HEPES 10; 0.1%BSA, pH7.4, and 40 nM AS605240 or DMSO alone). Seventy-five human islets per lane were perifused at 0.25ml/min. Solutions were switched to 50mM KCl KRB (50 mM KCl replaced an equivalent amount

of NaCl) as indicated. Perifusate was stored at -20^{o}C and analyzed for insulin *via* ELISA (ALPCO, Salem, NH).

DNA and Adenovirus Constructs

The p110γ shRNA has been published previously (Li et al., 2006). A scrambled control sequence (GCTAAATAATCGGATGATGT) was generated using Genscript (Piscataway, NJ) siRNA target finder software, synthesized as a hairpin oligo with BamHI and HindIII restriction sites on the 5' and 3' ends, respectively, and ligated into the pRNAT-H1.1/Shuttle vector (Clontech, Mountain View, CA). For most experiments these were transfected into INS-1 832/13 or human beta cells by lipid transfection (Lipofectamine, 2000), followed by 72 hrs of culture. For some experiments expression was *via* recombinant adenovirus produced by transferring the expression cassettes into the Adeno-X viral vector (Clontech) followed by adenovirus production in HEK293 cells. HEK293 cell lysates were used to infect INS-1 832/13 cells for 5 hours at a concentration previously determined for maximum infection efficiency. Cells were then washed and cultured for an additional 72 hours.

The VAMP-pHlourin construct was from Prof. G. Miesenboeck (University of Oxford). The NPY-mCherry and IAPP-mCherry were created by ligating the mCherry sequence (Prof. R. Tsien, UC San Diego) in place of the RFP of an NPY-RFP construct (Prof. G. Rutter, Imperial College London) or the emerald of an IAPP-emerald construct (Obermüller et al., 2005).

Pharmacologic Inhibition of p110γ

5-quinoxilin-6-methylene-1,3-thiazolidine-2,4-dione (AS605240), from Merck Serono (Geneva, Switzerland), is an ATP-competitive inhibitor of p110γ (IC_{50} = 8 nM).

Culture media was supplemented with 40 nM AS605240 in dimethyl sulfoxide (DMSO) or an equal volume of DMSO alone. This compound selectively targets p110γ (IC_{50} = 60 nM, 270 nM, 300 nM for p110α, β, δ, respectively) and exhibits no notable activity against a wide array of protein kinases at 1 μM (Camps et al., 2005). Consistent with a lack of effect on the class 1A PI3Ks, treatment of INS-1 832/13 cells overnight with 40 nM AS605240 did not block PI3K activation in response to high K^+, which activates type 1A PI3K through an autocrine insulin effect (Barker et al., 2002). This was assessed by recruitment of the GFP-tagged PH domain of the general receptor for phosphoinositides (GFP-$GRP1_{PH}$; 25), where 25 mM KCl elicited a 2.7+/-0.4 fold increase in DMSO-treated cells (n=11) and a 2.9+/-0.2 fold increase in AS605240-treated cells (n=9).

Immunoblotting

Lysates were subjected to SDS-PAGE and transferred to polyvinylidene difluoride membranes (Millipore Corporation, Billerica, MA), probed with primary antibodies (anti-p110γ anti-p110β and anti-β-actin, Santa Cruz Biotechnology, Santa Cruz, CA), detected with peroxidase-conjugated secondary anti-mouse or anti-rabbit antibodies (Santa Cruz Biotechnology) and visualized by chemiluminescence (ECL-Plus, GE Healthcare, Mississauga, Canada) and exposure to X-ray film (Fujifilm, Tokyo, Japan). Western blot analysis of F- and G-actin was performed using the G-actin/F-actin In Vivo Assay Kit (Cytoskeleton Inc., Denver, USA). Densitometry was expressed relative to total actin.

Electrophysiology

We used the standard whole-cell technique with the sine+DC lockin function of an EPC10 amplifier and Patchmaster software (HEKA Electronics, Lambrecht/Pfalz,

Germany). Experiments were performed at 32-35^{o}C. Extracellular bath solution for depolarization trains contained (in mM): 118 NaCl, 20 TEA, 5.6 KCl, 1.2 $MgCl_2$•$6H_2O$, 2.6 $CaCl_2$, 5 glucose and 5 HEPES (pH 7.4 with NaOH). Pipette solution for depolarization trains contained (in mM): 125 Cs-glutamate, 10 CsCl, 10 NaCl, 1 $MgCl_2$•$6H_2O$, 0.05 EGTA, 5 HEPES and 3 MgATP (pH 7.15 with CsOH). For some experiments, the pipette solution also contained 0.1 mM cAMP or 10 μM latrunculin as indicated. For Ca^{2+} infusion experiments the extracellular bath contained (in mM): 138 NaCl, 5.6 KCl, 1.2 $MgCl_2$•$6H_2O$, 2.6 $CaCl_2$, 5 glucose and 5 HEPES (pH 7.4 with NaOH). Pipette solution for Ca^{2+} infusion contained (in mM): 125 K-glutamate, 10 NaCl, 10 KCl, 1 $MgCl_2$•$6H_2O$, 5 $CaCl_2$, 10 EGTA, 5 HEPES and 3 MgATP (pH 7.1 with KOH) for 200 nM free-Ca^{2+}. Patch pipettes, pulled from borosilicate glass and coated with Sylgard, had resistances of 3-4 MΩ when filled with pipette solution. Whole-cell capacitance responses were normalized to initial cell size and expressed as femtofarad per picofarad (fF/pF).

Microscopy

An Olympus IX71 inverted microscope with a PlanApo 100X objective (NA 1.45, Olympus Canada, Markham, Canada) was used for TIRF microscopy. Excitation was established with a 488nm Argon laser and a 543nm He-Ne laser (Melles Griot, Carlsbad, CA), passing through a laser combiner, single mode optical fibre with laser coupler (458-633nm) and an IX2-RFAEVA-2 TIRFM illuminator (Olympus Canada). Emission was separated with a GFP/RFP dichroic (Chroma, Rockingham, VT), filtered with a GFP (520-535nm) or RFP filter set (590-650nm, Chroma) and projected onto a back-illuminated Rolera-Mgi Plus EMCCD camera (Q Imaging, Surrey, Canada) operated by

InVivo version 3.2.0. (Media Cybernetics, Bethesda, MD). For TIRF/patch-clamp experiments cells were imaged (16.7Hz) with a Cascade II 512 EMCCD camera (Photometrics, Tucson, USA) and cell capacitance was recorded as above. For visualization of actin, cells were fixed with Z-FIX (Anatech Ltd., Battle Creek, MI) and stained with Alexa Fluor 488-conjugated phalloidin (Invitrogen).

For epifluorescence microscopy cells were fixed and stained for actin as above and positively identified as beta cells by immunostaining (rabbit anti-insulin primary antibody; donkey anti-rabbit IgG secondary antibody conjugated to Texas Red, Santa Cruz Biotechnology). Cells were imaged with an Olympus BX61 upright microscope and a 60x LumPlanFI objective (0.9 NA). Excitation was with a DG4 light source with either a TRITC or FITC filter set (Semrock, Rochester, NY). For clarity, only the green channel (F-actin staining) is shown. Images were captured with a Retiga Exi CCD camera (Q Imaging) operated by InVivo version 3.2.0 (Media Cybernetics).

For electron microscopy, cells were prefixed in 2.5% glutaraldehyde in cacodylate buffer solution (pH 7.3) for 1.5 hr. at room temperature, then washed and post fixed with 1% osmium tetroxide in the same buffer for 1.5 hrs. Following a wash in distilled water, the sample was dehydrated in a graded series of ethanol solutions (50%, 70%, 90%, 10 minutes each) before the final two additional 10-minute with absolute ethanol. Samples were then embedded in Spurr's resin and cured at 70^{o}C for 10 hrs. Ultrathin sections were stained with 2% uranyl acetate for 30 minutes and lead citrate for 5 minutes. Micrographs were taken at 75 Kv with a Hitachi transmission electron microscope H-7000 (Tokyo, Japan). All imaging data was analyzed with either ImageJ 1.38x (NIH) or Image Pro Plus v6.2 (Media Cybernetics).

3.4 RESULTS

3.4.1 p110γ expression, and effect of knockdown or pharmacological inhibition on exocytosis and secretion

Expression of p110γ was confirmed in INS-1 832/13 cells and mouse and human islets by western blot **(Figure 17A)** in agreement with previous reports (Li et al., 2006; MacDonald et al., 2004; Muller et al., 2007). Expression of an shRNA construct targeted against p110γ (sh-p110γ) (Li et al., 2006) in INS-1 832/13 cells reduced p110γ expression by 78% (n=3) compared with a scrambled shRNA (sh-scrambled) control **(Figure 17A,B)**. Expression of the class 1A p110β isoform, which can functionally compensate for p110γ (Guillermet-Guibert et al., 2008), was not affected by the p110γ shRNA **(Figure 17A,B)**.

Whole-cell membrane capacitance changes and voltage-dependent Ca^{2+} channel (VDCC) activity were monitored in INS-1 832/13 cells expressing sh-p110γ or sh-scrambled **(Figure 17).** The capacitance response to a 500 ms membrane depolarization was decreased by 56%, ($p<0.01$, n=20 and 19), upon p110γ knockdown **(Figure 17C,D).** The Ca^{2+} current charge during this depolarization was not different between groups (–4.82±0.64 and –6.62±0.93 pC/pF; n=20 and 18, ns). When normalized to Ca^{2+} charge, the exocytotic response was reduced 45% by knockdown of p110γ **(**$p<0.01$, **Figure 17E).**

We used membrane depolarization trains to further assess the effect of p110γ knockdown on exocytosis. The total capacitance response was decreased by 45% upon expression of sh-p110γ (n=20 and 18, $p<0.05$) **(Figure 18A,B)**. Notably, the response to the first two depolarizations, considered to represent exocytosis of the readily releasable granule pool (Kanno et al., 2004), was markedly blunted (by 54%, $p<0.01$). A two-pulse

analysis estimates a 60% reduction in readily releasable pool size from 22.4±5.3 to 9.1±1.3 fF/pF ($p<0.05$).

Similarly, overnight inhibition of p110γ with 40 nM AS605240 ablated the exocytotic response of human beta cells identified by positive insulin immunostaining (n=18 cells from 5 donors, $p<0.001$) **(Figure 18C,D)**, without affecting Ca^{2+} currents (-0.61±0.13 *versus* -0.69±0.19 pC/pF, n=15-18 cells from 5 donors). Consistent with an impairment of insulin granule exocytosis *per se*, inhibition of p110γ (40 nM AS605240) in human islets resulted in a 51% reduction in peak insulin secretion to depolarization by 50 mM KCl (n=11 groups from 4 donors, $p<0.05$) **(Figure 18E)**.

Direct infusion of Ca^{2+} into the cell is often used as a measure of the Ca^{2+}-dependent recruitment of granules and their subsequent exocytosis (Kanno et al., 2004). The capacitance response to infusion of 200 nM free Ca^{2+} was blunted by expression of sh-p110γ in both INS-1 832/13 and human beta cells **(Figure 18F-I)**. Upon knockdown of p110γ the exocytotic response at 30-60 seconds was ablated in the INS-1 832/13 (n=8, $p<0.01$) and human beta cells (n=7 cells from 2 donors, $p<0.05$).

Figure 17: p110γ expression, and effect of knockdown on exocytosis in INS-1 832/13 cell.

In panel **(A)**, expression of p110γ was confirmed by western blot of protein lysates from INS-1 832/13 cells, mouse islets and human islets and (*left*). Expression of p110γ, but not the related p110β, was reduced by an adenovirus-delivered sh-p110γ construct in INS-1 832/13 cells (*right*).

In panel **(B)**, the average expression levels of p110γ and p110β in the sh-p110γ INS-1 832/13 cells is shown normalized to β-actin and expressed as a percentage of the sh-scramble control.

Panel **(C)** shows capacitance and Ca^{2+} current recordings from INS-1 832/13 cells expressing sh-scramble (*black lines*) or sh-p110γ (*grey lines*).

In panels **(D)** and **(E)**, the average capacitance response is shown, normalized to cell size and Ca^{2+} current charge.

**-$p<0.01$.

(JK and GMP both contributed to the western blot experiments. GMP performed the electrophysiological experiments.)

Figure 17

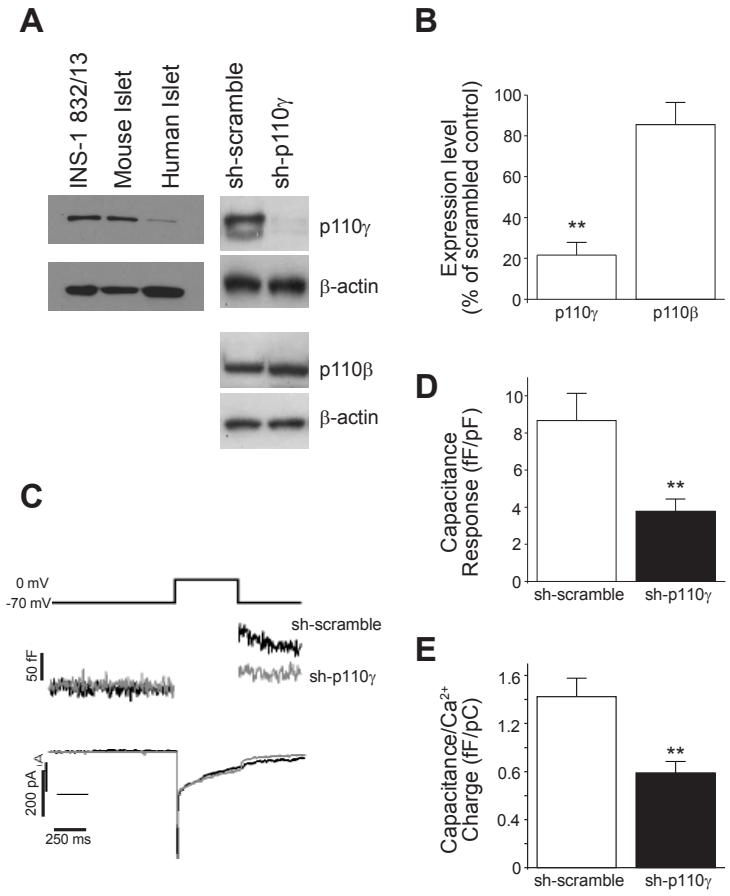
A
INS-1 832/13
Mouse Islet
Human Islet
sh-scramble
sh-p110γ
p110γ
β-actin
p110β
β-actin
B
Expression level
(% of scrambled control)
100
80
60
40
20
0
**
p110γ
p110β
C
0 mV
-70 mV
sh-scramble
sh-p110γ
50 fF
200 pA
250 ms
D
Capacitance
Response (fF/pF)
10
8
6
4
2
0
**
sh-scramble
sh-p110γ
E
Capacitance/Ca2+
Charge (fF/pC)
1.6
1.2
0.6
0.4
0
**
sh-scramble
sh-p110γ

Figure 18: Effect of p110γ knockdown or pharmacological inhibition on exocytosis and insulin secretion.

In panel **(A)** representative capacitance recordings are shown from INS-1 832/13 cells expressing sh-p110γ (*grey lines*) or sh-scrambled (*black lines*). Panel **(B)** shows the average capacitance response during each depolarization for cells expressing sh-p110γ (*black circles*) or sh-scrambled (*open circles*), and the total capacitance change over the depolarization train (*inset*).

In panel **(C)** representative capacitance recordings are shown from human β-cells, identified by positive insulin immunostaining, treated overnight with DMSO (*black lines*) or the p110γ inhibitor AS605240 (40 nM, *grey lines*). Panel **(D)** shows the average capacitance response during each depolarization for human β-cells treated overnight with DMSO (*open circles*) or the p110γ inhibitor AS605240 (40 nM, *black circles*).

In panel **(E)**, insulin secretion was measured by perifusion of isolated human islets following overnight treatment with DMSO (*open circles*) or 40 nM AS605240 (*black circles*).

In panel **(F)** exocytosis was stimulated in INS-1 832/13 cells expressing sh-p110γ or sh-scrambled by direct infusion of 200 nM free Ca^{2+} and observed as an increase in capacitance. A representative trace is shown. In panel **(G)** the average rate of capacitance increase at steady state (30-60 seconds) is shown.

Panels **(H)** and **(I)** show the same as **(F)** and **(G)**, except data is from human β-cells expressing sh-p110γ or the sh-scramble.

* $p<0.05$, ** $p<0.01$ and *** $p<0.001$

(GMP performed the electrophysiological experiments. JMF performed the secretion experiments.)

Figure 18

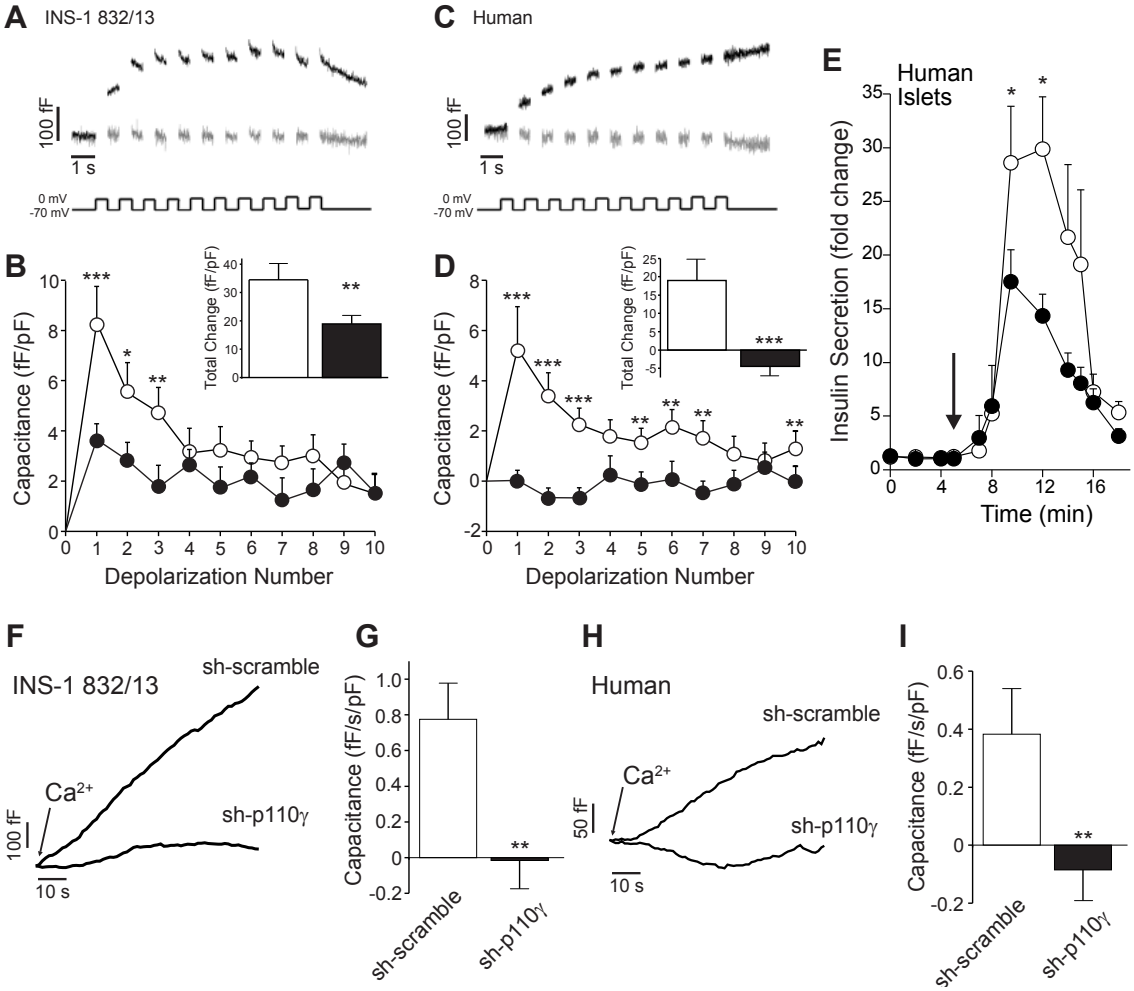
A
INS-1 832/13
100 fF
1 s
0 mV
-70 mV
B
Capacitance (fF/pF)
Depolarization Number
Total Change (fF/pF)
C
Human
D
E
Human Islets
Insulin Secretion (fold change)
Time (min)
F
INS-1 832/13
sh-scramble
sh-p110γ
Ca2+
100 fF
10 s
G
Capacitance (fF/s/pF)
H
Human
50 fF
I

3.4.2 Role of p110γ in secretory granule recruitment to the plasma membrane

We further examined the role of p110γ in insulin granule exocytosis by simultaneous TIRF and whole-cell capacitance measurements. In INS-1 833/15 cells expressing the granule marker VAMP-pHluorin the capacitance response was abolished following p110γ inhibition (40 nM AS605240) **(Figure 19A,B)**. Similarly, the exocytotic event frequency measured by TIRF was reduced by 62% (n=7, $p<0.001$) following inhibition of p110γ **(Figure 19C-E)**. Finally, after normalizing to the initial granule density inhibition of p110γ was no longer seen to blunt the exocytotic response **(Figure 19F)**, suggesting that the impaired exocytosis was likely not due to a reduced efficiency of Ca^{2+}-stimulated exocytosis *per se*.

We therefore examined the effect of p110γ knockdown on the density of membrane-associated insulin granules by targeting mCherry to secretory granules using neuropeptide Y (NPY) (Tsuboi and Rutter, 2003). TIRF microscopy revealed that knockdown of p110γ results in a 38 and 41% reduction in membrane-associated secretory granules in INS-1 832/13 (n=15-16, $p<0.001$) and human beta cells (n=29-30 cells from 4 donors, $p<0.001$), respectively **(Figure 20A,B)**, This was confirmed by electron microscopy in INS-1 832/13 cells **(Figure 20C,D)**, where inhibition of p110γ (40 nM AS605240) reduced the number of secretory granules near (<100 nm) the plasma membrane by 37% (n=55-56, $p<0.01$). Inhibition of p110γ was also associated with an increased ($p<0.05$) number of granules at >100 nm from the plasma membrane **(Figure 20D)**.

Figure 19: Effect of p110γ pharmacological inhibition on insulin granule recruitment in INS-1 cells.

INS-1 833/15 cells expressing a granule-targeted VAMP-pHluorin construct were simultaneously studied by whole-cell capacitance measurements and laser TIRF microscopy.

In panel **(A)**, a representative capacitance recording during a train of membrane depolarizations is shown from INS-1 833/15 cells treated overnight with 40 nM AS605240 (*grey lines*) or DMSO (*black lines*).

Panel **(B)**, shows the cumulative capacitance change over the depolarization train.

Panel **(C)** shows maximum intensity projections over the course of the 10sec depolarization protocol, illustrating exocytotic release sites in DMSO and AS605240 treated cells.

Panel **(D)** shows the rate of exocytotic events visualized during depolarization trains over time applied to INS-1 833/15 treated overnight with DMSO (*open circles*) or 40 nM AS605240 (*black circles*).

Panel **(E)** shows the total rate of exocytotic events observed by TIRF over the depolarization train.

Panel **(F)** shows the total rate of exocytotic events observed by TIRF over the depolarization train normalized to the initial granule number.

*** $p<0.001$

(GMP performed the electrophysiological and imaging experiments)

Figure 19

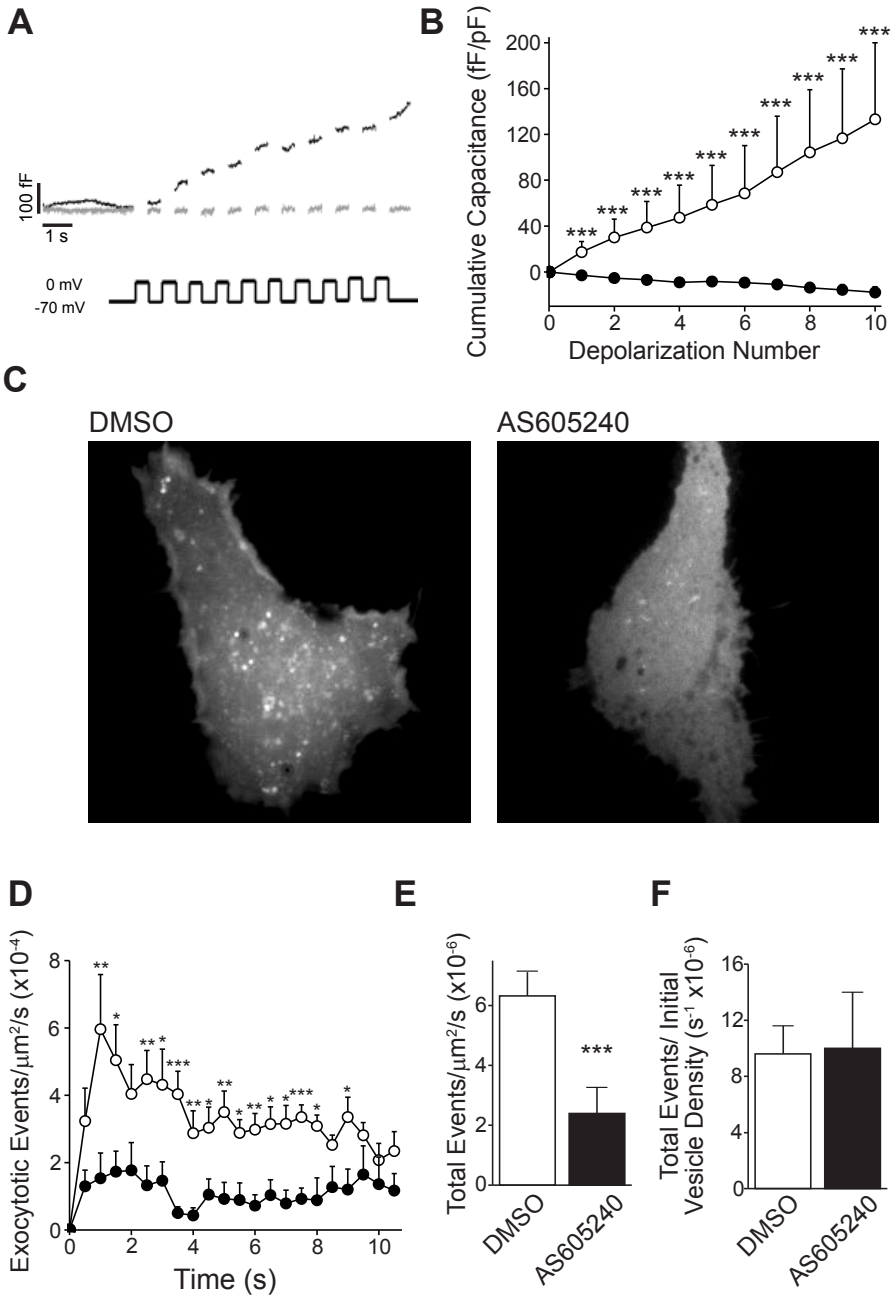
A
100 fF
1 s
0 mV
-70 mV
B
Cumulative Capacitance (fF/pF)
Depolarization Number
C
DMSO
AS605240
D
Exocytotic Events/μm²/s (x10⁻⁴)
Time (s)
E
Total Events/μm²/s (x10⁻⁶)
DMSO
AS605240
F
Total Events/ Initial Vesicle Density (s⁻¹ x10⁻⁶)
DMSO
AS605240

Figure 20: Effect of p110γ pharmacological inhibition or knockdown on insulin granule localization in INS-1 cells and human beta cells.

Panel **(A)** shows representative images of membrane-associated granules imaged by TIRF microscopy from INS-1 832/13 cells and human beta cells expressing either sh-scramble or sh-p110γ together with the granule-targeted NPY-mCherry.

Panel **(B)** shows the average membrane-associated granule density from the TIRF images, normalized to total membrane area.

In panel **(C)**, representative electron micrographs were obtained from INS-1 832/13 cells under control conditions (DMSO) or following inhibition of p110γ (40 nM AS605240).

Panel **(D)** shows the average number of granules per section located less-than, and greater-than, 100 nm from the plasma membrane.

*-$p<0.05$, **-$p<0.01$ and *** $p<0.001$

(GMP performed the TIRF imaging experiments; GMP, JK and BJB contributed to TIRF data analysis, JK prepared all sampled for EM experiments and analyzed al EM data)

Figure 20

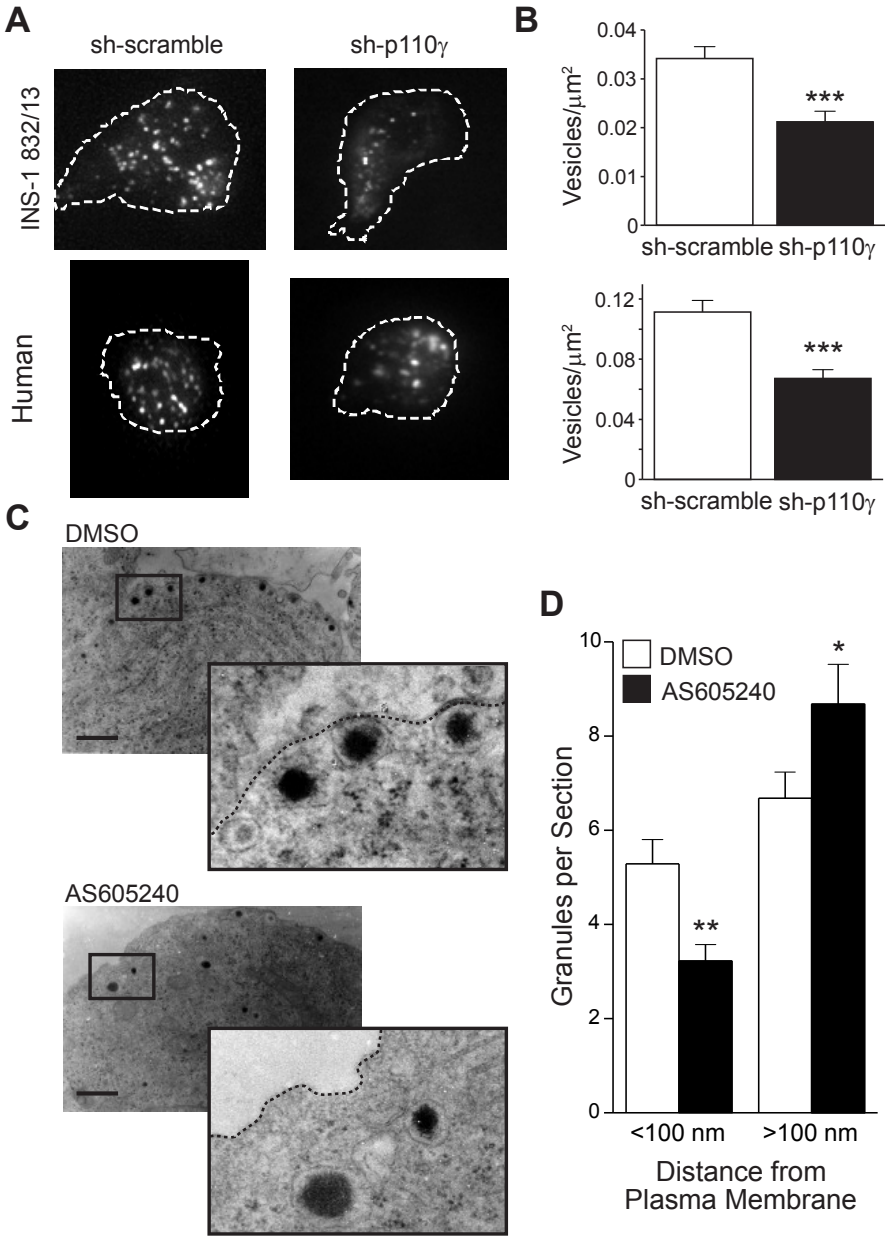
A
sh-scramble
sh-p110γ
INS-1 832/13
Human
B
Vesicles/μm²
0.04
0.03
0.02
0.01
0
***
sh-scramble sh-p110γ
0.12
0.08
0.04
0
***
sh-scramble sh-p110γ
C
DMSO
AS605240
D
DMSO
AS605240
Granules per Section
10
8
6
4
2
0
**
*
<100 nm
>100 nm
Distance from
Plasma Membrane

3.4.3 Role of p110γ in regulation of cortical F-actin density

Since cortical actin network integrity is an important determining factor in secretory granule recruitment and docking (Burgoyne and Cheek, 1987; Jewell et al., 2008; Li et al., 1994) we studied the effect of p110γ inhibition on cortical F-actin in INS-1 832/13 cells, human islets and mouse beta cells. The cortical F-actin network in INS-1 832/13 cells, assessed by TIRF microscopy, was increased after inhibition of p110γ (40 nM AS605240) **(Figure 21A)**. This was associated with a 53% reduction in the density of NPY-mCherry labeled granules at the plasma membrane (n=20, $p<0.01$). Western blotting for purified F- and total globular (G-) actin confirmed that F-actin, as a proportion of total actin, was increased by p110γ inhibition in INS-1 832/13 cells (n=3, $p<0.05$) and human islets (n=3 donors, $p<0.05$) **(Figure 21B,C)**.

The PtdIns(3,4,5)P_3 phosphatase activity of PTEN antagonizes PI3K signaling. We therefore examined the effect of p110γ inhibition (40 nM AS605240) on F-actin in control mouse beta cells (RIP-cre$^+$) and those lacking PTEN (RIP-cre$^+$/PTEN$^{fl/fl}$) (Kulkarni et al., 1999b). Cortical F-actin was visualized by epi-fluorescence **(Figure 22A)**. Analysis by random line scans **(Figure 22A *bottom*)** demonstrated that peak F-actin staining was increased 1.7-fold ($p<0.001$, n=10-11) by p110γ inhibition in control beta cells, but not in beta cells lacking PTEN (n=10-11) **(Figure 22)**.

Figure 21: Effect of p110γ pharmacological inhibition on cortical F-actin density.

In panel **(A)**, INS-1 832/13 cells expressing the granule targeted NPY-mCherry (*red*) were treated overnight with DMSO or AS605240 (40 nM) and subsequently stained for F-actin with Alexa 488 conjugated phalloidin (*green*) and imaged by TIRF microscopy. In panel **(B)**, the content of filamentous actin (F) and free globular-actin (G) was determined by immunoblotting of cell lysates from INS-1 832/13 cells and human islets treated overnight with DMSO or AS605240 (40 nM). Acute (10 minute) treatment with phalloidin (1 μM) or latrunculin (10 μM) were used as controls for actin polymerization and de-polymerization, respectively.

In panel **(C)**, the F-actin content is shown as a percentage of total actin.

*-$p<0.05$

(JK and GMP performed the imaging experiments; GMP performed the western blot experiments)

Figure 21

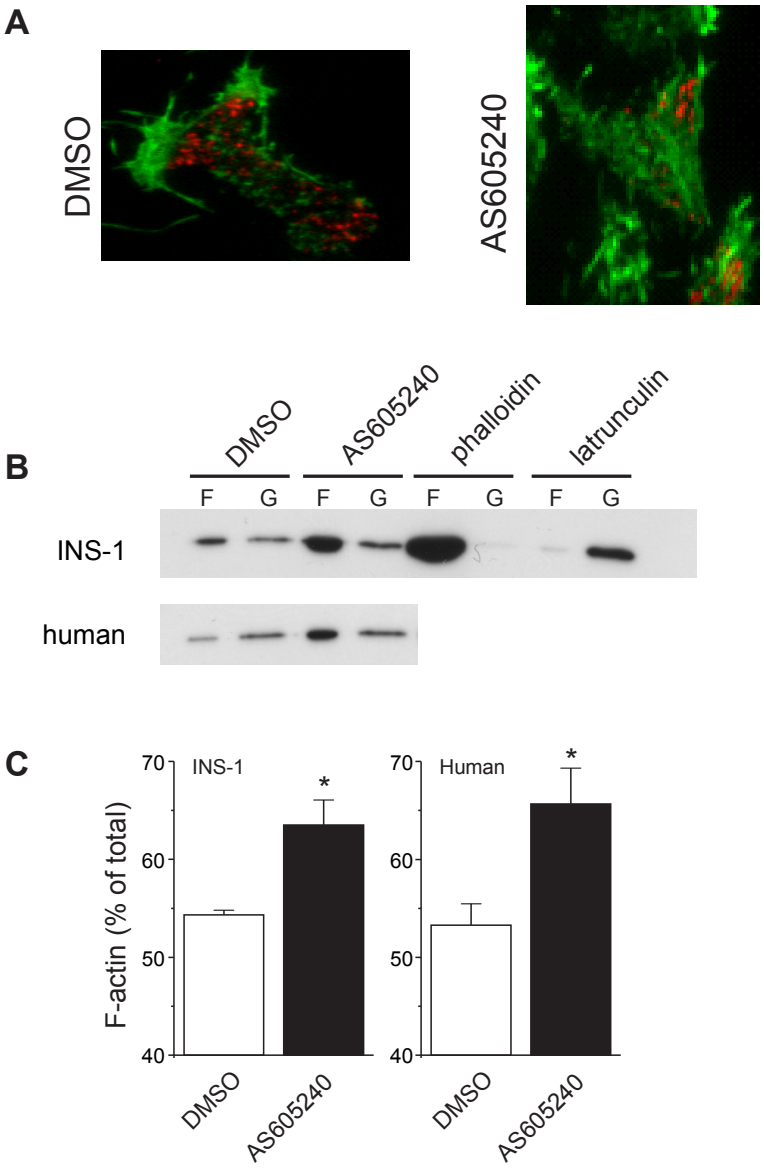
A
DMSO
AS605240
B
DMSO
AS605240
phalloidin
latrunculin
F G F G F G F G
INS-1
human
C
INS-1
Human
F-actin (% of total)
70
60
50
40
*
*
DMSO
AS605240
DMSO
AS605240

Figure 22: Effect of p110γ pharmacological inhibition on cortical F-actin density following PTEN deletion.

In panel **(A)**, beta cells from RIP-cre^{+} control mice or RIP-cre^{+}/PTEN$^{fl/fl}$ mice lacking the lipid phosphatase PTEN were stained for F-actin with Alexa Fluor 488-conjugated phalloidin and examined by epi-fluorescence. Representative images are shown at top, with representative intensity line scans for F-actin staining intensity below.

In panel **(B)**, the average F-actin peak intensities are shown.

**-$p<0.01$

(GMP performed imaging experiments, JK and BJB contributed to data analysis)

Figure 22:

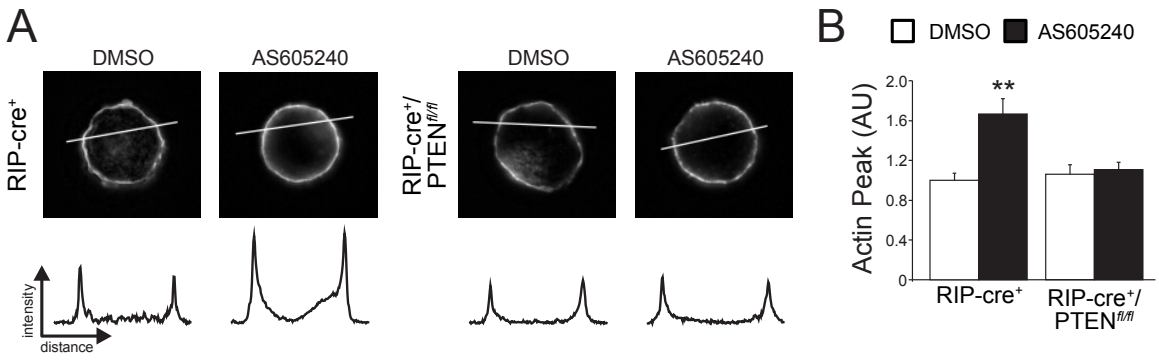
A
DMSO
AS605240
DMSO
AS605240
RIP-cre+
RIP-cre+/ PTENfl/fl
intensity
distance
B
DMSO
AS605240
Actin Peak (AU)
2.0
1.6
1.2
0.8
0.4
0
**
RIP-cre+
RIP-cre+/ PTENfl/fl

3.4.4 Acute F-actin disruption restores vesicle docking and exocytosis following PI3Kγ inhibition

Since the reduction in membrane-associated granules is associated with increased cortical F-actin, we examined whether disruption of F-actin could restore the membrane localization of secretory granules and exocytosis following p110γ inhibition. Inhibition of p110γ (40 nM AS605240) increased F-actin staining by 2-fold (n=25-26, $p<0.001$) **(Figure 23A,B)**. This was associated with a 37% (n=25-26, $p<0.001$) reduction in membrane-associated secretory granules, labeled in this experiment with a granule-targeted IAPP-mCherry construct.

As cAMP inhibits actin polymerization through PKA-dependent phosphorylation of monomeric actin (Ohta et al., 1987) and an indirect inhibition of the Rho family of GTPases (reviewed in (Howe, 2004; Roscioni et al., 2008)), we examined whether increased cAMP could reduce F-actin density and rescue granule recruitment following p110γ inhibition. Indeed, acute treatment with the cAMP-raising agent forskolin (5 □M, 10 minutes) reversed the effects of p110γ inhibition on cortical F-actin (n=34, $p<0.001$) and membrane granule density (n=30, $p<0.001$) in the INS-1 832/13 cells **(Figure 23A,B).**

Additionally, 10-minute treatment with the actin-depolymerizing agent Latrunculin B (10 μM) reduced actin staining in both control (n=28, $p<0.001$) and AS605240-treated (n=21, $p<0.001$) INS-1 832/13 cells **(Figure 23A,B).** This acute de-polymerization of F-actin increased the density of membrane-associated vesicles by 2.2-fold compared with p110γ inhibition alone (n=16, $p<0.001$) **(Figure 23A,B).** Thus,

secretory granules remain present in the cell following p110γ inhibition and can reach the plasma membrane upon disruption of the cortical actin barrier.

Finally, acute forskolin treatment (5 μM, 10 minutes, n=25) restored membrane-proximal granule density to control levels in INS-1 832/13 cells expressing sh-p110γ ($p<0.05$) **(Figure 24A).** Inclusion of cAMP (100 μM) in the patch-clamp pipette resulted in complete restoration of exocytosis following p110γ knockdown (n=10) **(Figure 24B,C).** Similarly the capacitance response of INS-1 832/13 **(Figure 24D,E)**, and human beta cells **(Figure 24F,G)** to a single 500 ms depolarization from -70 to 0 mV, which was blunted in following p110γ inhibition (n=14-20, $p<0.01$ and n=15-17 cells from 5 donors, $p<0.001$), could be rapidly reversed by intracellular dialysis of either 100 μM cAMP (INS-1, n=14; human, n=9 from 5 donors) or 10 μM latrunculin (INS-1, n=9; human n=12 from 5 donors). Thus, depolymerization of actin and restoration of the membrane-associated granule pool is sufficient to rescue exocytosis following p110γ inhibition.

Figure 23: Effect of forced F-actin depolymerization on membrane targeting of granules following p110γ inhibition.

Panel **(A)** shows representative INS-1 832/13 cells expressing the granule-targeted IAPP-mCherry construct (*red*) treated overnight with DMSO or 40 nM AS605240, then for 10-minutes with forskolin (5 μM) or latrunculin (10 μM) as indicated, and imaged by TIRF microscopy following staining for actin (*green*).

Panel **(B)** shows intensity line scans, obtained in a double-blinded manner, for actin from the regions indicated in panel **(A)**.

Panel **(C)** shows average actin line scan area under the curve.

Panel **(D)** shows average membrane associated granule density.

-$p<0.01$ and *-$p<0.001$ compared with control unless indicated otherwise.

(JK performed imaging experiments and analyzed data)

Figure 23

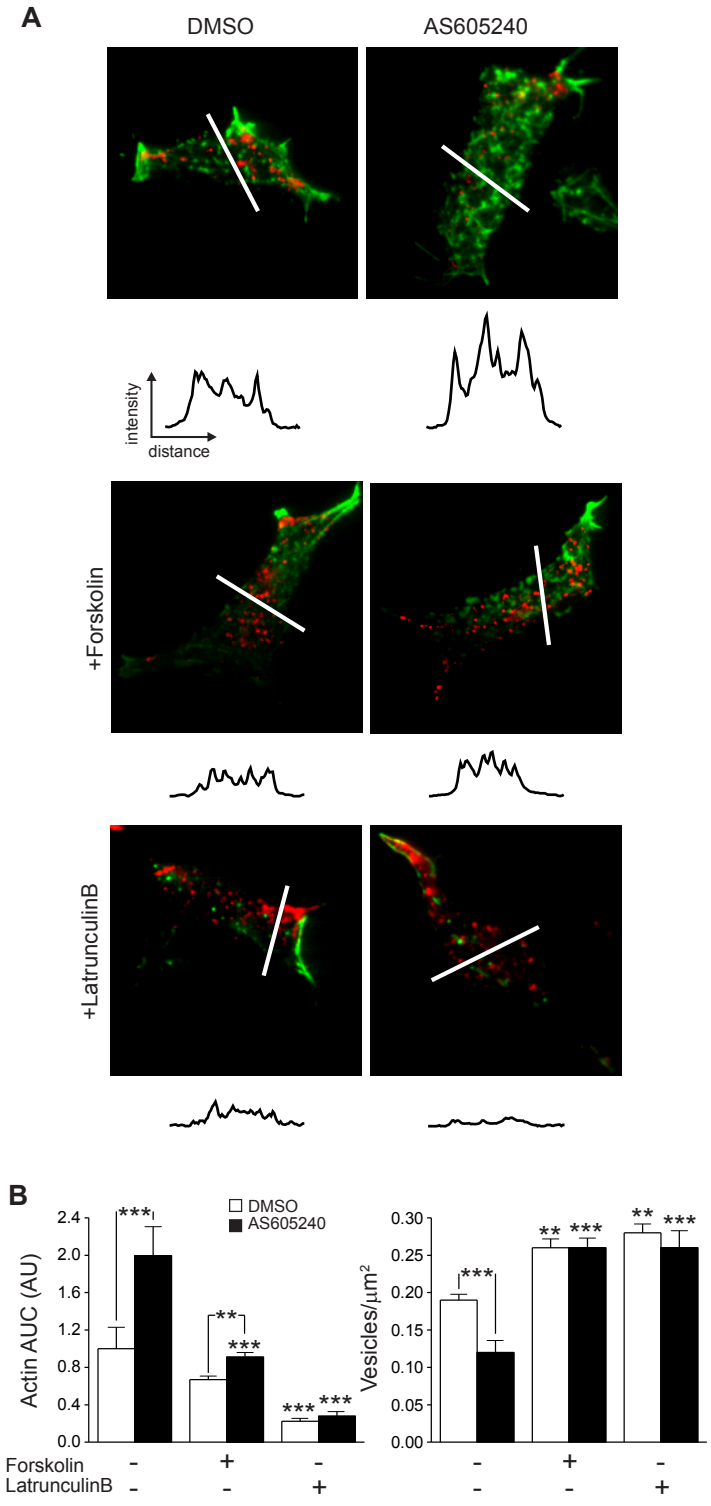
A
DMSO
AS605240
intensity
distance
+Forskolin
+LatrunculinB
B
DMSO
AS605240
Actin AUC (AU)
Vesicles/µm²
Forskolin
LatrunculinB

Figure 24: Effect of forced F-actin depolymerization on exocytosis following p110γ inhibition.

In panel **(A)**, membrane-associated secretory granules were visualized by TIRF microscopy in INS-1 832/13 cells co-expressing an NPY-mCherry and either sh-scramble or sh-p110γ. Addition of forskolin (5 μM, 10-minutes) resulted in the recovery of membrane-associated secretory granules.

In panel **(B)**, representative membrane capacitance traces are shown from INS-1 832/13 cells expressing sh-scramble (*black lines*) or sh-p110γ (*grey lines*) with 100 μM cAMP included in the patch pipette.

Panel **(C)** shows the average capacitance response for each depolarization and the total response over the course of the depolarization train (*inset*) for cells expressing sh-scramble (*open*) or shp110γ (*black*) with cAMP in the patch pipette. The response from cells expressing sh-p110γ in the absence of cAMP is also shown for comparison (*grey*).

Panel **(D)** shows representative membrane capacitance responses to a single depolarization from -70 to 0 mV by INS-1 832/13 cells treated with DMSO or the p110γ inhibitor alone or with 100 μM cAMP or 10 μM Latrunculin B in the patch pipette.

Panel **(E)** shows average capacitance responses.

Panels **(F)** and **(G)** are the same as **(D)** and **(E)**, but with human beta cells.

-$p<0.01$ and *-$p<0.001$ compared with control unless indicated otherwise.

(GMP performed imaging and electrophysiological experiments in panels A and B (and analyzed data); JK performed electrophysiological experiments (and analyzed data) in panels C and D)

Figure 24

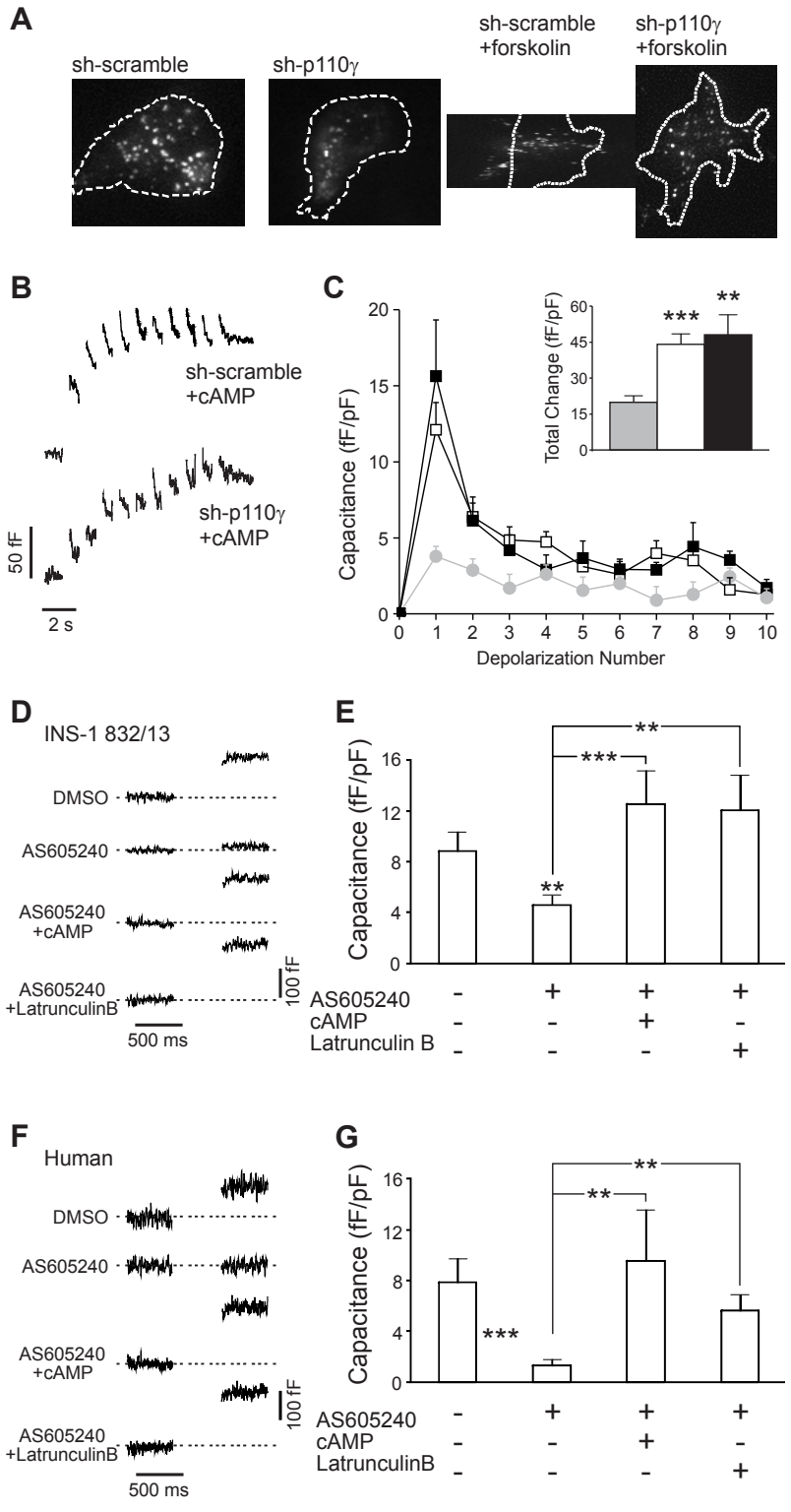
A
sh-scramble
sh-p110γ
sh-scramble +forskolin
sh-p110γ +forskolin
B
sh-scramble +cAMP
sh-p110γ +cAMP
50 fF
2 s
C
Capacitance (fF/pF)
Depolarization Number
Total Change (fF/pF)
***
**
D
INS-1 832/13
DMSO
AS605240
AS605240 +cAMP
AS605240 +LatrunculinB
100 fF
500 ms
E
Capacitance (fF/pF)
AS605240
cAMP
Latrunculin B
F
Human
DMSO
AS605240
AS605240 +cAMP
AS605240 +LatrunculinB
100 fF
500 ms
G
Capacitance (fF/pF)
AS605240
cAMP
LatrunculinB

3.5 DISCUSSION

Previous studies have demonstrated that knockout of p110γ results in a blunted glucose-stimulated insulin response, particularly during the first phase of secretion (MacDonald et al., 2004). We have now examined the underlying mechanism for regulation of insulin secretion by p110γ. This PI3K isoform positively regulates the size of the membrane-associated pool of insulin granules, likely through the modulation of cortical F-actin density. Therefore we now identify a previously un-described role for PI3Kγ in the regulation of cortical actin and targeting of insulin granules to the plasma membrane in pancreatic beta cells.

The tyrosine kinase activated isoforms of PI3K (class 1A) account for as much as 80% of islet PI3K activity (Eto et al., 2002). The class 1B isoform, p110γ is expressed in insulinoma cells, rodent islets and human islets ((MacDonald et al., 2004) and **Figure 19**) where it contributes a minor fraction of PI3K activity (Trümper et al., 2001). The non-selective nature of commonly used PI3K inhibitors may account for earlier findings ascribing both negative (Eto et al., 2002; Hagiwara et al., 1995; Zawalich et al., 2002) and positive (Straub and Sharp, 1996a; Straub and Sharp, 1996b) roles to PI3K in insulin secretion. Indeed, the various PI3Ks may play distinct roles in the regulation of insulin secretion in an isoform-specific manner (Kolic et al., 2013). This is further supported by the observation that, while p110γ displays basal activity (Sasaki et al., 2007), it is glucose-independent in INS-1 cells and thus likely does not contribute to increased PI3K activity following autocrine insulin feedback (Barker et al., 2002). This is consistent with our finding that p110γ inhibition did not blunt high K^+-stimulated PtdIns(3,4,5)P_3 formation (see Materials and Methods).

Consistent with the lack of first phase secretion in the p110γ knockout mouse (MacDonald et al., 2004), we observed a reduction of the early exocytotic response during membrane depolarization in both INS-1 and human beta cells following p110γ knockdown or pharmacological inhibition. This was paralleled by a similar reduction in the peak insulin secretory response to KCl following p110γ inhibition in human islets. However, we did not examine whether second phase of insulin secretion was affected by p110γ inhibition or knockdown. Reduced exocytosis was not due to the inhibition of voltage-dependent Ca^{2+} channel activity, and defective Ca^{2+} stimulated exocytosis was also demonstrated in response to direct Ca^{2+} infusion following knockdown of p110γ. While the lack of exocytotic response to Ca^{2+} infusion during latter time points (i.e. 30-60 seconds) may be indicative of a reduced Ca^{2+}-induced granule recruitment, since the readily releasable pool of granules is expected to be already depleted (Kanno et al., 2004), the exact role of p110γ in glucose- and Ca^{2+}-dependent granule recruitment *per se* remains unknown. Nonetheless, these results suggest a reduction in the size of the readily releasable granule pool and blunted refilling during prolonged Ca^{2+} stimulation.

There was no increase, and often a net negative change, in membrane capacitance in many experiments following p110γ inhibition. This was most noticeable following pharmacological inhibition with AS605240, likely due to a more complete inhibition of p110γ compared with the shRNA approach. The absence of a capacitance response is not necessarily indicative of an absence of exocytosis however, since this reports the net balance of exocytosis and endocytosis. In the present context, since PtdIns(4,5)P_2 is an important regulator of endocytosis (Schmidt et al., 1985; Sun et al., 2007; Zoncu et al., 2007), a reduced capacitance response may result from an increased Ca^{2+}-stimulated

endocytosis (Tsuboi and Rutter, 2003). To address this we simultaneously monitored exocytosis visually while measuring whole-cell capacitance changes in INS-1 cells. In these experiments, the exocytotic release of granule content was indeed blunted following p110γ inhibition **(Figure 19)**.

Reduced exocytosis can be explained either by an inability of membrane-associated granules to undergo exocytosis in response to a Ca^{2+} stimulus, or simply by a lack of membrane-associated granules. While impaired synaptic-like vesicle exocytosis may also contribute, the present data clearly demonstrates a reduced membrane-localized insulin granule pool by EM analysis, consistent with our TIRF imaging. This is not secondary to reduced insulin content since this is increased in the p110γ knockout mice (MacDonald et al., 2004) and following p110γ knockdown in INS-1 cells (Li et al., 2006); and acute disruption of F-actin can rapidly recover insulin granules at the plasma membrane **(Figure 23)**.

The integrity of the cortical F-actin network is an important determinant of granule recruitment to the plasma membrane in chromaffin (Burgoyne and Cheek, 1987) and beta cells (Jewell et al., 2008; Li et al., 1994). The cortical actin network can act as a physical barrier to granule translocation (Rutter and Hill, 2006), and can inhibit granule docking through the direct occlusion of Syntaxin-4 binding sites (Jewell et al., 2008). Indeed, decreased membrane-associated insulin granule density following p110γ inhibition is associated with increased F-actin **(Figures 21-23)**. While we have not examined the time-course of F-actin staining, we have observed that overnight inhibition of p110γ is required to blunt the exocytotic response. We ascribe this to the time necessary for increased F-actin to cause the depletion of the membrane-associated

granule pool. Thus, the overall reduction of membrane-associated granules following p110γ inhibition is likely related to the rate at which pre-existing membrane-associated granules are either basally released or internally recycled. A functional role for increased F-actin density in the inhibition of granule trafficking to the plasma membrane is demonstrated by the ability of actin depolymerization to acutely restore granule targeting and exocytosis **(Figure 23)**.

Only a minor fraction of the PI3K activity in insulin secreting cells is contributed by p110γ (Trümper et al., 2001) making it difficult to determine the effect of p110γ inhibition on whole-cell phosphoinositide levels. A role for p110γ lipid kinase activity in the regulation of cortical F-actin density is, however, indicated by the ability of the ATP-competitive inhibitor AS605240 (Camps et al., 2005) to mimic the effect of p110γ knockdown and the reversal of this by deletion of the PtdIns(3,4,5)P_3 phosphatase PTEN. The exact mechanism by which p110γ regulates cortical F-actin remains unclear, as phosphoinositides are complex regulators of cytoskeletal rearrangement (Insall and Weiner, 2001; Tsakiridis et al., 1999). It is interesting to note that the Rho GTPases, such as Rac1 and Cdc42 which have important roles in insulin secretion (Wang et al., 2007) also regulate actin (Yin and Janmey, 2003), and are activated by the lipid products of PI3K (Ridley, 2006; Welch et al., 2003). Additionally, increased PtdIns(4,5)P_2, which may be secondary to p110γ inhibition, could lead to actin assembly through the dissociation of actin capping proteins (including gelsolin) and/or activation of the WASP family proteins and the Arp2/3 complex (Schmidt and Hall, 2002). Thus, several potential actin-regulating proteins may act downstream of p110γ.

The p110γ isoform exhibits significant basal lipid kinase activity (Sasaki et al., 2007). While it is unlikely that p110γ is a key mediator of dynamic actin remodeling in response to glucose since it is not activated upon glucose-stimulation (Trümper et al., 2001), a role in stimulated granule translocation cannot be ruled out since this PI3K isoform can be activated by the incretin hormone GIP in INS-1 cells (Trümper et al., 2001) Furthermore, insulin secretion from HIT-T15 cells stimulated by GIP and the related VIP and PACAP peptides can be significantly blunted by wortmannin independent of cAMP generation *per se* (Straub and Sharp, 1996a; Straub and Sharp, 1996b), similar to what we have observed with forskolin and the direct infusion of cAMP.

In summary, we now demonstrate that the p110γ isoform of PI3K is necessary for insulin granule recruitment to the plasma membrane and maintenance of a membrane-associated readily releasable pool of secretory granules in model cell lines and in humans. This is mediated at least in part through the regulation of cortical F-actin, and represents a previously unknown function for a non-classical PI3K in the control of pancreatic beta cell function.

3.6 CONCLUDING REMARKS

The studies described here confirmed the expression p110γ at the protein level in mouse and human islets, as well as in a rat insulin secreting cell line (INS-1 832/13). PI3Kγ has been well studied in the context of various autoimmune and inflammatory diseases. Pharmacological inhibition of p110γ in mice results in a reduced susceptibility to autoimmune and inflammatory conditions such as rheumatoid arthritis (Okkenhaug, 2013; Okkenhaug and Vanhaesebroeck, 2003), and selective p110γ inhibitors have been called the "aspirin of the 21st century" (Rückle et al., 2006).

However, PI3Ks have a long recognized role in glucose homeostasis and insulin signaling (Okkenhaug and Vanhaesebroeck, 2003; Vanhaesebroeck et al., 2012). PI3Kγ knockout mice show impairment in insulin secretion, and shRNA-mediated knockdown of p110γ in INS-1E cells similarly decreases GSIS (Li et al., 2006). An increase in insulin content is also seen in islets from PI3Kγ$^{-/-}$ mice, and in INS-1E cells where p110γ has been knocked down (Li et al., 2006). Our studies confirm that p110γ shRNA-mediated knockdown, or pharmacological inhibition impairs insulin secretion and exocytosis, and show that this is mediated in part through the regulation of cortical F-actin and granule recruitment to the plasma membrane. However, we did not see an increase in insulin content following p110γ shRNA-mediated knockdown. Whilst we do not understand the exact reason for this discrepancy, a simple explanation may be due to the difference in cell clonal lines studied (INS-1E vs. INS-1 832/13)

Thus, given the popularity of PI3Kγ-specific inhibitors, monitoring for hyperglycemia may be advised when these agents are used in humans, given the secretory defects detected in our (and other) studies.

The exact mechanism by which p110γ regulates cortical F-actin and granule recruitment to the plasma membrane remains unclear. Whilst specific inhibition of class 1A PI3Ks is associated with a slight decrease in the SNARE proteins SNAP-25 and Syntaxin (Aoyagi et al., 2012), we did not examine the expression levels of either protein, or other SNARE-related proteins following the inhibition or knockdown of the class 1B PI3Kγ isoform. However, live cell TIRF imaging indicated that whilst there was a decrease in the number of exocytotic events following p110γ inhibition, when normalized to initial vesicle density, there was no difference in the number of exocytotic events, again suggesting that the increase of cortical F-actin density limits the recruitment of vesicles to the plasma membrane. This is supported by the need for overnight pharmacological inhibition of p110γ to observe any changes in granule number.

Several potential actin-regulating proteins (such as the Rho GTPases, Rac1 and Cdc42 which have important roles in insulin secretion also regulate actin dynamics) may act downstream of p110γ. It is also interesting to note that the lipid products of PI3K activate these Rho GTPases. Thus the next chapter investigates the possible role of the small GTPase protein Rac1 in p110γ-mediated regulation of cortical F-actin.

Chapter 4

Insulin secretion induced by glucose-dependent insulinotropic polypeptide requires PI3Kγ in rodent and human beta cells

A version of the following chapter is in revisions with the Journal of Biological Chemistry.

Jelena Kolic, Aliya F. Spigelman, Alannah M. Smith, Jocelyn E. Manning Fox, and Patrick E. MacDonald

Contributions by co-authors to the figures presented are stated in the figure legends, accompanied by the appropriate co-authors initials.

4.1 ABSTRACT

PI3Kγ, a G-protein coupled class 1B phosphoinositol-3-kinase, exhibits a basal glucose-independent activity in beta cells and can be activated by the glucose-dependent insulinotropic polypeptide (GIP). We therefore investigated the role of the PI3Kγ catalytic subunit (p110γ) in insulin secretion and beta cell exocytosis stimulated by GIP. We inhibited p110γ with AS604850 (1 μmol/l), or depleted it using an shRNA adenovirus in mouse and human islets and beta cells. Inhibition of PI3Kγ blunted the exocytotic and insulinotropic response to GIP receptor activation, while responses to the glucagon-like peptide 1 (GLP-1) receptor agonist exendin-4 (Ex-4) were unchanged. Downstream we find that GIP, much like glucose stimulation, activates the small GTPase protein Rac1 to induce actin remodeling. Inhibition of PI3Kγ blocked these effects of GIP. While Ex-4 could also stimulate actin remodeling, this was not prevented by p110γ inhibition. Finally, forced actin depolymerization with Latrunculin B restored the exocytotic response of beta cells to GIP during PI3Kγ inhibition, demonstrating that the loss of GIP-induced actin depolymerization was indeed limiting exocytosis.

4.2 INTRODUCTION

Both rodent and human beta cells express G-protein coupled receptors that are activated by peptide hormones of the secretin family: GIP (glucose dependent insulinotropic peptide) and GLP-1 (glucagon-like peptide-1) (Dillon et al., 1993; Gremlich et al., 1995; Thorens et al., 1993; Usdin et al., 1993; Volz et al., 1995). These are released from the intestine following a nutrient stimulus, and act to increase insulin secretion from pancreatic beta cells (Drucker, 2006; Holst and Gromada, 2004; Mojsov et al., 1987; Pederson and Brown, 1976).

Pathological conditions, such as diabetes and metabolic syndrome, are associated with disturbances in the incretin-signaling pathway (Knop et al., 2007; Nauck et al., 1993a; Vilsbøll et al., 2001). Whilst still controversial, a number of studies suggest that secretion of GIP (but not its incretin effect) is preserved in T2D (Calanna et al., 2013; Nauck et al., 1993a; Vilsbøll et al., 2001), whilst the incretin effect of GLP-1 is maintained, but its secretion is blunted (Nauck et al., 1993a; Nauck et al., 1986; Vilsbøll and Knop, 2007; Vilsbøll et al., 2001).

Both GIP and GLP-1 mediate their incretin effect by binding to their respective 7-transmembrane domain G-protein coupled receptors (GIP-R and GLP1-R) (Dillon et al., 1993; Gremlich et al., 1995; Kapeller et al., 1994; Thorens, 1992). GIP-R and GLP1-R activation leads to the activation of adenylate cyclase, and a subsequent rise in intracellular cAMP. This potentiates insulin through both PKA, and the guanine nucleotide exchange factor Epac, and an increase in cytosolic Ca^{2+} (Drucker, 2013; Roscioni et al., 2008; Seino et al., 2009; Song et al., 2011; Yabe and Seino, 2011).

Certain anitdiabetic drugs, such as Exenatide, exploit the GLP-1 pathway by activating the GLP-1 receptor (Barnett, 2007; Edwards, 2004).

Class 1 Phosphatidylinositol 3-OH kinases (PI3Ks) are implicated in incretin receptor signaling (Friedrichsen et al., 2006; Straub and Sharp, 1996b; Trümper et al., 2001). The non-selective PI3K inhibitor wortmannin partially inhibits GIP-stimulated insulin secretion in a clonal beta cell line, in a manner independent of cAMP generation (Straub and Sharp, 1996b). Whilst the best studied PI3Ks (type 1A) are activated through tyrosine kinase receptors (Kaneko et al., 2010), the lone type 1B PI3K isoform PI3Kγ is activated by G-protein βγ subunits (Stoyanov et al., 1995). Furthermore, GIP has previously been shown to directly activate PI3Kγ activity in INS-1 cells, as measured by an increase in the production of its main phosphorylation product PtdIns(3,4,5)P_3 (Trümper et al., 2001). We demonstrated previously that PI3Kγ is required for a robust insulin secretory response by promoting actin depolymerization and insulin granule recruitment to the plasma membrane (Pigeau et al., 2009).

Given the importance of incretin action to secretory dysfunction in T2D, we now examine the requirement for PI3Kγ in incretin-stimulated insulin secretion. We demonstrate that pharmacological inhibition, or shRNA-mediated knockdown of p110γ impairs the insulinotropic effects of GIP-R (but not GLP-1-R) activation in mouse and human islets. We show that GIP is a potent stimulator of insulin granule exocytosis, an effect that is blunted with p110γ inhibition or knockdown. Furthermore, we show that p110γ inhibition prevents GIP-induced actin depolymerization, likely by preventing activation of the small GTPase protein Rac1. Finally, we show that forced actin depolymerization restores the insulinotropic effects of GIP in cells lacking functional

p110γ. Thus, we demonstrate that in addition to the classical cAMP pathway, PI3K signaling through p110γ is required for the full insulinotropic effect of GIP.

4.3 MATERIALS AND METHODS

Cells and Cell Culture

Islets from male C57/BL6 mice were isolated by collagenase digestion and then handpicked. Human islets, from 14 healthy donors (53 +/- 5 years of age), were from either the Clinical Islet Laboratory at the University of Alberta, or the IsletCore program at the Alberta Diabetes Institute: islets were dispersed to single cells in Ca^{2+}-free buffer. INS-1 832/13 cells were a gift of Prof. Christopher Newgard (Duke University). Islet and cell culture was as described previously (Kolic et al., 2013; Pigeau et al., 2009). All studies were approved by the Animal Care and Use Committee and the Human Research Ethics Board at the University of Alberta.

DNA and Adenovirus Constructs

The p110γ shRNA and scrambled control sequence were previously published (Pigeau et al., 2009). Expression was via recombinant adenovirus produced by transferring the expression cassettes into the Adeno-X viral vector (Clontech) followed by adenovirus production in HEK293 cells as previously described.

Pharmacologic Inhibitors and Peptides

AS604850 (2,2-Difluoro-benzo[1,3]dioxol-5-ylmethylene)-thiazolidine-2,4-dione) (Selleckchem, Houston, TX) is a selective, competitive inhibitor of p110γ (IC_{50} = 250 nmol/l for p110γ *versus* 4.5 μmol/l for p110α, and > 20 μmol/l for p110β) (Camps et al., 2005). It exhibits no notable activity against a wide array of kinases at concentrations of 1 μmol/l. Latrunculin B, a potent actin-depolymerizing agent was from Sigma Aldrich Canada (Oakville, Canada). GIP and GLP-1 (7-36) peptides were from AnaSpec

(Fremont, CA). Exendin-4 was from Sigma Aldrich Canada (Oakville, Canada).

Immunoblotting

Cell lysates were subjected to SDS-PAGE and transferred to polyvinylidene difluoride membranes (Millipore, Billerica, MA), probed with primary antibodies (anti-p110α, anti-p110β, anti-p110γ [Cell Signaling Technology, Beverly, MA], anti-β-actin [Santa Cruz Biotechnology, Santa Cruz, CA], anti-Rac1 [Cytoskeleton, Denver, CO]). Detection was with peroxidase-conjugated secondary anti-rabbit and anti-mouse antibodies (GE Healthcare, Mississauga, Canada), and visualization by chemiluminescence (ECL-Plus; GE Healthcare, Mississauga, Canada) and exposure to X-ray film (Fujifilm, Tokyo, Japan).

Rac1 Activation Assay

INS-1 cells were treated overnight with AS604850 (1 μmol/l) (or DMSO vehicle). Cells were pre-incubated for 2 hours in 1 mmol/l glucose Krebs ringer buffer (KRB) (in mmol/l: 115 NaCl, 5 KCl, 24 $NaHCO_3$, 2.5 $CaCl_2$, 1 $MgCl_2$, and 10 HEPES; pH 7.4). Cells were then stimulated for 25 min with either 1 or 16.7 mmol/l glucose KRB. For GIP stimulation experiments, 100 nmol/l GIP was included in the 16.7 mmol/l glucose KRB. Rac1 activity was determined with glutathione *S*-transferase (GST)-P21-activated kinase binding domain (GST-PBD) as described in the Rac1 Pull Down Activation Biochem Kit manual (Cytoskeleton, Inc., Denver, CO).

Insulin Secretion Measurements

Islets (either mouse or human) were treated overnight with 1 μmol/l AS604850, (or vehicle), or infected with a p110γ shRNA adenovirus (or scrambled control) for 72

hours. Static insulin secretion measurements were performed at 37°C in Krebs ringer buffer (KRB) (in mmol/l: 115 NaCl, 5 KCl, 24 $NaHCO_3$, 2.5 $CaCl_2$, 1 $MgCl_2$, 10 HEPES; and 0.1% BSA, pH 7.4), as described previously (Kolic et al., 2013; Pigeau et al., 2009). For GIP (100 nmol/l), Ex-4 (100 nmol/l), GLP-1 (10 nmol/l) or Latrunculin B (10 μmol/l) stimulation experiments, the peptides were present during the 60 min 16.7 mmol/l glucose KRB stimulation. Human islet perifusion was performed at 37°C using a Brandel SF-06 system (Gaithersburg, MD) after a 2 hour pre-incubation in KRB with 1 mmol/l glucose. Thirty-five islets per lane were perifused (0.5 ml/min) with KRB with glucose as indicated. Samples, stored at -20°C, were assayed for insulin via enzyme-linked immunosorbent assay (MSD, Rockville, MD).

Electrophysiology

We used the standard whole-cell technique with the sine+DC lockin function of an EPC10 amplifier and Patchmaster software (HEKA Electronics, Lambrecht/Pfalz, Germany). Experiments were performed at 32–35°C. Solutions used for capacitance measurements are previously described (Kolic et al., 2013; Pigeau et al., 2009). For GIP (100 nmol/l) or Ex-4 (100 nmol/l) stimulation experiments, the peptides were added to the bath solution. For infusion experiments, the pipette solution also contained 10 μmol/l Latrunculin B. Capacitance responses and Ca^{2+} currents were normalized to initial cell size and expressed as femtofarad per picofarad (fF/pF) and picoampere per pF (pA/pF). Mouse beta cells were identified by size and the presence of a voltage-gated Na^{+} current that inactivates at approximately –90 mV whereas human beta cells were positively identified by insulin immunostaining.

Actin Staining

Mouse islets were dispersed into single cells onto coverslips as previously described (Pigeau et al., 2009). Cells were treated overnight with the AS604850 inhibitor (1 μmol/l), (or vehicle). For GIP, Ex-4 and Latrunculin B experiments cells were treated as indicated. Immediately following treatment, cells were fixed with Z-FIX (Anatech, Battle Creek, MI, USA) and stained for insulin with rabbit anti-insulin primary antibody (Santa Cruz, CA) and Alexa Fluor 594 goat anti-rabbit secondary antibody (Life Technologies Inc., Carlsbad, CA). Cells were also stained for filamentous actin (F-actin) with Alexa Fluor 488-conjugated phalloidin (Life Technologies Inc., Carlsbad, CA). Cells were imaged with a Zeiss Axio Observer.Z1 microscope and ×63 Plan ApoChromat objective (1.4 NA). Excitation was with a COLIBRITM (Carl Zeiss Canada, Toronto, Canada) LED light source with 495 or 555 nm filter set. Only insulin-positive cells were used for F-actin intensity measurement, which were analyzed using ImageJ software.

Statistical Analysis

For single-cell electrophysiology or imaging studies, the n-values represent the number of cells studied from at least three individual experiments. For secretion and perifusion studies, n-values represent numbers of distinct islet preparations from at least three individual experiments. Electrophysiological data was extracted using FitMaster v2.32 (HEKA Electronik). All data was analyzed using the Student t-test, or *post hoc* Tukey test following a two-way ANOVA where more than 2 groups were present. Statistical outliers were removed using the Grubb's test. Data is expressed as means±SE, and $p<0.05$ was considered significant.

4.4 RESULTS

4.4.1 p110γ inhibition blunts the insulinotropic effect of GIP receptor activation in mouse and human islets

Expression of the p110γ catalytic subunit of PI3K was confirmed by western blot in INS-1 832/13 cells, mouse islets, and human islets **(Figure 25A)**. The p110γ inhibitor, AS604850 (1 μmol/l, overnight) did not alter expression of p110γ protein in INS-1 832/13 cells **(Figure 25B)**. Because PI3K catalytic isoforms could possibly compensate for each other, we examined the effects of AS604850 on protein expression of p110α and p110β in INS-1 832/13 cells and found no difference following p110γ inhibition **(Figure 25B)**.

Consistent with previous findings, the pharmacological inhibition of p110γ (AS604850, 1 μmol/l, overnight) decreased GSIS from mouse islets by 50% **(**n=18 from 7 distinct experiments, $p<0.05$; **Figure 25C)**. The insulinotropic effect of GIP (100 nmol/l) was blunted by 46% following inhibition of p110γ **(**n=17 from 7 distinct experiments, $p<0.01$; **Figure 25C)**. There was no significant change in insulin content following overnight p110γ inhibition **(**n=18 from 7 distinct experiments, **Figure 25C (*inset*))**, nor was there a change in GIP-R or GLP-1-R mRNA expression as measured by qPCR **(Figure 25E).** The insulinotropic response to GIP was also blunted following p110γ inhibition in islets from 6 individual human donors (**Figure 26)**. This suggests that GIP-induced insulin secretion requires p110γ activity, in line with previous demonstration that GIP can directly activate p110γ in INS-1 cells (Trümper et al., 2001), and that GIP-dependent insulin secretion is blunted by the non-selective PI3K antagonist wortmannin (Straub and Sharp, 1996b).

4.4.2 p110γ inhibition does not impair the insulinotropic effect of GLP-1 receptor activation in mouse and human islets

p110γ-/- mice have been shown to have an impaired insulin secretory response from isolated islets in response to high glucose (MacDonald et al., 2004). However, chronic Ex-4 administration to these mice rescued the secretory defect (Li et al., 2006). We thus examined the insulinotropic effects of GLP-1 (10 nmol/l), and the GLP-1 analogue Exendin-4 (100 nmol/l) (Ex-4) following p110γ pharmacological inhibition in isolated islets. We found that insulin secretion in response to either GLP-1 or Ex-4 was not blunted following p110γ inhibition in mouse islets **(**n=16, from 6 distinct experiments **Figure 25D)**. Similarly, Ex-4 remained able to stimulate insulin secretion from islets of 6 individual human donors **(Figure 26)**. This suggests that insulin secretion stimulated by the GIP-R, but not the GLP-1-R, requires p110γ.

Figure 25: Expression of p110γ, and GIP and GLP-1 receptor-stimulated insulin secretion following p110γ inhibition.

Panel **(A)** shows expression of p110γ was by western blot of protein lysates from INS-1 832/13 (I), mouse islets (M), and human islets (H).

Panel **(B)** shows p110γ, p110α, and p110β protein expression levels from INS-1 832/13 cells following overnight treatment with either the DMSO vehicle, or the specific p110γ pharmacological inhibitor AS604850. β-actin protein expression was used as a loading control.

Panel **(C)** shows glucose and GIP (100 nmol/l) stimulated insulin secretion measured from mouse islets treated overnight with either DMSO (*open bars*) or AS604850 (1 μmol/l) (*black bars*).

Panel **(D)** shows glucose and GLP-1 (10 nmol/l) or Ex-4 (100 nmol/l) stimulated insulin secretion measured from mouse islets treated overnight with either DMSO (*open bars*) or AS604850 (1 μmol/l) (*black bars*). *Insets* show total insulin content.

Panel **(E)** shows GLP-1-R *(left)* and GIP-R *(right)* mRNA expression in mouse islets (treated overnight with either DMSO (*open bars*) or AS604850 (1 μmol/l) (*black bars*).

*-p <0.5, ** -p <0.01, ns = non significant.

(JK performed westernblot experiments and qPRC, AS performed GSIS experiments and ran ELISAs, JK analyzed all data.)

Figure 25

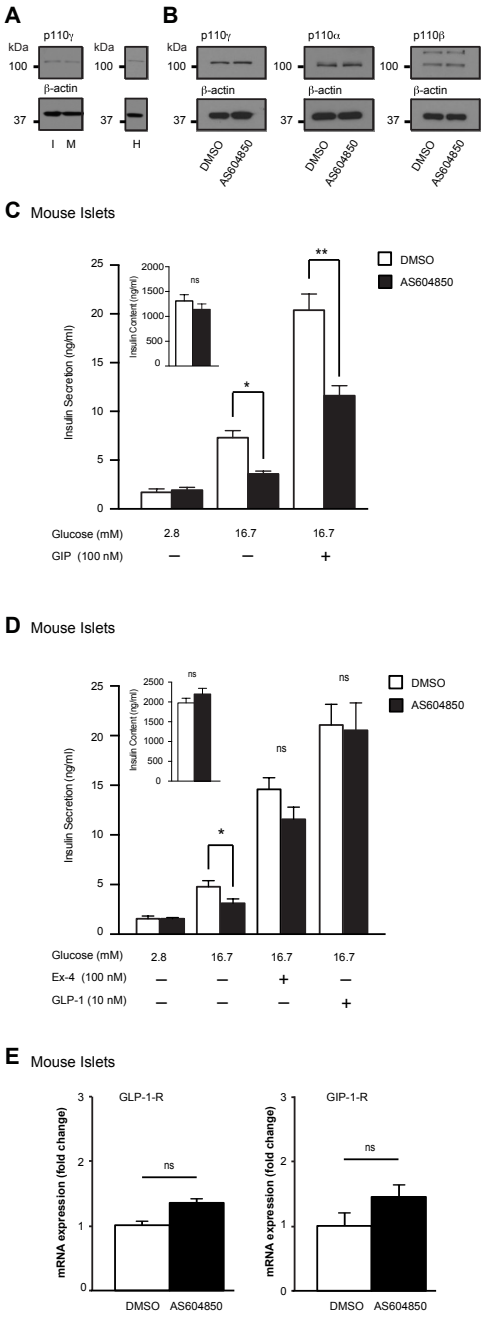
A
p110γ
kDa
100
β-actin
37
I M
H
B
p110γ
p110α
p110β
DMSO
AS604850
C Mouse Islets
Insulin Secretion (ng/ml)
Insulin Content (ng/ml)
ns
*
**
DMSO
AS604850
Glucose (mM) 2.8 16.7 16.7
GIP (100 nM) – – +
D Mouse Islets
Ex-4 (100 nM) – – + –
GLP-1 (10 nM) – – – +
E Mouse Islets
GLP-1-R
GIP-1-R
mRNA expression (fold change)

Figure 26: GIP and GLP-1 receptor activation stimulated insulin secretion following p110γ pharmacological inhibition in human islets.

Panels **(A-F)** show glucose (HG) and GIP (100 nmol/l) (*left*) or Ex-4 (100 nmol/l) (*right*) stimulated insulin secretion from human islets treated overnight with either DMSO (*open circles*) or AS604850 (1 μmol/l) (*black circles*). Each individual donor is shown in separate panels.

Panel **(G)** shows average glucose (*open bars*) and GIP (100 nmol/l) (*grey bars*) or Ex-4 (*black bars*) stimulated insulin secretion from the six donors shown as the stimulation index (fold-increase over a low-glucose control)

*-p <0.5, ** -p <0.01, ns = non significant.

(JK performed GSIS experiments, and analyzed data, AS ran the ELISAs.)

Figure 26:

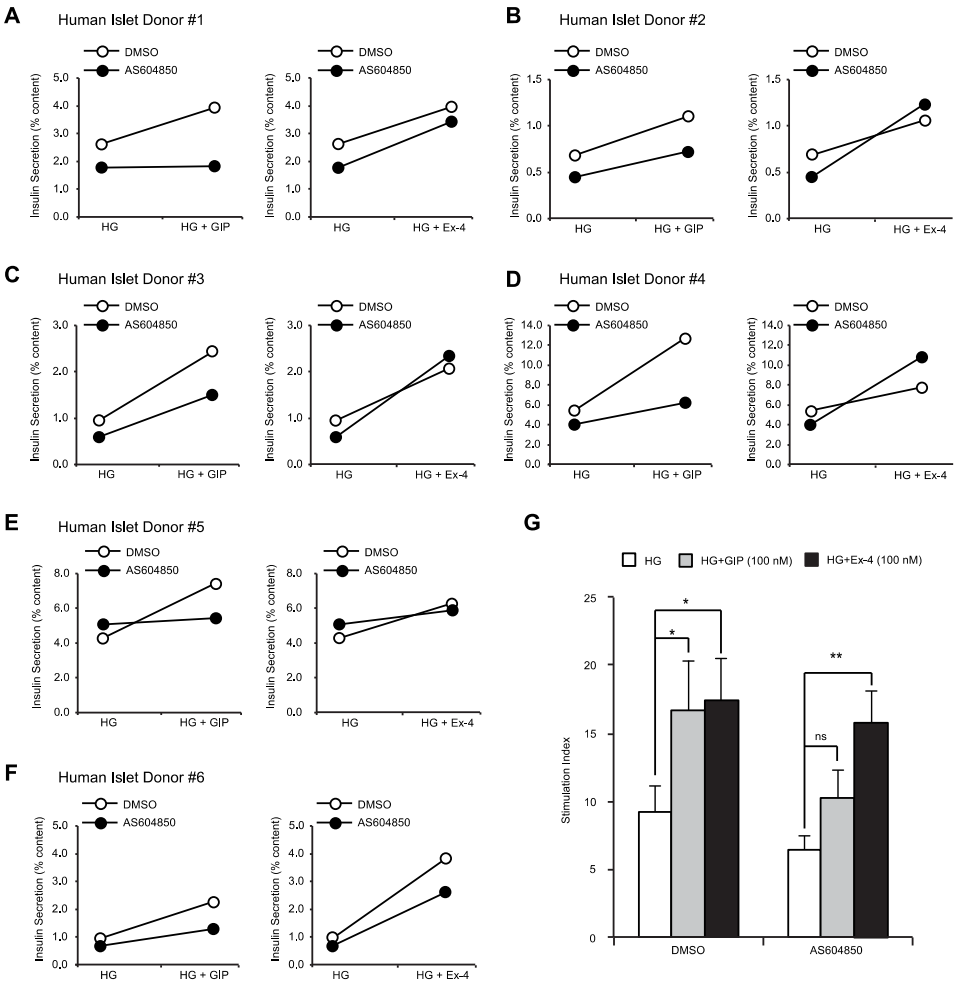
A
Human Islet Donor #1
DMSO
AS604850
Insulin Secretion (% content)
HG
HG + GIP
HG + Ex-4
B
Human Islet Donor #2
C
Human Islet Donor #3
D
Human Islet Donor #4
E
Human Islet Donor #5
F
Human Islet Donor #6
G
HG
HG+GIP (100 nM)
HG+Ex-4 (100 nM)
Stimulation Index
ns
DMSO
AS604850

4.4.3 p110γ inhibition prevents GIP-induced exocytosis in mouse and human beta cells

We next monitored whole-cell capacitance increases in response to a train of membrane depolarizations as a measure of exocytosis following p110γ inhibition. Compared to the control response, AS604850 (1 μmol/l, overnight) decreased exocytosis by 60% **(**n=15-18, p<0.01; **Figure 27A)** in mouse beta cells. GIP treatment (100 nmol/l) increased exocytosis in control cells by 2.3 fold **(**n=15-17, p<0.05; **Figure 27A,B)**, an effect that was blunted following p110γ inhibition **(**n=16-17; **Figure 27B)**. Conversely, Ex-4 treatment (100 nmol/l) increased exocytosis in control cells by 2.6 fold **(**n=15-19, p<0.01; **Figure 27A,C)**, and p110γ inhibition did not blunt the ability of Ex-4 to stimulate the exocytotic response (n=16-19, **Figure 27C**).

We subsequently monitored whole-cell capacitance following p110γ inhibition in human beta cells (identified by positive immunostaining for insulin). Similar to the mouse data, inhibition of p110γ decreased the exocytotic response by 50% **(**n=20-23, p<0.01; **Figure 28A)**. GIP treatment (100 nmol/l) increased exocytosis in control cells by 1.8 fold **(**n=19-23, p<0.01; **Figure 28A,B)**, and this was severely blunted following p110γ inhibition **(**n=17-19; **Figure 28B)**.

Figure 27: GIP and GLP-1 receptor-stimulated insulin secretion following p110γ inhibition in human islets.

In panel **(A)**, (*left*) representative capacitance recordings are shown from mouse beta cells treated overnight with vehicle DMSO (*grey lines*) or AS604850 (1 μmol/l) (*black lines*). (*right*) Average cumulative capacitance response during each depolarization step for beta cells treated overnight with DMSO (*open circles*) or AS604850 (1 μmol/l) (*black circle*) are shown.

Panel **(B)**, shows the same as A, except cells were additionally treated with GIP (100 nmol/l).

Panel **(C)**, shows the same as A, except cells were additionally treated with Ex-4 (100 nmol/l).

*- $p < 0.5$, **- $p < 0.01$.

(JK performed electrophysiological experiments, and analyzed data.)

Figure 27

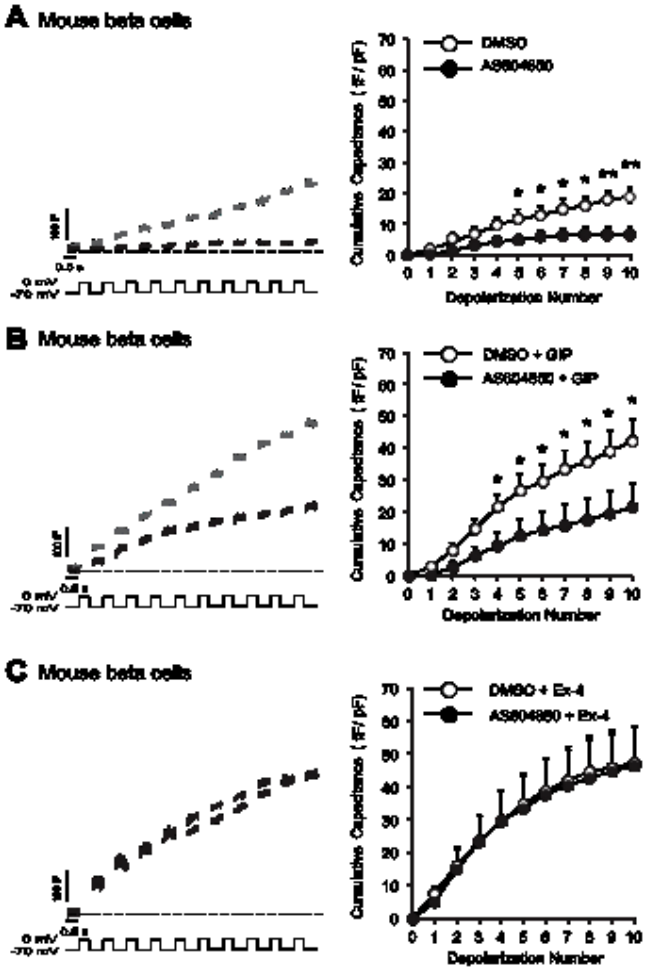
A Mouse beta cells
DMSO
AS604850
Cumulative Capacitance (fF/pF)
Depolarization Number
B Mouse beta cells
DMSO + GIP
AS604850 + GIP
Cumulative Capacitance (fF/pF)
Depolarization Number
C Mouse beta cells
DMSO + Ex-4
AS604850 + Ex-4
Cumulative Capacitance (fF/pF)
Depolarization Number

Figure 28: GIP-stimulated exocytosis following p110γ inhibition in human beta cells.

Panel **(A)**, (*left*) shows representative capacitance recordings are from human beta cells treated overnight with vehicle DMSO (*grey lines*) or AS604850 (1 μmol/l) (*black lines*). (*right*) Average cumulative capacitance response during each depolarization step for human beta cells treated overnight with DMSO (*open circles*) or AS604850 (1 μmol/l) (*black circle*) are shown.

Panel **(B)** shows the same as A, except cells were additionally treated with GIP (100 nmol/l; 1 hr.).

- $p < 0.01$, *- $p < 0.001$.

(JK performed electrophysiological experiments, and analyzed data.)

Figure 28

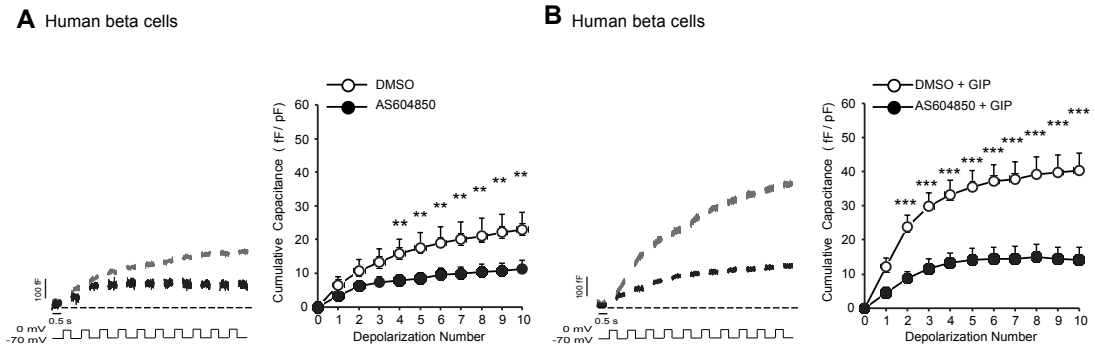
A Human beta cells
B Human beta cells
DMSO
AS604850
DMSO + GIP
AS604850 + GIP
Cumulative Capacitance (fF / pF)
Depolarization Number
100 fF
0.5 s
0 mV
-70 mV

4.4.4 p110γ knockdown impairs the response to GIP in mouse and human islets

Knockdown of p110γ, using an adenoviral-shRNA construct (Adsh-p110γ) that reduces p110γ expression by 78% (Pigeau et al., 2009), results in impaired insulin exocytosis when compared with a scrambled control. Adsh-p110γ had no effect on expression of the class 1A PI3K p110β, which can functionally compensate for p110γ. In line with our observations using pharmacological inhibition, shRNA-mediated knockdown of p110γ impaired the insulinotropic effects of GIP (100 nmol/l) in mouse islets measured during perifusion **(**n=4,4, $p<0.05$; **Figure 29A,B)**. Similarly, the insulinotropic effects of GIP (100 nmol/l) were also severely blunted in human islets infected with Adsh-p110γ **(**n=15-17, from 6 distinct donors, $p<0.05$; **Figure 29C)**. Insulin content was not significantly changed during any treatment conditions. p110γ knockdown also severely impaired the ability of GIP (100 nmol/l) to increase exocytosis in mouse beta cells **(**n=15-18, $p<0.01$; **Figure 29D,E)**.

Figure 29: GIP-stimulated insulin secretion and exocytosis following p110γ knockdown.

In panel **(A)**, insulin secretion was measured by perifusion of isolated mouse islets infected with Adsh-scram (*open circles*) or Adsh-p110γ (*black circles*). 16.7 mmol/l glucose was perifused at 10 min.

Panel **(B)** shows the same as A, except cells were additionally perifused with GIP (100 nmol/l; added at 10 min.)

In panel **(C)**, static insulin secretion was measured from human islets infected with Adsh-scram (*open bars*) or Adsh-p110γ (*black bars*) shown as the stimulation index (fold-increase over a low glucose control). Glucose and GIP concentrations were as indicated.

Panel **(D)**, (*left*) shows representative capacitance recordings from mouse beta cells infected with Adsh-scram (*grey lines*) or sh-p110γ (*black lines*). (*right*) Average cumulative capacitance response during each depolarization step for mouse beta cells infected with Adsh-scram *(grey lines*) or Adsh-p110γ (*black lines*) are shown.

Panel **(E)** shows the same as C, except cells were additionally treated with GIP (100 nmol/l; 1 hr.).

*- $p < 0.5$, **- $p < 0.01$, ***-$p < 0.001$.

(JK performed GSIS and electrophysiological experiments, ran ELISAs, and analyzed data.)

Figure 29

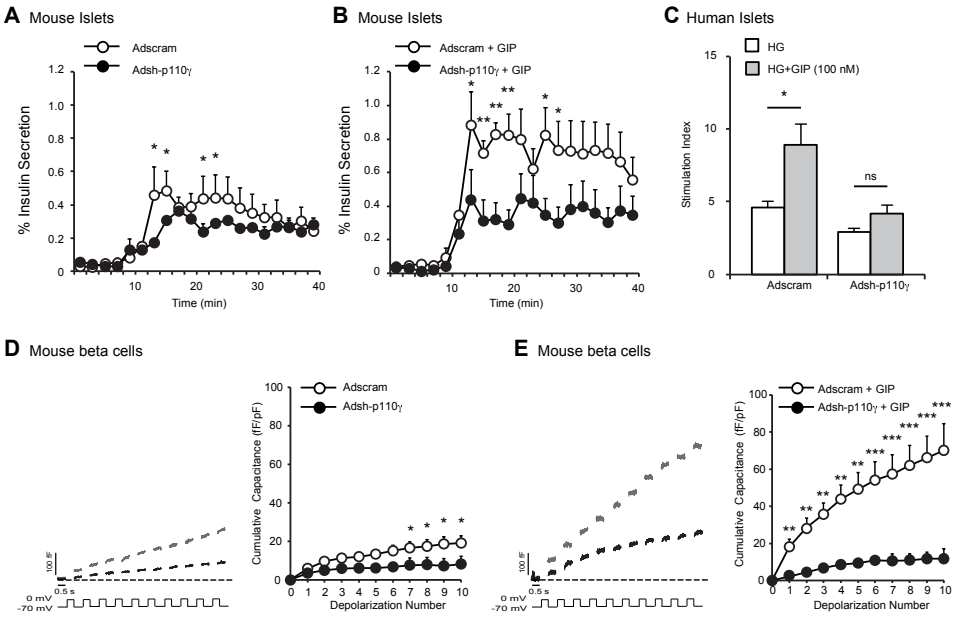
A Mouse Islets
Adscram
Adsh-p110γ
% Insulin Secretion
Time (min)
B Mouse Islets
Adscram + GIP
Adsh-p110γ + GIP
% Insulin Secretion
Time (min)
C Human Islets
HG
HG+GIP (100 nM)
Stimulation Index
ns
Adscram
Adsh-p110γ
D Mouse beta cells
100 fF
0.5 s
0 mV
-70 mV
Adscram
Adsh-p110γ
Cumulative Capacitance (fF/pF)
Depolarization Number
E Mouse beta cells
100 fF
0.5 s
0 mV
-70 mV
Adscram + GIP
Adsh-p110γ + GIP
Cumulative Capacitance (fF/pF)
Depolarization Number

4.4.5 p110γ inhibition blunts Rac1 activation

Next, we explored the mechanism by which p110γ inhibition impairs the insulinotropic effects of GIP. Small GTPase proteins, such as Rac1, are implicated in the insulin secretory response, having well-defined roles in actin remodeling (Kalwat and Thurmond, 2013; Kowluru, 2010; Li et al., 2004; Wang and Thurmond, 2009). Recent studies in beta cell specific Rac1-knockout (betaRac1-/-) mice, demonstrate that Rac1 controls glucose-stimulated insulin secretion by promoting cytoskeletal rearrangement and recruitment of insulin-containing granules to the plasma membrane (Asahara et al., 2013). In addition, INS-1 832/13 cells lacking Rac1 or the ability to activate Rac1 fail to show actin depolymerization in response to high glucose, and exhibit a decreased insulin secretory response (Asahara et al., 2013; Li et al., 2004).

Because p110γ inhibition is associated with increased actin polymerization and a reduction in insulin granules at the plasma membrane (Pigeau et al., 2009), we examined Rac1 activation in INS-1 832/13 treated with AS604850 (1 μmol/l). We found that p110γ inhibition severely impaired glucose-stimulated Rac1 activation, without affecting total Rac1 levels **(**n=3, $p<0.01$; **Figure 30A,B)**. Compared to vehicle treated cells, glucose stimulated Rac1 activation was decreased by 76% in AS604850-treated cells **(**n=3, $p<0.01$; **Figure 30A,B)**.

4.4.6 GIP activates Rac1 in a p110γ-dependent manner

GLP-1 receptor activation has been postulated to activate Rac1 through PKA mediated activation of the serine/threonine-protein kinase PAK 1 (Kalwat and Thurmond, 2013). We now show that GIP stimulates Rac1 activation in INS-1 cells **(Figure 30C,D)** under low glucose conditions. GIP (100 nmol/l, 25 min) increased Rac1 activation by 4.3 fold **(**n=3, $p<0.05$; **Figure 30C,D)**. However, when p110γ activity was inhibited, GIP mediated Rac1 activation was blocked **(Figure 30E,F)**, suggesting a role for p110γ in GIP mediated activation of Rac1.

Figure 30: Glucose and GIP mediated Rac1 activation following p110γ pharmacological inhibition in INS1 832/13 cells.

Panel **(A)** shows representative blots of activated Rac1, and total Rac1 in response to high glucose in cells treated overnight with either DMSO or AS604850 (1 μmol/l).

Panel **(B)**, shows average Rac1 activation (normalized to total Rac1 present) in response to glucose in cells treated overnight with either DMSO (*open bar*) or AS604850 (1 μmol/l) (*black bar*).

In panel **(C)** a representative blot of activated Rac1 in response to GIP (100 nmol/l, 25 min) is shown.

In panel **(D)** average Rac1 activation (normalized to total Rac1 present) in response to GIP (100 nmol/l, 25 min) (*black bar*) is shown.

Panel **(E)** shows representative blots of activated Rac1, and total Rac1 in response to GIP (100 nmol/l, 25 min) in cells treated overnight with either DMSO or AS604850 (1 μmol/l). (Images are from different parts of the same gel).

Panel **(F)** shows average Rac1 activation (normalized to total Rac1 present) in response to GIP (100 nmol/l, 25 min) (*black bar*) in cells treated overnight with either DMSO (*open bars*) or AS604850 (1 μmol/l) (*black bars*).

*- $p < 0.5$, **- $p < 0.01$.

(JK performed Rac1 activation assays, and analyzed data.)

Figure 30

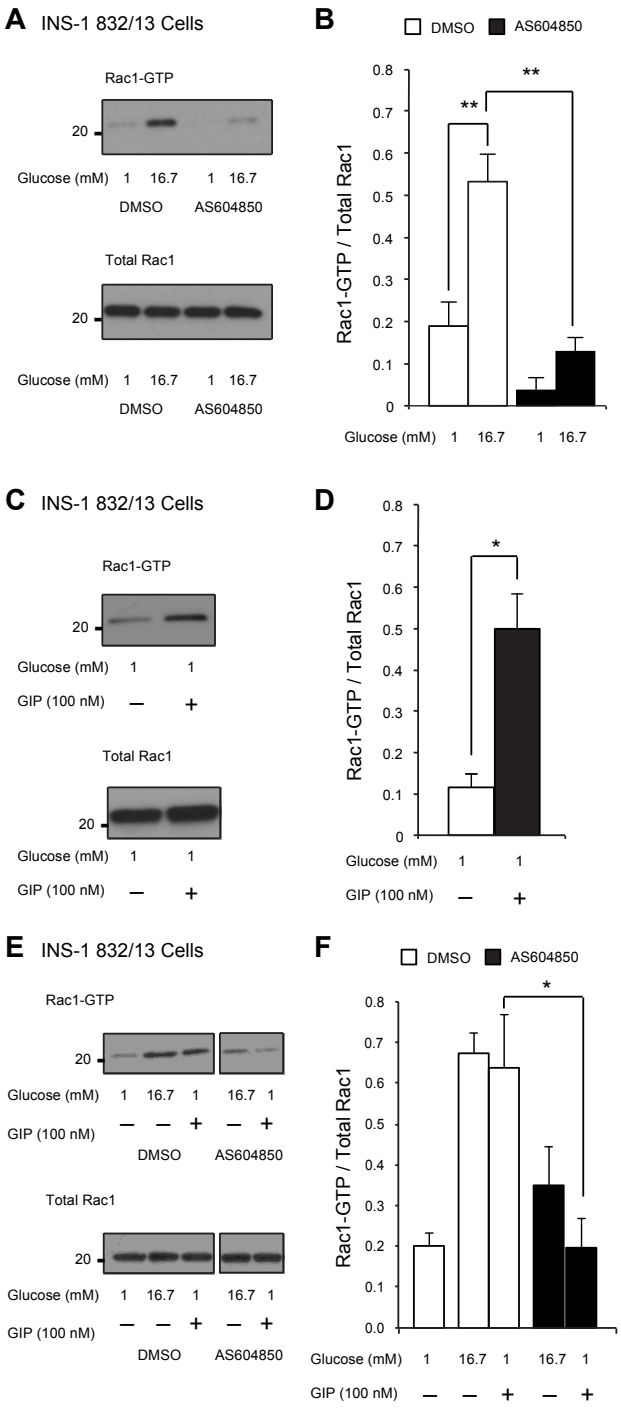
A INS-1 832/13 Cells
Rac1-GTP
20
Glucose (mM) 1 16.7 1 16.7
DMSO AS604850
Total Rac1
20
Glucose (mM) 1 16.7 1 16.7
DMSO AS604850
B
DMSO AS604850
Rac1-GTP / Total Rac1
0.8
0.7
0.6
0.5
0.4
0.3
0.2
0.1
0
**
**
Glucose (mM) 1 16.7 1 16.7
C INS-1 832/13 Cells
Rac1-GTP
20
Glucose (mM) 1 1
GIP (100 nM) – +
Total Rac1
20
Glucose (mM) 1 1
GIP (100 nM) – +
D
Rac1-GTP / Total Rac1
0.8
0.7
0.6
0.5
0.4
0.3
0.2
0.1
0
*
Glucose (mM) 1 1
GIP (100 nM) – +
E INS-1 832/13 Cells
Rac1-GTP
20
Glucose (mM) 1 16.7 1 16.7 1
GIP (100 nM) – – + – +
DMSO AS604850
Total Rac1
20
Glucose (mM) 1 16.7 1 16.7 1
GIP (100 nM) – – + – +
DMSO AS604850
F
DMSO AS604850
Rac1-GTP / Total Rac1
0.8
0.7
0.6
0.5
0.4
0.3
0.2
0.1
0.0
*
Glucose (mM) 1 16.7 1 16.7 1
GIP (100 nM) – – + – +

4.4.7 GIP and GLP-1 receptor activation stimulates actin depolymerization

We, and others, have shown that cortical actin is an important determinant of the exocytotic response (Jewell et al., 2008; Kalwat and Thurmond, 2013; Pigeau et al., 2009). We know that p110γ inhibition blunts exocytosis by increasing cortical actin density, and limiting the number of insulin containing granules at the plasma membrane (Pigeau et al., 2009). Rac1 activation is necessary to induce a secretory response (Asahara et al., 2013; Li et al., 2004) and mediates actin reorganization in response to glucose (Asahara et al., 2013). Thus, we examined whether GIP and GLP-1 receptor activation affects cortical actin. We find that both GIP (100 nmol/l) and Ex-4 (100 nmol/l induce actin depolymerization in mouse beta cells. After 5 min treatment, cortical actin intensity was decreased by 29% (n=55-65, $p<0.001$; **Figure 31A,B)** with GIP (100 nmol/l), and by 31% **(**n=75-85, $p<0.001$; **Figure 31C,D)** with Ex-4 (100 nmol/l). This effect was maintained over 60 minutes **(Figure 31B,D)** In comparison, Latrunculin B (10 μmol/l, 2 min), a potent actin-depolymerizing agent used as a positive control, reduced actin intensity by 64-65% **(**n=40-60, $p<0.001$; **Figure 31B,D)**.

Figure 31: GIP and GLP-1 receptor activation induces actin depolymerization in mouse beta cells.

Panel **(A)** shows dispersed mouse beta cells treated with water control, GIP (100 nmol/l), or Latrunculin B (10 μmol/l) for indicated time periods, and subsequently fixed with Z-FIX. Cells were stained for insulin (red) and F-actin (green). Representative images are shown at top with representative intensity line scans for F-actin staining intensity below.

Panel **(B)** shows average peak actin intensities following treatments.

Panel **(C)** shows the same as A, except cells were treated with Ex-4 (100 nmol/l) instead of GIP.

Panel **(D)** shows average peak actin intensities following treatments.

- $p < 0.01$, *-$p < 0.001$.

(JK, and AMS (under the supervision of JK) performed imaging experiments, and analyzed data.)

Figure 31

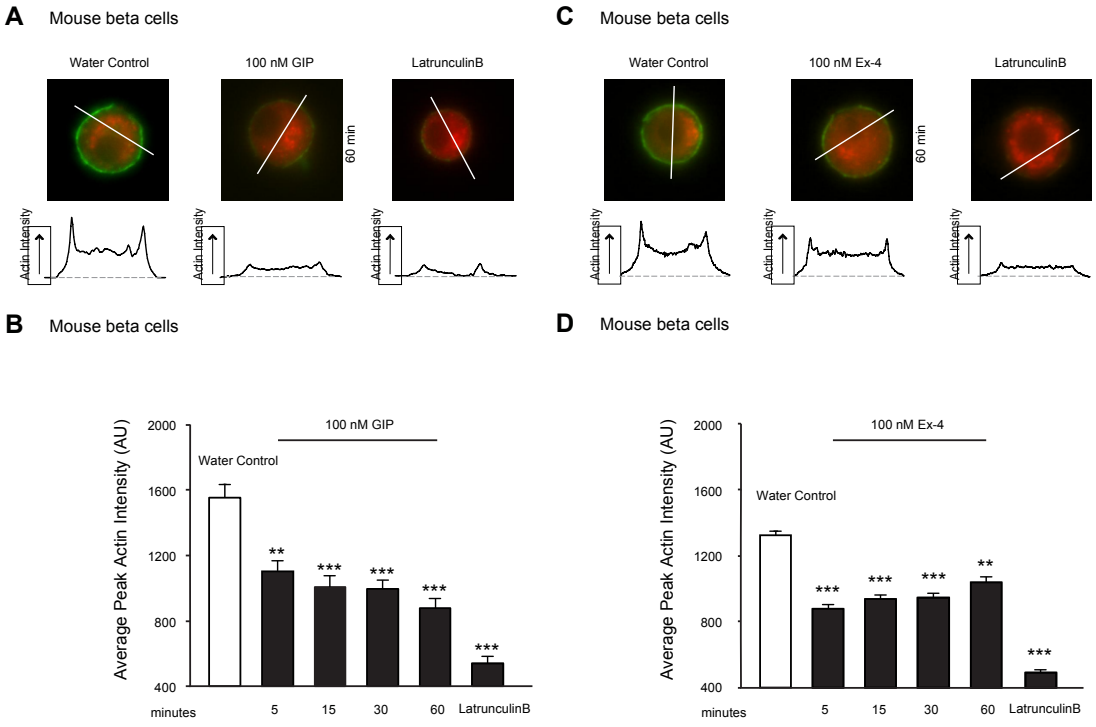
A
Mouse beta cells
Water Control
100 nM GIP
LatrunculinB
60 min
Actin Intensity
C
Mouse beta cells
Water Control
100 nM Ex-4
LatrunculinB
60 min
Actin Intensity
B
Mouse beta cells
Average Peak Actin Intensity (AU)
2000
1600
1200
800
400
100 nM GIP
Water Control
**
***
***
***
***
minutes
5
15
30
60
LatrunculinB
D
Mouse beta cells
Average Peak Actin Intensity (AU)
2000
1600
1200
800
400
100 nM Ex-4
Water Control
***
***
***
**
***
minutes
5
15
30
60
LatrunculinB

4.4.8 p110γ is required for GIP (but not GLP-1) receptor–mediated actin depolymerization

Since we show that p110γ inhibition prevents the insulinotropic effects of GIP, and cortical actin dynamics are essential to insulin secretion (Kalwat and Thurmond, 2013), we examined whether p110γ inhibition impairs the ability of GIP to depolymerize actin. In dispersed mouse beta cells, we show that pharmacological inhibition of p110γ reduced the ability of GIP to depolymerize actin. In vehicle treated cells, GIP (100 nmol/l, 5 min) depolymerized cortical F-actin by 30% (n=88-93 from 4 mice, $p<0.01$; **Figure 32A,B)**. This was prevented by p110γ inhibition **(**n=89-90 from 4 mice, p=ns; **Figure 32A,B).** Both vehicle and AS604850 treated cells responded to Latrunculin B treatment **(**n=61-71 from 4 mice, $p<0.001$; **Figure 32A,B)**.

Conversely, inhibition of p110γ was not able to prevent actin depolymerization induced by the GLP-1 receptor agonist Ex-4. Ex-4 (100 nmol/l, 5min), decreased actin density by 32%, **(**n=66-88 from 4 mice, $p<0.001$; **Figure 32A,B)**, and by 37% in AS604850 treated cells **(**n= 64-89 from 4 mice, $p<0.001$; **Figure 32A,B)**, suggesting that p110γ is not required for GLP-1 receptor -induced actin depolymerization.

Figure 32: p110γ pharmacological inhibition prevents GIP induced actin depolymerization in mouse beta cells.

Panel **(A)** shows representative images of dispersed mouse beta cells treated overnight with either DMSO or AS604850, and water control, GIP (100 nmol/l), Ex-4 (100 nmol/l), or Latrunculin B (10 μmol/l) for indicated time periods are shown. Representative images are shown at top with representative intensity line scans for F-actin staining intensity below.

Panel **(B)** shows average peak actin intensities following treatments are shown.

*- p <0.5, **- p <0.01, *** or ###-p<0.001, ns = non significant.

(JK performed imaging experiments, and analyzed data.)

Figure 32

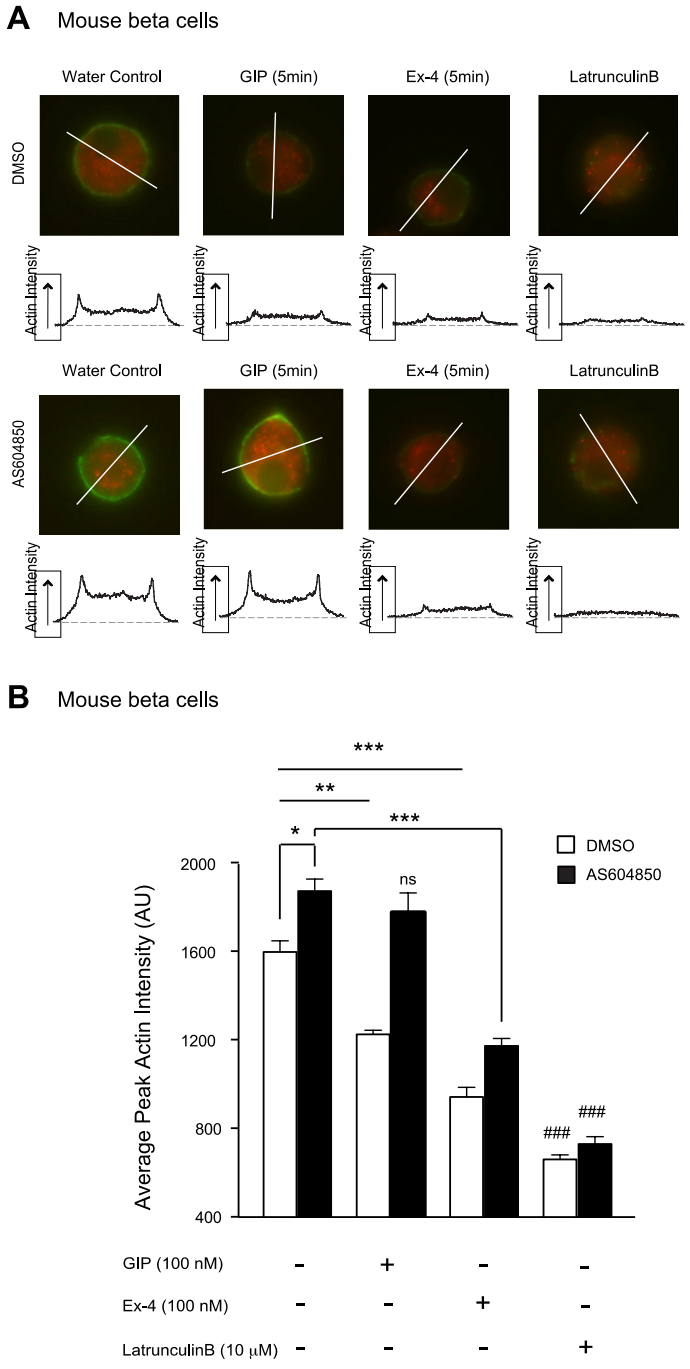
A
Mouse beta cells
Water Control
GIP (5min)
Ex-4 (5min)
LatrunculinB
DMSO
AS604850
Actin Intensity
B
Mouse beta cells
Average Peak Actin Intensity (AU)
2000
1600
1200
800
400
DMSO
AS604850
ns
###
GIP (100 nM)
Ex-4 (100 nM)
LatrunculinB (10 μM)

4.4.9 Forced actin depolymerization restores GIP-mediated exocytosis and insulin secretion following p110γ inhibition or knockdown

We next determined if the impairment of GIP's ability to increase exocytosis and insulin secretion following p110γ inhibition is due in part to its inability to cause actin depolymerization. Upon intracellular dialysis of Latrunculin B (10 μmol/l via the patch-pipette), the GIP-stimulated capacitance response of mouse beta cells was unaffected by shRNA-mediated p110γ knockdown **(**n=12-15**; Figure 33A)**. Thus, forced depolymerization of actin was sufficient to rescue the GIP-stimulated exocytotic response. Accordingly, the blunted secretory response to GIP observed following p110γ inhibition was reversed following acute treatment of islets with Latrunculin B (10 μmol/l) **(**n=4; **Figure 33B).** Together, these data suggest that the impaired insulinotropic effect of GIP seen following p110γ inhibition may be mediated by its inability to effectively depolymerize actin in these cells.

Figure 33: Forced disruption F-actin restores the insulinotropic effects of GIP.

Panel **(A)** *(left)* shows representative membrane capacitance traces from mouse beta cells infected with Adsh-scram (*grey lines*) or Adsh-p110γ (*black lines*), treated with GIP (100 nmol/l, 1hr) and 10 μmol/l Latrunculin B included in the patch pipette. *(right)* shows the average capacitance response over the course of the depolarization trains.

Panel **(B)** shows glucose stimulated insulin secretion in the presence of GIP (100 nmol/l) and/or Latrunculin B (10 μmol/l) measured from mouse beta islets treated overnight with either DMSO (*open bars*) or AS604850 (1 μmol/l) (*black bars*).

*- $p < 0.5$.

(JK and AMS (under supervision of JK) performed electrophysiological experiments; AS performed GSIS experiments and ran ELISAs, JK analyzed all data.)

Figure 33

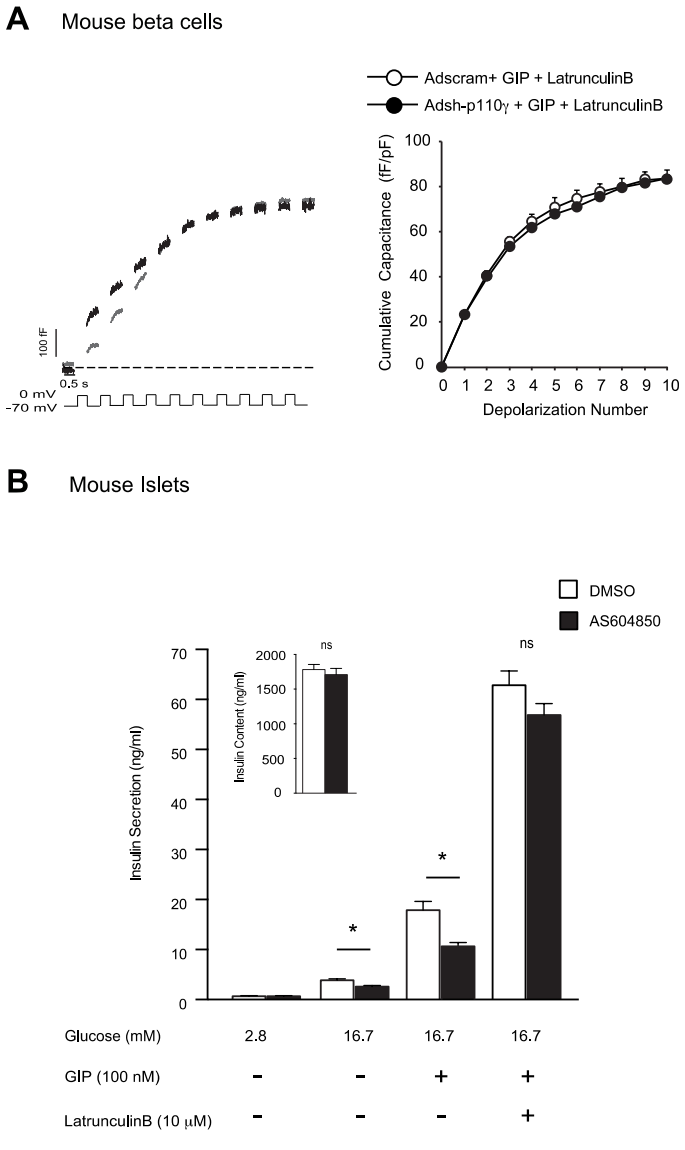
A
Mouse beta cells
Adscram+ GIP + LatrunculinB
Adsh-p110γ + GIP + LatrunculinB
Cumulative Capacitance (fF/pF)
Depolarization Number
100 fF
0.5 s
0 mV
-70 mV
B
Mouse Islets
DMSO
AS604850
Insulin Secretion (ng/ml)
Insulin Content (ng/ml)
ns
Glucose (mM) 2.8 16.7 16.7 16.7
GIP (100 nM) - - + +
LatrunculinB (10 μM) - - - +

4.5 DISCUSSION

We have previously shown that the G-protein coupled PI3Kγ is a positive regulator of insulin secretion, by controlling cortical actin density and targeting secretory granules to the plasma membrane (Pigeau et al., 2009). The two incretin hormones GIP and GLP-1 signal through distinct G_s coupled G-protein receptors; their major mechanism of action being linked to a rise in cAMP (Campbell and Drucker, 2013; Drucker, 2013).

GIP is shown to stimulate PI3Kγ activity, as measured by an increase in PIP_3 production in insulinoma cells (Trümper et al., 2001). GIP signaling has also been linked to a wortmannin-sensitive pathway (Straub and Sharp, 1996b). Conversely, the insulin secretory defect of PI3Kγ KO mice is reversed following chronic Ex-4 treatment, suggesting that PI3Kγ is not required for the insulinotropic actions of GLP-1 (MacDonald et al., 2004). GLP-1-R (or GIP-R) activation increases intracellular cAMP, which subsequently activates PKA. This has been postulated to activate Rac1 through PKA mediated activation of the serine/threonine-protein kinase PAK 1 (Kalwat and Thurmond, 2013).

Thus, we now investigated whether PI3Kγ is required for GIP and/or GLP-1 receptor-induced insulin secretion, and examine the role of GIP-mediated Rac1 activation and actin remodeling. We find that selective inhibition of p110γ, or sh-RNA mediated knockdown, impairs the insulinotropic effects of GIP in both mouse and human islets. This does not appear due to loss of the GIP-R since mRNA expression of either this or GLP-1-R is not reduced following p110γ inhibition.

We also find that both GIP and Ex-4 are potent activators of insulin exocytosis,

and that p110γ inhibition or knockdown blocks the GIP-mediated facilitation of exocytosis. This is consistent with work by Straub *et al*. (1996) who found that wortmannin inhibits the insulinotropic effect of GIP (but not forskolin) in HIT insulinoma cells. The authors linked this effect to the possible inhibition of a "novel exocytosis-linked G-protein βγ subunit activated PI3K" (Straub and Sharp, 1996b), which our work now demonstrates is PI3Kγ.

Surprisingly, our results indicate that the insulinotropic effects of GLP-1 or its analogue Ex-4 are not impaired following p110γ inhibition. The ability of Ex-4 to stimulate exocytosis is also not impaired following p110γ inhibition. These results are consistent with earlier observations showing that Ex-4 rescues the glucose-stimulated secretory defect in islets from p110γ-/- mice (Li et al., 2006), and suggests that the GIP-R and GLP-1-R are differentially coupled to PI3Kγ.

The GLP-1-R has been linked to activation of class 1A PI3Ks through trans-activation of the epidermal growth factor (EGF) receptor in the beta cell (Buteau et al., 2003). While it is possible, since PI3Kα and –β (class 1A PI3Ks) also regulate insulin secretion (Kaneko et al., 2010; Kolic et al., 2013), that these kinases may link the GLP-1-R to actin depolymerization, it should be noted that selective inhibition of these isoforms increases insulin secretion (Kolic et al., 2013). This finding is inconsistent with a positive role in the GLP-1-dependent insulin secretion.

Recent reports suggest that p110γ-/- mice are protected from obesity-induced inflammation and insulin resistance (Becattini et al., 2011; Kobayashi et al., 2011; Wymann and Solinas, 2013). These studies suggest that p110γ inhibition may be beneficial, as it would limit the inflammatory response associated with obesity. These

studies were however done *in vivo*, in mice ubiquitously lacking p110γ (Becattini et al., 2011; Kobayashi et al., 2011; Wymann and Solinas, 2013). PI3Kγ is highly expressed in cells of the immune system (Bernstein et al., 1998; Randis et al., 2008). The improvements in insulin resistance in p110γ-/- mice are largely due to protection from inflammatory stress resulting from a high fat diet (Becattini et al., 2011; Kobayashi et al., 2011; Wymann and Solinas, 2013), which may mask an underlying role of p110γ as a positive regulator of insulin secretion in beta cells. Also, any defect in GIP's insulinotropic effects in these mice would be completely masked by the intact GLP-1 signaling, which is not impaired following p110γ inhibition.

Our results point to a mechanism by which GIP is able to activate the small GTPase protein Rac1 to induce actin depolymerization. p110γ has previously been shown to be involved in the activation of Rac1 in immune cells (Rommel et al., 2007). PtdIns(3,4,5)P_3 and Gβγ both activate Rac1 by activating Rac-specific guanine nucleotide exchange factor (GEF) activity (Innocenti et al., 2003; Welch et al., 2002).

Small GTPase proteins, such as Rac1, have been implicated in the insulin secretory response (Asahara et al., 2013; Li et al., 2004; Wang and Thurmond, 2009). Insulin-producing cells lacking Rac1, or in which the ability of Rac1 to be activated is blocked, lack glucose-stimulated actin remodeling and show impaired insulin secretion (Asahara et al., 2013; Li et al., 2004; Wang and Thurmond, 2009). Dispersed beta cells from betaRac1-/- mice, also show a reduction in insulin granule recruitment to the plasma membrane (Asahara et al., 2013), similar to what we reported previously upon loss of p110γ (Pigeau et al., 2009). Thus, we now suggest that the insulinotropic effects of GIP are blunted when p110γ is inhibited or knocked-down because GIP is unable to stimulate

Rac1 activation, and subsequently induce actin remodeling.

Filamentous actin can act as a barrier to insulin secretion by limiting vesicle fusion with the plasma membrane (Jewell et al., 2008; Orci et al., 1972; Pigeau et al., 2009; Thurmond et al., 2003; Tomas et al., 2006). Thus, we next determined whether forced actin depolymerization would restore the insulinotropic effects of GIP. We found that GIP-stimulated insulin secretion, and the GIP-potentiated capacitance response were no longer different upon actin depolymerization with Latrunculin B. These results further support the notion that GIP's ability to stimulate secretion in cells lacking p110γ activity is blunted in part by its inability to induce actin depolymerization in these cells.

In summary, we show that the insulinotropic effects of GIP are blunted following p110γ inhibition or knockdown in both mouse and human cells. We propose that this is due to the inability of GIP to stimulate Rac1 activation and cause actin depolymerization following p110γ inhibition. We also show that the insulinotropic effects of GLP-1 receptor activation are not affected following p110γ inhibition. This PI3Kγ-dependent pathway will facilitate insulin granule access to the plasma membrane to, in concert with classical cAMP/PKA-dependent signaling; potentiate Ca^{2+}-triggered exocytosis and insulin secretion.

4.6 CONCLUDING REMARKS

As PI3Kγ is highly expressed in cells of hematopoietic origin (Becattini et al., 2011; Wymann and Solinas, 2013; Wymann et al., 2003), the majority of studies examining the role of PI3Kγ signaling have so far been examined from an immunological perspective. Whole body Class I B PI3Kγ-deficient mice show impaired migration of neutrophils and macrophages toward chemoattractants (Hirsch et al., 2000; Li et al., 2000; Sasaki et al., 2000). Migration of hematopoietic cells towards sites of inflammation involves the activation of Rho family GTPases (Ridley, 2001; Ridley, 2006; Weiss-Haljiti et al., 2004). In macrophages, the chemokine RANTES (regulated on activation normal T cell expressed and secreted) activates the small GTPase Rac1 and its downstream target PAK, a response dependent on G_i GPCR activation and subsequent activation of p110γ (Weiss-Haljiti et al., 2004). Pharmacological inhibition or lack of p110γ expression results in similar reduction of Rac1 activation (Weiss-Haljiti et al., 2004).

Our studies implicate p110γ signaling in both glucose and GIP-mediated Rac1 activation in beta cells, and demonstrate that p110γ inhibition impairs the insulinotropic effect of GIP. Our results point to a mechanism by which GIP is able to activate the small GTPase protein Rac1, which may be contributing to the actin depolymerization seen. We implicate p110γ activation as the link between GIP and Rac1 activation. However, in other cell types (in particular, those of the immune system), PI3Kγ activation is pertussis toxin sensitive, thus implicating activation dependent on a $G_{i/o}$ GPCR (Stephens et al., 1997; Weiss-Haljiti et al., 2004). Whilst the GIP receptor is linked to a G_s protein (Campbell and Drucker, 2013; Drucker, 2006), and would thus logically not be a candidate PI3Kγ effector, PI3Kγ activation is dependent on the Gβγ subunit, rather than

the Gα subunit. Furthermore, GIP can activate p110γ in INS-1 cells (Trümper et al., 2001); and our data shows that the ability of GIP to stimulate insulin secretion and exocytosis is severely blunted following p110γ inhibition.

Surprisingly, the ability of GLP-1 to stimulate insulin secretion and exocytosis is not blunted following p110γ inhibition. However, this is supported by previous findings showing that chronic Ex-4 treatment in PI3Kγ-/- mice normalizes glucose stimulated insulin secretion (Li et al., 2006), and might explain why PI3Kγ-/- do not become diabetic and are only slightly glucose intolerant (MacDonald et al., 2004).

I attribute the ability of GLP-1 to maintain its insulinotropic effect following p110γ inhibition to the finding that p110γ inhibition does not prevent GLP-1-R activation–mediated actin depolymerization. Whilst this could suggest that GLP-1-R activation (as opposed to GIP-R activation) does not lead to the activation of p110γ in beta cells, another possible explanation lies with the ability of GLP-1 to activate the class 1A PI3Ks by transactivating the tyrosine kinase epidermal growth factor (EGF) receptor (EGFR) (Buteau et al., 2003). However, it should be noted that selective inhibition of these isoforms increases insulin secretion (Kolic et al., 2013). Whilst this would be inconsistent with a positive role in the GLP-1-dependent insulin secretion, I cannot rule out the possibility that acute activation of the class 1A PI3K by GLP-1 may be affecting insulin secretion in a positive manner. Furthermore, whilst I have not seen any changes in actin density following class 1A PI3Ks inhibition at the time points we studied, this does not rule out the possibility that they may be involved in the actin remodeling process. Thus, additional studies are required to determine the role of class 1A PI3K signaling in the incretin effect of GLP-1.

Chapter 5

Summary, General Discussion, and Future Directions

5.1 SUMMARY

The stimulus-secretion coupling pathway that connects glucose metabolism to ionic events and regulates insulin secretion from the pancreatic beta cell is well established, and the major ion channels involved are well characterized. However, this triggering pathway is only responsible for a fraction of insulin secreted from the beta cell. Many other events including the activation of cell surface receptors (such as tyrosine kinase and G-protein coupled receptors), as well as the remodeling of cytoskeletal filamentous actin are essential to insulin secretion, particularly following a prolonged stimulus.

Class 1 PI3Ks are involved in the regulation of insulin secretion in the beta cell, but the specific role of each isoform is not well understood. This thesis examines the specific role of each individual class 1 PI3K isoform expressed in islets (PI3Kα, -β and -γ) in insulin secretion, beta cell exocytosis, and actin remodeling. It also examines the role of PI3Kγ in the incretin effect of GIP and GLP-1 receptor activation. The following is a point form summary of the major finding of this thesis:

- I have confirmed the expression of p110α, -β and -γ in insulinoma cells, mouse islets and human islets.
- I showed that specific pharmacological inhibition of each isoform does not change protein expression levels of the other isoforms (which can sometimes compensate for each other), nor does it change expression of the regulatory subunit p85.
- I showed that p110α acts as a negative regulator of insulin secretion, as its

specific pharmacological inhibition or shRNA-mediated knockdown results in an increase in insulin secretion and beta cell exocytosis from mouse and human islets, and insulinoma cells.

- Acute p110α pharmacological inhibition had no effect on insulin secretion, whilst acute treatment with the non-specific PI3K inhibitor wortmannin significantly increased insulin secretion, suggesting that the acute insulinotropic effect of wortmannin is likely due to its inhibition of other PI3Ks.
- Conversely, I showed that the specific pharmacological inhibition of p110β had no effect on insulin secretion. Rather, I showed that p110β has a non-catalytic function in beta cell exocytosis and insulin secretion. Acute infusion of a catalytically inhibited p110β recombinant peptide (together with its regulatory subunit p85), restored the exocytotic response following shRNA-mediated knockdown on p110β.
- I showed that p110γ acts as a negative regulator of insulin secretion, as its specific pharmacological inhibition or shRNA-mediated knockdown decreased insulin secretion from mouse and human islets, and decreased exocytosis from mouse and human beta cells, and insulinoma cells.
- p110γ inhibition or knockdown was associated with an increase in F-actin density, and a decrease in insulin granule recruitment to the plasma membrane; agents that induced depolymerization of F-actin restored the number of granules at the plasma membrane and restored the exocytotic response.
- I demonstrated that GIP-R and GLP-1-R activation was associated with a decrease in cortical F-actin in mouse beta cells and that GIP-R activation induced the

activation of the small GTPase Rac1. However, p110γ inhibition blocked both glucose and GIP mediated activation of Rac1. Furthermore, p110γ inhibition blunted the insulinotropic effects of GIP-R (but not GLP-1-R) activation.

5.2 GENERAL DISCUSSION

The PI3K family of enzymes regulate many essential cellular functions such as growth control, metabolism, vascular homeostasis and inflammation (Vanhaesebroeck et al., 2012). Impairments in PI3K signaling are implicated in a number of human disease states including: cancer, diabetes, cardiovascular disease and inflammatory disorders such as rheumatoid arthritis (Banham-Hall et al., 2012; Becattini et al., 2011; Jia et al., 2008; Vogt et al., 2009; Wymann and Solinas, 2013). As such, a number of PI3K inhibitors have been developed and are currently being investigated for treatments of these (and other) disease states (reviewed by Cho, 2013). However, because PI3Ks are ubiquitously, and because they regulate such a wide range of signaling processes, it is important to understand the distinct roles of each PI3K isoforms.

Class 1 PI3Ks have a long recognized in the regulation of insulin secretion. Non-specific PI3K inhibitors wortmannin and LY294002 potentiate insulin secretion (Collier et al., 2004; Eto et al., 2002; Hagiwara et al., 1995; Zawalich et al., 2002). However, these observations conflict with *in vivo* data showing that mice lacking the beta cell IR, or IGF1R (and thus exhibit decreased downstream PI3K activity) exhibit glucose intolerance, have elevated C-peptide levels and show elevated levels of circulating insulin (Kulkarni et al., 2002). Furthermore beta cell specific *pik3r1* (βPik3r1KO) and *pik3r2* knockout (βPik3r2KO) (which encode for p85α and p85β regulatory subunits of PI3K) in mice results in glucose intolerance (Kaneko et al., 2010). However, knockout of the class 1B PI3K isoform, p110γ, is also associated with an impairment of glucose-stimulated insulin secretion (MacDonald et al., 2004).

The work presented in this thesis elucidates the distinct roles of individual Class 1 PI3K isoforms in the regulation of islet insulin secretion and beta cell exocytosis. Understanding how individual PI3K isoforms control normal physiology is key to designing PI3K-targeting drugs that work within a specific therapeutic window.

5.2.1 WHAT WE KNOW FROM GLOBAL TRANSGENIC MICE

Whole body Class 1A PI3K knockout mice are generally embryonically lethal as in the case of p110α or β knockout mice, suggesting that these kinases are essential to normal development (Bi et al., 2002; Bi et al., 1999; Foukas et al., 2006). However, kinase dead mutants tend to be viable, reach an advanced age and are able to reproduce (Ciraolo et al., 2008; Foukas et al., 2006). Whole body knockouts of the regulatory subunits p85α, or -β or the splice variants p50/55α, as well as p110γ knockouts are also viable (Chen et al., 2004; Hirsch et al., 2000; Terauchi et al., 1999; Ueki et al., 2002).

The general conclusion from the experiments described below is that lack of either p110α or p110β catalytic activity results in mice developing fasting hyperinsulineamia and glucose intolerance (Ciraolo et al., 2008; Foukas et al., 2006). This phenotype is much more pronounced with the heterozygous kinase dead p110α mice, as mice lacking p110β catalytic activity show only mild impairment in glucose handling (Ciraolo et al., 2008; Foukas et al., 2006). However, knockout of the regulatory subunits p85α, p85β or p50/55α results in lower circulating blood glucose levels and increased insulin sensitivity and improved isolated islet beta cell secretory function (Chen et al., 2004; Eto et al., 2002; Terauchi et al., 1999). Furthermore, knockout of p110γ, leads to impairments in GSIS and mild glucose intolerance (MacDonald et al., 2004).

5.2.1a p110α knockin mice

PI3Kα is essential to growth and metabolism as evident by the embryonic lethality of global gene knockout and knockin mice (Bi et al., 1999; Foukas et al., 2006). However, a heterozygous mutation in the p110α ATP binding site (leading to a kinase dead protein) is not lethal, and in contrast to knockout mice, expression levels of the regulatory subunit p85, and the catalytic subunits p110α, p110βand p110δ remain unaltered (Foukas et al., 2006). Expression levels of the IR or IRS (Insulin-Receptor Substrate) proteins are also not affected, but rather reduced activation of effector pathways such as PKB/AKT is seen. These mice show a severe impairment in signaling via IRS proteins, exhibit hyperinsulineamia and glucose intolerance, and develop increased beta cell mass. Whilst these mice are also smaller in weight than their wild-type littermates, they display increased adiposity and have elevated plasma leptin levels, suggesting leptin resistance, or impaired PI3K signaling in the hypothalamus.

It is difficult to discern whether the hyperinsulinemia in these mice is a direct result of loss of p110α activity, or whether it is secondary to the decreased peripheral insulin sensitivity (or a combination of both). It would be interesting to examine isolated islets from these animals and look at insulin secretion in response to glucose or look at exocytosis from individual beta cells. My data would suggest that isolated islets from these mice would show an increase in GSIS and individual beta cells would exhibit increased exocytosis (Kolic et al., 2013).

5.2.1b p110β catalytically inactive mice

PI3Kβ is also essential to growth and development, as mice deficient in the p110β catalytic subunit die in the embryonic state (Bi et al., 2002). Mouse mutants expressing a

catalytically inactive p110β (p110β$^{K805R/K805R}$) are viable and survive into adulthood, and unlike with p110α catalytically inactive mutants, homozygous loss of p110β catalytic activity is not lethal (Ciraolo et al., 2008; Foukas et al., 2006). However, 50% fewer homozygous mutants than expected are born, indicating some embryonic lethality with incomplete penetrance (Ciraolo et al., 2008). The expression levels of p85 and p110α are not affected in these mice, and p110α activity remains unaltered. Whilst catalytic function of p110β is shown to not be required for AKT activation following stimulation with insulin, insulin-evoked AKT activation does decline significantly faster in mutant mice. Furthermore, at 6 months of age, p110β$^{K805R/K805R}$ mice start to show increased plasma glucose levels and mild insulin resistance, accompanied by increased beta cell mass and hyperinsulinemia (Ciraolo et al., 2008).

It is very interesting that only the non-catalytic function of p110β is necessary for survival. This is reminiscent of my study, where only the non-catalytic function of p110β was necessary for GSIS. In regards to glycemia, p110β$^{K805R/K805R}$ mice are relatively comparable to their wild-type littermates until about 6 months of age, when they start to show mild hyperglycemia. Increased circulating plasma insulin levels would be suggestive of insulin resistance rather than beta cell failure, however this was not directly measured. My data suggests that isolated islets from p110β$^{K805R/K805R}$ mice would not show impairments in insulin secretion (Kolic et al., 2013). However due to the acute nature of my study, it would be more prudent to examine GSIS from isolated islets from p110β$^{K805R/K805R}$ mice.

5.2.1c p85α knockout mice

Homozygous Pik3r1-/- mice which lack the p85α regulatory subunit, but still maintain expression of p85β or the shorter splice variants p50/55α are viable (Terauchi et al., 1999). These mice show significant overexpression of p50α. (However, homozygous Pik3r1-/- mice that lack p85α and its splice variants p50/55α die within a few weeks of birth (Fruman et al., 2000)). PI3K activity in muscle and adipose tissue is decreased by 40-50% compared to wild-type controls; however, the generation of PIP_3 in response to insulin in adipocytes is paradoxically increased. Pik3r1-/- mice exhibit lower circulating blood glucose levels and increased insulin sensitivity, thought to be primarily due to increased glucose uptake into the muscle and adipose tissue (Terauchi et al., 1999). Insulin stimulated GLUT-4 translocation to the plasma membrane of these tissues is increased in Pik3r1-/- mice. This increase in GLUT-4 translocation is shown to be a result of the regulatory isoform switch from p85α to p50α in Pik3r1-/- mice with a subsequent increase in insulin-induced generation of PIP_3 (which promotes GLUT-4 translocation).

Isolated islets from Pik3r1-/- mice have also been examined to investigate the role of PI3K in beta cell secretory function (Eto et al., 2002). These islets have decreased insulin content and decreased insulin granule number in individual beta cells, but show higher glucose stimulated insulin release (Eto et al., 2002). Furthermore, the non-specific PI3K inhibitor wortmannin further increases insulin secretion in Pik3r1-/- mice (which still maintained some residual PI3K activity), suggesting that PI3K normally plays a suppressive role in GSIS (Eto et al., 2002). However, wortmannin also inhibits both class II and III PI3K isoforms, which may also have a role in insulin secretion (Dominguez and Holmes, 2011).

5.2.1d p50/55α knockout mice

Whole body mouse knockouts of the Class 1A regulatory subunits p50α and p55α (which are mostly expressed in insulin sensitive adipose, muscle and live tissues) are also viable (Chen et al., 2004). Expression levels of the p85 regulatory subunit in these mice are slightly decreased in muscle tissue, whilst expression levels of the catalytic subunits were not measured. These mice exhibit normal fasting glucose levels, but have lower fasting insulin levels and show enhanced insulin sensitivity following an insulin tolerance test. This enhancement in insulin sensitivity is a result of increased glucose uptake by muscle and adipose tissue, as well as more robust glucose metabolism.

5.2.1e p85β knockout mice

The Pik3r2 gene encodes for the regulatory subunit p85β, which is ubiquitously expressed, but at a lower level than p85α (Otsu et al., 1991). p85β-/- mice are viable; they are slightly smaller in size compared to their wild type littermates (Ueki et al., 2002). The expression levels of p85α or the splice variants p50/55α are unchanged in p85β-/- mice compared to wild type and PI3K activity induced by insulin is preserved. However, both fasting and fed plasma glucose and insulin levels are lower in p85β-/- mice, suggesting improved insulin sensitivity. Furthermore, PKB/AKT activity is increased in the muscles of these animals (but unchanged in the liver). The authors postulate that p85 may play a role in degradation of PIP_3 through stimulation of unknown phosphatases. Furthermore they suggest that p85 (which can exist as a monomer) may compete with p85-p110 dimer binding to IRS proteins and suggest that a moderate decrease in p85 protein expression may be beneficial, as it reduces these inhibitory effects of p85.

5.2.1f p110γ knockout mice

Mice lacking both alleles of the p110γ catalytic isoform (p110γ-/-) are viable, fertile and display a normal life-span (Hirsch et al., 2000). Lack of p110γ does not change the expression levels of other class 1 PI3K isoforms (Hirsch et al., 2000). Whilst fasting blood glucose levels are not different between p110γ-/- mice and wild type controls, p110γ-/- mice show an impaired glucose tolerance test, with significantly lower plasma insulin levels in response to an intraperitoneal (i.p.) glucose load (MacDonald et al., 2004). This decrease in insulin secretion in response to a glucose load is not due to reduced beta cell mass, as beta cell mass and insulin content is increased in p110γ-/- mice. Furthermore, *ex vivo* perfused pancreatic insulin secretion in response to arginine is not different between wild type and p110γ-/- mice. This data thus suggests that p110γ-/- mice show an impaired secretory defect, and suggest a positive role for PI3Kγ in insulin secretion.

5.2.2 WHAT WE KNOW FROM TISSUE SPECIFIC TRANSGENIC MICE

The alterations in glucose handling seen following whole body knockout (or knockin) of catalytic and regulatory subunits of class1A PI3Ks are mainly due to changes in insulin sensitivities in muscle, adipose, and liver tissues (Chen et al., 2004; Ciraolo et al., 2008; Foukas et al., 2006; Ueki et al., 2002). Thus, to examine the role of class1A PI3K signaling in beta cells, beta cell specific knockout mice that lacked the insulin receptor or the insulin-like growth factor 1 (IGF1) receptor (or both), were developed (described below).

5.2.2a Beta cell specific insulin receptor knockout mice

Mice lacking the beta cell insulin receptor (βIRKO) show an age-dependent progression in glucose intolerance (Kulkarni et al., 1999a). The expression of the insulin receptor in other tissues of the mouse is not affected, thus the glucose intolerance seen is not due to loss of insulin sensitivity. Beta cell mass is slightly reduced in βIRKO mice at 4 months of age but insulin content does not change drastically. Furthermore, there is no change in GLUT-2 expression in βIRKO mice compared to wild type. The authors suggest that the loss of first phase insulin secretion in βIRKO mice is due to beta cell secretory machinery impairments or intracellular alterations in glucose sensing.

5.2.2b Beta cell specific IGF1 receptor knockout mice

IGF1 receptor knockout mice (βIGFRKO) show increased fasting levels of insulin (Kulkarni et al., 2002). Isolated islets from βIGFRKO mice show impairments in GSIS and reduced expression of GLUT-2 and glucokinase. Furthermore, the normal suppressive effect of IGF1 on insulin secretion is lost in βIGFRKO islets. These mice also have an impaired glucose tolerance response, but show normal sensitivity to insulin. This suggests that the IGF1-R is important in the differentiation function of the beta cell.

5.2.2c Beta cell specific double insulin and IGF1 receptor knockout mice

Whilst beta cell specific knockout of either the insulin or IGF1 receptor in mice leads to mild impairments in glucose handling, beta cell double knockout mice, in which both receptors are disrupted develop a severe diabetic phenotype by three weeks of age (Ueki et al., 2006). This suggests some redundancy in IR and IGF1-R signaling. Isolated islets from these double knockout mice show severely blunted GSIS, as well as

impairments in Ca^{2+} oscillations and oxygen consumption. Islets from these mice also show evidence of increased beta cell apoptosis, as measured by increased TUNEL (Terminal deoxynucleotidyl transferase dUTP Nick End Labeling) (a method for detecting DNA fragmentation) positive cells, and exhibit a slight decrease in cell proliferation. Signs of reduced PI3K activity are also evident: absent PKB/AKT phosphorylation, reduced PDK1 protein expression in the cytosol, and FoxO1 nuclear restriction. However, paradoxically PTEN protein levels are higher in islets from double knockout mice. Direct measurements of PI3K activity or expression levels of PI3Ks were not assessed.

5.2.2d Beta cell specific p85α/p85β double knockout mice

Whole body p85α or p85β knockout mice show enhanced insulin sensitivity, and isolated islets from p85α knockout mice exhibit higher glucose stimulated insulin release (Eto et al., 2002; Terauchi et al., 1999; Ueki et al., 2002). To further examine the role of p85α and p85β in beta cells specifically, beta cell specific double knockout mice lacking both regulatory subunits were generated (Kaneko et al., 2010). This almost completely abolished PI3K activity in the beta cells, as measured by a marked reduction in glucose stimulated PIP_3 production and FoxO1 localization in the nucleus (PI3K protein expression was not measured). These mice exhibited glucose intolerance and decreased *in vivo* GSIS. Isolated islets from these mice also showed decreased glucose-stimulated exocytotic events and a decrease in Ca^{2+} influx. This was associated with a decreased expression of GLUT-2 and the transcription factor pdx1. Furthermore, expression levels of SNARE complex proteins were reduced, which could account for some of decrease in insulin exocytotic events observed.

5.2.3 WHAT WE KNOW FROM ACUTE NON-SPECIFIC CLASS 1 PI3K PHARMACOLOGICAL INHIBITION

Tissue specific knockout and knockin models are important in understanding how chronic genetic augmentation of PI3K signaling alters the regulation of glucose handling. However, these studies are only possible in animal models, and only offer explanations of how chronic genetic manipulation of PI3K signaling affects glucose handling. Long-term genetic knockdown can cause developmental problems in key glucose-sensing tissues, which could be contributing to the defects in glucose handling seen. In fact the majority of the tissue specific models described above are associated with a loss of beta cell mass and decreased expression of GLUT-2 and pdx-1. Thus the secretory defects seen are likely due to the chronic and complete ablation of PI3K activity. Furthermore, since numerous pharmacological PI3K inhibitors are currently being investigated for the treatments of diseases such as inflammatory disorders and cancer, it is essential to understand the effects of acute PI3K pharmacological inhibition on the regulation of glucose metabolism.

5.2.3a Effects of wortmannin on insulin secretion

Wortmannin, a pan PI3K inhibitor (with a similar potency *in vitro* for the class I, II, and III PI3K members) can also inhibit other PI3K related enzymes (at concentrations >1 μM) such as MLCK and mTOR, both of which are involved in insulin secretion (Iida et al., 1997; Le Bacquer et al., 2013; Niki et al., 1993; Penn et al., 1982; Yang et al., 2012). Wortmannin (50-100 nM) was first shown to increase GSIS in a MIN6 insulin-secreting cell line (Hagiwara et al., 1995). At these concentrations wortmannin significantly inhibited PI3K activity without affecting activities of other PI3K related enzymes (Hagiwara et al., 1995). However, at concentrations >1 μM, wortmannin was

shown to inhibit GSIS (Gao et al., 1996; Hagiwara et al., 1995). This is likely due to its inhibitory effects on MLCK and mTOR, as the inhibition of these enzymes suppresses insulin secretion (Iida et al., 1997; Le Bacquer et al., 2013; Niki et al., 1993; Yang et al., 2012).

The effects of wortmannin were also examined on glucose oxidation and intracellular Ca^{2+} handling in mouse islets (Eto et al., 2002). 100 nM wortmannin treatment does not affect glucose oxidation, nor does it affect intracellular ATP concentrations (Eto et al., 2002). Intracellular Ca^{2+} entry is also not affected by 100 nM wortmannin. These results suggested that the effects of wortmannin on GSIS are mediated at sites distal to cytosolic Ca^{2+} entry (Eto et al., 2002).

Furthermore, the effects of wortmannin were examined on IGF-1-mediated suppression, and GIP-mediated stimulation, of insulin release (Hagiwara et al., 1995; Straub and Sharp, 1996b). 50 nM wortmannin completely reverses the decrease in insulin secretion seen following IGF-1 treatment; whilst 100 nM wortmannin partially inhibits GIP-induced insulin secretion in clonal beta cell lines, thus further implicating a role for PI3K in GSIS.

5.2.3b Effects of acute PI3K inhibition on insulin secretion from ob/ob mice

The insulinotropic effects of wortmannin were also examined in isolated islets from ob/ob mice (a model of T2D) (Zawalich et al., 2002). Whilst wortmannin is a potent potentiator of insulin secretion from lean control mice, islets from ob/ob mice are immune to the insulinotropic effects of wortmannin. However, consistent with evidence of hyperinsulinemia in early stages of T2D, islets from ob/ob mice secrete more insulin in response to glucose alone. Furthermore, isolated islets from ob/ob mice are resistant to

the negative feedback effect that insulin can have on its own release (Loreti et al., 1974). Insulin sensing tissues in ob/ob mice, which become insulin resistant, also show signs of reduced PI3K activity (Kerouz et al., 1997); this is consistent with the loss of PI3K catalytic activity in mice leads to insulin intolerance (Foukas et al., 2006). These data taken together suggest that ob/ob mice are hyperinsulinemic because of the loss of beta cell PI3K activity, concurrent with the negative feedback effect insulin exerts on its own secretion (Loreti et al., 1974; Zawalich et al., 2002).

5.2.3c Acute effects of PI3K-PDK1-Akt inhibition on insulin secretion

Whilst wortmannin is an efficient PI3K inhibitor, it does not discriminate between the different PI3K classes. PIK-75 is a specific inhibitor for class 1A PI3K isoforms (Han and Zhang, 2010; Knight et al., 2006). PIK-75 acts as a specific inhibitor of p110α if used at a concentration of <300 nM (Knight et al., 2006). However, at concentration > 300 nM, PIK-75 also inhibits p110β. PIK-75 reduces AKT phosphorylation and increases GSIS from isolated mouse islets in a concentration dependent manner (Aoyagi et al., 2012). PIK-75 is however unable to induce insulin secretion in mice lacking both the p85α and p85β regulatory subunits. Interestingly, a more chronic (>24 hr) inhibition of class 1A PI3K activity with 500 nM PIK-75 is associated with a decrease in GSIS and a slight decrease in SNARE protein expression.

The increase in insulin secretion following acute PI3K inhibition is shown to be a result of an increase in newcomer granule fusion events, as seen through TIRF microscopy. Furthermore, expression of a constitutively active PDK1 blocks the potentiating effect of PIK-75, whilst PDK1 inhibition mimics the potentiating effects. Whilst this is in apparent contrast to βPDK1-/- mice which develop overt diabetes, it is

important to remember that genetic deletion of PDK1 affects beta cell development and substantially reduces beta cell mass (Hashimoto et al., 2006).

To further characterize this signaling pathway, downstream effectors of PDKI signaling (AKT and PKCζ) were examined in the potentiating effects of PIK-75 (Aoyagi et al., 2012). A constitutively active PKCζ does not block the potentiating effect of PIK-75, whilst a constitutively active AKT does. Furthermore, selective inhibition of AKT mimics the stimulatory effects of PIK-75. Whilst the downstream effector of AKT that is involved in this signaling pathway is currently unknown, MyosinVA is suggested as a possible target. Phosphorylation of MyosinVA (which is known to play a role in insulin granule trafficking) (Ivarsson et al., 2005) by AKT leads to its binding to the cytoskeleton (Yoshizaki et al., 2007). The inhibition of AKT activation would prevent MyosinVA phosphorylation, and it turn would allow an increased number of insulin granules to detach from the actin cytoskeleton, which would subsequently allow for more granules to fuse with the plasma membrane (Aoyagi et al., 2012).

5.2.4 WHAT WE KNOW FROM ACUTE ISOFORM SPECIFIC CLASS 1 PI3K PHARMACOLOGICAL INHIBITION OR KNOCKDOWN

Whilst a number of pharmacological PI3K inhibitors currently being investigated for the treatments of various disease states are pan-isoform PI3K inhibitors, isoform-specific inhibitors have also been generated (reviewed by Cho, 2013). Because PI3K signaling is ubiquitous to nearly all tissues, it is essential to understand the effects of acute specific PI3K pharmacological inhibition on the regulation of glucose metabolism.

5.2.4a PI3Kα is the primary insulin-responsive Class 1API3K

A number of specific PI3Kα inhibitors (including PIK-75 at concentrations < 300 nM) inhibit insulin-stimulated activation of AKT, and production of PIP_3 in cultured adipocytes (Knight et al., 2006). These inhibitors also reduce PI3K activity in insulin stimulated adipocytes, as shown though an *in vitro* PI3K assay from lysates immunoprecipitated for IRS protein. Furthermore, these specific PI3Kα inhibitors block insulin-induced glucose uptake *in vitro* in cultured adipocytes, and prevent an insulin-stimulated decrease in blood glucose following an insulin tolerance test in mice.

However, whilst specific PI3Kβ inhibitors also reduce PIP_3 production, they fail to block insulin-induced phosphorylation of AKT in cultured adipocytes (Knight et al., 2006). They also only slightly reduce PI3K activity from adipocyte lysates immunoprecipitated for IRS. Furthermore, PI3Kβ inhibitors have no effect on blood glucose levels during an insulin tolerance test. These data taken together suggest that PI3Kα is the primary insulin-responsive PI3K. My data also suggests that PI3Kα is the primary insulin-responsive class 1A PI3K in mouse and human beta cells (Kolic et al., 2013). I show that specific pharmacological inhibition of PI3Kα stimulates GSIS from isolated islets and exocytosis from individual beta cells, whilst specific pharmacological inhibition of PI3Kβ has no effect on exocytosis or insulin secretion.

Whilst I did not examine PIP_3 production in the presence of specific PI3Kα and PI3Kβ pharmacological inhibitors, I looked at recruitment of an AKT plekstrin homology domain (Tengholm and Meyer, 2002) to the plasma membrane as a surrogate for PI3K activity. Inhibition of PI3Kα reduced both basal and insulin-stimulated GFP-PH_{AKT} recruitment to the plasma membrane **(Figure 34)**. However whilst inhibition of PI3Kβ

blocked insulin-stimulated recruitment, it had no effect on basal levels of GFP-PH_{AKT} recruitment. These results are surprising as PI3Kβ inhibition has no effect on insulin secretion, but our measurements of insulin-stimulated GFP-PH_{AKT} recruitment indirectly indicate a decrease in insulin stimulated PIP_3 production **(Figure 34)**. However, caution should be taken with the interpretation of GFP-PH_{AKT} recruitment data as in our experiments we induce expression of the PH_{AKT} domain to levels that are much higher than found physiologically.

Knight *el al.* (2006) showed that the specific PI3Kβ inhibitor TGX-115 reduces insulin stimulated PIP_3 production in adipocytes (Knight et al., 2006). However, TGX-115 failed to block insulin induced AKT phosphorylation in these cells. Thus, this suggests that PI3Kβ may be contributing to a pool of insulin – stimulated PIP_3 production that is not independently required for AKT activation (and in our case insulin secretion). Knight *el al.* (2006) suggest that PI3Kβ contributes to a pool of PIP_3 which defines a threshold for the amount of PI3Kα activity required to stimulate downstream pathways. This theory is supported by experiments that show that the presence of TGX-115 shifts the concentration response curve for PIK-75-mediated inhibition of AKT phosphorylation. Thus, in the presence of TGX-115, a lower concentration of PIK-75 is needed to inhibit AKT phosphorylation. Whilst this is a plausible explanation for the catalytic role of PI3Kβ in insulin secretion, I did not test the effects of TGX-221 in the presence of PIK-75.

Figure 34: Affect of p110α inhibition on GFP-PH_{AKT} recruitment to the plasma membrane in INS-1 cells.

Figure 34 shows average basal and insulin-stimulated (200 nM; 20 min) GFP-PH_{AKT} recruitment to the plasma membrane in INS-1 832/13 cells. Cells were transfected with GFP-PH_{AKT} and treated overnight with DMSO (*open bars*), PIK-75 (100 nM) (*black bars*) or TGX-221 (*grey bars*) before stimulated with bovine insulin. This data is representative 10-25 cells per group.

** -$p < 0.01$

(JK and AMS (under supervision of JK) performed imaging experiments and analyzed data.)

Figure 34

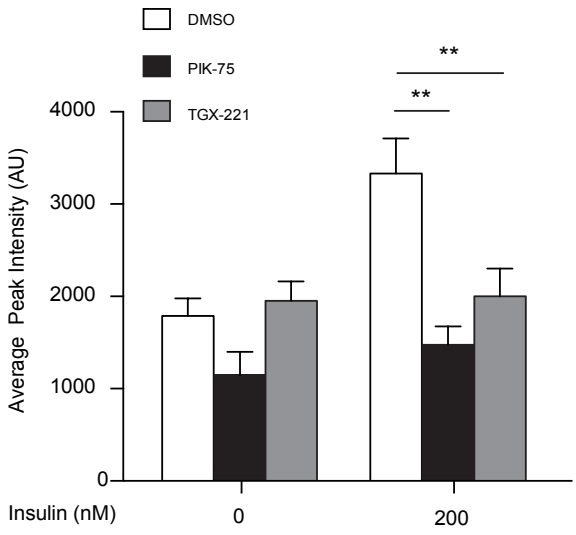
DMSO
PIK-75
TGX-221
**
**
4000
3000
2000
1000
0
Average Peak Intensity (AU)
Insulin (nM)
0
200

5.2.4b PI3Kβ has a catalytic independent role in insulin secretion

Whist shRNA-mediated knockdown of PI3Kα mimics the results of pharmacological inhibition, shRNA-mediated knockdown of PI3Kβ does not. We see a severe impairment of insulin secretion and exocytosis following shRNA-mediated knockdown of PI3Kβ (Kolic et al., 2013). This is suggestive of a catalytic independent or "scaffolding" function of PI3Kβ in insulin secretion and exocytosis **(Figure 35)**. To confirm this theory, we generated a catalytically inactive p110β mutant ($p110\beta^{K805R}$), and showed that defects in beta cell exocytosis were restored following overexpression of $p110\beta^{K805R}$. Furthermore, acute infusion of WTp110β (even in the presence of the TGX-221 catalytic inhibitor) enhanced insulin secretion in INS-1 cells. We did not determine the mechanism by which p110β acts in a non-kinase dependent matter in the beta cell as it was beyond the scope of our study, however possible mechanism by which p110β may act as a scaffolding protein are discussed in the concluding remarks section of chapter 2.

One significant limitation of my study is that I cannot rule out the possibility that the decrease in secretion and exocytosis seen following p110β knockdown is simply due to increased p110α activity. The removal of p110β may be removing competition for p110α binding to its tyrosine kinase receptor, and re-introducing $p110\beta^{K805R}$ or WTp110β may be displacing p110α binding and reducing its activity. I did not test whether p110α activity increases following knockdown of p110β, however Jia *et al.* (2008) showed that mice with conditional hepatocyte specific knockout of PI3Kβ showed higher fasting levels of insulin, and impaired insulin and glucose tolerance tests (Jia et al., 2008). No significant change in AKT activation in response to insulin was observed. If

PI3Kβ ablation is increasing p110α activity, an increase in AKT phosphorylation should have been observed. Furthermore, Ciraolo *et al.* (2008) also showed a kinase independent activity for p110β (described above in section 5.2.1b) in growth and development of mice (Ciraolo et al., 2008). Recruitment of p110α to the IRS receptor, or p110α activity was not altered following p110β ablation, thus further supporting a p110β kinase-independent function, rather than altered p110α activity .

Figure 35: Regulation of insulin secretion by PI3Kα and PI3Kβ.

Both shRNA mediated knockdown and pharmacological inhibition of PI3Kα increases insulin secretion from pancreatic islets. Pharmacological inhibition of PI3Kβ has no effect on insulin secretion, whilst shRNA mediated knockdown drastically blunts GSIS. We did not observe changes in F-actin density at the time points studied; however this does not rule out the possibility that actin remodeling is not affected, as both PIP_2 and PIP_3 are known to have essential roles in the actin remodeling process.

PI3Kβ is postulated to be contributing to a pool of PIP_3 that is not limiting to AKT activation; thus we see no effects on insulin secretion. However, PI3Kβ seems to have a non-catalytic function; perhaps by interacting with the SNARE protein complex, as PI3Kβ reduces granule number at the plasma membrane.

The mechanism by which PI3Kα inhibition or knockdown stimulates insulin secretion is still not fully understood. Whilst we did not see an increase in insulin granule number at the plasma membrane following PI3Kα inhibition, it has been suggested that Class 1 PI3Ks may control newcomer granule release, perhaps by controlling activation of MyosinVA.

Figure 35:

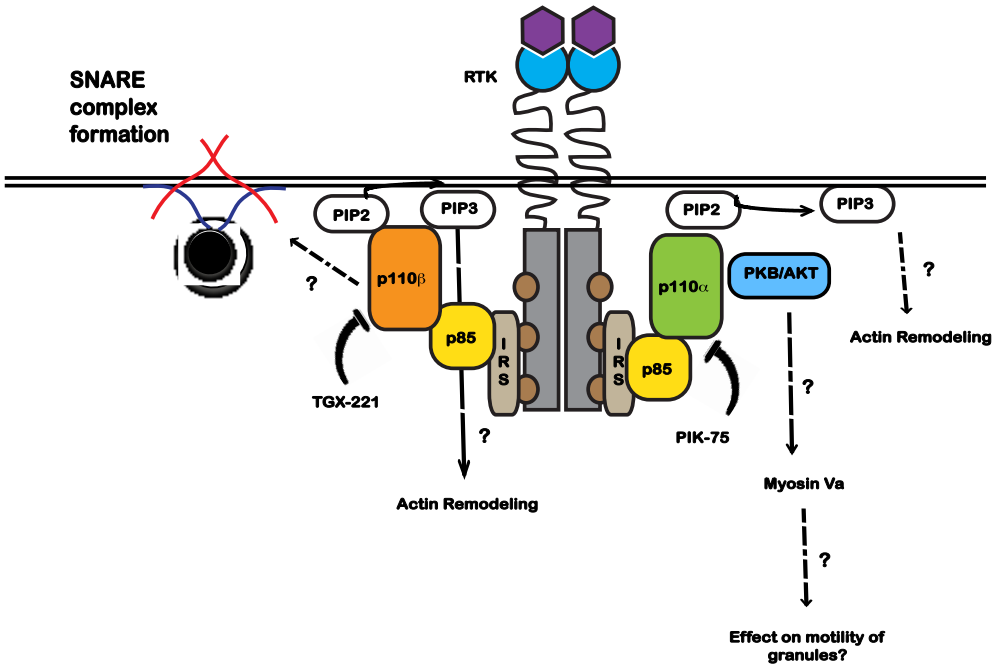
SNARE
complex
formation
RTK
PIP2
PIP3
p110β
p85
I
R
S
TGX-221
?
Actin Remodeling
PIP2
PIP3
p110α
PKB/AKT
p85
PIK-75
Actin Remodeling
Myosin Va
Effect on motility of
granules?

5.2.4c PI3Kγ is a positive regulator of insulin secretion

Whilst chronic genetic whole body ablation of p110γ in mice impairs glucose handling and insulin secretion (MacDonald et al., 2004), it is important to understand how p110γ affects insulin secretion in a more acute and tissue-specific setting. Li *et al.* (2006) showed that basal and glucose-stimulated insulin secretion are decreased by 30% in INS1-E cells following shRNA mediated knockdown of p110γ (Li et al., 2006). Furthermore, they showed that insulin content is increased by about 40%.

My studies confirm that p110γ is a positive regulator of insulin secretion and provide a mechanism by which p110γ regulates beta cell exocytosis (Pigeau et al., 2009). I show that the inhibition (or knockdown) of p110γ increases actin polymerization and prevents insulin granule recruitment to the plasma membrane. Furthermore I demonstrate that agents that induce actin depolymerization restore the exocytotic response following p110γ inhibition **(Figure 24)**. **Figure 36** is a summary of the proposed mechanism by which p110γ regulates cortical actin dynamics. Both specific pharmacological inhibition of p110γ and shRNA-mediated knockdown show similar results. This is essential because p110γ has a kinase-independent role in regulating phosphodiesterase 3B (PDE3B) activity (Patrucco et al., 2004; Perino et al., 2011). Depletion of p110γ lowers PDE3B activity and leads to increased levels of cAMP (Patrucco et al., 2004). In the beta cell, cAMP has a stimulatory role in insulin secretion through its activation of PKA and Epac (Roscioni et al., 2008; Seino et al., 2009). Thus, the increased levels of cAMP seen in whole body p110γ knockout mice should stimulate insulin secretion (Waddleton et al., 2008; Walz et al., 2007). However, the opposite effect is observed, suggesting that p110γ regulates insulin secretion independent of its effect on PDE3B activity.

Figure 36: PI3Kγ regulates beta cell exocytosis by controlling cortical actin polymerization.

Pharmacological inhibition or shRNA-mediated knockdown of PI3Kγ impairs insulin secretion and exocytosis. I show that this is mediated by an increase in cortical F-actin density, which prevents reserve pool (RP) insulin granule recruitment to the plasma membrane (Pigeau et al., 2009). This limits the number of granules in the readily releasable pool (RRP). However, PI3Kγ inhibition in beta cells lacking PTEN does not increase cortical F-actin density. Both PIP_2 and PIP_3 to play essential roles in actin remodeling (Insall and Weiner, 2001; Logan and Mandato, 2006; Papakonstanti and Stournaras, 2002; Sechi and Wehland, 2000; Yin and Janmey, 2003). High levels of PIP_2 are generally associated with an increase in actin polymerization, whereas low levels both block actin assembly and promote actin severing (Logan and Mandato, 2006; Sechi and Wehland, 2000; Yin and Janmey, 2003). PIP_2 activates the Arp 2/3 proteins, which induce actin polymerization, and inhibits the actin severing proteins gelsolin and cofilin (Uenishi et al., 2013; Tomas et al., 2010). PIP_3 can activate the small GTPase protein Rac1 (Innocenti et al., 2003; Welch et al., 2002). Rac1 has been ascribed both positive and negative roles in actin polymerization. However, in the beta cell, Rac1 seems to be involved in actin depolymerization as Rac1 deficiency prevents glucose induced actin depolymerization (Asahara et al., 2013; Li et al., 2004).

Figure 36

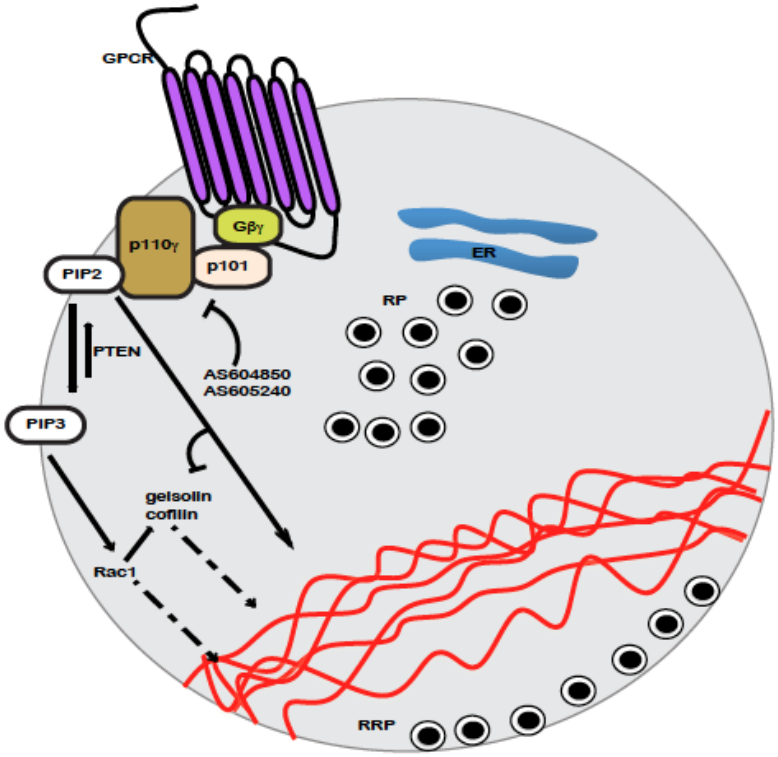
GPCR
Gβγ
p110γ
p101
PIP2
PTEN
PIP3
AS604850
AS605240
ER
RP
gelsolin
cofilin
Rac1
RRP

5.2.4d Role of PI3Kγ in GIP-R and GLP-R activation

I examined the role of p110γ in incretin effects of GIP-R and GLP-R activation. Surprisingly I found that the insulinotropic effect of GIP-R (but not GLP-R) activation is blunted by either inhibition of p110γ or shRNA-mediated knockdown. I saw no difference in insulin content following p110γ overnight inhibition, or knockdown, or following acute treatments with GIP, GLP-1 or Ex-4. This was in contrast to p110γ knockout animals where insulin content was increased from isolated islets (MacDonald et al., 2004). I also did not see decreased mRNA expression of GIP-R following overnight p110γ inhibition, suggesting that this was not a mechanism by which its insulinotropic effects were blunted. This was essential to my study because PI3Ks (including PI3Kγ) are implicated in the regulation of the nuclear transcription factor FoxO1 (Kim et al., 2005; Madeddu et al., 2008). PI3K-mediated FoxO1 phosphorylation leads to its translocation from the nucleus to the cytosol, and subsequent inactivation (Kim et al., 2005; Madeddu et al., 2008). FoxO1 can regulate GIP and GLP-1-R expression through the regulation of the transcription factor Wnt and its downstream effector TCF7L2 (Chiang et al., 2012; Essers et al., 2005; Shu et al., 2009).

Furthermore both GIP-R and GLP-1-R activation has also been associated with FoxO1 inactivation (Buteau et al., 2006; Kim et al., 2005). GLP-1-R activation mediates its effects on FoxO1 through the transactivation of EGFR and subsequent activation of class 1A PI3Ks (Buteau et al., 1999; Buteau et al., 2003; Buteau et al., 2006). However, the PI3K isoform involved in GIP-R-mediated FoxO1 regulation has not been examined.

Not measuring plasma membrane protein expression of GIP-R and GLP-1-R was a limitation to my study, as varying degrees of GIP-R or GLP-1-R internalization could

be occurring following p110γ inhibition or knockdown. GPCRs can be internalized (endocytosed) through the aid of clathrin coated pits (Goodman et al., 1996; Grady et al., 1995; Lin et al., 1998; Tolbert and Lameh, 1996; Widmann et al., 1995). By regulating proteins involved in clathrin-mediated endocytosis, PI3Ks (and their phosphoinositide substrates and products) are implicated in GPCR internalization (Gaidarov and Keen, 1999; Naga Prasad et al., 2002). However, there are currently no antibodies on the market that are able to definitively distinguish between the GIP-R and GLP-1-R; they are shown to be neither sensitive nor specific (Drucker et al., 1987; Panjwani et al., 2013; Pyke and Knudsen, 2013). I could however measure GIP or GLP-1 potentiated intracellular cAMP increase following p110γ inhibition or knockdown. Theoretically, if p110γ inhibition were causing receptor internalization, I would see a reduced cAMP signal in response to agonist stimulation.

5.2.5 WHAT WE HAVE LEARNED ABOUT CLASS 1 PI3K AND GPCR INVOLVEMENT IN ACTIN REMODELING

The remodeling of the actin cytoskeleton is essential to the insulin secretory response. However the signaling pathways that control the organization of the actin fiber assembly and disassembly are complex and are still not fully understood. Because the inhibition (or knockdown) of class 1 PI3K isoforms alters the exocytotic response downstream of intracellular Ca^{2+} entry, and alters granule recruitment to the plasma membrane, we examined the role of PI3Ks in remodeling of the actin cytoskeleton. Furthermore both the substrate (PIP_2) and the product (PIP_3) of class 1 PI3K activation are involved in actin remodeling, thus further implicating these kinases in the actin remodeling process (Insall and Weiner, 2001; Logan and Mandato, 2006) **(Figure 36)**.

5.2.5a Overnight inhibition of PI3Kα or -β inhibition does not change F-actin density

I did not see any changes in cortical F-actin density following overnight inhibition of either PI3Kα or PI3Kβ (Kolic et al., 2013). This is an unusual finding since PI3Kα in particular is responsible for a large pool of PIP_3 generation, which acts as an instructive cue for actin remodeling; unstimulated cells have very low levels of PIP_3 (Logan and Mandato, 2006). Furthermore, alterations in class 1 PI3K signaling in various cell types have previously been shown to involve changes in cortical actin dynamics.

The lack of change in cortical F-actin density observed following PI3Kα or PI3Kβ inhibition can be explained by a number of factors. I did not look at time course dependent cortical F-actin density following PI3Kα or PI3Kβ inhibition, but rather only examined cortical F-actin density following overnight inhibition of these kinases. Actin remodeling is a dynamic process, and thus by looking at F-actin density only at one time point it is possible that I missed seeing any changes. Furthermore, I did not examine stimulus-dependent actin remodeling following PI3Kα or PI3Kβ inhibition. It would be interesting to look at glucose-stimulated actin remodeling in the presence of PI3Kα or PI3Kβ inhibitors, or following their knockdown.

5.2.5b GIP-R and GLP-R activation stimulates actin depolymerization

My studies showed a novel mechanism by which GIP-R and GLP-1-R activation potentiates insulin secretion. I show that both GIP and Ex-4 are potent actin depolymerizing agents, and that they induce actin depolymerization in mouse beta cells. I can postulate that actin depolymerization allows for a greater population of insulin granules to be released following a glucose stimulus. I did not monitor granule

recruitment to the plasma membrane following GIP-R and GLP-1-R activation. However, I show that the actin depolymerizing ability of GIP is linked to p110γ activity, as p110γ inhibition prevents GIP-R activation–mediated actin remodeling in mouse beta cells. Furthermore, p110γ inhibition blunts the GIP-induced potentiation of exocytosis in beta cells, and insulin secretion in islets, thus linking its incretin effect to actin remodeling. p110γ inhibition does not impair GLP-1-R mediated actin remodeling, nor does it impair its ability to stimulate exocytosis and insulin secretion. This would explain why p110γ-/- mice do not have an impaired oral glucose tolerance test and why chronic Ex-4 treatment normalizes impaired GSIS fr0m p110γ-/- islets (Li et al., 2006).

Furthermore, I show that GIP-R activation activates Rac1 in INS1 cells independent of glucose stimulation. Rac1 activation is necessary for actin reorganization and the subsequent recruitment of secretory granules to the plasma membrane (Li et al., 2004). shRNA-mediated knockdown of Rac1 in INS-1 attenuates GSIS, and prevent glucose-induced actin depolymerization (Asahara et al., 2013). Thus my data further implicates GIP receptor activation in actin remodeling, and suggests an additional mechanism, in concert with classical cAMP/PKA-dependent signaling by which GIP potentiates insulin secretion.

5.2.5c Evidence suggesting that GIP induces actin depolymerization by activating the GIP-R

I show that GIP induced actin depolymerization is mainly due to its actions of the GIP-R. We examined the effects of GIP on cortical F-actin density in beta cells from beta cell specific GIP-R knockout mice (β-cell$^{GIP\text{-}R\text{-}/\text{-}}$) under low glucose conditions (unpublished data) (**Figure 37**). I show that GIP has a minimal effect on cortical F-actin

density in beta cells from β-cell$^{GIP\text{-}R\text{-}/\text{-}}$ mice, whilst Ex-4 induces actin depolymerization in the beta cells. Both GIP-R and GLP-1-R activation induces actin depolymerization in beta cells from control animals. Whilst my data has shown that p110γ has a role in GIP induced actin depolymerization, the mechanism by which GIP-R and GLP-1-R activation induces actin remodeling is currently not understood. I show that Rac1 activation induced by GIP requires functional p110γ. However, I did not directly examine whether blocking Rac1 activation prevents GIP induced actin depolymerization. Furthermore, I did not examine whether GLP-1-R activation induced Rac1 activation. However, it is suggested that both GIP-R and GLP-1-R activation activates serine/ threonine protein kinase PAK 1 in response to increased cAMP signaling and PAK 1 has previously been implicated Rac1 activation and actin remodeling (Nie et al., 2013; Nie et al., 2012). This suggests that GLP-1 would activate Rac1, but may not require functional p110γ to do so.

Figure 37: GIP induces actin remodeling in beta cells from wild type mice, but not in beta cells from mice lacking the GIP-R.

Panel **(A)** (*top*) shows representative images for F-actin staining (green) for each incubation period from WT mouse beta cells (with intensity line scans shown below each image). (*bottom*) shows representative images for F-actin staining for each incubation period with glucose, GIP (10 nM), Ex-4 (1 nM) or LatrunculinB (10 μm) from β-cell$^{GIP-R-/-}$ mouse beta cells (with intensity line scans shown below each image). Beta cells were identified by insulin staining (red).

Panel **(B)** shows mean F-actin intensities from 40-62 cells from three WT (*white bars*) or β-cell$^{GIP-R-/-}$ (*black bars*) mice from the treatment groups descried above.

***p<0.001 compared with the 2.8 glucose condition for each genotype, ###p<0.001 compared with the GIP (10 nM) WT vs. β-cell$^{GIP-R-/-}$ treatment.

(JK performed imaging experiments and analyzed data. Islets were received from the lab of Dr. Daniel Drucker in Lunenfeld Tanenbaum Research Institute)

Figure 37

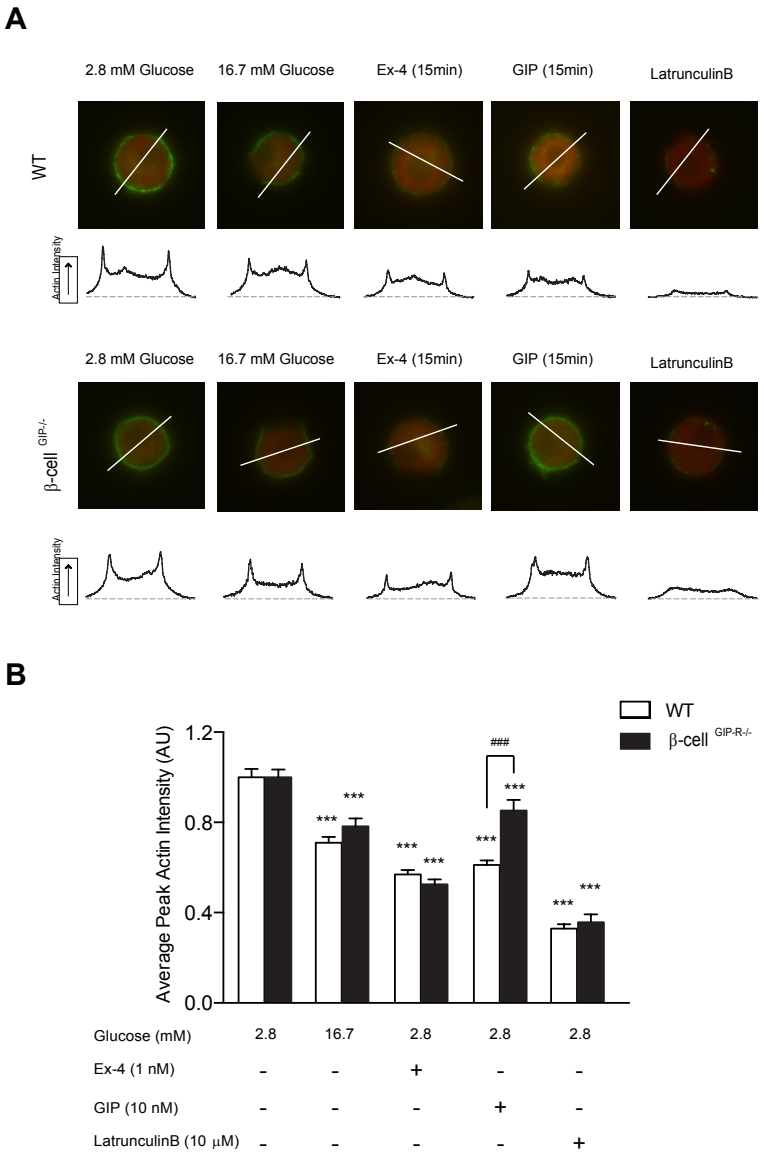
A
2.8 mM Glucose
16.7 mM Glucose
Ex-4 (15min)
GIP (15min)
LatrunculinB
WT
Actin Intensity
2.8 mM Glucose
16.7 mM Glucose
Ex-4 (15min)
GIP (15min)
LatrunculinB
β-cell GIP-/-
Actin Intensity
B
WT
β-cell GIP-R-/-
Average Peak Actin Intensity (AU)
1.2
0.8
0.4
0.0
###
***
Glucose (mM) 2.8 16.7 2.8 2.8 2.8
Ex-4 (1 nM) - - + - -
GIP (10 nM) - - - + -
LatrunculinB (10 μM) - - - - +

5.2.5d Additional evidence suggesting that activation of G-protein coupled receptors is involved in actin remodeling

The G_q - G-protein coupled receptor GPR40 is activated by long-chain fatty acids. Long-chain fatty acids potentiate insulin secretion from pancreatic β-cells. The long-chain fatty acid oleate is shown to potentiate GSIS from islets of wild-type mice; this effect is severely blunted in islets of mice lacking the GPR40 receptor (GPR40-/-) (Ferdaoussi et al., 2012). I show that this potentiation in GSIS is due to the downstream activation of a diacyl-glycerol (DAG)-sensitive kinase PKD1, and subsequent stimulation of cortical F-actin remodeling. Oleate is shown to induce actin depolymerization in wild-type beta cells, but is unable to do so in beta cells from GPR40-/- mice **(Figure 38A)**. Furthermore, I show that oleate-induced actin depolymerization in beta cells lacking PKD1 are blunted **(Figure 38B)**. This implicates GPCR activation in the actin remodeling process, and suggests that GPR40 activation stimulates GSIS at least in part by activation of PKD1 and subsequent induction of actin depolymerization. Thus, different GPCRs may use different signaling pathways to exert similar effects on actin.

Figure 38: GPR40 activation by oleate induces actin remodeling in beta cells.

Panel (A) (*left*) shows representative images for F-actin staining for each incubation period with intensity line scans shown below each image. Dashed lines represent the F-actin intensity means for the 2.8 mM glucose. Beta cells were identified by positive insulin immunostaining. (*right*) shows mean F-actin intensities from 40-62 cells from three WT (*white bars*) or GPR40-/- (*black bars*) mice. G, glucose; Latr, latrunculin; OL, oleate.

Panel (B) (*left*) shows representative images for F-actin staining (red) for each incubation condition with intensity line scans for F-actin staining intensity. Dashed lines represent the F-actin intensity means for the 2.8 G condition. Beta cells were identified by insulin staining (blue). (*right*) shows mean F-actin intensities from 20–35 cells, from three mice, of Ad-GFP (*white bars*)- or Ad-Cre (*black bars*)-infected Pkd1flox/flox islets.

*p<0.05, **p<0.01 and ***p<0.001 compared with the 2.8 G condition for each genotype, †p<0.001 compared with the respective condition in WT.

(JK performed imaging experiments and analyzed data (Ferdaoussi et al., 2012).)

Figure 38

A

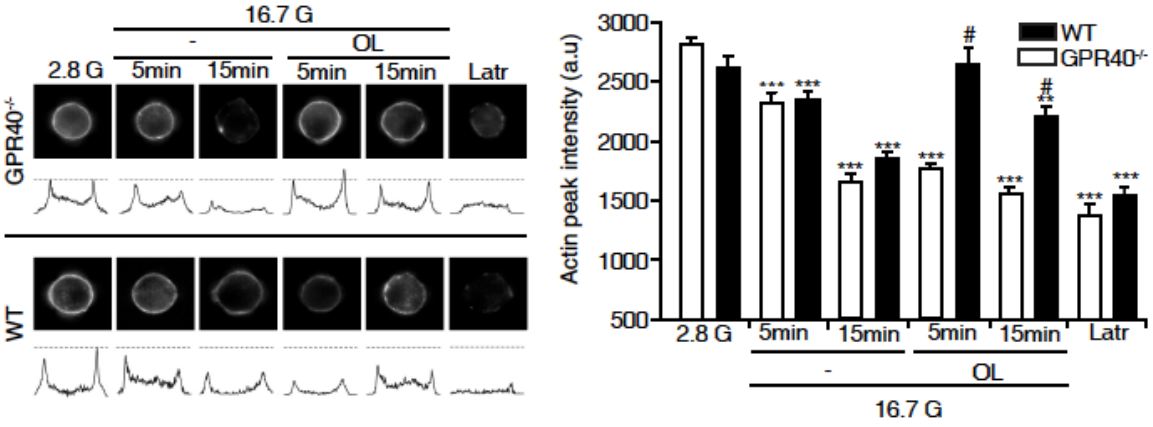
16.7 G
-
OL
2.8 G
5min
15min
5min
15min
Latr
GPR40-/-
WT
Actin peak intensity (a.u)
3000
2500
2000
1500
1000
500
WT
GPR40-/-
2.8 G
5min
15min
5min
15min
Latr
-
OL
16.7 G

B

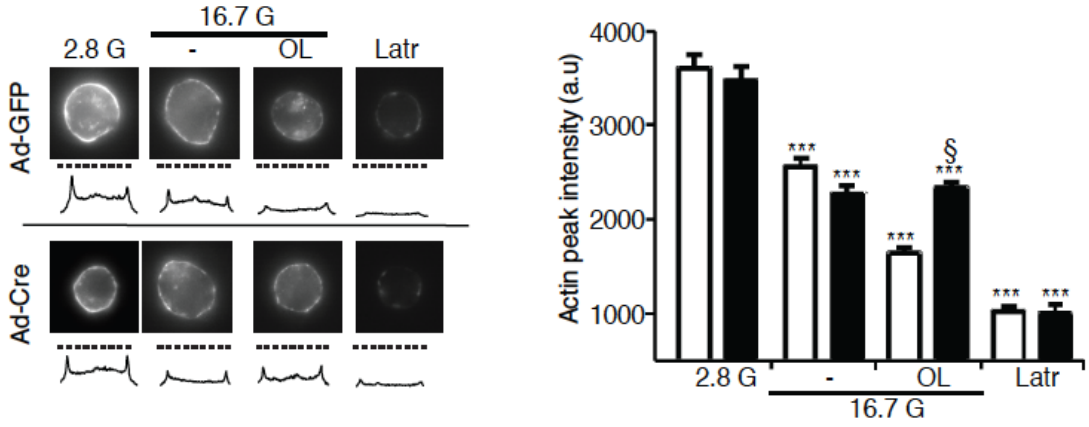
16.7 G
2.8 G
-
OL
Latr
Ad-GFP
Ad-Cre
Actin peak intensity (a.u)
4000
3000
2000
1000
2.8 G
-
OL
Latr
16.7 G

5.3 FUTURE DIRECTIONS

- Examine the plausible interaction between class 1 PI3Ks and SNARE protein expression. Specifically, does p110α or -β inhibition or knockdown affect expression levels of Syntaxin 1A or SNAP-25? If so, does this occur in a time – dependent manner?
- p110α inhibition increases exocytosis, but is also associated with a moderate reduction in insulin granules at the plasma membrane. Thus additional studies are needed to determine whether the specific inhibition or knockdown of p110α increases the number of insulin granule fusion events. This can be examined by simultaneous live cell TIRF microscopy and exocytotic measurements. If an increased number of newcomer fusion events is seen, MyosinVA would be a candidate protein to examine following p110α inhibition.
- Additional studies are required to determine the scaffolding or catalytic independent roles of p110β. Exactly how does p110β knockdown affect granule number at the plasma membrane?
- PIP_2 and PIP_3 levels are associated with changes in actin remodeling; however we did not see changes in cortical F-actin following p110α or -β inhibition. Further studies are required to examine stimulus and time-dependent actin remodeling in live cells, following p110α or -β inhibition. We can examine real-time actin remodeling in live cells using LifeAct actin visualization. LifeAct stains F-actin, but does not interfere with actin dynamics, thus allowing for live cell imaging (Kalwat and Thurmond, 2013; Riedl et al., 2008).

- The mechanism by which GIP-R and GLP-1-R activation induces actin remodeling is currently not understood. I show that GIP-R activation activates Rac1 and induces actin depolymerization. However, I did not determine whether specific inhibition of Rac1 blocks GIP-induced actin remodeling. Furthermore, the upstream and downstream molecular mechanisms involved haven not been studied. Possible candidate proteins to examine would be the small GTPase protein Cdc42, and the serine/threonine-protein kinase PAK 1.
- It is not currently clear as to why p110γ inhibition blunts the insulinotropic effect of GIP but not GLP-1-R activation. The simple explanation is that the GIP-R is coupled directly to p110γ, whilst the GLP-1-R is not. To study this, I need to examine PIP_3 production in response to GIP or GLP-1 receptor activation in cell lysates that have been immunoprecipitated for p110γ, To determine whether GIP or GLP-1 receptor activation transactivates the class 1A PI3Ks, I would also need to look at PIP_3 production in cell lysates that have been immunoprecipitated for p110α or p110β.
- Alternatively, p110γ inhibition or knockdown may be affecting the amounts of cAMP generated in response to GIP or GLP-1-R activation. Thus, cAMP levels should be measured under the above-described conditions. Both PKA and Epac are activated by cAMP, but cAMP exhibits a lower affinity for Epac. Thus we can also look at PKA and Epac activation in response to GIP or GLP-1-R activation following p110γ inhibition or knockdown.

5.4 CONCLUSIONS

This thesis presents clear evidence supporting distinct roles for individual class 1 PI3K isoforms in insulin secretion and beta cell exocytosis. PI3Kα has a negative role, as its pharmacological inhibition or shRNA-mediated knockdown increases insulin secretion and beta cell exocytosis. This is not due to an increase in granule numbers at the plasma membrane, changes in actin dynamics (at the time points studied), or differences in $[Ca^{2+}]_i$ responses. Thus I conclude that p110α exerts a negative effect on insulin secretion by limiting Ca^{2+}-dependent exocytosis. Further studies examining fusion events in live cells may show a role for p110α in controlling newcomer granule fusion.

In contrast, the catalytic function of PI3Kβ does not have a role in insulin secretion. However, I show that PI3Kβ has a non-catalytic function, as its shRNA-mediated knockdown significantly blunts insulin secretion and beta cell exocytosis. This in not due to changes in actin dynamics, or differences in $[Ca2+]_i$ responses but rather due to decreased granule numbers at the plasma membrane. Further studies are required to elucidate the scaffolding function of PI3Kβ in the beta cell.

My studies show that PI3Kγ has a positive role, as its pharmacological inhibition or knockdown blunts insulin secretion and beta cell exocytosis. I show that PI3Kγ has an important role in controlling cortical actin dynamics and granule recruitment to the plasma membrane, possibly due to its role in the activation of Rac1. Furthermore, I show that in concert with classical cAMP/PKA-dependent signaling GIP-R and GLP-1-R activation potentiates insulin secretion by inducing cortical actin depolymerization. I also show a role for PI3Kγ in the insulinotropic effect of GIP-R (but not GLP-1-R) activation; however further studies are needed to elucidate this interaction.

Both isoform specific and pan-PI3K inhibitors are currently being used for the treatment of various disease states. Thus considering the complexity of the role of PI3Ks in insulin secretion and beta cell exocytosis, it is essential to consider the implications of the clinical usage of PI3K inhibitors, and monitor patients for any signs of changes in glucose handling.

REFERENCE LIST

Alssema, M., Rijkelijkhuizen, J. M., Holst, J. J., Teerlink, T., Scheffer, P. G., Eekhoff, E. M. W., Gastaldelli, A., Mari, A., Hart, L. M., Nijpels, G., et al. (2013). Preserved GLP-1 and exaggerated GIP secretion in type 2 diabetes and relationships with triglycerides and ALT. *Eur. J. Endocrinol.* **169**, 421–430.

Andrianantoandro, E. and Pollard, T. D. (2006). Mechanism of actin filament turnover by severing and nucleation at different concentrations of ADF/cofilin. *Mol. Cell* **24**, 13–23.

Aoyagi, K., Ohara-Imaizumi, M., Nishiwaki, C., Nakamichi, Y., Ueki, K., Kadowaki, T. and Nagamatsu, S. (2012). Acute inhibition of PI3K-PDK1-Akt pathway potentiates insulin secretion through upregulation of newcomer granule fusions in pancreatic β-cells. *PLoS ONE* **7**, e47381.

Arcaro, A. and Wymann, M. P. (1993). Wortmannin is a potent phosphatidylinositol 3-kinase inhibitor: the role of phosphatidylinositol 3,4,5-trisphosphate in neutrophil responses. *Biochem. J.* **296 (Pt 2)**, 297–301.

Asahara, S., Shibutani, Y., Teruyama, K., Inoue, H. Y., Kawada, Y., Etoh, H., Matsuda, T., Kimura-Koyanagi, M., Hashimoto, N., Sakahara, M., et al. (2013). Ras-related C3 botulinum toxin substrate 1 (RAC1) regulates glucose-stimulated insulin secretion via modulation of F-actin. *Diabetologia* **56**, 1088–1097.

Ashcroft, F. M. and Rorsman, P. (1989). Electrophysiology of the pancreatic beta-cell. *Prog. Biophys. Mol. Biol.* **54**, 87–143.

Ashcroft, F. M. and Rorsman, P. (1990). ATP-sensitive K+ channels: a link between B-cell metabolism and insulin secretion. *Biochem. Soc. Trans.* **18**, 109–111.

Aspinwall, C. A., Qian, W. J., Roper, M. G., Kulkarni, R. N., Kahn, C. R. and Kennedy, R. T. (2000). Roles of insulin receptor substrate-1, phosphatidylinositol 3-kinase, and release of intracellular Ca2+ stores in insulin-stimulated insulin secretion in beta -cells. *J. Biol. Chem.* **275**, 22331–22338.

Ayscough, K. R., Stryker, J., Pokala, N., Sanders, M., Crews, P. and Drubin, D. G. (1997). High rates of actin filament turnover in budding yeast and roles for actin in establishment and maintenance of cell polarity revealed using the actin inhibitor latrunculin-A. *J. Cell Biol.* **137**, 399–416.

Banham-Hall, E., Clatworthy, M. R. and Okkenhaug, K. (2012). The Therapeutic Potential for PI3K Inhibitors in Autoimmune Rheumatic Diseases. *Open Rheumatol J* **6**, 245–258.

Barclay, J. W., Morgan, A. and Burgoyne, R. D. (2005). Calcium-dependent regulation

of exocytosis. *Cell Calcium* **38**, 343–353.

Barden, J. A., Miki, M., Hambly, B. D. and Remedios, Dos, C. G. (1987). Localization of the phalloidin and nucleotide-binding sites on actin. *Eur. J. Biochem.* **162**, 583–588.

Barg, S., Eliasson, L., Renström, E. and Rorsman, P. (2002). A subset of 50 secretory granules in close contact with L-type Ca2+ channels accounts for first-phase insulin secretion in mouse beta-cells. *Diabetes* **51 Suppl 1**, S74–82.

Barg, S., Huang, P., Eliasson, L., Nelson, D. J., Obermüller, S., Rorsman, P., Thévenod, F. and Renström, E. (2001). Priming of insulin granules for exocytosis by granular Cl(-) uptake and acidification. *J. Cell. Sci.* **114**, 2145–2154.

Barker, C. J., Leibiger, I. B., Leibiger, B. and Berggren, P.-O. (2002). Phosphorylated inositol compounds in beta -cell stimulus-response coupling. *Am. J. Physiol. Endocrinol. Metab.* **283**, E1113–22.

Barnett, A. (2007). Exenatide. *Expert Opin Pharmacother* **8**, 2593–2608.

Barroso, I., Luan, J., Middelberg, R. P. S., Harding, A.-H., Franks, P. W., Jakes, R. W., Clayton, D., Schafer, A. J., O'Rahilly, S. and Wareham, N. J. (2003). Candidate gene association study in type 2 diabetes indicates a role for genes involved in beta-cell function as well as insulin action. *PLoS Biol.* **1**, E20.

Becattini, B., Marone, R., Zani, F., Arsenijevic, D., Seydoux, J., Montani, J.-P., Dulloo, A. G., Thorens, B., Preitner, F., Wymann, M. P., et al. (2011). PI3Kγ within a nonhematopoietic cell type negatively regulates diet-induced thermogenesis and promotes obesity and insulin resistance. *Proc. Natl. Acad. Sci. U.S.A.* **108**, E854–63.

Bell, G. I., Santerre, R. F. and Mullenbach, G. T. (1983). Hamster preproglucagon contains the sequence of glucagon and two related peptides. *Nature* **302**, 716–718.

Bernal-Mizrachi, E., Wen, W., Stahlhut, S., Welling, C. M. and Permutt, M. A. (2001). Islet beta cell expression of constitutively active Akt1/PKB alpha induces striking hypertrophy, hyperplasia, and hyperinsulinemia. *J. Clin. Invest.* **108**, 1631–1638.

Bernstein, H. G., Keilhoff, G., Reiser, M., Freese, S. and Wetzker, R. (1998). Tissue distribution and subcellular localization of a G-protein activated phosphoinositide 3-kinase. An immunohistochemical study. *Cell. Mol. Biol. (Noisy-le-grand)* **44**, 973–983.

Bi, L., Okabe, I., Bernard, D. J. and Nussbaum, R. L. (2002). Early embryonic lethality in mice deficient in the p110beta catalytic subunit of PI 3-kinase. *Mamm. Genome* **13**, 169–172.

Bi, L., Okabe, I., Bernard, D. J., Wynshaw-Boris, A. and Nussbaum, R. L. (1999). Proliferative defect and embryonic lethality in mice homozygous for a deletion in the p110alpha subunit of phosphoinositide 3-kinase. *J. Biol. Chem.* **274**, 10963–10968.

Bishop, A. L. and Hall, A. (2000). Rho GTPases and their effector proteins. *Biochem. J.* **348 Pt 2**, 241–255.

Blikstad, I., Markey, F., Carlsson, L., Persson, T. and Lindberg, U. (1978). Selective assay of monomeric and filamentous actin in cell extracts, using inhibition of deoxyribonuclease I. *Cell* **15**, 935–943.

Bokvist, K., Ammälä, C., Ashcroft, F. M., Berggren, P. O., Larsson, O. and Rorsman, P. (1991). Separate processes mediate nucleotide-induced inhibition and stimulation of the ATP-regulated K(+)-channels in mouse pancreatic beta-cells. *Proc. Biol. Sci.* **243**, 139–144.

Brachmann, S. M., Ueki, K., Engelman, J. A., Kahn, R. C. and Cantley, L. C. (2005). Phosphoinositide 3-kinase catalytic subunit deletion and regulatory subunit deletion have opposite effects on insulin sensitivity in mice. *Mol. Cell. Biol.* **25**, 1596–1607.

Braekman, J. C., Daloze, D., Moussiaux, B. and Riccio, R. (1987). Jaspamide from the Marine Sponge Jaspis johnstoni. *J. Nat. Prod.* **50**, 994–995.

Braun, M., Ramracheya, R., Bengtsson, M., Zhang, Q., Karanauskaite, J., Partridge, C., Johnson, P. R. and Rorsman, P. (2008). Voltage-gated ion channels in human pancreatic beta-cells: electrophysiological characterization and role in insulin secretion. *Diabetes* **57**, 1618–1628.

Brunn, G. J., Williams, J., Sabers, C., Wiederrecht, G., Lawrence, J. C. and Abraham, R. T. (1996). Direct inhibition of the signaling functions of the mammalian target of rapamycin by the phosphoinositide 3-kinase inhibitors, wortmannin and LY294002. *EMBO J.* **15**, 5256–5267.

Bubb, M. R., Senderowicz, A. M., Sausville, E. A., Duncan, K. L. and Korn, E. D. (1994). Jasplakinolide, a cytotoxic natural product, induces actin polymerization and competitively inhibits the binding of phalloidin to F-actin. *J. Biol. Chem.* **269**, 14869–14871.

Burgoyne, R. D. and Cheek, T. R. (1987). Reorganisation of peripheral actin filaments as a prelude to exocytosis. *Biosci. Rep.* **7**, 281–288.

Bustelo, X. R., Sauzeau, V. and Berenjeno, I. M. (2007). GTP-binding proteins of the Rho/Rac family: regulation, effectors and functions in vivo. *Bioessays* **29**, 356–370.

Buteau, J., Foisy, S., Joly, E. and Prentki, M. (2003). Glucagon-like peptide 1 induces pancreatic beta-cell proliferation via transactivation of the epidermal growth factor receptor. *Diabetes* **52**, 124–132.

Buteau, J., Foisy, S., Rhodes, C. J., Carpenter, L., Biden, T. J. and Prentki, M. (2001). Protein kinase Czeta activation mediates glucagon-like peptide-1-induced pancreatic beta-cell proliferation. *Diabetes* **50**, 2237–2243.

Buteau, J., Roduit, R., Susini, S. and Prentki, M. (1999). Glucagon-like peptide-1 promotes DNA synthesis, activates phosphatidylinositol 3-kinase and increases transcription factor pancreatic and duodenal homeobox gene 1 (PDX-1) DNA binding activity in beta (INS-1)-cells. *Diabetologia* **42**, 856–864.

Buteau, J., Spatz, M. L. and Accili, D. (2006). Transcription factor FoxO1 mediates glucagon-like peptide-1 effects on pancreatic beta-cell mass. *Diabetes* **55**, 1190–1196.

Cabrera, O., Berman, D. M., Kenyon, N. S., Ricordi, C., Berggren, P.-O. and Caicedo, A. (2006). The unique cytoarchitecture of human pancreatic islets has implications for islet cell function. *Proc. Natl. Acad. Sci. U.S.A.* **103**, 2334–2339.

Cai, E. P., Casimir, M., Schroer, S. A., Luk, C. T., Shi, S. Y., Choi, D., Dai, X.-Q., Hajmrle, C., Spigelman, A. F., Zhu, D., et al. (2012). In vivo role of focal adhesion kinase in regulating pancreatic β-cell mass and function through insulin signaling, actin dynamics, and granule trafficking. *Diabetes* **61**, 1708–1718.

Calanna, S., Christensen, M., Holst, J. J., Laferrère, B., Gluud, L. L., Vilsbøll, T. and Knop, F. K. (2013). Secretion of glucose-dependent insulinotropic polypeptide in patients with type 2 diabetes: systematic review and meta-analysis of clinical studies. *Diabetes Care* **36**, 3346–3352.

Campbell, J. E. and Drucker, D. J. (2013). Pharmacology, physiology, and mechanisms of incretin hormone action. *Cell Metab.* **17**, 819–837.

Camps, M., Rückle, T., Ji, H., Ardissone, V., Rintelen, F., Shaw, J., Ferrandi, C., Chabert, C., Gillieron, C., Françon, B., et al. (2005). Blockade of PI3Kgamma suppresses joint inflammation and damage in mouse models of rheumatoid arthritis. *Nat. Med.* **11**, 936–943.

Carlier, M. F., Ducruix, A. and Pantaloni, D. (1999). Signalling to actin: the Cdc42-N-WASP-Arp2/3 connection. *Chem. Biol.* **6**, R235–40.

Castellano, E. and Downward, J. (2011). RAS Interaction with PI3K: More Than Just Another Effector Pathway. *Genes Cancer* **2**, 261–274.

Chasserot-Golaz, S., Hubert, P., Thiersé, D., Dirrig, S., Vlahos, C. J., Aunis, D. and Bader, M. F. (1998). Possible involvement of phosphatidylinositol 3-kinase in regulated exocytosis: studies in chromaffin cells with inhibitor LY294002. *J. Neurochem.* **70**, 2347–2356.

Chaussade, C., Rewcastle, G. W., Kendall, J. D., Denny, W. A., Cho, K., Grønning, L. M., Chong, M. L., Anagnostou, S. H., Jackson, S. P., Daniele, N., et al. (2007).

Evidence for functional redundancy of class IA PI3K isoforms in insulin signalling. *Biochem. J.* **404**, 449–458.

Chen, D., Mauvais-Jarvis, F., Bluher, M., Fisher, S. J., Jozsi, A., Goodyear, L. J., Ueki, K. and Kahn, C. R. (2004). p50alpha/p55alpha phosphoinositide 3-kinase knockout mice exhibit enhanced insulin sensitivity. *Mol. Cell. Biol.* **24**, 320–329.

Chen, G., Hohmeier, H. E., Gasa, R., Tran, V. V. and Newgard, C. B. (2000). Selection of insulinoma cell lines with resistance to interleukin-1beta- and gamma-interferon-induced cytotoxicity. *Diabetes* **49**, 562–570.

Chen, Y. A. and Scheller, R. H. (2001). SNARE-mediated membrane fusion. *Nat. Rev. Mol. Cell Biol.* **2**, 98–106.

Chiang, Y.-T. A., Ip, W. and Jin, T. (2012). The role of the Wnt signaling pathway in incretin hormone production and function. *Front Physiol* **3**, 273.

Cho, D. (2013). Despite Lukewarm Clinical Benefit of PI3K Inhibitors, Optimism Remains Regarding Biomarkers and Combination Therapy. *am.asco.org*

Chu, K. S., Negrete, G. R. and Konopelski, J. P. (1991). Asymmetric total synthesis of (+)-jasplakinolide. *J. Org. Chem.* **56**, 5196–5202.

Ciraolo, E., Iezzi, M., Marone, R., Marengo, S., Curcio, C., Costa, C., Azzolino, O., Gonella, C., Rubinetto, C., Wu, H., et al. (2008). Phosphoinositide 3-kinase p110beta activity: key role in metabolism and mammary gland cancer but not development. *Sci Signal* **1**, ra3.

Collier, J. J., White, S. M., Dick, G. M. and Scott, D. K. (2004). Phosphatidylinositol 3-kinase inhibitors reveal a unique mechanism of enhancing insulin secretion in 832/13 rat insulinoma cells. *Biochem. Biophys. Res. Commun.* **324**, 1018–1023.

Cooper, J. A. (1987). Effects of cytochalasin and phalloidin on actin. *J. Cell Biol.* **105**, 1473–1478.

Crespo, P., Xu, N., Simonds, W. F. and Gutkind, J. S. (1994). Ras-dependent activation of MAP kinase pathway mediated by G-protein beta gamma subunits. *Nature* **369**, 418–420.

Creutzfeldt, W., Ebert, R., Nauck, M. and Stöckmann, F. (1983). Disturbances of the entero-insular axis. *Scand. J. Gastroenterol. Suppl.* **82**, 111–119.

Curry, D. L., Bennett, L. L. and Grodsky, G. M. (1968). Dynamics of insulin secretion by the perfused rat pancreas. *Endocrinology* **83**, 572–584.

Danaei, G., Finucane, M. M., Lu, Y., Singh, G. M., Cowan, M. J., Paciorek, C. J., Lin, J. K., Farzadfar, F., Khang, Y.-H., Stevens, G. A., et al. (2011). National, regional, and global trends in fasting plasma glucose and diabetes prevalence since

1980: systematic analysis of health examination surveys and epidemiological studies with 370 country-years and 2·7 million participants. *Lancet* **378**, 31–40.

Dancker, P. and Löw, I. (1979). Complex influence of cytochalasin B on actin polymerization. *Z. Naturforsch., C, Biosci.* **34**, 555–557.

Dean, P. M. and Matthews, E. K. (1968). Electrical activity in pancreatic islet cells. *Nature* **219**, 389–390.

Dean, P. M. and Matthews, E. K. (1970a). Electrical activity in pancreatic islet cells: effect of ions. *J. Physiol. (Lond.)* **210**, 265–275.

Dean, P. M. and Matthews, E. K. (1970b). Glucose-induced electrical activity in pancreatic islet cells. *J. Physiol. (Lond.)* **210**, 255–264.

Dhanvantari, S. and Brubaker, P. L. (1998). Proglucagon processing in an islet cell line: effects of PC1 overexpression and PC2 depletion. *Endocrinology* **139**, 1630–1637.

Dillon, J. S., Tanizawa, Y., Wheeler, M. B., Leng, X. H., Ligon, B. B., Rabin, D. U., Yoo-Warren, H., Permutt, M. A. and Boyd, A. E. (1993). Cloning and functional expression of the human glucagon-like peptide-1 (GLP-1) receptor. *Endocrinology* **133**, 1907–1910.

Disanza, A., Steffen, A., Hertzog, M., Frittoli, E., Rottner, K. and Scita, G. (2005). Actin polymerization machinery: the finish line of signaling networks, the starting point of cellular movement. *Cell. Mol. Life Sci.* **62**, 955–970.

Dominguez, R. and Holmes, K. C. (2011). Actin structure and function. *Annu Rev Biophys* **40**, 169–186.

Doyle, D. A., Morais Cabral, J., Pfuetzner, R. A., Kuo, A., Gulbis, J. M., Cohen, S. L., Chait, B. T. and MacKinnon, R. (1998). The structure of the potassium channel: molecular basis of K+ conduction and selectivity. *Science* **280**, 69–77.

Drucker, D. J. (2003). Glucagon-like peptides: regulators of cell proliferation, differentiation, and apoptosis. *Mol. Endocrinol.* **17**, 161–171.

Drucker, D. J. (2006). The biology of incretin hormones. *Cell Metab.* **3**, 153–165.

Drucker, D. J. (2013). Incretin action in the pancreas: potential promise, possible perils, and pathological pitfalls. *Diabetes* **62**, 3316–3323.

Drucker, D. J., Philippe, J., Mojsov, S., Chick, W. L. and Habener, J. F. (1987). Glucagon-like peptide I stimulates insulin gene expression and increases cyclic AMP levels in a rat islet cell line. *Proc. Natl. Acad. Sci. U.S.A.* **84**, 3434–3438.

Dupre, J., Ross, S. A., Watson, D. and Brown, J. C. (1973). Stimulation of insulin

secretion by gastric inhibitory polypeptide in man. *J. Clin. Endocrinol. Metab.* **37**, 826–828.

Edwards, C. M. B. (2004). GLP-1: target for a new class of antidiabetic agents? *J R Soc Med* **97**, 270–274.

El-Kholy, W., MacDonald, P. E., Lin, J.-H., Wang, J., Fox, J. M., Light, P. E., Wang, Q., Tsushima, R. G. and Wheeler, M. B. (2003). The phosphatidylinositol 3-kinase inhibitor LY294002 potently blocks K(V) currents via a direct mechanism. *FASEB J.* **17**, 720–722.

Elliott, R. M., Morgan, L. M., Tredger, J. A., Deacon, S., Wright, J. and Marks, V. (1993). Glucagon-like peptide-1 (7-36)amide and glucose-dependent insulinotropic polypeptide secretion in response to nutrient ingestion in man: acute post-prandial and 24-h secretion patterns. *J. Endocrinol.* **138**, 159–166.

Elrick, H., Stimmler, L., Hlad, C. J. and Arai, Y. (1964). Plasma insulin response to oral and intravenous glucose administration. *J. Clin. Endocrinol. Metab.* **24**, 1076–1082.

Engelman, J. A., Luo, J. and Cantley, L. C. (2006). The evolution of phosphatidylinositol 3-kinases as regulators of growth and metabolism. *Nat. Rev. Genet.* **7**, 606–619.

Essers, M. A. G., de Vries-Smits, L. M. M., Barker, N., Polderman, P. E., Burgering, B. M. T. and Korswagen, H. C. (2005). Functional interaction between beta-catenin and FOXO in oxidative stress signaling. *Science* **308**, 1181–1184.

Eto, K., Yamashita, T., Tsubamoto, Y., Terauchi, Y., Hirose, K., Kubota, N., Yamashita, S., Taka, J., Satoh, S., Sekihara, H., et al. (2002). Phosphatidylinositol 3-kinase suppresses glucose-stimulated insulin secretion by affecting post-cytosolic [Ca(2+)] elevation signals. *Diabetes* **51**, 87–97.

Farilla, L., Bulotta, A., Hirshberg, B., Li Calzi, S., Khoury, N., Noushmehr, H., Bertolotto, C., Di Mario, U., Harlan, D. M. and Perfetti, R. (2003). Glucagon-like peptide 1 inhibits cell apoptosis and improves glucose responsiveness of freshly isolated human islets. *Endocrinology* **144**, 5149–5158.

Fehmann, H. C. and Habener, J. F. (1992). Insulinotropic hormone glucagon-like peptide-I(7-37) stimulation of proinsulin gene expression and proinsulin biosynthesis in insulinoma beta TC-1 cells. *Endocrinology* **130**, 159–166.

Fenteany, G. and Zhu, S. (2003). Small-molecule inhibitors of actin dynamics and cell motility. *Curr Top Med Chem* **3**, 593–616.

Ferdaoussi, M., Bergeron, V., Zarrouki, B., Kolic, J., Cantley, J., Fielitz, J., Olson, E. N., Prentki, M., Biden, T., MacDonald, P. E., et al. (2012). G protein-coupled receptor (GPR)40-dependent potentiation of insulin secretion in mouse islets is

mediated by protein kinase D1. *Diabetologia* **55**, 2682–2692.

Fischer, R. S. and Fowler, V. M. (2003). Tropomodulins: life at the slow end. *Trends Cell Biol.* **13**, 593–601.

Foukas, L. C., Claret, M., Pearce, W., Okkenhaug, K., Meek, S., Peskett, E., Sancho, S., Smith, A. J. H., Withers, D. J. and Vanhaesebroeck, B. (2006). Critical role for the p110alpha phosphoinositide-3-OH kinase in growth and metabolic regulation. *Nature* **441**, 366–370.

Friedrichsen, B. N., Neubauer, N., Lee, Y. C., Gram, V. K., Blume, N., Petersen, J. S., Nielsen, J. H. and Møldrup, A. (2006). Stimulation of pancreatic beta-cell replication by incretins involves transcriptional induction of cyclin D1 via multiple signalling pathways. *J. Endocrinol.* **188**, 481–492.

Fruman, D. A. (2010). Regulatory subunits of class IA PI3K. *Curr. Top. Microbiol. Immunol.* **346**, 225–244.

Fruman, D. A., Mauvais-Jarvis, F., Pollard, D. A., Yballe, C. M., Brazil, D., Bronson, R. T., Kahn, C. R. and Cantley, L. C. (2000). Hypoglycaemia, liver necrosis and perinatal death in mice lacking all isoforms of phosphoinositide 3-kinase p85 alpha. *Nat. Genet.* **26**, 379–382.

Fruman, D. A., Meyers, R. E. and Cantley, L. C. (1998). Phosphoinositide kinases. *Annu. Rev. Biochem.* **67**, 481–507.

Fujimoto, K. and Polonsky, K. S. (2009). Pdx1 and other factors that regulate pancreatic beta-cell survival. *Diabetes Obes Metab* **11 Suppl 4**, 30–37.

Gaidarov, I. and Keen, J. H. (1999). Phosphoinositide-AP-2 interactions required for targeting to plasma membrane clathrin-coated pits. *J. Cell Biol.* **146**, 755–764.

Galkin, V. E., Orlova, A., Kudryashov, D. S., Solodukhin, A., Reisler, E., Schröder, G. F. and Egelman, E. H. (2011). Remodeling of actin filaments by ADF/cofilin proteins. *Proc. Natl. Acad. Sci. U.S.A.* **108**, 20568–20572.

Galletta, B. J., Chuang, D. Y. and Cooper, J. A. (2008). Distinct roles for Arp2/3 regulators in actin assembly and endocytosis. *PLoS Biol.* **6**, e1.

Gao, Z., Konrad, R. J., Collins, H., Matschinsky, F. M., Rothenberg, P. L. and Wolf, B. A. (1996). Wortmannin inhibits insulin secretion in pancreatic islets and beta-TC3 cells independent of its inhibition of phosphatidylinositol 3-kinase. *Diabetes* **45**, 854–862.

Gatof, D., Kilic, G. and Fitz, J. G. (2004). Vesicular exocytosis contributes to volume-sensitive ATP release in biliary cells. *Am. J. Physiol. Gastrointest. Liver Physiol.* **286**, G538–46.

Gerst, J. E. (2003). SNARE regulators: matchmakers and matchbreakers. *Biochim. Biophys. Acta* **1641**, 99–110.

Goddette, D. W. and Frieden, C. (1986a). Actin polymerization. The mechanism of action of cytochalasin D. *J. Biol. Chem.* **261**, 15974–15980.

Goddette, D. W. and Frieden, C. (1986b). The kinetics of cytochalasin D binding to monomeric actin. *J. Biol. Chem.* **261**, 15970–15973.

Goldschmidt-Clermont, P. J., Machesky, L. M., Baldassare, J. J. and Pollard, T. D. (1990). The actin-binding protein profilin binds to PIP2 and inhibits its hydrolysis by phospholipase C. *Science* **247**, 1575–1578.

Goodman, O. B., Krupnick, J. G., Santini, F., Gurevich, V. V., Penn, R. B., Gagnon, A. W., Keen, J. H. and Benovic, J. L. (1996). Beta-arrestin acts as a clathrin adaptor in endocytosis of the beta2-adrenergic receptor. *Nature* **383**, 447–450.

Graceffa, P. and Dominguez, R. (2003). Crystal structure of monomeric actin in the ATP state. Structural basis of nucleotide-dependent actin dynamics. *J. Biol. Chem.* **278**, 34172–34180.

Grady, E. F., Slice, L. W., Brant, W. O., Walsh, J. H., Payan, D. G. and Bunnett, N. W. (1995). Direct observation of endocytosis of gastrin releasing peptide and its receptor. *J. Biol. Chem.* **270**, 4603–4611.

Gremlich, S., Porret, A., Hani, E. H., Cherif, D., Vionnet, N., Froguel, P. and Thorens, B. (1995). Cloning, functional expression, and chromosomal localization of the human pancreatic islet glucose-dependent insulinotropic polypeptide receptor. *Diabetes* **44**, 1202–1208.

Guillermet-Guibert, J., Bjorklof, K., Salpekar, A., Gonella, C., Ramadani, F., Bilancio, A., Meek, S., Smith, A. J. H., Okkenhaug, K. and Vanhaesebroeck, B. (2008). The p110beta isoform of phosphoinositide 3-kinase signals downstream of G protein-coupled receptors and is functionally redundant with p110gamma. *Proc. Natl. Acad. Sci. U.S.A.* **105**, 8292–8297.

Gunn, R. M. and Hailes, H. C. (2008). Insights into the PI3-K-PKB-mTOR signalling pathway from small molecules. *J Chem Biol* **1**, 49–62.

Hagiwara, S., Sakurai, T., Tashiro, F., Hashimoto, Y., Matsuda, Y., Nonomura, Y. and Miyazaki, J. (1995). An inhibitory role for phosphatidylinositol 3-kinase in insulin secretion from pancreatic B cell line MIN6. *Biochem. Biophys. Res. Commun.* **214**, 51–59.

Halliburton, W. D. (1887). On Muscle-Plasma. *J. Physiol. (Lond.)* **8**, 133–202.

Han, M. and Zhang, J. Z. H. (2010). Class I phospho-inositide-3-kinases (PI3Ks) isoform-specific inhibition study by the combination of docking and molecular

dynamics simulation. *J Chem Inf Model* **50**, 136–145.

Hansen, T., Andersen, C. B., Echwald, S. M., Urhammer, S. A., Clausen, J. O., Vestergaard, H., Owens, D., Hansen, L. and Pedersen, O. (1997). Identification of a common amino acid polymorphism in the p85alpha regulatory subunit of phosphatidylinositol 3-kinase: effects on glucose disappearance constant, glucose effectiveness, and the insulin sensitivity index. *Diabetes* **46**, 494–501.

Hanson, P. I., Heuser, J. E. and Jahn, R. (1997). Neurotransmitter release - four years of SNARE complexes. *Curr. Opin. Neurobiol.* **7**, 310–315.

Hare, K. J. (2010). Role of GLP-1 induced glucagon suppression in type 2 diabetes mellitus. *Dan Med Bull* **57**, B4181.

Hashimoto, N., Kido, Y., Uchida, T., Asahara, S.-I., Shigeyama, Y., Matsuda, T., Takeda, A., Tsuchihashi, D., Nishizawa, A., Ogawa, W., et al. (2006). Ablation of PDK1 in pancreatic beta cells induces diabetes as a result of loss of beta cell mass. *Nat. Genet.* **38**, 589–593.

Hay, J. C., Fisette, P. L., Jenkins, G. H., Fukami, K., Takenawa, T., Anderson, R. A. and Martin, T. F. (1995). ATP-dependent inositide phosphorylation required for Ca(2+)-activated secretion. *Nature* **374**, 173–177.

Hayakawa, M., Kawaguchi, K.-I., Kaizawa, H., Koizumi, T., Ohishi, T., Yamano, M., Okada, M., Ohta, M., Tsukamoto, S.-I., Raynaud, F. I., et al. (2007). Synthesis and biological evaluation of sulfonylhydrazone-substituted imidazo[1,2-a]pyridines as novel PI3 kinase p110alpha inhibitors. *Bioorg. Med. Chem.* **15**, 5837–5844.

Hazeki, O., Okada, T., Kurosu, H., Takasuga, S., Suzuki, T. and Katada, T. (1998). Activation of PI 3-kinase by G protein betagamma subunits. *Life Sci.* **62**, 1555–1559.

Heasman, S. J. and Ridley, A. J. (2008). Mammalian Rho GTPases: new insights into their functions from in vivo studies. *Nat. Rev. Mol. Cell Biol.* **9**, 690–701.

Heinemann, C., Rüden, von, L., Chow, R. H. and Neher, E. (1993). A two-step model of secretion control in neuroendocrine cells. *Pflugers Arch.* **424**, 105–112.

Henquin, J.-C., Ishiyama, N., Nenquin, M., Ravier, M. A. and Jonas, J.-C. (2002). Signals and pools underlying biphasic insulin secretion. *Diabetes* **51 Suppl 1**, S60–7.

Herman, W. H. and Zimmet, P. (2012). Type 2 diabetes: an epidemic requiring global attention and urgent action. *Diabetes Care* **35**, 943–944.

Hille, B. (1992). *Ionic channels of excitable membranes*. Sinauer Associates Inc.

Hirsch, E., Katanaev, V. L., Garlanda, C., Azzolino, O., Pirola, L., Silengo, L., Sozzani, S., Mantovani, A., Altruda, F. and Wymann, M. P. (2000). Central role

for G protein-coupled phosphoinositide 3-kinase gamma in inflammation. *Science* **287**, 1049–1053.

Hohmeier, H. E., Mulder, H., Chen, G., Henkel-Rieger, R., Prentki, M. and Newgard, C. B. (2000). Isolation of INS-1-derived cell lines with robust ATP-sensitive K+ channel-dependent and -independent glucose-stimulated insulin secretion. *Diabetes* **49**, 424–430.

Holmes, K. C. (2009). Structural biology: actin in a twist. *Nature* **457**, 389–390.

Holmes, K. C., Popp, D., Gebhard, W. and Kabsch, W. (1990). Atomic model of the actin filament. *Nature* **347**, 44–49.

Holst, J. J. and Gromada, J. (2004). Role of incretin hormones in the regulation of insulin secretion in diabetic and nondiabetic humans. *Am. J. Physiol. Endocrinol. Metab.* **287**, E199–206.

Hong, D. H., Choi, I.-W., Son, Y. K., Kim, D.-J., Na, S. H., Jung, W.-K., Yoon, Y. W. and Park, W. S. (2013). The effect of PI3 kinase inhibitor LY294002 on voltage-dependent K(+) channels in rabbit coronary arterial smooth muscle cells. *Life Sci.* **92**, 916–922.

Hooshmand-Rad, R., Hájková, L., Klint, P., Karlsson, R., Vanhaesebroeck, B., Claesson-Welsh, L. and Heldin, C. H. (2000). The PI 3-kinase isoforms p110(alpha) and p110(beta) have differential roles in PDGF- and insulin-mediated signaling. *J. Cell. Sci.* **113 Pt 2**, 207–214.

Howe, A. K. (2004). Regulation of actin-based cell migration by cAMP/PKA. *Biochim. Biophys. Acta* **1692**, 159–174.

Humtsoe, J. O. and Kramer, R. H. (2010). Differential epidermal growth factor receptor signaling regulates anchorage-independent growth by modulation of the PI3K/AKT pathway. *Oncogene* **29**, 1214–1226.

Hügl, S. R., White, M. F. and Rhodes, C. J. (1998). Insulin-like growth factor I (IGF-I)-stimulated pancreatic beta-cell growth is glucose-dependent. Synergistic activation of insulin receptor substrate-mediated signal transduction pathways by glucose and IGF-I in INS-1 cells. *J. Biol. Chem.* **273**, 17771–17779.

Iida, Y., Senda, T., Matsukawa, Y., Onoda, K., Miyazaki, J. I., Sakaguchi, H., Nimura, Y., Hidaka, H. and Niki, I. (1997). Myosin light-chain phosphorylation controls insulin secretion at a proximal step in the secretory cascade. *American Journal of Physiology* **273**, E782–9.

Innocenti, M., Frittoli, E., Ponzanelli, I., Falck, J. R., Brachmann, S. M., Di Fiore, P. P. and Scita, G. (2003). Phosphoinositide 3-kinase activates Rac by entering in a complex with Eps8, Abi1, and Sos-1. *J. Cell Biol.* **160**, 17–23.

Insall, R. H. and Weiner, O. D. (2001). PIP3, PIP2, and cell movement--similar messages, different meanings? *Dev. Cell* **1**, 743–747.

Isgandarova, S., Jones, L., Forsberg, D., Loncar, A., Dawson, J., Tedrick, K. and Eitzen, G. (2007). Stimulation of actin polymerization by vacuoles via Cdc42p-dependent signaling. *J. Biol. Chem.* **282**, 30466–30475.

Ivarsson, R., Jing, X., Waselle, L., Regazzi, R. and Renström, E. (2005). Myosin 5a controls insulin granule recruitment during late-phase secretion. *Traffic* **6**, 1027–1035.

Jackson, M. B. and Chapman, E. R. (2006). Fusion pores and fusion machines in Ca2+-triggered exocytosis. *Annu Rev Biophys Biomol Struct* **35**, 135–160.

Jackson, S. P., Schoenwaelder, S. M., Goncalves, I., Nesbitt, W. S., Yap, C. L., Wright, C. E., Kenche, V., Anderson, K. E., Dopheide, S. M., Yuan, Y., et al. (2005). PI 3-kinase p110beta: a new target for antithrombotic therapy. *Nat. Med.* **11**, 507–514.

Jacobsson, G., Bean, A. J., Scheller, R. H., Juntti-Berggren, L., Deeney, J. T., Berggren, P. O. and Meister, B. (1994). Identification of synaptic proteins and their isoform mRNAs in compartments of pancreatic endocrine cells. *Proc. Natl. Acad. Sci. U.S.A.* **91**, 12487–12491.

Janmey, P. A., Chaponnier, C., Lind, S. E., Zaner, K. S., Stossel, T. P. and Yin, H. L. (1985). Interactions of gelsolin and gelsolin-actin complexes with actin. Effects of calcium on actin nucleation, filament severing, and end blocking. *Biochemistry* **24**, 3714–3723.

Jayaram, B., Syed, I., Kyathanahalli, C. N., Rhodes, C. J. and Kowluru, A. (2011). Arf nucleotide binding site opener [ARNO] promotes sequential activation of Arf6, Cdc42 and Rac1 and insulin secretion in INS 832/13 β-cells and rat islets. *Biochem. Pharmacol.* **81**, 1016–1027.

Jean, S. and Kiger, A. A. (2014). Classes of phosphoinositide 3-kinases at a glance. *J. Cell. Sci.* **127**, 923–928.

Jewell, J. L., Luo, W., Oh, E., Wang, Z. and Thurmond, D. C. (2008). Filamentous actin regulates insulin exocytosis through direct interaction with Syntaxin 4. *J. Biol. Chem.* **283**, 10716–10726.

Jia, S., Liu, Z., Zhang, S., Liu, P., Zhang, L., Lee, S. H., Zhang, J., Signoretti, S., Loda, M., Roberts, T. M., et al. (2008). Essential roles of PI(3)K-p110beta in cell growth, metabolism and tumorigenesis. *Nature* **454**, 776–779.

Kahn, M., Nakanishi, H., Su, T., Lee, J. Y. and Johnson, M. E. (1991). Design and synthesis of nonpeptide mimetics of jaspamide. *Int J Pept Protein Res* **38**, 324–334.

Kalwat, M. A. and Thurmond, D. C. (2013). Signaling mechanisms of glucose-induced F-actin remodeling in pancreatic islet β cells. *Exp. Mol. Med.* **45**, e37.

Kalwat, M. A., Wiseman, D. A., Luo, W., Wang, Z. and Thurmond, D. C. (2012). Gelsolin associates with the N terminus of syntaxin 4 to regulate insulin granule exocytosis. *Mol. Endocrinol.* **26**, 128–141.

Kaneko, K., Ueki, K., Takahashi, N., Hashimoto, S., Okamoto, M., Awazawa, M., Okazaki, Y., Ohsugi, M., Inabe, K., Umehara, T., et al. (2010). Class IA phosphatidylinositol 3-kinase in pancreatic β cells controls insulin secretion by multiple mechanisms. *Cell Metab.* **12**, 619–632.

Kang, F., Purich, D. L. and Southwick, F. S. (1999). Profilin promotes barbed-end actin filament assembly without lowering the critical concentration. *J. Biol. Chem.* **274**, 36963–36972.

Kang, L., He, Z., Xu, P., Fan, J., Betz, A., Brose, N. and Xu, T. (2006). Munc13-1 is required for the sustained release of insulin from pancreatic beta cells. *Cell Metab.* **3**, 463–468.

Kanno, T., Ma, X., Barg, S., Eliasson, L., Galvanovskis, J., Göpel, S., Larsson, M., Renström, E. and Rorsman, P. (2004). Large dense-core vesicle exocytosis in pancreatic beta-cells monitored by capacitance measurements. *Methods* **33**, 302–311.

Kapeller, R., Prasad, K. V., Janssen, O., Hou, W., Schaffhausen, B. S., Rudd, C. E. and Cantley, L. C. (1994). Identification of two SH3-binding motifs in the regulatory subunit of phosphatidylinositol 3-kinase. *J. Biol. Chem.* **269**, 1927–1933.

Kerouz, N. J., Hörsch, D., Pons, S. and Kahn, C. R. (1997). Differential regulation of insulin receptor substrates-1 and -2 (IRS-1 and IRS-2) and phosphatidylinositol 3-kinase isoforms in liver and muscle of the obese diabetic (ob/ob) mouse. *J. Clin. Invest.* **100**, 3164–3172.

Kieffer, T. J., McIntosh, C. H. and Pederson, R. A. (1995). Degradation of glucose-dependent insulinotropic polypeptide and truncated glucagon-like peptide 1 in vitro and in vivo by dipeptidyl peptidase IV. *Endocrinology* **136**, 3585–3596.

Kim, S.-J., Winter, K., Nian, C., Tsuneoka, M., Koda, Y. and McIntosh, C. H. S. (2005). Glucose-dependent insulinotropic polypeptide (GIP) stimulation of pancreatic beta-cell survival is dependent upon phosphatidylinositol 3-kinase (PI3K)/protein kinase B (PKB) signaling, inactivation of the forkhead transcription factor Foxo1, and down-regulation of bax expression. *J. Biol. Chem.* **280**, 22297–22307.

Kinosian, H. J., Newman, J., Lincoln, B., Selden, L. A., Gershman, L. C. and Estes, J. E. (1998). Ca2+ regulation of gelsolin activity: binding and severing of F-actin. *Biophys. J.* **75**, 3101–3109.

Kiraly-Borri, C. E., Morgan, A., Burgoyne, R. D., Weller, U., Wollheim, C. B. and Lang, J. (1996). Soluble N-ethylmaleimide-sensitive-factor attachment protein and N-ethylmaleimide-insensitive factors are required for Ca2+-stimulated exocytosis of insulin. *Biochem. J.* **314 (Pt 1)**, 199–203.

Kitamura, T., Nakae, J., Kitamura, Y., Kido, Y., Biggs, W. H., Wright, C. V. E., White, M. F., Arden, K. C. and Accili, D. (2002). The forkhead transcription factor Foxo1 links insulin signaling to Pdx1 regulation of pancreatic beta cell growth. *J. Clin. Invest.* **110**, 1839–1847.

Knight, Z. A., Gonzalez, B., Feldman, M. E., Zunder, E. R., Goldenberg, D. D., Williams, O., Loewith, R., Stokoe, D., Balla, A., Toth, B., et al. (2006). A pharmacological map of the PI3-K family defines a role for p110alpha in insulin signaling. *Cell* **125**, 733–747.

Knop, F. K., Vilsbøll, T., Højberg, P. V., Larsen, S., Madsbad, S., Vølund, A., Holst, J. J. and Krarup, T. (2007). Reduced incretin effect in type 2 diabetes: cause or consequence of the diabetic state? *Diabetes* **56**, 1951–1959.

Kobayashi, N., Ueki, K., Okazaki, Y., Iwane, A., Kubota, N., Ohsugi, M., Awazawa, M., Kobayashi, M., Sasako, T., Kaneko, K., et al. (2011). Blockade of class IB phosphoinositide-3 kinase ameliorates obesity-induced inflammation and insulin resistance. *Proc. Natl. Acad. Sci. U.S.A.* **108**, 5753–5758.

Kolic, J., Spigelman, A. F., Plummer, G., Leung, E., Hajmrle, C., Kin, T., Shapiro, A. M. J., Manning Fox, J. E. and MacDonald, P. E. (2013). Distinct and opposing roles for the phosphatidylinositol 3-OH kinase catalytic subunits p110α and p110β in the regulation of insulin secretion from rodent and human beta cells. *Diabetologia* **56**, 1339–1349.

Kowluru, A. (2010). Small G proteins in islet beta-cell function. *Endocr. Rev.* **31**, 52–78.

Koyasu, S. (2003). The role of PI3K in immune cells. *Nat. Immunol.* **4**, 313–319.

Kreymann, B., Williams, G., Ghatei, M. A. and Bloom, S. R. (1987). Glucagon-like peptide-1 7-36: a physiological incretin in man. *Lancet* **2**, 1300–1304.

Kubota, A., Yamada, Y., Yasuda, K., Someya, Y., Ihara, Y., Kagimoto, S., Watanabe, R., Kuroe, A., Ishida, H. and Seino, Y. (1997). Gastric inhibitory polypeptide activates MAP kinase through the wortmannin-sensitive and -insensitive pathways. *Biochem. Biophys. Res. Commun.* **235**, 171–175.

Kulkarni, R. N., Brüning, J. C., Winnay, J. N., Postic, C., Magnuson, M. A. and Kahn, C. R. (1999a). Tissue-specific knockout of the insulin receptor in pancreatic beta cells creates an insulin secretory defect similar to that in type 2 diabetes. *Cell* **96**, 329–339.

Kulkarni, R. N., Holzenberger, M., Shih, D. Q., Ozcan, U., Stoffel, M., Magnuson,

M. A. and Kahn, C. R. (2002). beta-cell-specific deletion of the Igf1 receptor leads to hyperinsulinemia and glucose intolerance but does not alter beta-cell mass. *Nat. Genet.* **31**, 111–115.

Kulkarni, R. N., Jhala, U. S., Winnay, J. N., Krajewski, S., Montminy, M. and Kahn, C. R. (2004). PDX-1 haploinsufficiency limits the compensatory islet hyperplasia that occurs in response to insulin resistance. *J. Clin. Invest.* **114**, 828–836.

Kulkarni, R. N., Winnay, J. N., Daniels, M., Brüning, J. C., Flier, S. N., Hanahan, D. and Kahn, C. R. (1999b). Altered function of insulin receptor substrate-1-deficient mouse islets and cultured beta-cell lines. *J. Clin. Invest.* **104**, R69–75.

Kurig, B., Shymanets, A., Bohnacker, T., Prajwal, Brock, C., Ahmadian, M. R., Schaefer, M., Gohla, A., Harteneck, C., Wymann, M. P., et al. (2009). Ras is an indispensable coregulator of the class IB phosphoinositide 3-kinase p87/p110gamma. *Proc. Natl. Acad. Sci. U.S.A.* **106**, 20312–20317.

Lacy, P. E., Klein, N. J. and Fink, C. J. (1973). Effect of cytochalasin B on the biphasic release of insulin in perifused rat islets. *Endocrinology* **92**, 1458–1468.

Le Bacquer, O., Queniat, G., Gmyr, V., Kerr-Conte, J., Lefebvre, B. and Pattou, F. (2013). mTORC1 and mTORC2 regulate insulin secretion through Akt in INS-1 cells. *J. Endocrinol.* **216**, 21–29.

Leech, C. A., Dzhura, I., Chepurny, O. G., Kang, G., Schwede, F., Genieser, H.-G. and Holz, G. G. (2011). Molecular physiology of glucagon-like peptide-1 insulin secretagogue action in pancreatic β cells. *Prog. Biophys. Mol. Biol.* **107**, 236–247.

Leibiger, B., Moede, T., Uhles, S., Barker, C. J., Creveaux, M., Domin, J., Berggren, P.-O. and Leibiger, I. B. (2010). Insulin-feedback via PI3K-C2alpha activated PKBalpha/Akt1 is required for glucose-stimulated insulin secretion. *FASEB J.* **24**, 1824–1837.

LeRoith, D., Taylor, S. I. and Olefsky, J. M. (2004). *Diabetes Mellitus*. Lippincott Williams & Wilkins.

Li, G., Rungger-Brändle, E., Just, I., Jonas, J. C., Aktories, K. and Wollheim, C. B. (1994). Effect of disruption of actin filaments by Clostridium botulinum C2 toxin on insulin secretion in HIT-T15 cells and pancreatic islets. *Mol. Biol. Cell* **5**, 1199–1213.

Li, J., Luo, R., Kowluru, A. and Li, G. (2004). Novel regulation by Rac1 of glucose- and forskolin-induced insulin secretion in INS-1 beta-cells. *Am. J. Physiol. Endocrinol. Metab.* **286**, E818–27.

Li, J., Song, J., Cassidy, M. G., Rychahou, P., Starr, M. E., Liu, J., Li, X., Epperly, G., Weiss, H. L., Townsend, C. M., et al. (2012). PI3K p110α/Akt Signaling Negatively Regulates Secretion of the Intestinal Peptide Neurotensin Through

Interference of Granule Transport. *Mol. Endocrinol.*

Li, L.-X., MacDonald, P. E., Ahn, D. S., Oudit, G. Y., Backx, P. H. and Brubaker, P. L. (2006). Role of phosphatidylinositol 3-kinasegamma in the beta-cell: interactions with glucagon-like peptide-1. *Endocrinology* **147**, 3318–3325.

Li, Y., Hansotia, T., Yusta, B., Ris, F., Halban, P. A. and Drucker, D. J. (2003). Glucagon-like peptide-1 receptor signaling modulates beta cell apoptosis. *J. Biol. Chem.* **278**, 471–478.

Li, Z., Jiang, H., Xie, W., Zhang, Z., Smrcka, A. V. and Wu, D. (2000). Roles of PLC-beta2 and -beta3 and PI3Kgamma in chemoattractant-mediated signal transduction. *Science* **287**, 1046–1049.

Lin, H. C., Duncan, J. A., Kozasa, T. and Gilman, A. G. (1998). Sequestration of the G protein beta gamma subunit complex inhibits receptor-mediated endocytosis. *Proc. Natl. Acad. Sci. U.S.A.* **95**, 5057–5060.

Liu, Y., Shi, S., Gu, Z., Du, Y., Liu, M., Yan, S., Gao, J., Li, J., Shao, Y., Zhong, W., et al. (2013). Impaired autophagic function in rat islets with aging. *Age (Dordr)* **35**, 1531–1544.

Loew, E. R., Gray, J. S. and Ivy, A. C. (1940). Is a duodenal hormone involved in carbohydrate metabolism? *American Journal of Physiology* **129**, 659–663.

Logan, M. R. and Mandato, C. A. (2006). Regulation of the actin cytoskeleton by PIP2 in cytokinesis. *Biol. Cell* **98**, 377–388.

Lopez-Ilasaca, M., Crespo, P., Pellici, P. G., Gutkind, J. S. and Wetzker, R. (1997). Linkage of G protein-coupled receptors to the MAPK signaling pathway through PI 3-kinase gamma. *Science* **275**, 394–397.

Loreti, L., Dunbar, J. C., Chen, S. and Foà, P. P. (1974). The autoregulation of insulin secretion in the isolated pancreatic islets of lean (obOb) and obese-hyperglycemic (obob) mice. *Diabetologia* **10**, 309–315.

Luo, J., McMullen, J. R., Sobkiw, C. L., Zhang, L., Dorfman, A. L., Sherwood, M. C., Logsdon, M. N., Horner, J. W., DePinho, R. A., Izumo, S., et al. (2005). Class IA phosphoinositide 3-kinase regulates heart size and physiological cardiac hypertrophy. *Mol. Cell. Biol.* **25**, 9491–9502.

Lynen, F. (1937). *Ueber die giftstoffe des knollenblätterpilzes*.

Ma, L., Bindokas, V. P., Kuznetsov, A., Rhodes, C., Hays, L., Edwardson, J. M., Ueda, K., Steiner, D. F. and Philipson, L. H. (2004). Direct imaging shows that insulin granule exocytosis occurs by complete vesicle fusion. *Proc. Natl. Acad. Sci. U.S.A.* **101**, 9266–9271.

MacDonald, P. E., El-Kholy, W., Riedel, M. J., Salapatek, A. M. F., Light, P. E. and Wheeler, M. B. (2002). The multiple actions of GLP-1 on the process of glucose-stimulated insulin secretion. *Diabetes* **51 Suppl 3**, S434–42.

MacDonald, P. E., Joseph, J. W., Yau, D., Diao, J., Asghar, Z., Dai, F., Oudit, G. Y., Patel, M. M., Backx, P. H. and Wheeler, M. B. (2004). Impaired glucose-stimulated insulin secretion, enhanced intraperitoneal insulin tolerance, and increased beta-cell mass in mice lacking the p110gamma isoform of phosphoinositide 3-kinase. *Endocrinology* **145**, 4078–4083.

Machesky, L. M. and Insall, R. H. (1998). Scar1 and the related Wiskott-Aldrich syndrome protein, WASP, regulate the actin cytoskeleton through the Arp2/3 complex. *Curr. Biol.* **8**, 1347–1356.

Machesky, L. M., Atkinson, S. J., Ampe, C., Vandekerckhove, J. and Pollard, T. D. (1994). Purification of a cortical complex containing two unconventional actins from Acanthamoeba by affinity chromatography on profilin-agarose. *J. Cell Biol.* **127**, 107–115.

Machesky, L. M., Mullins, R. D., Higgs, H. N., Kaiser, D. A., Blanchoin, L., May, R. C., Hall, M. E. and Pollard, T. D. (1999). Scar, a WASp-related protein, activates nucleation of actin filaments by the Arp2/3 complex. *Proc. Natl. Acad. Sci. U.S.A.* **96**, 3739–3744.

Madeddu, P., Kraenkel, N., Barcelos, L. S., Siragusa, M., Campagnolo, P., Oikawa, A., Caporali, A., Herman, A., Azzolino, O., Barberis, L., et al. (2008). Phosphoinositide 3-kinase gamma gene knockout impairs postischemic neovascularization and endothelial progenitor cell functions. *Arterioscler. Thromb. Vasc. Biol.* **28**, 68–76.

Maier, U., Babich, A. and Nürnberg, B. (1999). Roles of non-catalytic subunits in gbetagamma-induced activation of class I phosphoinositide 3-kinase isoforms beta and gamma. *J. Biol. Chem.* **274**, 29311–29317.

Margolis, B. and Skolnik, E. Y. (1994). Activation of Ras by receptor tyrosine kinases. *J. Am. Soc. Nephrol.* **5**, 1288–1299.

Matheny, R. W. and Adamo, M. L. (2010). PI3K p110 alpha and p110 beta have differential effects on Akt activation and protection against oxidative stress-induced apoptosis in myoblasts. *Cell Death Differ.* **17**, 677–688.

McCulloch, L. J., van de Bunt, M., Braun, M., Frayn, K. N., Clark, A. and Gloyn, A. L. (2011). GLUT2 (SLC2A2) is not the principal glucose transporter in human pancreatic beta cells: implications for understanding genetic association signals at this locus. *Mol. Genet. Metab.* **104**, 648–653.

McIntyre, N., Holdsworth, C. D. and Turner, D. S. (1964). New interpretation of oral glucose tolerance. *Lancet* **2**, 20–21.

Meier, J. J. and Nauck, M. A. (2008). Is secretion of glucagon-like peptide-1 reduced in type 2 diabetes mellitus? *Nat Clin Pract Endocrinol Metab* **4**, 606–607.

Meier, J. J. and Nauck, M. A. (2010). Is the diminished incretin effect in type 2 diabetes just an epi-phenomenon of impaired beta-cell function? *Diabetes* **59**, 1117–1125.

Meier, J. J., Gallwitz, B., Salmen, S., Goetze, O., Holst, J. J., Schmidt, W. E. and Nauck, M. A. (2003a). Normalization of glucose concentrations and deceleration of gastric emptying after solid meals during intravenous glucagon-like peptide 1 in patients with type 2 diabetes. *J. Clin. Endocrinol. Metab.* **88**, 2719–2725.

Meier, J. J., Gallwitz, B., Siepmann, N., Holst, J. J., Deacon, C. F., Schmidt, W. E. and Nauck, M. A. (2003b). Gastric inhibitory polypeptide (GIP) dose-dependently stimulates glucagon secretion in healthy human subjects at euglycaemia. *Diabetologia* **46**, 798–801.

Meissner, H. P. and Schmelz, H. (1974). Membrane potential of beta-cells in pancreatic islets. *Pflugers Arch.* **351**, 195–206.

Miyawaki, K., Yamada, Y., Yano, H., Niwa, H., Ban, N., Ihara, Y., Kubota, A., Fujimoto, S., Kajikawa, M., Kuroe, A., et al. (1999). Glucose intolerance caused by a defect in the entero-insular axis: a study in gastric inhibitory polypeptide receptor knockout mice. *Proc. Natl. Acad. Sci. U.S.A.* **96**, 14843–14847.

Mojsov, S., Weir, G. C. and Habener, J. F. (1987). Insulinotropin: glucagon-like peptide I (7-37) co-encoded in the glucagon gene is a potent stimulator of insulin release in the perfused rat pancreas. *J. Clin. Invest.* **79**, 616–619.

Moore, B. (1906). On the treatment of Diabetus mellitus by acid extract of Duodenal Mucous Membrane. *Biochem. J.* **1**, 28–38.

Morton, W. M., Ayscough, K. R. and McLaughlin, P. J. (2000). Latrunculin alters the actin-monomer subunit interface to prevent polymerization. *Nat. Cell Biol.* **2**, 376–378.

Muller, D., Huang, G. C., Amiel, S., Jones, P. M. and Persaud, S. J. (2007). Gene expression heterogeneity in human islet endocrine cells in vitro: the insulin signalling cascade. *Diabetologia* **50**, 1239–1242.

Muller, D., Huang, G. C., Amiel, S., Jones, P. M. and Persaud, S. J. (2006). Identification of insulin signaling elements in human beta-cells: autocrine regulation of insulin gene expression. *Diabetes* **55**, 2835–2842.

Murga, C., Fukuhara, S. and Gutkind, J. S. (2000). A novel role for phosphatidylinositol 3-kinase beta in signaling from G protein-coupled receptors to Akt. *J. Biol. Chem.* **275**, 12069–12073.

Naga Prasad, S. V., Laporte, S. A., Chamberlain, D., Caron, M. G., Barak, L. and

Rockman, H. A. (2002). Phosphoinositide 3-kinase regulates beta2-adrenergic receptor endocytosis by AP-2 recruitment to the receptor/beta-arrestin complex. *J. Cell Biol.* **158**, 563–575.

Nakanishi, S., Kakita, S., Takahashi, I., Kawahara, K., Tsukuda, E., Sano, T., Yamada, K., Yoshida, M., Kase, H. and Matsuda, Y. (1992). Wortmannin, a microbial product inhibitor of myosin light chain kinase. *J. Biol. Chem.* **267**, 2157–2163.

Nauck, M. A., Heimesaat, M. M., Orskov, C., Holst, J. J., Ebert, R. and Creutzfeldt, W. (1993a). Preserved incretin activity of glucagon-like peptide 1 [7-36 amide] but not of synthetic human gastric inhibitory polypeptide in patients with type-2 diabetes mellitus. *J. Clin. Invest.* **91**, 301–307.

Nauck, M. A., Kleine, N., Orskov, C., Holst, J. J., Willms, B. and Creutzfeldt, W. (1993b). Normalization of fasting hyperglycaemia by exogenous glucagon-like peptide 1 (7-36 amide) in type 2 (non-insulin-dependent) diabetic patients. *Diabetologia* **36**, 741–744.

Nauck, M., Stöckmann, F., Ebert, R. and Creutzfeldt, W. (1986). Reduced incretin effect in type 2 (non-insulin-dependent) diabetes. *Diabetologia* **29**, 46–52.

Neher, E. (1998). Vesicle pools and Ca2+ microdomains: new tools for understanding their roles in neurotransmitter release. *Neuron* **20**, 389–399.

Nevins, A. K. and Thurmond, D. C. (2003). Glucose regulates the cortical actin network through modulation of Cdc42 cycling to stimulate insulin secretion. *Am. J. Physiol., Cell Physiol.* **285**, C698–710.

Nevins, A. K. and Thurmond, D. C. (2006). Caveolin-1 functions as a novel Cdc42 guanine nucleotide dissociation inhibitor in pancreatic beta-cells. *J. Biol. Chem.* **281**, 18961–18972.

Nguyen, K.-T. T., Tajmir, P., Lin, C. H., Liadis, N., Zhu, X.-D., Eweida, M., Tolasa-Karaman, G., Cai, F., Wang, R., Kitamura, T., et al. (2006). Essential role of Pten in body size determination and pancreatic beta-cell homeostasis in vivo. *Mol. Cell. Biol.* **26**, 4511–4518.

Nie, J., Lilley, B. N., Pan, Y. A., Faruque, O., Liu, X., Zhang, W., Sanes, J. R., Han, X. and Shi, Y. (2013). SAD-A potentiates glucose-stimulated insulin secretion as a mediator of glucagon-like peptide 1 response in pancreatic β cells. *Mol. Cell. Biol.* **33**, 2527–2534.

Nie, J., Sun, C., Faruque, O., Ye, G., Li, J., Liang, Q., Chang, Z., Yang, W., Han, X. and Shi, Y. (2012). Synapses of amphids defective (SAD-A) kinase promotes glucose-stimulated insulin secretion through activation of p21-activated kinase (PAK1) in pancreatic β-Cells. *J. Biol. Chem.* **287**, 26435–26444.

Niki, I., Okazaki, K., Saitoh, M., Niki, A., Niki, H., Tamagawa, T., Iguchi, A. and Hidaka, H. (1993). Presence and possible involvement of Ca/calmodulin-dependent protein kinases in insulin release from the rat pancreatic beta cell. *Biochem. Biophys. Res. Commun.* **191**, 255–261.

Nunemaker, C. S., Zhang, M. and Satin, L. S. (2004). Insulin feedback alters mitochondrial activity through an ATP-sensitive K+ channel-dependent pathway in mouse islets and beta-cells. *Diabetes* **53**, 1765–1772.

Nunoi, K., Yasuda, K., Tanaka, H., Kubota, A., Okamoto, Y., Adachi, T., Shihara, N., Uno, M., Xu, L. M., Kagimoto, S., et al. (2000). Wortmannin, a PI3-kinase inhibitor: promoting effect on insulin secretion from pancreatic beta cells through a cAMP-dependent pathway. *Biochem. Biophys. Res. Commun.* **270**, 798–805.

Nylander, S., Kull, B., Björkman, J. A., Ulvinge, J. C., Oakes, N., Emanuelsson, B. M., Andersson, M., Skärby, T., Inghardt, T., Fjellström, O., et al. (2012). Human target validation of phosphoinositide 3-kinase (PI3K)β: effects on platelets and insulin sensitivity, using AZD6482 a novel PI3Kβ inhibitor. *J. Thromb. Haemost.* **10**, 2127–2136.

Oh, E., Kalwat, M. A., Kim, M.-J., Verhage, M. and Thurmond, D. C. (2012). Munc18-1 regulates first-phase insulin release by promoting granule docking to multiple syntaxin isoforms. *J. Biol. Chem.* **287**, 25821–25833.

Ohta, Y., Akiyama, T., Nishida, E. and Sakai, H. (1987). Protein kinase C and cAMP-dependent protein kinase induce opposite effects on actin polymerizability. *FEBS Lett.* **222**, 305–310.

Okkenhaug, K. (2013). Signaling by the phosphoinositide 3-kinase family in immune cells. *Annu. Rev. Immunol.* **31**, 675–704.

Okkenhaug, K. and Vanhaesebroeck, B. (2003). PI3K-signalling in B- and T-cells: insights from gene-targeted mice. *Biochem. Soc. Trans.* **31**, 270–274.

Orci, L., Gabbay, K. H. and Malaisse, W. J. (1972). Pancreatic beta-cell web: its possible role in insulin secretion. *Science* **175**, 1128–1130.

Otsu, M., Hiles, I., Gout, I., Fry, M. J., Ruiz-Larrea, F., Panayotou, G., Thompson, A., Dhand, R., Hsuan, J. and Totty, N. (1991). Characterization of two 85 kd proteins that associate with receptor tyrosine kinases, middle-T/pp60c-src complexes, and PI3-kinase. *Cell* **65**, 91–104.

Pacold, M. E., Suire, S., Perisic, O., Lara-Gonzalez, S., Davis, C. T., Walker, E. H., Hawkins, P. T., Stephens, L., Eccleston, J. F. and Williams, R. L. (2000). Crystal structure and functional analysis of Ras binding to its effector phosphoinositide 3-kinase gamma. *Cell* **103**, 931–943.

Panjwani, N., Mulvihill, E. E., Longuet, C., Yusta, B., Campbell, J. E., Brown, T. J.,

Streutker, C., Holland, D., Cao, X., Baggio, L. L., et al. (2013). GLP-1 receptor activation indirectly reduces hepatic lipid accumulation but does not attenuate development of atherosclerosis in diabetic male ApoE(-/-) mice. *Endocrinology* **154**, 127–139.

Papakonstanti, E. A. and Stournaras, C. (2002). Association of PI-3 kinase with PAK1 leads to actin phosphorylation and cytoskeletal reorganization. *Mol. Biol. Cell* **13**, 2946–2962.

Patrucco, E., Notte, A., Barberis, L., Selvetella, G., Maffei, A., Brancaccio, M., Marengo, S., Russo, G., Azzolino, O., Rybalkin, S. D., et al. (2004). PI3Kgamma modulates the cardiac response to chronic pressure overload by distinct kinase-dependent and -independent effects. *Cell* **118**, 375–387.

Patzelt, C. and Schiltz, E. (1984). Conversion of proglucagon in pancreatic alpha cells: the major endproducts are glucagon and a single peptide, the major proglucagon fragment, that contains two glucagon-like sequences. *Proc. Natl. Acad. Sci. U.S.A.* **81**, 5007–5011.

Pederson, R. A. and Brown, J. C. (1976). The insulinotropic action of gastric inhibitory polypeptide in the perfused isolated rat pancreas. *Endocrinology* **99**, 780–785.

Penn, E. J., Brocklehurst, K. W., Sopwith, A. M., Hales, C. N. and Hutton, J. C. (1982). Ca2+--Calmodulin dependent myosin light-chain phosphorylating activity in insulin-secreting tissues. *FEBS Lett.* **139**, 4–8.

Perino, A., Ghigo, A., Ferrero, E., Morello, F., Santulli, G., Baillie, G. S., Damilano, F., Dunlop, A. J., Pawson, C., Walser, R., et al. (2011). Integrating cardiac PIP3 and cAMP signaling through a PKA anchoring function of p110γ. *Mol. Cell* **42**, 84–95.

Persaud, S. J., Asare-Anane, H. and Jones, P. M. (2002). Insulin receptor activation inhibits insulin secretion from human islets of Langerhans. *FEBS Lett.* **510**, 225–228.

Pigeau, G. M., Kolic, J., Ball, B. J., Hoppa, M. B., Wang, Y. W., Rückle, T., Woo, M., Manning Fox, J. E. and MacDonald, P. E. (2009). Insulin granule recruitment and exocytosis is dependent on p110gamma in insulinoma and human beta-cells. *Diabetes* **58**, 2084–2092.

Poirier, M. A. M., Xiao, W. W., Macosko, J. C. J., Chan, C. C., Shin, Y. K. Y. and Bennett, M. K. M. (1998). The synaptic SNARE complex is a parallel four-stranded helical bundle. *Nat Struct Mol Biol* **5**, 765–769.

Pollard, T. D. (2007). Regulation of actin filament assembly by Arp2/3 complex and formins. *Annu Rev Biophys Biomol Struct* **36**, 451–477.

Pollard, T. D., Blanchoin, L. and Mullins, R. D. (2000). Molecular mechanisms controlling actin filament dynamics in nonmuscle cells. *Annu Rev Biophys Biomol*

Struct **29**, 545–576.

Pons, S., Asano, T., Glasheen, E., Miralpeix, M., Zhang, Y., Fisher, T. L., Myers, M. G., Sun, X. J. and White, M. F. (1995). The structure and function of p55PIK reveal a new regulatory subunit for phosphatidylinositol 3-kinase. *Mol. Cell. Biol.* **15**, 4453–4465.

Pressel, D. M. and Misler, S. (1990). Sodium channels contribute to action potential generation in canine and human pancreatic islet B cells. *J. Membr. Biol.* **116**, 273–280.

Pyke, C. and Knudsen, L. B. (2013). The glucagon-like peptide-1 receptor--or not? *Endocrinology* **154**, 4–8.

Randis, T. M., Puri, K. D., Zhou, H. and Diacovo, T. G. (2008). Role of PI3Kdelta and PI3Kgamma in inflammatory arthritis and tissue localization of neutrophils. *Eur. J. Immunol.* **38**, 1215–1224.

Regazzi, R., Wollheim, C. B., Lang, J., Theler, J. M., Rossetto, O., Montecucco, C., Sadoul, K., Weller, U., Palmer, M. and Thorens, B. (1995). VAMP-2 and cellubrevin are expressed in pancreatic beta-cells and are essential for Ca(2+)-but not for GTP gamma S-induced insulin secretion. *EMBO J.* **14**, 2723–2730.

Reisler, E. (1993). Actin molecular structure and function. *Curr. Opin. Cell Biol.* **5**, 41–47.

Reisler, E. and Egelman, E. H. (2007). Actin structure and function: what we still do not understand. *J. Biol. Chem.* **282**, 36133–36137.

Remedios, dos, C. and Chhabra, D. (2010). *Actin-Binding Proteins and Disease*. Springer Verlag.

Ridley, A. J. (2001). Rho GTPases and cell migration. *J. Cell. Sci.* **114**, 2713–2722.

Ridley, A. J. (2006). Rho GTPases and actin dynamics in membrane protrusions and vesicle trafficking. *Trends Cell Biol.* **16**, 522–529.

Riedl, J., Crevenna, A. H., Kessenbrock, K., Yu, J. H., Neukirchen, D., Bista, M., Bradke, F., Jenne, D., Holak, T. A., Werb, Z., et al. (2008). Lifeact: a versatile marker to visualize F-actin. *Nat. Methods* **5**, 605–607.

Robinson, R. C., Turbedsky, K., Kaiser, D. A., Marchand, J. B., Higgs, H. N., Choe, S. and Pollard, T. D. (2001). Crystal structure of Arp2/3 complex. *Science* **294**, 1679–1684.

Roche, S., Downward, J., Raynal, P. and Courtneidge, S. A. (1998). A function for phosphatidylinositol 3-kinase beta (p85alpha-p110beta) in fibroblasts during mitogenesis: requirement for insulin- and lysophosphatidic acid-mediated signal

transduction. *Mol. Cell. Biol.* **18**, 7119–7129.

Rohatgi, R., Ma, L., Miki, H., Lopez, M., Kirchhausen, T., Takenawa, T. and Kirschner, M. W. (1999). The interaction between N-WASP and the Arp2/3 complex links Cdc42-dependent signals to actin assembly. *Cell* **97**, 221–231.

Rommel, C., Camps, M. and Ji, H. (2007). PI3K delta and PI3K gamma: partners in crime in inflammation in rheumatoid arthritis and beyond? *Nat. Rev. Immunol.* **7**, 191–201.

Rondas, D., Tomas, A. and Halban, P. A. (2011). Focal adhesion remodeling is crucial for glucose-stimulated insulin secretion and involves activation of focal adhesion kinase and paxillin. *Diabetes* **60**, 1146–1157.

Rondas, D., Tomas, A., Soto-Ribeiro, M., Wehrle-Haller, B. and Halban, P. A. (2012). Novel mechanistic link between focal adhesion remodeling and glucose-stimulated insulin secretion. *J. Biol. Chem.* **287**, 2423–2436.

Rorsman, P. and Renström, E. (2003). Insulin granule dynamics in pancreatic beta cells. *Diabetologia* **46**, 1029–1045.

Rorsman, P., Eliasson, L., Kanno, T., Zhang, Q. and Göpel, S. (2011). Electrophysiology of pancreatic β-cells in intact mouse islets of Langerhans. *Prog. Biophys. Mol. Biol.* **107**, 224–235.

Rorsman, P., Eliasson, L., Renström, E., Gromada, J., Barg, S. and Göpel, S. (2000). The Cell Physiology of Biphasic Insulin Secretion. *News Physiol. Sci.* **15**, 72–77.

Roscioni, S. S., Elzinga, C. R. S. and Schmidt, M. (2008). Epac: effectors and biological functions. *Naunyn Schmiedebergs Arch. Pharmacol.* **377**, 345–357.

Ross, S. A., Brown, J. C. and Dupre, J. (1977). Hypersecretion of gastric inhibitory polypeptide following oral glucose in diabetes mellitus. *Diabetes* **26**, 525–529.

Rossner, S., Fuchsbrunner, K., Lange-Dohna, C., Hartlage-Rübsamen, M., Bigl, V., Betz, A., Reim, K. and Brose, N. (2004). Munc13-1-mediated vesicle priming contributes to secretory amyloid precursor protein processing. *J. Biol. Chem.* **279**, 27841–27844.

Rouillé, Y., Westermark, G., Martin, S. K. and Steiner, D. F. (1994). Proglucagon is processed to glucagon by prohormone convertase PC2 in alpha TC1-6 cells. *Proc. Natl. Acad. Sci. U.S.A.* **91**, 3242–3246.

Rutter, G. A. and Hill, E. V. (2006). Insulin vesicle release: walk, kiss, pause ... then run. *Physiology (Bethesda)* **21**, 189–196.

Rückle, T., Schwarz, M. K. and Rommel, C. (2006). PI3Kgamma inhibition: towards an 'aspirin of the 21st century'? *Nat Rev Drug Discov* **5**, 903–918.

Sadoul, K. K., Berger, A. A., Niemann, H. H., Weller, U. U., Roche, P. A. P., Klip, A. A., Trimble, W. S. W., Regazzi, R. R., Catsicas, S. S. and Halban, P. A. P. (1997). SNAP-23 is not cleaved by botulinum neurotoxin E and can replace SNAP-25 in the process of insulin secretion. *J. Biol. Chem.* **272**, 33023–33027.

Sadoul, K., Lang, J., Montecucco, C., Weller, U., Regazzi, R., Catsicas, S., Wollheim, C. B. and Halban, P. A. (1995). SNAP-25 is expressed in islets of Langerhans and is involved in insulin release. *J. Cell Biol.* **128**, 1019–1028.

Saltiel, A. R. and Pessin, J. E. (2007). *Mechanisms of Insulin Action*. Springer.

Sasaki, A. T., Janetopoulos, C., Lee, S., Charest, P. G., Takeda, K., Sundheimer, L. W., Meili, R., Devreotes, P. N. and Firtel, R. A. (2007). G protein-independent Ras/PI3K/F-actin circuit regulates basic cell motility. *J. Cell Biol.* **178**, 185–191.

Sasaki, T., Irie-Sasaki, J., Jones, R. G., Oliveira-dos-Santos, A. J., Stanford, W. L., Bolon, B., Wakeham, A., Itie, A., Bouchard, D., Kozieradzki, I., et al. (2000). Function of PI3Kgamma in thymocyte development, T cell activation, and neutrophil migration. *Science* **287**, 1040–1046.

Saxena, R., Hivert, M.-F., Langenberg, C., Tanaka, T., Pankow, J. S., Vollenweider, P., Lyssenko, V., Bouatia-Naji, N., Dupuis, J., Jackson, A. U., et al. (2010). Genetic variation in GIPR influences the glucose and insulin responses to an oral glucose challenge. *Nat. Genet.* **42**, 142–148.

Schliwa, M. (1982). Action of cytochalasin D on cytoskeletal networks. *J. Cell Biol.* **92**, 79–91.

Schmidt, A. and Hall, A. (2002). Guanine nucleotide exchange factors for Rho GTPases: turning on the switch. *Genes Dev.* **16**, 1587–1609.

Schmidt, W. E., Siegel, E. G. and Creutzfeldt, W. (1985). Glucagon-like peptide-1 but not glucagon-like peptide-2 stimulates insulin release from isolated rat pancreatic islets. *Diabetologia* **28**, 704–707.

Scrocchi, L. A., Brown, T. J., MaClusky, N., Brubaker, P. L., Auerbach, A. B., Joyner, A. L. and Drucker, D. J. (1996). Glucose intolerance but normal satiety in mice with a null mutation in the glucagon-like peptide 1 receptor gene. *Nat. Med.* **2**, 1254–1258.

Sechi, A. S. and Wehland, J. (2000). The actin cytoskeleton and plasma membrane connection: PtdIns(4,5)P(2) influences cytoskeletal protein activity at the plasma membrane. *J. Cell. Sci.* **113 Pt 21**, 3685–3695.

Seino, S. and Bell, G. I. (2008). *Pancreatic Beta Cell in Health and Disease*. Springer.

Seino, S., Takahashi, H., Fujimoto, W. and Shibasaki, T. (2009). Roles of cAMP signalling in insulin granule exocytosis. *Diabetes Obes Metab* **11 Suppl 4**, 180–188.

Shaw, J. E., Sicree, R. A. and Zimmet, P. Z. (2010). Global estimates of the prevalence of diabetes for 2010 and 2030. *Diabetes Res. Clin. Pract.* **87**, 4–14.

Shu, L., Matveyenko, A. V., Kerr-Conte, J., Cho, J.-H., McIntosh, C. H. S. and Maedler, K. (2009). Decreased TCF7L2 protein levels in type 2 diabetes mellitus correlate with downregulation of GIP- and GLP-1 receptors and impaired beta-cell function. *Hum. Mol. Genet.* **18**, 2388–2399.

Sjölund, K., Sandén, G., Håkanson, R. and Sundler, F. (1983). Endocrine cells in human intestine: an immunocytochemical study. *Gastroenterology* **85**, 1120–1130.

Smith, G. C., Ong, W. K., Rewcastle, G. W., Kendall, J. D., Han, W. and Shepherd, P. R. (2012). Effects of acutely inhibiting PI3K isoforms and mTOR on regulation of glucose metabolism in vivo. *Biochem. J.* **442**, 161–169.

Smith, P. A., Bokvist, K., Arkhammar, P., Berggren, P. O. and Rorsman, P. (1990). Delayed rectifying and calcium-activated K+ channels and their significance for action potential repolarization in mouse pancreatic beta-cells. *J. Gen. Physiol.* **95**, 1041–1059.

Song, M. S., Salmena, L. and Pandolfi, P. P. (2012). The functions and regulation of the PTEN tumour suppressor. *Nat. Rev. Mol. Cell Biol.* **13**, 283–296.

Song, W.-J., Seshadri, M., Ashraf, U., Mdluli, T., Mondal, P., Keil, M., Azevedo, M., Kirschner, L. S., Stratakis, C. A. and Hussain, M. A. (2011). Snapin mediates incretin action and augments glucose-dependent insulin secretion. *Cell Metab.* **13**, 308–319.

Söllner, T., Bennett, M. K., Whiteheart, S. W., Scheller, R. H. and Rothman, J. E. (1993a). A protein assembly-disassembly pathway in vitro that may correspond to sequential steps of synaptic vesicle docking, activation, and fusion. *Cell* **75**, 409–418.

Söllner, T., Whiteheart, S. W., Brunner, M., Erdjument-Bromage, H., Geromanos, S., Tempst, P. and Rothman, J. E. (1993b). SNAP receptors implicated in vesicle targeting and fusion. *Nature* **362**, 318–324.

Spector, I., Shochet, N. R., Blasberger, D. and Kashman, Y. (1989). Latrunculins--novel marine macrolides that disrupt microfilament organization and affect cell growth: I. Comparison with cytochalasin D. *Cell Motil. Cytoskeleton* **13**, 127–144.

Spector, I., Shochet, N. R., Kashman, Y. and Groweiss, A. (1983). Latrunculins: novel marine toxins that disrupt microfilament organization in cultured cells. *Science* **219**, 493–495.

Spurlin, B. A. and Thurmond, D. C. (2006). Syntaxin 4 facilitates biphasic glucose-stimulated insulin secretion from pancreatic beta-cells. *Mol. Endocrinol.* **20**, 183–193.

Stephens, L. R., Eguinoa, A., Erdjument-Bromage, H., Lui, M., Cooke, F., Coadwell, J., Smrcka, A. S., Thelen, M., Cadwallader, K., Tempst, P., et al. (1997). The G beta gamma sensitivity of a PI3K is dependent upon a tightly associated adaptor, p101. *Cell* **89**, 105–114.

Stephens, L. R., Jackson, T. R. and Hawkins, P. T. (1993). Agonist-stimulated synthesis of phosphatidylinositol(3,4,5)-trisphosphate: a new intracellular signalling system? *Biochim. Biophys. Acta* **1179**, 27–75.

Stoyanov, B., Volinia, S., Hanck, T., Rubio, I., Loubtchenkov, M., Malek, D., Stoyanova, S., Vanhaesebroeck, B., Dhand, R. and Nürnberg, B. (1995). Cloning and characterization of a G protein-activated human phosphoinositide-3 kinase. *Science* **269**, 690–693.

Straub, F. B. (1943). Actin, II. *Stud Inst Med Chem Univ Szeged*.

Straub, S. G. and Sharp, G. W. (1996a). A wortmannin-sensitive signal transduction pathway is involved in the stimulation of insulin release by vasoactive intestinal polypeptide and pituitary adenylate cyclase-activating polypeptide. *J. Biol. Chem.* **271**, 1660–1668.

Straub, S. G. and Sharp, G. W. (1996b). Glucose-dependent insulinotropic polypeptide stimulates insulin secretion via increased cyclic AMP and [Ca2+]1 and a wortmannin-sensitive signalling pathway. *Biochem. Biophys. Res. Commun.* **224**, 369–374.

Stutchfield, J. and Howell, S. L. (1984). The effect of phalloidin on insulin secretion from islets of Langerhans isolated from rat pancreas. *FEBS Lett.* **175**, 393–396.

Sun, Y., Carroll, S., Kaksonen, M., Toshima, J. Y. and Drubin, D. G. (2007). PtdIns(4,5)P2 turnover is required for multiple stages during clathrin- and actin-dependent endocytic internalization. *J. Cell Biol.* **177**, 355–367.

Sutton, R. B., Fasshauer, D., Jahn, R. and Brunger, A. T. (1998). Crystal structure of a SNARE complex involved in synaptic exocytosis at 2.4 A resolution. *Nature* **395**, 347–353.

Swanston-Flatt, S. K., Carlsson, L. and Gylfe, E. (1980). Actin filament formation in pancreatic beta-cells during glucose stimulation of insulin secretion. *FEBS Lett.* **117**, 299–302.

Taminato, T., Seino, Y., Goto, Y., Inoue, Y. and Kadowaki, S. (1977). Synthetic gastric inhibitory polypeptide. Stimulatory effect on insulin and glucagon secretion in the rat. *Diabetes* **26**, 480–484.

Tengholm, A. and Meyer, T. (2002). A PI3-kinase signaling code for insulin-triggered insertion of glucose transporters into the plasma membrane. *Curr. Biol.* **12**, 1871–1876.

Terauchi, Y., Tsuji, Y., Satoh, S., Minoura, H., Murakami, K., Okuno, A., Inukai, K., Asano, T., Kaburagi, Y., Ueki, K., et al. (1999). Increased insulin sensitivity and hypoglycaemia in mice lacking the p85 alpha subunit of phosphoinositide 3-kinase. *Nat. Genet.* **21**, 230–235.

Thorens, B. (1992). Expression cloning of the pancreatic beta cell receptor for the gluco-incretin hormone glucagon-like peptide 1. *Proc. Natl. Acad. Sci. U.S.A.* **89**, 8641–8645.

Thorens, B., Porret, A., Bühler, L., Deng, S. P., Morel, P. and Widmann, C. (1993). Cloning and functional expression of the human islet GLP-1 receptor. Demonstration that exendin-4 is an agonist and exendin-(9-39) an antagonist of the receptor. *Diabetes* **42**, 1678–1682.

Thurmond, D. C., Gonelle-Gispert, C., Furukawa, M., Halban, P. A. and Pessin, J. E. (2003). Glucose-stimulated insulin secretion is coupled to the interaction of actin with the t-SNARE (target membrane soluble N-ethylmaleimide-sensitive factor attachment protein receptor protein) complex. *Mol. Endocrinol.* **17**, 732–742.

Toft-Nielsen, M. B., Damholt, M. B., Madsbad, S., Hilsted, L. M., Hughes, T. E., Michelsen, B. K. and Holst, J. J. (2001). Determinants of the impaired secretion of glucagon-like peptide-1 in type 2 diabetic patients. *J. Clin. Endocrinol. Metab.* **86**, 3717–3723.

Tolbert, L. M. and Lameh, J. (1996). Human muscarinic cholinergic receptor Hm1 internalizes via clathrin-coated vesicles. *J. Biol. Chem.* **271**, 17335–17342.

Tomas, A., Yermen, B., Min, L., Pessin, J. E. and Halban, P. A. (2006). Regulation of pancreatic beta-cell insulin secretion by actin cytoskeleton remodelling: role of gelsolin and cooperation with the MAPK signalling pathway. *J. Cell. Sci.* **119**, 2156–2167.

Tourrel, C., Bailbé, D., Meile, M. J., Kergoat, M. and Portha, B. (2001). Glucagon-like peptide-1 and exendin-4 stimulate beta-cell neogenesis in streptozotocin-treated newborn rats resulting in persistently improved glucose homeostasis at adult age. *Diabetes* **50**, 1562–1570.

Trümper, A., Trümper, K., Trusheim, H., Arnold, R., Göke, B. and Hörsch, D. (2001). Glucose-dependent insulinotropic polypeptide is a growth factor for beta (INS-1) cells by pleiotropic signaling. *Mol. Endocrinol.* **15**, 1559–1570.

Tsakiridis, T., Tong, P., Matthews, B., Tsiani, E., Bilan, P. J., Klip, A. and Downey, G. P. (1999). Role of the actin cytoskeleton in insulin action. *Microsc. Res. Tech.* **47**, 79–92.

Tsuboi, T. and Rutter, G. A. (2003). Multiple forms of "kiss-and-run" exocytosis revealed by evanescent wave microscopy. *Curr. Biol.* **13**, 563–567.

Ueki, K., Okada, T., Hu, J., Liew, C. W., Assmann, A., Dahlgren, G. M., Peters, J. L., Shackman, J. G., Zhang, M., Artner, I., et al. (2006). Total insulin and IGF-I resistance in pancreatic beta cells causes overt diabetes. *Nat. Genet.* **38**, 583–588.

Ueki, K., Yballe, C. M., Brachmann, S. M., Vicent, D., Watt, J. M., Kahn, C. R. and Cantley, L. C. (2002). Increased insulin sensitivity in mice lacking p85beta subunit of phosphoinositide 3-kinase. *Proc. Natl. Acad. Sci. U.S.A.* **99**, 419–424.

Uenishi, E., Shibasaki, T., Takahashi, H., Seki, C., Hamaguchi, H., Yasuda, T., Tatebe, M., Oiso, Y., Takenawa, T. and Seino, S. (2013). Actin dynamics regulated by the balance of neuronal Wiskott-Aldrich syndrome protein (N-WASP) and cofilin activities determines the biphasic response of glucose-induced insulin secretion. *J. Biol. Chem.* **288**, 25851–25864.

Ui, M., Okada, T., Hazeki, K. and Hazeki, O. (1995). Wortmannin as a unique probe for an intracellular signalling protein, phosphoinositide 3-kinase. *Trends Biochem. Sci.* **20**, 303–307.

Usdin, T. B., Mezey, E., Button, D. C., Brownstein, M. J. and Bonner, T. I. (1993). Gastric inhibitory polypeptide receptor, a member of the secretin-vasoactive intestinal peptide receptor family, is widely distributed in peripheral organs and the brain. *Endocrinology* **133**, 2861–2870.

Vadas, O., Burke, J. E., Zhang, X., Berndt, A. and Williams, R. L. (2011). Structural basis for activation and inhibition of class I phosphoinositide 3-kinases. *Sci Signal* **4**, re2.

Vanhaesebroeck, B. and Waterfield, M. D. (1999). Signaling by distinct classes of phosphoinositide 3-kinases. *Exp. Cell Res.* **253**, 239–254.

Vanhaesebroeck, B., Guillermet-Guibert, J., Graupera, M. and Bilanges, B. (2010). The emerging mechanisms of isoform-specific PI3K signalling. *Nat. Rev. Mol. Cell Biol.* **11**, 329–341.

Vanhaesebroeck, B., Leevers, S. J., Ahmadi, K., Timms, J., Katso, R., Driscoll, P. C., Woscholski, R., Parker, P. J. and Waterfield, M. D. (2001). Synthesis and function of 3-phosphorylated inositol lipids. *Annu. Rev. Biochem.* **70**, 535–602.

Vanhaesebroeck, B., Stephens, L. and Hawkins, P. (2012). PI3K signalling: the path to discovery and understanding. *Nat. Rev. Mol. Cell Biol.* **13**, 195–203.

Vanhaesebroeck, B., Welham, M. J., Kotani, K., Stein, R., Warne, P. H., Zvelebil, M. J., Higashi, K., Volinia, S., Downward, J. and Waterfield, M. D. (1997). P110delta, a novel phosphoinositide 3-kinase in leukocytes. *Proc. Natl. Acad. Sci. U.S.A.* **94**, 4330–4335.

Vilsbøll, T. and Knop, F. K. (2007). [Effect of incretin hormones GIP and GLP-1 for the pathogenesis of type 2 diabetes mellitus]. *Ugeskr. Laeg.* **169**, 2101–2105.

Vilsbøll, T., Krarup, T., Deacon, C. F., Madsbad, S. and Holst, J. J. (2001). Reduced postprandial concentrations of intact biologically active glucagon-like peptide 1 in type 2 diabetic patients. *Diabetes* **50**, 609–613.

Vlahos, C. J., Matter, W. F., Hui, K. Y. and Brown, R. F. (1994). A specific inhibitor of phosphatidylinositol 3-kinase, 2-(4-morpholinyl)-8-phenyl-4H-1-benzopyran-4-one (LY294002). *J. Biol. Chem.* **269**, 5241–5248.

Vogt, P. K., Gymnopoulos, M. and Hart, J. R. (2009). PI 3-kinase and cancer: changing accents. *Curr. Opin. Genet. Dev.* **19**, 12–17.

Voigt, P., Brock, C., Nürnberg, B. and Schaefer, M. (2005). Assigning functional domains within the p101 regulatory subunit of phosphoinositide 3-kinase gamma. *J. Biol. Chem.* **280**, 5121–5127.

Voigt, P., Dorner, M. B. and Schaefer, M. (2006). Characterization of p87PIKAP, a novel regulatory subunit of phosphoinositide 3-kinase gamma that is highly expressed in heart and interacts with PDE3B. *J. Biol. Chem.* **281**, 9977–9986.

Volz, A., Göke, R., Lankat-Buttgereit, B., Fehmann, H. C., Bode, H. P. and Göke, B. (1995). Molecular cloning, functional expression, and signal transduction of the GIP-receptor cloned from a human insulinoma. *FEBS Lett.* **373**, 23–29.

Waddleton, D., Wu, W., Feng, Y., Thompson, C., Wu, M., Zhou, Y.-P., Howard, A., Thornberry, N., Li, J. and Mancini, J. A. (2008). Phosphodiesterase 3 and 4 comprise the major cAMP metabolizing enzymes responsible for insulin secretion in INS-1 (832/13) cells and rat islets. *Biochem. Pharmacol.* **76**, 884–893.

Walker, E. H., Pacold, M. E., Perisic, O., Stephens, L., Hawkins, P. T., Wymann, M. P. and Williams, R. L. (2000). Structural determinants of phosphoinositide 3-kinase inhibition by wortmannin, LY294002, quercetin, myricetin, and staurosporine. *Mol. Cell* **6**, 909–919.

Walz, H. A., Wierup, N., Vikman, J., Manganiello, V. C., Degerman, E., Eliasson, L. and Holst, L. S. (2007). Beta-cell PDE3B regulates Ca2+-stimulated exocytosis of insulin. *Cell. Signal.* **19**, 1505–1513.

Wang, J. L., Easom, R. A., Hughes, J. H. and McDaniel, M. L. (1990). Evidence for a role of microfilaments in insulin release from purified beta-cells. *Biochem. Biophys. Res. Commun.* **171**, 424–430.

Wang, L., Liu, Y., Yan Lu, S., Nguyen, K.-T. T., Schroer, S. A., Suzuki, A., Mak, T. W., Gaisano, H. and Woo, M. (2010). Deletion of Pten in pancreatic ß-cells protects against deficient ß-cell mass and function in mouse models of type 2 diabetes. *Diabetes* **59**, 3117–3126.

Wang, Z. and Thurmond, D. C. (2009). Mechanisms of biphasic insulin-granule exocytosis - roles of the cytoskeleton, small GTPases and SNARE proteins. *J. Cell.*

Sci. **122**, 893–903.

Wang, Z., Oh, E. and Thurmond, D. C. (2007). Glucose-stimulated Cdc42 signaling is essential for the second phase of insulin secretion. *J. Biol. Chem.* **282**, 9536–9546.

Wegner, A., Aktories, K., Ditsch, A., Just, I., Schoepper, B., Selve, N. and Wille, M. (1994). Actin-gelsolin interaction. *Adv. Exp. Med. Biol.* **358**, 97–104.

Wehland, J. and Weber, K. (1981). Actin rearrangement in living cells revealed by microinjection of a fluorescent phalloidin derivative. *Eur. J. Cell Biol.* **24**, 176–183.

Weiss-Haljiti, C., Pasquali, C., Ji, H., Gillieron, C., Chabert, C., Curchod, M.-L., Hirsch, E., Ridley, A. J., Hooft van Huijsduijnen, R., Camps, M., et al. (2004). Involvement of phosphoinositide 3-kinase gamma, Rac, and PAK signaling in chemokine-induced macrophage migration. *J. Biol. Chem.* **279**, 43273–43284.

Welch, H. C. E., Coadwell, W. J., Ellson, C. D., Ferguson, G. J., Andrews, S. R., Erdjument-Bromage, H., Tempst, P., Hawkins, P. T. and Stephens, L. R. (2002). P-Rex1, a PtdIns(3,4,5)P3- and Gbetagamma-regulated guanine-nucleotide exchange factor for Rac. *Cell* **108**, 809–821.

Wen, P. J., Osborne, S. L., Zanin, M., Low, P. C., Wang, H.-T. A., Schoenwaelder, S. M., Jackson, S. P., Wedlich-Söldner, R., Vanhaesebroeck, B., Keating, D. J., et al. (2011). Phosphatidylinositol(4,5)bisphosphate coordinates actin-mediated mobilization and translocation of secretory vesicles to the plasma membrane of chromaffin cells. *Nat Commun* **2**, 491.

Wennerberg, K., Rossman, K. L. and Der, C. J. (2005). The Ras superfamily at a glance. *J. Cell. Sci.* **118**, 843–846.

Whalley, N. M., Pritchard, L. E., Smith, D. M. and White, A. (2011). Processing of proglucagon to GLP-1 in pancreatic α-cells: is this a paracrine mechanism enabling GLP-1 to act on β-cells? *J. Endocrinol.* **211**, 99–106.

Wheeler, M. B., Gelling, R. W., McIntosh, C. H., Georgiou, J., Brown, J. C. and Pederson, R. A. (1995). Functional expression of the rat pancreatic islet glucose-dependent insulinotropic polypeptide receptor: ligand binding and intracellular signaling properties. *Endocrinology* **136**, 4629–4639.

Wheeler, M. B., Sheu, L., Ghai, M., Bouquillon, A., Grondin, G., Weller, U., Beaudoin, A. R., Bennett, M. K., Trimble, W. S. and Gaisano, H. Y. (1996). Characterization of SNARE protein expression in beta cell lines and pancreatic islets. *Endocrinology* **137**, 1340–1348.

Whitman, M., Downes, C. P., Keeler, M., Keller, T. and Cantley, L. (1988). Type I phosphatidylinositol kinase makes a novel inositol phospholipid, phosphatidylinositol-3-phosphate. *Nature* **332**, 644–646.

Widenmaier, S. B., Sampaio, A. V., Underhill, T. M. and McIntosh, C. H. S. (2009). Noncanonical activation of Akt/protein kinase B in {beta}-cells by the incretin hormone glucose-dependent insulinotropic polypeptide. *J. Biol. Chem.* **284**, 10764–10773.

Widmann, C., Dolci, W. and Thorens, B. (1995). Agonist-induced internalization and recycling of the glucagon-like peptide-1 receptor in transfected fibroblasts and in insulinomas. *Biochem. J.* **310 (Pt 1)**, 203–214.

Wieland, T. and Faulstich, H. (1978). Amatoxins, phallotoxins, phallolysin, and antamanide: the biologically active components of poisonous Amanita mushrooms. *CRC Crit. Rev. Biochem.* **5**, 185–260.

Wulf, E., Deboben, A., Bautz, F. A., Faulstich, H. and Wieland, T. (1979). Fluorescent phallotoxin, a tool for the visualization of cellular actin. *Proc. Natl. Acad. Sci. U.S.A.* **76**, 4498–4502.

Wymann, M. P. and Solinas, G. (2013). Inhibition of phosphoinositide 3-kinase γ attenuates inflammation, obesity, and cardiovascular risk factors. *Ann. N. Y. Acad. Sci.* **1280**, 44–47.

Wymann, M. P., Björklöf, K., Calvez, R., Finan, P., Thomast, M., Trifilieff, A., Barbier, M., Altruda, F., Hirsch, E. and Laffargue, M. (2003). Phosphoinositide 3-kinase gamma: a key modulator in inflammation and allergy. *Biochem. Soc. Trans.* **31**, 275–280.

Wymann, M. P., Bulgarelli-Leva, G., Zvelebil, M. J., Pirola, L., Vanhaesebroeck, B., Waterfield, M. D. and Panayotou, G. (1996). Wortmannin inactivates phosphoinositide 3-kinase by covalent modification of Lys-802, a residue involved in the phosphate transfer reaction. *Mol. Cell. Biol.* **16**, 1722–1733.

Xu, G., Stoffers, D. A., Habener, J. F. and Bonner-Weir, S. (1999). Exendin-4 stimulates both beta-cell replication and neogenesis, resulting in increased beta-cell mass and improved glucose tolerance in diabetic rats. *Diabetes* **48**, 2270–2276.

Yabe, D. and Seino, Y. (2011). Two incretin hormones GLP-1 and GIP: comparison of their actions in insulin secretion and β cell preservation. *Prog. Biophys. Mol. Biol.* **107**, 248–256.

YALOW, R. S. and BERSON, S. A. (1960). Immunoassay of endogenous plasma insulin in man. *J. Clin. Invest.* **39**, 1157–1175.

Yang, J., Dolinger, M., Ritaccio, G., Mazurkiewicz, J., Conti, D., Zhu, X. and Huang, Y. (2012). Leucine stimulates insulin secretion via down-regulation of surface expression of adrenergic α2A receptor through the mTOR (mammalian target of rapamycin) pathway: implication in new-onset diabetes in renal transplantation. *J. Biol. Chem.* **287**, 24795–24806.

Yang, S.-N. and Berggren, P.-O. (2006). The role of voltage-gated calcium channels in pancreatic beta-cell physiology and pathophysiology. *Endocr. Rev.* **27**, 621–676.

Yano, H., Nakanishi, S., Kimura, K., Hanai, N., Saitoh, Y., Fukui, Y., Nonomura, Y. and Matsuda, Y. (1993). Inhibition of histamine secretion by wortmannin through the blockade of phosphatidylinositol 3-kinase in RBL-2H3 cells. *J. Biol. Chem.* **268**, 25846–25856.

Yin, H. L. and Janmey, P. A. (2003). Phosphoinositide regulation of the actin cytoskeleton. *Annu. Rev. Physiol.* **65**, 761–789.

Yoshizaki, T., Imamura, T., Babendure, J. L., Lu, J.-C., Sonoda, N. and Olefsky, J. M. (2007). Myosin 5a is an insulin-stimulated Akt2 (protein kinase Bbeta) substrate modulating GLUT4 vesicle translocation. *Mol. Cell. Biol.* **27**, 5172–5183.

Yu, J., Zhang, Y., McIlroy, J., Rordorf-Nikolic, T., Orr, G. A. and Backer, J. M. (1998). Regulation of the p85/p110 phosphatidylinositol 3'-kinase: stabilization and inhibition of the p110alpha catalytic subunit by the p85 regulatory subunit. *Mol. Cell. Biol.* **18**, 1379–1387.

Zawalich, W. S. and Zawalich, K. C. (2000). A link between insulin resistance and hyperinsulinemia: inhibitors of phosphatidylinositol 3-kinase augment glucose-induced insulin secretion from islets of lean, but not obese, rats. *Endocrinology* **141**, 3287–3295.

Zawalich, W. S., Tesz, G. J. and Zawalich, K. C. (2002). Inhibitors of phosphatidylinositol 3-kinase amplify insulin release from islets of lean but not obese mice. *J. Endocrinol.* **174**, 247–258.

Zhao, L. and Vogt, P. K. (2008a). Class I PI3K in oncogenic cellular transformation. *Oncogene* **27**, 5486–5496.

Zhao, L. and Vogt, P. K. (2008b). Helical domain and kinase domain mutations in p110alpha of phosphatidylinositol 3-kinase induce gain of function by different mechanisms. *Proc. Natl. Acad. Sci. U.S.A.* **105**, 2652–2657.

Zhao, L. and Vogt, P. K. (2010). Hot-spot mutations in p110alpha of phosphatidylinositol 3-kinase (pI3K): differential interactions with the regulatory subunit p85 and with RAS. *Cell Cycle* **9**, 596–600.

Zheng, Z., Amran, S. I., Thompson, P. E. and Jennings, I. G. (2011). Isoform-selective inhibition of phosphoinositide 3-kinase: identification of a new region of nonconserved amino acids critical for p110α inhibition. *Mol. Pharmacol.* **80**, 657–664.

Zoncu, R., Perera, R. M., Sebastian, R., Nakatsu, F., Chen, H., Balla, T., Ayala, G., Toomre, D. and De Camilli, P. V. (2007). Loss of endocytic clathrin-coated pits upon acute depletion of phosphatidylinositol 4,5-bisphosphate. *Proc. Natl. Acad. Sci.*

U.S.A. **104**, 3793–3798.

Zunz, E. and La Barre, J. (1930). Contributions A L'Étude Des Variations Physiologiques De La Sécrétion Interne Du Pancreas -- VIII. – Répercussion de l'activité exocrine du pancréas sur l'insulino-sécrétion. *Arch Physiol Biochem* **33**, 142–158.